The Interaction of p21Ras with Neurofibromin

Beth A. Sermon

1997

Submitted in partial fulfilment of the requirements of the University of London
for the degree of Doctor of Philosophy

University College London
University of London

and

National Institute For Medical Research
Mill Hill
London

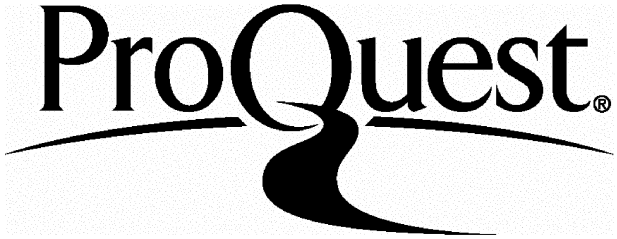

Contents

Figures

Tables

Abbreviations

GAP	GTPase-activating Protein
NF1	Neurofibromin
p120-GAP	Full length mammalian GAP
GAP_{344}	Catalytic domain of p120-GAP
$NF1_{334}$	Catalytic domain of neurofibromin
NF1-GST	Catalytic domain of neurofibromin as a fusion protein with glutathione S-transferase
GST	Glutathione S-transferase
I_{50}	Concentration at which 50% inhibition is observed
EC_{50}	Effective concentration for 50% of the effect observed
EDTA	Ethylenediamine tetraacetic acid
Tris	Tris(hydroxymethyl)aminomethane
MOPS	3-[N-Morpholino]propanesulfonic acid
IPTG	Isopropyl-D-thiogalactopyranoside
mantGTP	2' (3')-*O*-*N*-methylanthraniloyl-GTP
mantGDP	2' (3')-*O*-*N*-methylanthraniloyl-GDP
GTP	Guanosine triphosphate
GDP	Guanosine diphosphate
GDP-[NH]P	Guanosine 5'-[β,γ-imido]triphosphate
GDP-[CH_2]P	Guanosine 5'-(β,γ-methylene)triphosphate
PDGF	Platelet derived growth factor
EGF	Eosinophil derived growth factor
PMSF	Phenyl Methyl Sulfonyl Fluoride
SDS PAGE	Sodium dodecyl sulphate polyacrylamide gel electrophoresis
TEMED	N, N, N', N'- tetramethylethylenediamine
HPLC	High performance liquid chromatography
TBA	Tetra-butyl ammonium hydroxide
TEAB	Triethylammonium bicarbonate
SPA	Scintillation proximity assay
BSA	Bovine serum albumin

CMC	Critical micellar concentration
DPH Carboxylic acid	*p*-((6-phenyl)-1,3,5-hexatrienyl) benzoic acid
DPH	1,6-diphenyl-1,3,5-hexatriene
Phosphatidic acid	β-stearoyl-γ-arachidonyl-L-α-phosphatidic acid
Ras	Protein product of the Harvey-*ras* gene (in all experiments this refers to wild-type Ras truncated at residue 166, except where otherwise specified)

Abstract

*ras*genes encode guanine nucleotide binding proteins that act as molecular switches for signal transduction pathways controlling cell growth and differentiation. In the GTP-bound form the Ras protein is active and interacts with effector proteins to propagate a signal from the outside of the cell to the nucleus or cytoskeleton. Ras has a low intrinsic GTPase activity which is accelerated by the GTPase-activating proteins (GAPs), p120-GAP and neurofibromin. Two aspects of the interaction between Ras and the catalytic domain of neurofibromin ($NF1_{334}$) have been studied.

(1) The GTPase-activating activity of both p120-GAP and neurofibromin are inhibited by mitogenic lipids such as phosphatidic acid and arachidonic acid. Previous data on the differential inhibition of the two GAPs led to the hypothesis that both were effectors in a Ras-controlled mitogenic pathway. The mechanism of inhibition of $NF1_{334}$ by arachidonic acid was studied by measuring the catalytic activity under multiple turnover conditions, using *p*-((6-phenyl)-1,3,5-hexatrienyl)benzoic acid as a fluorescent probe for ligands binding to GAPs and using a scintillation proximity assay to measure direct binding of Ras to $NF1_{334}$. The inhibition by arachidonic acid included a major component that is competitive with Ras.GTP and an additional non-competitive type effect consistent with protein denaturing activity. This suggested that insomuch as the mitogenic effects of lipids are mediated via inhibition of GAPs, GAPs are not Ras effector proteins.

(2) Basic residues within the catalytic domains of p120-GAP and neurofibromin have been suggested to play an important role in GAP-stimulated catalysis and Ras binding. Two invariant arginine residues within $NF1_{334}$, R1276 and R1391, were mutated to alanine and their effects on maximal catalysis (k_{cat}) and affinity (K_d) for Ras measured under single turnover conditions. Both R1276 and R1391 are required for efficient catalysis by $NF1_{334}$ as removal of either results in a 1000-fold loss of activity. R1276 is not thought to be directly involved in Ras binding as the affinity of R1276A for H-Ras or [Leu61]H-Ras is only moderately reduced (ca. 3-fold). The reduction in affinity of R1391A for H-Ras is more marked (ca. 10-20 fold) but most notable for [Leu61]H-Ras (ca. 100-fold) suggesting a role for this residue in Ras binding. The high affinity of [Leu61]H-Ras for $NF1_{334}$ over H-Ras is completely lost with the R1391 $NF1_{334}$, suggesting that the high affinity is related to an interaction with R1391 of $NF1_{334}$

Chapter 1

Introduction

1.1 Ras Superfamily of GTPases

ras oncogenes were initially identified as the transforming elements of acutely oncogenic Harvey (H-*ras*) and Kirsten (K-*ras*) rat sarcoma viruses (Harvey, 1964; Kirsten and Mayer, 1967). A third *ras* gene (N-*ras*) was identified from a neuroblastoma cell line (Hall *et al*, 1983). Subsequent studies revealed that many of these retrovirally transduced sequences represented mammalian cellular proto-oncogenes (c-*ras*) that had been activated by point mutation (Barbacid, 1987). Activated c-*ras* genes have been shown to play a role in neoplasia, being frequently implicated in many types of human cancer (Forrester *et al*, 1987; Bos, 1989; Rhodenhuis, 1992). Current estimates suggest that 30% of all cancers harbour mutations in one of the three related *ras* genes, with mutation frequencies varying from 0-100% depending on the individual tumour. The Ras protein gains its oncogenic potential by selective substitution of single amino acids in the so-called 'hot spot' positions (12, 13 and 61) of the H-, K- or N-*ras* genes.

These three highly-related mammalian *ras* proto-oncogenes encode the 21 kiloDalton guanine nucleotide binding proteins, Ras. The Ras proteins are members of a large superfamily which contains 50-60 small GTPases which share sequence homology with Ras (Macara *et al*, 1996). Members of the superfamily function as molecular switches and control a wide variety of cellular processes. On the basis of sequence and functional homology, Ras-like GTPases can be grouped into six subfamilies, **Rac/Rho**, **Rab/Ypt**, **Ran/TC4**, **Arf**, **Rad** and **Ras**. It has recently been proposed that **Rin**, a neuron-specific and calmodulin-binding small G-protein, and **Rit**, define a novel subfamily of Ras-related proteins which use a new mechanism of membrane association (Lee *et al*, 1996). **Rin** may be involved in calcium mediated signalling within neurons.

To date, at least ten distinct **Rac/Rho** family proteins (ie: Rac1, Rac2, RhoA, RhoB, RhoC, RhoE, RhoG, TC10, G25K and Cdc42Hs) have been identified in mammalian cells, the most recent being RhoE (Foster *et al*, 1996). These share approximately 30% amino acid identity with Ras proteins. **Rho** family proteins have been implicated in a wide variety of biological activities including motility and mitosis (Takai *et al*, 1995) apoptosis (Jimenez *et al*, 1995) cell cycle progression (Olson *et al*, 1995) transformation

(Prendergast *et al*, 1995; Symons, 1996) and morphological changes (Hall, 1994). Evidence for the role of Rho family proteins in regulating cytoskeletal dynamics has come from observations that these proteins can profoundly affect the polymerization and organization of actin (reviewed by Takai *et al*, 1995; Nobes and Hall, 1995; Tapon and Hall, 1997). In mammalian fibroblasts, Rho causes actin stress fibre formation in response to lysophosphatidic acid (Paterson *et al*, 1990; Ridley and Hall, 1992; Ridley, 1995), Rac stimulates membrane ruffling induced by platelet-derived growth factor (Ridley *et al*, 1992; Ridley, 1994) and Cdc42 induces filopodia formation in response to bradykinin. In addition, Rac proteins are essential components of the NADPH oxidase system that generates the superoxide anion (O_2^-) in phagocytes (Segal *et al*, 1993; Bokoch, 1994).

At least thirty **Rab** GTPases (e.g Rab 1-6, BRL-Ras, Smg25-A, -B, -C and the yeast proteins Ypt1 and Sec4) have been identified. The **Arf** family is divided functionally into the **Arf** (ADP ribosylation factor) and **Arl** (Arf-like) proteins. Several **Arf** (Arf1-6) and at least ten **Arl** proteins have been identified. Both Rab and Arf proteins have been shown to play essential roles in the assembly, loading and targeting of vesicles to appropriate cellular compartments during endocytosis and secretion (Fischer von Mollard *et al*, 1994; Gruenberg and Maxfield, 1995; Boman and Kahn, 1995). However, no cellular roles for Arls have as yet been identified.

The exact function(s) of the **Ran/TC4** family of GTPases remains unclear, although studies by Moore and Blobel (1993) and Melchior and Gerace (1995) have identified **Ran** as an essential component of nuclear protein import machinery (reviewed by Rush *et al*, 1996; Koepp and Silver, 1996).

Several members of the **Rad** subfamily have been identified, namely Rad (Ras associated with diabetes) (Reynet and Kahn, 1993; Zhu *et al*, 1995), Gem (immediate early gene expressed in mitogen stimulated T-cells) (Maguire *et al*, 1994) and Kir (tyrosine kinase inducible ras-like) (Cohen *et al*, 1994). These proteins are unique among the Ras superfamily of G-proteins since their intracellular level is transcriptionally regulated. Recent experiments have suggested that Rad is involved in skeletal muscle motor function

and cytoskeletal organization (Zhu *et al*, 1996). Gem is thought to be a regulatory protein which may participate in receptor-mediated signal transduction at the plasma membrane. Other experiments have suggested that Kir could be involved in processes of invasion or metastasis in mammalian (Cohen *et al*, 1994) and yeast cells (Dorin *et al*, 1995) or could form a link between Ca^{2+}/calmodulin and growth factor signal transduction pathways (Fischer *et al*, 1996).

Finally, members of the **Ras** branch of the superfamily (i.e Ras, Rap1A, Rap1B, Rap2, R-Ras, RalA, RalB and TC21) are regulators of signal transduction pathways that control cell growth and differentiation (Cox *et al*, 1994; Graham *et al*, 1994; Khosravi-Far and Der, 1994; Prendergast and Gibbs, 1993; Hall, 1993; Urano *et al*, 1996).

1.1.1 Biochemistry of Ras

Ras itself forms a central molecular switch whose activity is governed by modulation of the ratio of bound GTP to GDP (Bourne *et al*, 1990; 1991). Ras proteins bind the guanine nucleotides GDP and GTP with high affinities (K_d ca. 10^{-12}M), and exist in two distinct conformations, dependent upon the nature of the nucleotide bound to the protein (Wittinghofer and Pai, 1991). The main differences between the GTP and GDP-bound forms of Ras reside in the switch I and switch II regions of the protein. The switch I region is defined by loop 2 (residues ca. 28-40) which has been shown to play an important role in the interaction with the downstream effector (Polakis and McCormick, 1993). Switch II is formed from residues 59-76 and is also thought to be required for effector binding. In the GTP-bound form, Ras is active and interacts with effector proteins to propagate a signal from the outside of the cell to the nucleus or cytoskeleton (Boguski and McCormick, 1993; McCormick and Wittinghofer, 1996). Ras cycles between the active GTP-bound form and the inactive GDP-bound form. This process, shown in figure 1, is referred to as 'switching' (Milburn *et al*, 1990; Stouten *et al*, 1993) and is accompanied by a major conformational change in the Ras protein centred around the switch II region.

Figure 1: The GDP / GTP cycle of Ras

Schematic view of signal transduction from the cell surface to the nucleus via the regulatory cycle of the *ras*-gene product, Ras. Exchange factors catalyse the activation of Ras in transferring it into the GTP bound form. Deactivation by intrinsic GTP hydrolysis of Ras can be accelerated by GTPase activating proteins. Only the GTP-bound Ras is able to interact strongly with effector molecules to transmit a downstream signal.

[Taken from Wittinghofer and Herrmann (1995)]

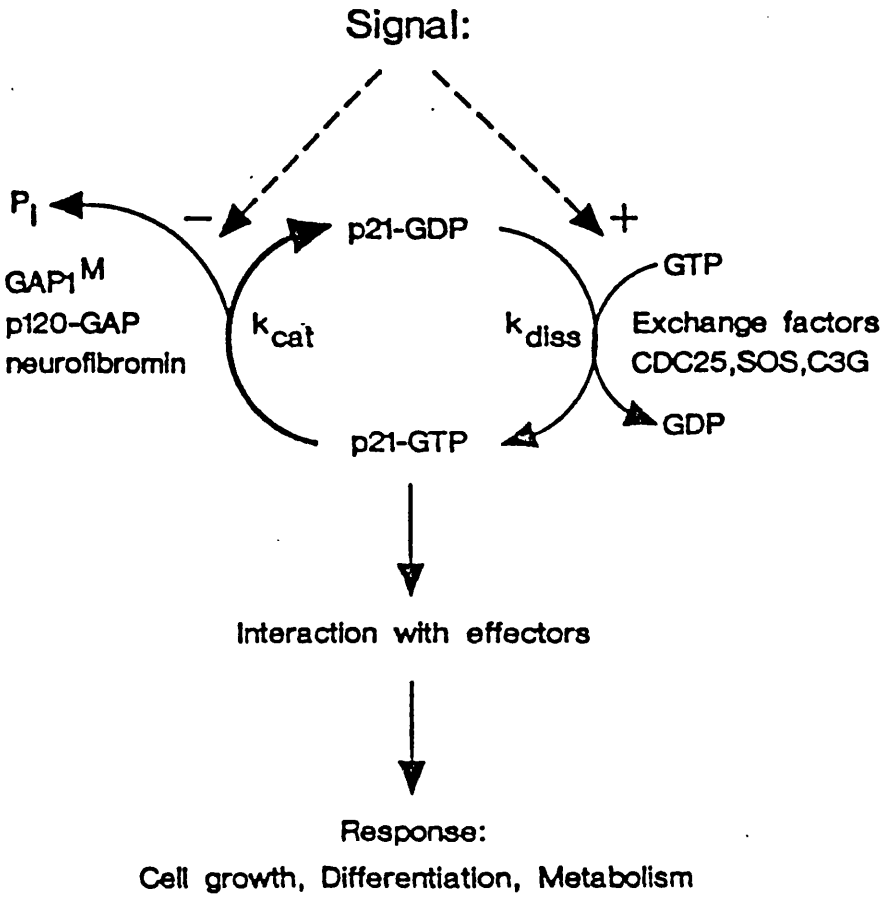
Signal:
P$_i$
−
+
p21-GDP
GAP1^M
p120-GAP
neurofibromin
k$_{cat}$
k$_{diss}$
GTP
Exchange factors
CDC25,SOS,C3G
GDP
p21-GTP
Interaction with effectors
Response:
Cell growth, Differentiation, Metabolism

The rate of interconversion of nucleotides is controlled by the rate of dissociation of GDP from the protein.GDP complex (k_{diss}) and the rate of hydrolysis of bound-GTP (k_{hyd}). Ras proteins possess low intrinsic rates of GDP dissociation and GTP hydrolysis (Barbacid, 1987; Grand and Owen 1991; Lowy *et al*, 1991; Lowy and Willumsen, 1993), rate constants for these processes being ca. 0.005 and 0.01 min^{-1}, respectively (Lowe *et al*, 1991; John *et al*, 1988). Intrinsic GTP hydrolysis activity converts the GTP-bound form of Ras to the GDP-bound form. Inactive Ras is subsequently converted back to the active GTP-bound form via an exchange process which involves the dissociation of GDP from the protein giving rise to a transient 'empty' state, followed by rebinding of GTP. GTP will be the predominant nucleotide to rebind since it is present at a higher intracellular concentration than GDP. Under steady state conditions, the rate of conversion of Ras.GTP to Ras.GDP equals that of conversion of Ras.GDP to Ras.GTP i.e k_{hyd} [Ras.GTP] = k_{diss} [Ras.GDP]. Therefore, the ratio of Ras.GTP to Ras.GDP will be equal to the ratio of k_{diss} to k_{hyd} (Lowe and Skinner, 1994).

However, this ratio may be modulated by two classes of regulatory proteins which regulate the cellular function of Ras by controlling the relative concentrations of active and inactive forms of the protein. Guanine nucleotide exchange proteins (GEFs) regulate the GDP dissociation rate. There are two types of GEF classified on the basis of their ability to stimulate (Guanine nucleotide dissociation stimulator, GDS) or inhibit (GDI) the rate of nucleotide exchange. The GTPase activating proteins (GAPs) accelerate the rate of GTP hydrolysis. Both classes of regulators will be discussed in more detail in section 1.2.

1.1.2 Three-dimensional structure of Ras

Ras superfamily members exhibit high degrees of amino acid homology. These regions of homology are confined to the N-terminal guanine nucleotide binding region which lies within the catalytic domain. The 165 amino acid catalytic domain is more than 90% identical among the three mammalian Ras genes with the N-terminal 86 amino acids being identical. Over the past few years X-ray diffraction studies have contributed greatly to the understanding of the structure and mechanism of action of Ras. Such studies have led to

an indepth understanding not only of the interaction of Ras with both nucleotide and magnesium but also of the structural differences between diphosphate and triphosphate-bound protein and the effects of point mutations that lead to cell transformation. More recently progress is being made in understanding the structural elements involved in Ras-effector interactions. The three-dimensional crystal structures of the guanine nucleotide binding domain (G-domain) of truncated wild-type and mutated Ras complexed with either GDP, caged GTP, non-hydrolyzable (GDP-[CH_2]P; GDP-[NH]P; mant dGDP-[NH]P) GTP analogues, have been determined (residues 1-171, De Vos *et al*, 1988; Milburn *et al*, 1990; Tong *et al*, 1991; Prive *et al*, 1992; residues 1-166, Pai *et al*, 1989; 1990; Schlichting *et al*, 1990; Krengel *et al*, 1990; Brunger *et al*, 1990; Franken *et al*, 1993; Scheidig *et al*, 1995).

Figure 2 shows the three-dimensional structure of Ras complexed to the non-hydrolyzable GTP analogue, GDP-[NH]P (Pai *et al*, 1990). The overall backbone structure of Ras is comprised of a six-stranded β-sheet forming a hydrophobic core, five α-helices and nine interconnecting loops (Pai *et al*, 1989; Milburn *et al*, 1990). Of the six strands, five are antiparallel whilst the other is parallel. The essential regions for Ras function include all strands of the central β-sheet, several connecting loops and adjacent helices. Analysis of the crystal structure of Ras.GDP-[NH]P (Pai *et al*, 1989; 1990) revealed that all looped regions are exposed on the surface of the protein, and residues from these loops have been shown to be critical for a number of functional properties of the Ras proteins, namely phosphate binding, guanine nucleotide binding, magnesium ion coordination, binding of the putative effector and neutralizing Y13-259 antibody.

i) Phosphate binding domain

Three patches of conserved residues were found to be important for binding the nucleotide phosphate groups, namely residues 10-17 (GAGGVGKS) in loop 1 (phosphate binding loop), residues 32-40 (YDPTIEDSY) in loop 2 (switch I) and residues 57-60 (DTAGQE) in loop 4 (switch II). The phosphate binding loop (residues 10-17) is not flexible but in fact very rigid in the Ras.GDP-[NH]P crystal structure (Pai *et al*, 1989). Residues from the switch I region such as Asp33, Pro34 and Thr35, are particularly

inflexible. However, Thr35 which co-ordinates the nucleotide and Mg^{2+} may be more flexible in the absence of the γ-phosphate group (Pai *et al*, 1990). Residues in loop4 have the highest mobility and are very poorly defined in the GTP structure but not in the GDP structure (Milburn *et al*, 1990).

Figure 3a illustrates the interactions between the GDP-[NH]P nucleotide analogue and Ras. The α-phosphate of the guanine nucleotide forms a hydrogen bond with the main chain of Ala18. The β-phosphate is hydrogen bonded to the main chain amide groups of residues 13-17 which point towards and are within 3.5Å of the phosphate oxygens, creating a polarized local electrostatic field (Pai *et al*, 1990). Lys16, in particular, stretches across the phosphates forming an ion pair interaction with the γ-phosphate and hydrogen bonding with the main chain oxygens of residues 10 and 11. In addition to being co-ordinated through hydrogen bonding to the amide nitrogen of Lys16, the γ-phosphate also interacts with the main chain amide and hydroxyl groups of Thr35, Tyr32 and Gly60. Co-ordination through Lys16 is thought to aid in the hydrolysis of GTP by increasing the hydrophilicity of the γ-phosphate and the acidity of the leaving GDP (Pai *et al*, 1990).

ii) Guanine base binding domain

The residues involved in coordinating the guanine base are also shown in Figure 3a. The guanine base of the nucleotide is bound by interaction with two patches of conserved residues, residues 116-119 of loop 8 (also refered to as the guanine specificity region) which is very rigid and residues 145-147 of loop 10. These amino acids (Phe28, Asn116, Lys117, Asp119, Ser145, Ala146 and Lys147) form a deep narrow groove which has great specificity for the guanine base (Tong *et al*, 1991). The guanine base is sandwiched between the aliphatic part of the Lys117 side chain on one side and the aromatic side chain of Phe28 on the other, both of which participate in hydrophobic interactions with the guanine base. The guanine base is also held in position by additional polar interactions between the O6 of the guanine ring and the amide nitrogen of Ala146 and the exocyclic 2-amino group and the endocyclic N1 of the guanine and the carboxylate group of Asp119. In addition, Asp119 is able to form contacts with the side chain hydroxyl of

Figure 2: Three-dimensional structure of Ras.GDP-[NH]P

Cartoon representation of the structure of the Ras protein (residues 1-166) complexed with the GTP nucleotide analogue, GDP-[NH]P. Secondary structure elements, $\alpha 1$-$\alpha 5$ are helices, $\beta 1$-$\beta 6$ are β-strands and L1-L10 are loop regions. The most conserved sequences are in loops 1, 4, 6 and 10. The position and conformation of the bound non-hydrolyzable nucleotide analogue, GDP-[NH]P is represented by GTP in this diagram.

[Taken from Wittinghofer and Pai (1991)]

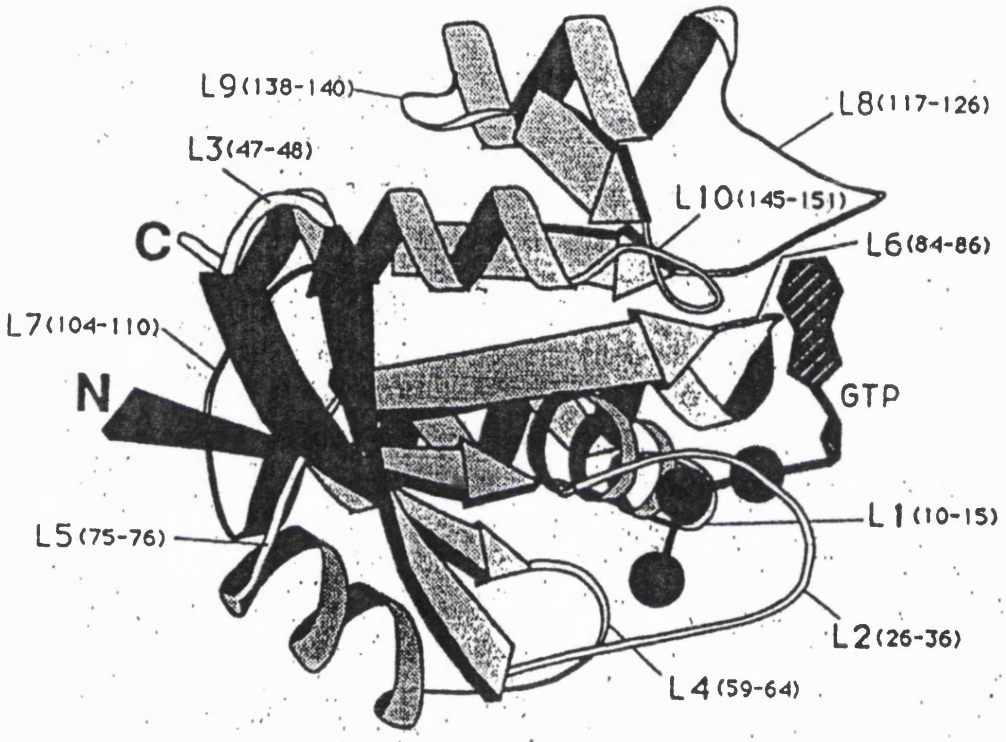
L9(138-140)
L8(117-126)
L3(47-48)
L10(145-151)
C
L6(84-86)
L7(104-110)
N
GTP
L1(10-15)
L5(75-76)
L2(26-36)
L4(59-64)

Figure 3(a): Scheme showing the interactions between GDP-[NH]P and Ras

Dashed lines indicate hydrogen bonds (<3.4Å). Distances between donor and acceptor atoms (in Å) are indicated next to the labels except where one residue makes several bonds, in which case the distances are given next to the dashed lines. Wat: water molecule; MC: main chain.

[Data taken from Pai *et al* (1990)]

Figure 3(b) Schematic drawing of the magnesium binding site on Ras

The diagram shows the ligands involved in the first co-ordination sphere of the magnesium ion. The magnesium ion is held in position by hydrogen bonding to both the β- and γ-phosphates, the side chain hydroxyl groups of Ser17 and Thr35. Asp57 is indirectly involved in co-ordinating the magnesium ion through hydrogen bonding to an intermediate water molecule, Wat173 which interacts with the Mg^{2+}, and by stabilizing Ser17.

[Taken from Pai *et al* (1990)]

(a)

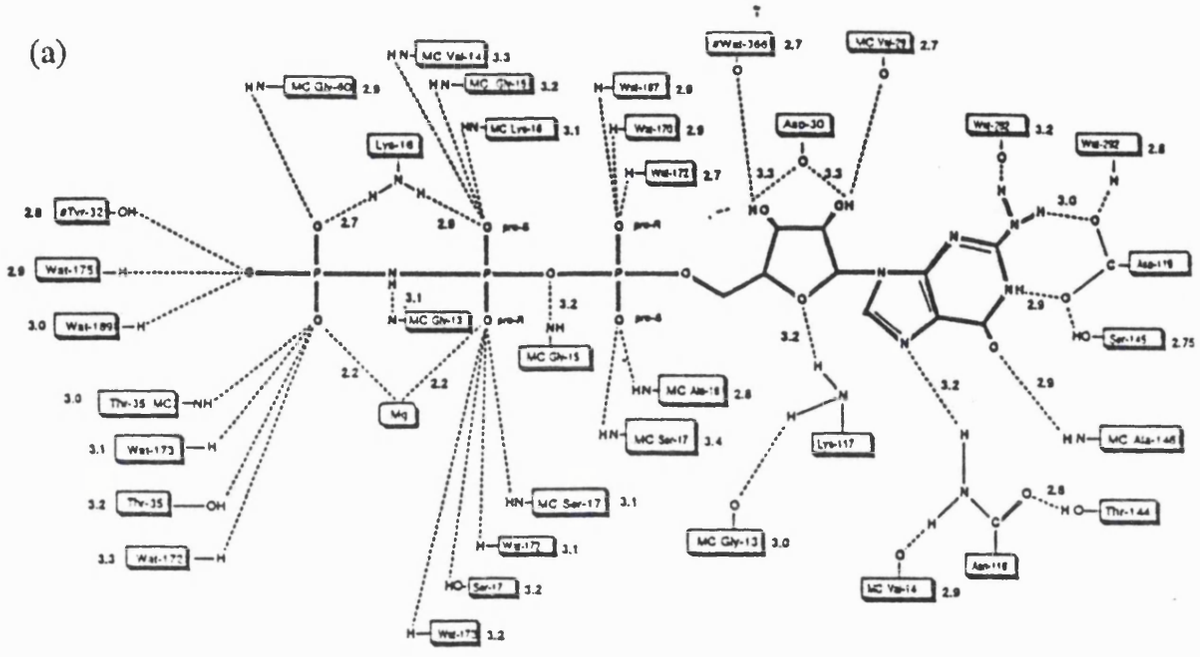

(b)

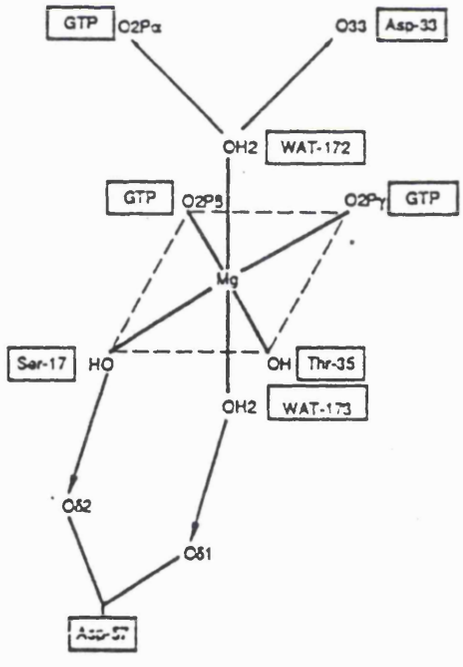
GTP
O2Pα
O33
Asp-33
OH2
WAT-172
GTP
O2Pβ
O2Pγ
GTP
Mg
Ser-17
HO
OH
Thr-35
OH2
WAT-173
Oδ2
Oδ1

Ser145, with the amino group of Lys147 and with Wat292.

Asn116 is able to orientate the three elements which are involved in nucleotide binding; the phosphate binding loop (residues 10-17), residues 116-119 and residues 146-148, by forming hydrogen bonds with the purine ring, the side chain of Thr144 and with the main chain oxygen atom of Val14. The amino group of Lys117 assists Asn116 by forming a hydrogen bond with the main chain carbonyl group of Gly13 in the phosphate binding loop.

iii) Magnesium binding domain

The residues of Ras involved in co-ordinating the magnesium ion are shown in figure 3b. Such co-ordination is achieved through hydrogen bonding of the Mg^{2+} ion to both the β- and γ-phosphates, the side chain hydroxyl groups of Ser17 and Thr35 (Pai *et al*, 1989). Asp57 is indirectly involved in co-ordinating the magnesium ion through hydrogen bonding to an intermediate water molecule, Wat173 which interacts with the Mg^{2+}, and by stabilizing Ser17.

iv) Effector binding domain

There are now several strong candidates for Ras effectors that include protein kinases, lipid kinases and guanine nucleotide exchange factors (discussed in section 1.2.2). Structural information on the interaction between the Ras binding domains of effectors and Ras.GTP is now available. Ras effectors preferentially bind to the GTP-bound form of Ras. The switch mechanism involves a guanine-nucleotide dependent conformational change in two discrete regions of Ras, referred to as switch I and switch II (Pai *et al*, 1989; Milburn *et al*, 1990). This structural rearrangement occurs during the switching between the GTP and GDP-bound states and is directed by the loss of the γ-phosphate and alterations in the co-ordination of magnesium. The switch I region is defined by residues 30-38 which form part of loop2 and the second β-strand. Residues 32-38 of this motif are conserved among all members of the Ras subfamily. The switch II region is composed of residues 60-76 and is highly mobile and therefore able to exist in a variety of conformations (Pai *et al*, 1990). Residues 61-64 in particular are able to adopt at least

Figure 4(a): Schematic drawing of the active conformation of Ras.GDP-[NH]P

This conformation of residues is proposed to be required for competent hydrolysis of GTP and the activation of the nucleophilic water molecule. In this complex, Gln61, assisted by the carbonyl group of Thr35, is proposed to activate Wat175. Gln63 may play an indirect role in GTP hydrolysis by stabilizing Gln61 in its proper activating orientation or increasing its proton withdrawing potential. The γ-phosphate is hydrogen bonded to Thr35, Gly60 and Lys16. In addition, Thr35 forms a hydrogen bond with the Mg^{2+} ion.

[Taken from Pai *et al* (1990)]

Figure 4(b) Schematic diagram indicating the changes in interactions between nucleotide and protein occurring upon GTP hydrolysis

In the transition from the active to inactive form of Ras, the hydrogen bond between the main chain of Thr35 and the γ-phosphate bond is broken. At the same time, the side chain hydroxyl is no longer co-ordinated to the magnesium ion and swings away from the protein into the solvent. This change is accompanied by movements of adjacent residues such as Tyr32, Asp33, Pro34 and Ile36. In addition, the hydrogen bond between the backbone of Gly60 and the γ-phosphate is lost leading to conformational changes of loop 4.

[Taken from Wittinghofer and Pai (1991)]

(a)

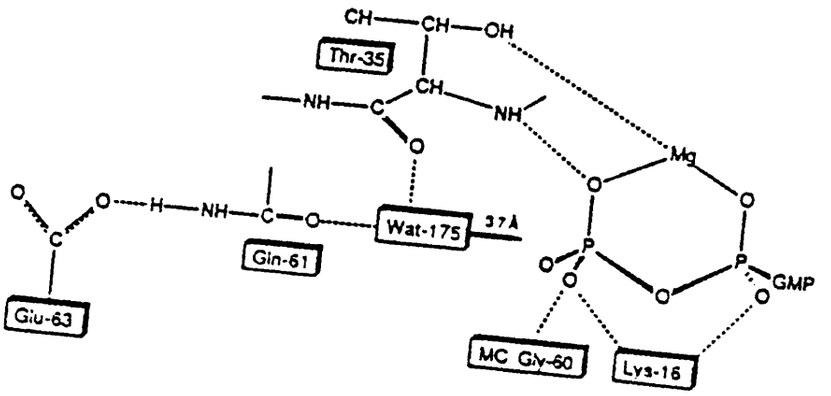
Thr-35
Gln-61
Wat-175
3.7 Å
Glu-63
MC Gly-60
Lys-16
GMP

(b)

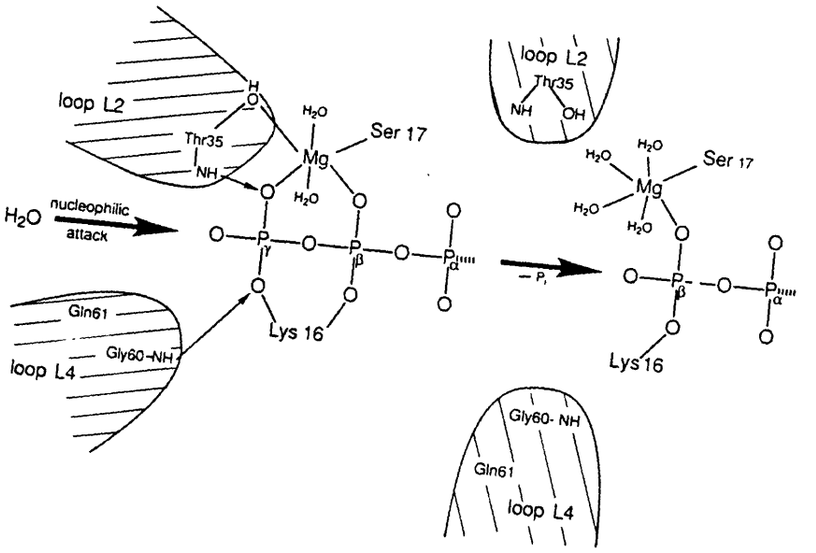
loop L2
Thr35
Ser 17
nucleophilic attack
Gln61
Gly60-NH
loop L4
Lys 16
Gly60- NH

two different conformations. This ability to exist in different conformations may reflect the requirement for Ras to interact with different effector targets (Moodie *et al*, 1995). However, the switch II region of Ras is not thought to be involved in the binding of the Raf-1 Ras binding domain (Nassar *et al*, 1995). Sequence differences outside the actual core effector domain are responsible for modulating the interactions between the GTP-binding protein and the effector.

Figure 4a shows the conformational state of Ras which is proposed to be competent for GTP hydrolysis. Figure 4b indicates the changes in interactions between nucleotide and Ras occurring upon hydrolysis of GTP. The prescence of a nucleotide-associated conformational change in Ras involving residues 31-39 has been directly observed by X-ray crystallography (Pai *et al*, 1990; Tong *et al*, 1991) and by magnetic resonance spectroscopy (Halkides *et al*, 1994; Miller *et al*, 1993; 1992). The crystallographic data has suggested that the co-ordination of the Thr35 hydroxyl group by the magnesium ion is the driving force behind the conformational change.

Upon hydrolysis, residues 32-36 in the switch I region change orientation, with their side chains flipping out into the solvent. The hydrogen bonds between the main chain of Thr35, Tyr32 and the γ-phosphate are lost upon hydrolysis. At the same time the side chain hydroxyl of Thr35 is no longer coordinated to the magnesium ion and swings away from the protein, pointing out towards the solvent (Schlichting *et al*, 1990). This process also invokes changes in the positions of adjacent residues, in particular, Tyr32, Asp33, Pro34 and Ile36. Tyr32 interacts more strongly with the ring of Pro34 in the GDP-bound state (Schlichting *et al*, 1990). Residues 36 and 38 adopt different side chain orientations depending upon the nature of the nucleotide bound. In the GDP-bound complex, the hydrophobic side chain of Ile36 becomes exposed to the solvent, compensating for the loss of interaction energy which occurs when Thr35 is no longer in contact with the Mg^{2+} and the γ-phosphate. In the switch II region upon hydrolysis, hydrogen bonding of residues 60 and 61 with the γ-phosphate are proposed to be lost, inducing a structural change which alters the conformation of loop 4 and reorientates the α2-helix.

Solution structures of Ras obtained by molecular dynamics (Foley *et al*, 1992) and magnetic resonance spectroscopy (Halkides *et al*, 1994; Miller *et al*, 1993; Bellew *et al*, 1996; Halkides *et al*, 1996) have shown that the Thr35 forms a weaker hydrogen bond with the γ-phosphate in solution than in the X-ray structure. This is interpreted as showing that the Thr35-Mg^{2+} interaction is incidental to the conformational change, rather than its driving force. Fernando-Diaz (1995) has suggested that the co-ordination of the γ-phosphate by Thr35 is the actual driving force for the conformational transition accompanying GTP hydrolysis. A number of mechanisms for GTP hydrolysis have been proposed and these will be discussed in section 1.1.4.

1.1.3 Mutations of Ras

Activating point mutations which give rise to Ras which is constitutively locked in the active GTP-bound form, can be mapped to regions within the catalytic domain to which important functions have been assigned, and fall into three main biochemical categories.

The first group of mutations are those which confer aggressive growth promoting properties onto Ras, and include those at codons 12, 13, 59, 61 and 63, (Fasano *et al*, 1984; Manne *et al*, 1985; Colby *et al*, 1986) all of which lie near the sites of interaction of the Ras protein with the β- and γ-phosphates of the bound GTP. These transforming mutations result in proteins which have a reduced intrinsic GTPase activity and an altered guanine nucleotide dissociation rate (Gibbs *et al*, 1985; Barbacid, 1987; Feig and Cooper, 1988a). Although still able to bind GAP, these proteins are unresponsive to acceleration by GAP or NF1 proteins. The net result of such mutations is that Ras remains in an 'active' GTP-bound conformation which will eventually lead to cellular transformation. Gln61, in particular, is thought to be directly involved in the catalytic process and mutations at this position lead to a loss of GAP stimulation *in vitro*, although binding to GAP is unaffected. For example, the strongly activating mutation Leu61 resulted in a protein which possessed a higher affinity for GAP than wild-type Ras (Krengel *et al*, 1990), a 5-fold increase in nucleotide exchange rate and a reduced GTPase activity.

The second class of mutations include those at codons 28, 116-119, 144 and 146, all of

which are at sites involved in the interaction of Ras with the purine base of GTP. These mutations lead to proteins with an overall lowered affinity for guanine nucleotides. (Der *et al*, 1986a; Feig *et al*, 1986; Feig and Cooper, 1988a; Reinstein *et al*, 1991), resulting from an increased rate of nucleotide dissociation. Since the release of GDP is rate-limiting for normal Ras and mammalian cells contain a much higher concentration of GTP than GDP, these mutations will ultimately result in accumulation of the active GTP-bound form of Ras. These mutations have eliminated the requirement for a guanine nucleotide dissociation stimulator (GDS) utilized by normal Ras to accelerate the otherwise slow dissociation of GDP from the protein.

The third set of mutations are those which affect the biological activity of Ras without altering nucleotide binding or the intrinsic GTPase activity. These so-called 'effector' mutations are found within three regions of the primary structure. The effector region (i.e. switch I) located between residues 32-40 and the switch II region incorporating residues 60-76, undergo significant changes in position upon GTP binding. In addition, both the effector domain and the α3 domain (residues 101-103) are involved in binding to the Ras effector(s). Mutations in the effector region have been shown to block activation of Ras by GAP (Adari *et al*, 1988). Most of the effector site mutations that block GAP activation of cellular Ras also lead to deleterious effects on the transforming activity of Ras. Substitutions at positions 35, 36 and 38 lead to Ras proteins which are unresponsive to GAP (Adari *et al*, 1988; Cales *et al*, 1988). Mutants such as Asp38Ala are impaired in binding to GAP and in their ability to be activated by GAP. Other effector mutants, such as Asp38Glu and Asp33Asn show almost wild-type affinity for GAP but are totally unresponsive to GAP activation (Krengel *et al*, 1990; Marshall and Hettich, 1993). These mutations are not always transforming since although Ras remains in its active GTP-bound form, interaction with its downstream effector may be prevented due to changes in the effector binding site. In addition, mutations in both the effector region (Pro34Ser) and the α3 region (Asp92Lys) renders Ras defective for interaction with GAPs (Morcos *et al*, 1996).

A residue which has an important role in Ras function is the cysteine at position 186 which

is required for post-translational modification and membrane localization (Willumsen *et al*, 1984). Single point mutations within the viral H-Ras protein (Cys186Ser, Val187Thr) gave rise to a Ser186 mutant which was not post-translationally modified and was defective for transformation and a Thr187 mutant which was transformation-competent and the protein was processed normally.

Several mutants warrant particular attention since they are dominant inhibitors that interfere with the role of endogenous wild-type Ras proteins within the cell. Substitutions at both Gln61 and Cys186 (Gibbs *et al*, 1989) give rise to a dominant inhibitor which is thought to inhibit Ras function by sequestering a downstream effector for Ras. In addition, a single mutation of serine at position 17 to Asn, Cys or Ala, (Feig and Cooper, 1988b; Cai *et al*, 1990; Stacey *et al*, 1991) gives rise to a dominant inhibitor whose role is to sequester an upstream effector for Ras. The dominant inhibitory effects are thought to be due to the improper co-ordination of the Mg^{2+} ion (Farnsworth and feig, 1991)

1.1.4 Mechanism of GTP Hydrolysis

1.1.4.1 Intrinsic GTP Hydrolysis

The chemical mechanism of intrinsic GTP hydrolysis in both elongation factor-Tu (EF-Tu) (Eccleston and Webb, 1982), and Ras (Feuerstein *et al*, 1989) has been shown biochemically to follow a direct in-line transfer of the terminal phosphate from GTP to water. This is achieved via a direct attack of the γ-phosphate by a water molecule, resulting in the inversion of configuration at the γ-phosphate. Structural analysis revealed two water molecules (Wat175 and Wat189) which are close enough to the γ-phosphate group to carry out an in-line nucleophilic attack. Of the two, Wat175 would appear to be the more likely candidate for this role since it is bound directly opposite to the β, γ-bond. Activation of Wat175, by the removal of a proton, might be mediated by interaction with functional groups within Ras which possess general base-like properties, i.e. have either an ability to abstract protons or an affinity for protons. Such interactions are thought to perform several functions, to increase the nucleophilicity of the attacking water molecule by abstraction of a proton, to increase the electrophilicity of the γ-phosphorous and the acidity of the leaving group, (thus lowering the activation energy of the reaction) and to

stabilize the transition state of the GTPase reaction.

Recent model studies (Maegley *et al*, 1996) have indicated that the transition state for GTP hydrolysis at the active site of Ras is dissociative rather than associative in character. A dissociative transition state is dominated by bond cleavage. The bond to the outgoing leaving group is fully or nearly broken whilst the bond to the incoming nucleophile is absent or barely formed. This results in a loss of charge on the phosphoryl group being transferred. Such a chemical perspective provides a good basis from which to discuss previously proposed mechanisms for catalysis.

Pai *et al* (1990) proposed a mechanism referred to as the general base 61 (GB61) mechanism, which identified a crucial role for Gln61 in the catalytic process by acting as a general base for the nucleophilic water molecule. Gln61, which is characterized by a large functional side chain, is present in most GTPases (except in EF-Tu, which has a His at the same site) including heterotrimeric G-proteins (Gln-204 in $G_{i\alpha 1}$; Glu-203 in $G_{t\alpha}$ and Gln-227 in $G_{s\alpha\text{-}L}$) (Graziano and Gilman, 1989). This residue forms part of the highly mobile switch II region (residues 61-65) in Ras, which is in close proximity to the putative nucleophilic water molecule. As such, it is able to adopt several conformations, one of which involves the carboxamide group of Gln61 linking the side chain of Glu63 and the nucleophile. It is thought that Glu63 may assist in either the orientation of Gln61 for correct activation of the nucleophile, or its proton removing ability.

Based on (i) the configuration of these residues within the active site, (ii) the mutations at Gln61 which decrease the intrinsic GTPase rate, and (iii) the mobility of loop4, with at least two conformations found for each of the residues 61-64, it was suggested that one of the conformations of the Gln61 side chain, would result in the polarization of the nucleophilic Wat175 by the formation of a hydrogen bond between either the amide nitrogen or the carbonyl atom of the side chain and the Wat175. Gln61 is assisted by the backbone of Thr35 in facilitating the nucleophilic attack on the γ-phosphate by activating Wat175. Since the half life of Ras.GTP has been determined to be 20 minutes at 37°C (John *et al*, 1988), it has been suggested that the full conformational change may be a

slow reaction involving more than a change in the orientation of one or two residues.

The general base mechanism has gained support from a number of other studies. Gln61 is highly conserved in most small GTPases, except in the Ras-related Rap protein family (Pizon *et al*, 1988; Kitayama *et al*, 1989) where a threonine rather than a glutamine is present at position 61. Rap proteins have a lower intrinsic GTPase rate than Ras which is not stimulated by RasGAP, however, mutation of Thr61 to glutamine increases the intrinsic GTPase to a rate similar to that observed for Ras (Frech *et al*, 1990) and renders the mutant protein partially sensitive to activation by RasGAP. In Ras, position 61 will not tolerate any other amino acid apart from glutamine, and such a substitution results in a mutant protein with a reduced GTPase activity that can no longer be activated by GAP (Der *et al*, 1986b; Vogel *et al*, 1988). Similarly, mutation of the corresponding residue in EF-Tu, His84, to glycine reduces the GTPase activity, suggesting that His84 performs a similar function in EF-Tu to that of Gln61 in Ras. Frech *et al* (1994) have also studied the involvement of the Gln61 side chain in the intrinsic hydrolysis event and the results were in agreement with Pai *et al* (1990). Substitution of Gln61 for Glu resulted in a 20-fold increase in GTP hydrolysis consistent with role of Gln61 as a general base. It has been proposed that the positioning of the negatively charged Glu near to the attacking water would stabilize the change in charge distribution that occurs in proceeding from the ground state to the transition state for GTP hydrolysis i.e. the migration of negative charge away from the attacking water and transferred phosphoryl group. The increase in hydrolysis would also result from better positioning of the attacking water molecule with respect to the γ-phosphoryl group or from an increase in the strength of the hydrogen bond to the attacking water molecule in the transition state. However, despite the good structural evidence, this mechanism is not yet conclusive.

Maegley *et al*, (1996) have argued against general base catalysis from a chemical perspective. In a dissociative transition state, there is little bond formation to the incoming water nucleophile and therefore little charge development. Therefore, there would be little advantage of removing a proton from the attacking water in the transition state. In addition, no significant proton transfer from the attacking water to Gln61 is expected in

a dissociative transition state.

Alternative models for the mechanism of hydrolysis based on more recent theoretical (Langen *et al*, 1992) and experimental (Prive *et al*, 1992; Chung *et al*, 1993) studies, have argued against the general base model, at least in terms of its applicability to the intrinsic hydrolysis reaction. Gln61 is a poor base and as such would be unable to activate a critically positioned water molecule. Mutation of Gln61 to residues with better water-activating groups, such as glutamate or histidine, did not increase the level of hydrolysis as would be expected, but gave the same low hydrolysis activity as the Leu61 mutant.

If Gln61 is not the general base in the intrinsic hydrolysis reaction, one would expect to find another residue in the vicinity of the water molecule which could perform a similar function. However, no other obvious residues in appropriate positions for the role of general base have been identified by either structural analysis or mutagenesis studies. This adds support to studies which have suggested that the mechanism of GTP hydrolysis may be 'substrate-assisted' in which the general base may be the GTP itself (Schweins *et al*, 1994; 1995) or other nearby water molecules. However, from a chemical perspective, protonation of the γ-phosphoryl group in the transition state is not the preferred path for a dissociative reaction and would in fact have an anticatalytic effect. Such a process would be expected to destabilise rather than stabilise a dissociative transition state since protonation stablizes the electron density on the phosphoryl oxygen. The dissociative transition state is achieved by the donation of electron density from the phosphoryl oxygen atoms.

Prive *et al* (1992) have proposed an alternative model for the Ras GTPase reaction, referred to as the 'transition-state stabilization' mechanism. In this model, functional groups of the side chain of Gln61 have a role in stabilizing the transition state, by forming a specific stabilization complex with the pentavalent phosphate intermediate of the hydrolysis reaction. Such roles have also been suggested for Lys16, the backbone amide of Gly60 and the bound Mg^{2+} ion of Ras. The β- and γ-phosphates are electrostatically stabilized in such a configuration due to ionic interactions with the Mg^{2+} and the amino

group of Lys16 and hydrogen bonding with the main chain amides of residues 13-17, 35 and 60. These interactions serve to fix the flexible phosphate groups in a specific conformation and reduce the charge density at the γ-phosphorous atom. The role of Ras is that of a catalyst whose function is to lower the activation energy required to reach the transition state.

However, Langen *et al* (1992) have reported that the distance between the amide group and the γ-phosphate is in the order of 6Å, so that a significant amount of energy would have to be expended in order to move the Gln61 residue towards the γ-phosphate, more than would be expended if a nearby water molecule were to stabilize the transition state whilst keeping Gln61 in its original position. From a chemical point of view, negative charge does not accumulate on the γ-phosphoryl group in a dissociative transition state, therefore these interactions are not predicted to provide electrostatic catalysis in a dissociative reaction. However, the increase in negative charge on the non-bridging β-phosphoryl oxygens in the transition state allows electrostatic interactions to be catalytic.

More recently it has been proposed that catalysis occurs by a stabilization of the GDP leaving group. The β-γ bridge oxygen undergoes the largest change in charge upon reaching the transition state. In the GTP ground state, it is attached to electron withdrawing phosphoryl groups and thus has a low electron density. However, in a dissociative transition state this bond is nearly broken. The backbone amide of Gly13 donates a hydrogen bond to the β-γ bridge oxygen of GTP that is strengthened in the transition state. Other interactions can also contribute to the modest catalysis of Ras. Interactions of the β non-bridging oxygens with Lys16 and Mg^{2+} may be strengthened in the transition state. Interactions that are not strengthened electrostatically in the transition state may also be catalytic. Hydrogen bonds between the nucleophilic water, Gln61 and Thr35 may help position the water with respect to the γ-phosphoryl group and lower the entropic barrier for the reaction.

Active sites are thought of as transition state templates that provide electrostatic and geometrical complementarity and allow exploitation of the changes between the ground

and transition states. Although the catalytic advantage from increased hydrogen bond strength can be large, the overall catalysis by Ras is only 10^3-fold. Therefore in order to achieve a low intrinsic reaction rate, Ras may not maximise the difference in ground versus transition state hydrogen bond strength. This could be achieved by using a hydrogen bond donor such as a backbone amide that is weak relative to positively charged side chains, by leaving possible stabilizing hydrogen bond interactions unfulfilled or by forming an active site with a relatively high effective dielectric. Other enzymes such as GAPs might then maximize the rate enhancement by more precise positioning of the backbone amide hydrogen bond and/or by positioning a second stronger hydrogen bond donor for interaction with the β-γ bridge oxygen or by altering the electrostatic environment of the active site.

However, despite evidence that the Ras-catalyzed GTPase reaction proceeds by a dissociative transition state with no significant transfer, a hydrogen bond acceptor such as a general base could still assist in the overall process of GTP hydrolysis in several ways. Firstly, the general base could participate in the loss of a proton from water which occurs after the rate limiting transition state. Secondly, even in a dissociative transition state there is a small amount of nucleophilic participation in GTP hydrolysis. Hydrogen bonds from the water protons to Gln61 and Thr35 can be strengthened to a small extent in the transition state. Thirdly, a general base could aid in the positioning of the nucleophilic water with respect to the γ-phosphoryl group.

This transition state stabilization model also lends support to and attempts to explain the transforming mutations at positions 12 and 61 which interfere with the GTPase activity. The transition state stabilization is unable to tolerate amino acids other than glutamine at position 61 or glycine at position 12. Mutation of Gln61 to asparagine produces a protein which is deficient in its GTPase activity. Since asparagine has a shorter side chain than glutamine, the residue may not be able to reach and interact with the transition state which precedes hydrolysis. In the transition-state model, the Gln61 is in close proximity to the α-carbon of residue 12. Replacement of Gly12 with any other amino acid (except proline) will affect the position of Gln61, interfere with the formation of the transition state and

lead to mutant proteins with a reduced intrinsic GTPase activity which will ultimately be transforming. For example, the reduction in the GTPase activity observed upon replacement of Gly12 with either valine or alanine was proposed to be due to the side chains of these residues directly blocking the approach of the Gln61 side chain in the transition state. In addition, replacement of alanine with the bulkier branched threonine side chain at position 59, causes a conformational shift in residues 59-61 resulting from the formation of a hydrogen bond between the threonine hydroxyl group and the main chain carbonyl oxygen of Pro34. This interaction causes residue 59 to be displaced from its position in the loop 2 region along with several other residues including the critical Gln61 residue, resulting in it no longer being in a position to stabilize the transition state.

1.1.4.2 GAP-activated hydrolysis

The intrinsic GTPase activity of Ras is accelerated 10^5-fold by the GTPase activating proteins, p120-GAP and neurofibromin. The exact mechanism by which GAP accelerates the intrinsic GTPase activity of Ras is not yet known, but several hypotheses exist. Such a stimulation might be achieved in several ways. GAP could either i) induce or accelerate a conformational change in the Ras catalytic site, thus enabling the amino acids to align in the correct manner and with the correct charge state for optimal catalysis, ii) stabilize the transition state by controlling the orientation of the Gln61 residue. In such a position, GAP could select the most favourable conformation of loop 4 for hydrolysis and fix the orientation of Gln61 in a position similar to that assumed by the analogous residue in transducin-$\alpha(G_t)$ and $G_{\alpha i1}$ in the transition state complex, iii) shield the solvent-exposed residues of loops 2 and 4 at the active site from the surrounding water, to lower the dielectric constant thus enhancing important electrostatic interactions within the active site, to protonate the leaving group or to change the pKa of the γ-phosphate with the consequent acceleration of the reaction rate or iv) provide additional amino acids which could stabilize charges developed in the transition state of the GTPase reaction.

If the mechanism of GAP-stimulated hydrolysis were to involve the donation of residues from GAP into the catalytic site of Ras, there are a number of conserved residues within the catalytic domain of GAP that might fulfill such a role. It has been suggested that one

of the highly conserved arginine residues within the catalytic domain of p120-GAP might play an important role in the stabilization of the transition state of the GTPase reaction. This theory has gained support from observations of the GTPase mechanism in large GTP-binding proteins. Heterotrimeric G-proteins contain a conserved arginine residue (Arg178 in $G_{i\alpha 1}$, Arg174 in $G_{t\alpha}$ and Arg201 in $G_{s\alpha\text{-}L}$) in their active site which is able to contact the developing charge of the transition state. Arg174 is thought to be critical for the higher intrinsic GTP hydrolysis observed in G_α proteins (Noel *et al*, 1993; Coleman *et al*, 1994; Sondek *et al*, 1994) in comparison to Ras, since it acts as an inbuilt intrinsic GTPase activating protein (GAP) and guanine dissociation inhibitor (GDI) for G_α, similar to the extrinsic GAPs that are required for accelerating the GTPase activity in Ras. This GAP-GDI combination has therefore overridden the need for a GTPase activating protein in this system. Mutation of this arginine in G-proteins was found to decrease the rate of the hydrolysis reaction. Additional support has come from studies described by Landis *et al* (1989) of G-protein mutants, in which mutation of the conserved arginine has impaired the GTPase activity.

In the case of small GTP-binding proteins, therefore, the role of GAP may be to provide residues such as arginine to the active site to accelerate the GTPase rate, in a similar manner to the active site arginine of G-proteins. This topic is covered in more detail in chapter 4.

1.1.5 Kinetics of GTP hydrolysis

Ras has been isolated as a heterogeneous mixture of Ras.nucleotide complexes (Feuerstein *et al*, 1987) comprising mainly of (ribo)-GDP with traces of dGDP, (ribo)-GTP and dGTP. In the absence of nucleotide, the `apoprotein' has been shown to be thermally less stable than the complexes of Ras with nucleotide (Feuerstein *et al*, 1987), but has the advantage of enabling accurate binding constants to be measured. Binding of GDP and GTP to the nucleotide-free Ras protein has been shown to occur very rapidly, with association rate constants in the order of $1.5 \times 10^6\ M^{-1}.s^{-1}$ and $3 \times 10^6\ M^{-1}.s^{-1}$ (Feuerstein *et al*, 1987; Neal *et al*, 1988). In contrast, the dissociation constants which were measured in the presence of excess Mg^{2+}, were very low, $10^{-4}\ s^{-1}$ for Ras.GTP and $10^{-5}\ s^{-1}$ for

Ras.GDP (Feuerstein *et al*, 1987; Neal *et al*, 1988). The binding constants for the magnesium-nucleotide complexes are in the order of 10^{10}-10^{11} M^{-1} (Feuerstein *et al*, 1987; Neal *et al*, 1988; John *et al*, 1990).

Amino acid sequences and crystallographic studies have indicated that the nucleotide binding sites of Ras and EF-Tu from *E.coli* (Jurnak, 1985) are very similar and possibly share a common chemical mechanism for hydrolysis (Eccleston and Webb, 1982). However, whereas the association rate constants for the binding of GTP and GDP to Ras are very similar, the association rate constants of GTP and GDP to EF-Tu at 0°C are 1 x 10^4 M^{-1}. s^{-1} and 2.6 x 10^5 M^{-1}. s^{-1}, respectively (Fasano *et al*, 1978). These differences in association rate constants for binding of GTP and GDP to EF-Tu were confirmed by Eccleston *et al* (1981) and interpreted as showing a two-step binding mechanism comprising a binding step followed by a conformational change. John *et al* (1990) proposed that the binding of guanine nucleotides to Ras also involved a two-step mechanism, in which an initial rapid binding step is followed by a second slow isomerization step.

Since H-Ras has no tryptophan residues, the change in the relatively weak intrinsic fluorescence induced by nucleotide binding, nucleotide exchange or the GTPase reaction, is small. The fluorescence signal has been improved by substituting an amino acid residue that may be affected by events at the active site, for a single tryptophan residue (Skelly *et al*, 1990; Antonny *et al*, 1991; Yamasaki *et al*, 1994). Another approach has been to use nucleotides with a fluorescence label such as GTP or GDP-[NH]P labelled at the 2' and 3' positions of the ribose moiety with the fluorescent methylanthraniloyl (mant) group. Mant-labelled nucleotides have been employed to study association kinetics (John *et al*, 1989, 1990) GTPase kinetics (Neal *et al*, 1990; Rensland *et al*, 1991; Moore *et al*, 1993) and the mechanism of GAP interaction with Ras (Rensland *et al*, 1991; Moore *et al*, 1993). MantGTP and mantGDP have similar properties to their parent nucleotides in terms of the kinetics of their interaction with N-Ras. The rate constants determined for reactions involving mant-nucleotides were found to be within a factor of two of those obtained with the parent nucleotides. In addition, the presence of the mant moiety on the

ribose group of guanine nucleotides does not affect the binding affinity of the nucleotides for N-Ras since the 2', 3'-hydroxyl groups of the nucleotide point away from the protein, towards the solvent. The mant-nucleotides were demonstrated to be environmentally sensitive and show a large enhancement of fluorescence upon binding to N-Ras, 3.2-fold for mantGTP and 2.8-fold for mantGDP (Neal *et al*, 1990).

Neal *et al* (1990) have described a minimal GTP hydrolysis mechanism for N-Ras using mantGTP to probe for conformational changes which can be distinguished on the basis of their kinetics. An underlying feature of this mechanism is the proposed rate-limiting isomerization step which precedes and limits the rate of the cleavage step. Neal and colleagues noted that a solution of N-Ras.mantGTP incubated at 30°C exhibited an 8-10% exponential decrease in fluorescence which occurred with a first order rate constant similar to that for the cleavage of mantGTP by Ras. This initially suggested that the change in fluorescence represented the cleavage step in the intrinsic GTPase. However, incubation of Ras complexed with a non-hydrolyzable GTP analogue mantGDP-[NH]P, also produced a decrease in fluorescence which was biphasic and smaller in amplitude to that observed with mantGTP. If the fluorescence change represents an isomerization step, then the fluorescence change would be expected to be similar regardless of the nature of the nucleotide bound to Ras. The rate constant of the second fluorescence change was similar to that of mantGTP. This suggested that the fluorophore was monitoring a structural change occurring during the conversion of Ras.mantGTP to Ras.mantGDP. Neal *et al* (1990) interpreted this decrease in fluorescence as representing either a i) conformational change in the Ras.mantGTP complex which occurs during the cleavage step and changes the local environment of the fluorophore, or ii) a conformation change which occurs during the release of phosphate from the N-Ras.mantGDP.Pi complex, or iii) a conformation change of the N-Ras.mantGTP complex which precedes and limits the rate of the cleavage step. Such conformational changes have been recognized for the nucleoside triphosphatase transducing system of myosin (Bagshaw *et al*, 1974). In the case of Ras, the large free energy change associated with the conversion of Ras.GTP to Ras.GDP.Pi and Ras.GDP could well involve a protein conformation change. Since mantpGDP-[NH]P is not hydrolyzed by Ras under the conditions of the experiment, it was

suggested that the basic mechanism of the Ras GTPase cycle involves a slow rate-limiting isomerization step which precedes and limits the rate of the cleavage step (Neal *et al*, 1988, 1990; Eccleston *et al*, 1991). This mechanism is shown in the scheme below. The steps contributing most to the overall catalytic rate of GTP hydrolysis were the cleavage step (k_2) and the GDP dissociation step (k_4), the other forward steps being fast and the reverse rate constants being slow.

$$\underset{}{R + GTP} \underset{1}{\rightleftharpoons} \underset{}{R.GTP} \underset{2a}{\rightleftharpoons} \underset{}{R.GTP^*} \underset{2b}{\rightleftharpoons} \underset{}{R.GDP.Pi} \underset{3}{\rightleftharpoons} \underset{}{R.GDP} \underset{4}{\rightleftharpoons} \underset{}{R + GDP}$$

Moore *et al* (1992, 1993) also studied the kinetic mechanism of GTP hydrolysis using Ras complexed to either mantGTP or mantGDP-[NH]P and reached the same conclusion as Neal *et al* (1988; 1990). In the absence of GAP, a biphasic decrease in fluorescence was observed with Ras.mantGTP. The second phase occurred with the same rate constant as the cleavage step and was accelerated by GAP. A biphasic decrease in fluorescence was also observed with the Ras.mantGDP-[NH]P complex depite the absence of cleavage by Ras. The rate constant of the second phase of the fluorescence change was accelerated by GAP. The first process had not previously been observed by Neal *et al* (1990) due to the timescale of their experiments. The second phase was equivalent to that described by Neal *et al* (1990) and was suggested to represent a conformational change of the complex, which precedes and controls the rate of the cleavage step. It was suggested that this slow fluorescence change might represent the formation of an active conformation in which Gln61 can activate a water molecule, a process which is accelerated by GAP.

Thus, GAP was able to accelerate the second process associated with both Ras.mantGTP and Ras.mantGDP-[NH]P complexes, in a linear manner, dependent upon the concentration of GAP (Moore *et al*, 1993). In the presence of GAP or NF1, a rapid increase in fluorescence was observed, proposed to represent initial complex formation between Ras.mantGTP and GAP, followed by a second slow decrease in fluorescence proposed to represent the isomerization process. This is consistent with the conclusions of Neal *et al* (1990) that GAP accelerates the rate of the isomerization step which

precedes and limits the cleavage step. This finding does not eliminate the possibility that GAP also contributes catalytic groups that enhance the chemical cleavage rate. Increasing the salt concentration was found to decrease the affinity of GAP for Ras.mantGTP and increase the rate of the conformational change, k_2, (Eccleston *et al*, 1993). Eccleston *et al* (1993) reported an inhibition of p120-GAP and neurofibromin by NaCl. Inhibition of p120-GAP and neurofibromin by salts has previously been observed by several groups (Gibbs *et al*, 1988; Antonny *et al*, 1991; Weismuller and Wittinghofer, 1992) and has been proposed to be a general effect of ionic strength rather than a specific ion (Antonny *et al*, 1991). Ammonium sulphate was found to be about 3-fold more potent than NaCl (Eccleston *et al*, 1993).

Studies by Antonny *et al* (1991) also led to a similar conclusion using the fluorescence of a single tryptophan, engineered into Ras either at positions 56 or 64, as a conformational probe for time-resolved biochemical studies of Ras.GTP and Ras.GTPγS. Both mutants demonstrated a slow fluorescence change, demonstrating a 5% decrease in tryptophan fluorescence, which occurred with rate constants similar to those of the intrinsic Ras GTPase, following the binding of GTPγS. This suggested that, in the absence of GAP, a slow conformational change precedes and limits the cleavage step, since GTPγS would be expected to be cleaved more slowly than GTP. However, p120-GAP did not accelerate this fluorescence change suggesting that this step is not involved in the GAP-accelerated mechanism.

A biphasic decrease in fluorescence was also observed by Rensland *et al* (1991) with H-Ras.mantGTP. However, Rensland *et al* (1991) have argued against the presence of a rate limiting step before GTP cleavage, at least in H-Ras. Using mant-nucleotides, Rensland and colleagues observed that the interaction of the non-hydrolyzable analogue mantGDP-[NH]P with Ras, induced a 5% fluorescence decrease which was faster than that observed for mantGTP and occurred with a smaller amplitude. Moore *et al* (1993) have suggested that the rate constant for this process probably corresponds to the fast phase observed in their experiments, since Rensland *et al* (1991) only measured the fluorescence changes occurring over 17min and would not have observed the slower phase described by Moore

et al (1993). In support of this, the fluorescence change observed by Rensland *et al* (1991) was not accelerated by GAP, consistent with the results of Moore *et al* (1993). In contrast, the very slow decrease in fluorescence associated with mantGTPγS was accelerated by GAP (Rensland *et al*, 1991). Hydrolysis of mantGTPγS was not measured in these experiments. This suggested that the fluorescence change does not represent a rate-limiting step preceding hydrolysis but rather occurs either at the hydrolysis step or upon the release of inorganic phosphate. This discrepancy could be due to differences between H-Ras and N-Ras, buffer conditions, differences in the ratio of 2' to 3' mant isomers in the Ras complexes or differences in the timescales over which the experiments were performed. Mant-nucleotides exist as an equilibrium mixture of the 2' and 3' isomers (Cremo *et al*, 1990). Eccleston *et al* (1991) showed that > 97% of the nucleotide bound to Ras in all the complexes studied was the 3' isomer. Rensland *et al* (1991) and Moore *et al* (1993) showed that the slow change in fluorescence proposed to represent the hydrolysis of Ras.mantGTP cannot be accounted for by an isomerization of the nucleotide analogue, since the ratio of the 2' and 3' isomers of mantGTP is not altered upon hydrolysis. Moore *et al* (1993) were able to exclude nucleotide dissociation as an alternative explanation for the fluorescence change. The conformational change associated with the isomerization step must be a reversible process to enable Ras.mantGTP to be regenerated at a later point in the GTPase cycle. Such a conformational change may be related to the different conformations of residues 58-65 in the Ras crystal structure.

Both interpretations of the nature of the slow fluorescence change are consistent with two classes of hydrolysis mechanism. One suggests that the basic mechanism of catalysis is the same for the intrinsic GTPase and the GAP-activated GTPase. The role of GAP in such a mechanism would therefore be to stabilize a particular conformation of residues at the active site on Ras, such that the catalytic reaction is favoured. Alternatively, the mechanism of GAP-activated catalysis may be different from the intrinsic Ras GTPase. GAP may provide additional amino acids to the active site on Ras, to accelerate the catalytic reaction. The mechanism suggested by Neal *et al* (1990) would be consistent with the first model since only the rate-controlling conformational change must be accelerated by GAP. The results of Rensland *et al* (1991) would be consistent with either

model since it is the hydrolysis reaction itself which is accelerated by GAP.

1.2 Regulators of ras GTPase cycle

1.2.1 GTPase activating proteins (GAPs)

Two distinct types of mammalian RasGAPs have been described, p120-GAP and neurofibromin (NF1), both of which accelerate the conversion of Ras.GTP to Ras.GDP, (reviewed by McCormick *et al*, 1991; McCormick, 1992; Polakis and McCormick, 1992; McCormick, 1995). In recent years, several more mammalian GAPs have been isolated. These include p100GAP1m (the mammalian homologue of *Drosophila* Gap1) (Maekawa *et al*, 1993; 1994), DGAP1 (RasGAP homologue in *Drosophila*) (Faix and Dittrich, 1996), IQGAP1 (Weissbach *et al*, 1994) a human protein related to a RasGAP homologue (Sar1/Gap1) from the fission yeast *S.pombe* and IQGAP2, a human protein that is 62% identical to IQGAP1 (Brill *et al*, 1996). These IQGAPs interact with the Rho-family GTPases (Cdc42H and Rac1). This finding and the presence of a potential actin-binding domain has led to the suggestion that IQGAPs might play roles in the Cdc42 and Rac1-controlled generation of specific polymerized actin structures. In addition, another human gene, related to *Drosophila* Gap1 has been identified which appears to be distinct from p100GAP. There are perhaps many more RasGAPs which are still undiscovered.

1.2.1.1 p120-GAP

The first GAP to be characterized was p120-GAP, a cytosolic protein with an Mr of 120,000, found in all mammalian cells, that catalytically accelerates GTP hydrolysis of normal mammalian Ras proteins but not that of mutant Ras proteins with oncogenic potential (Trahey and McCormick, 1987; Gibbs *et al*, 1988). Two yeast (*S. cerevisiae*) proteins with both functional and sequence homologueies to RasGAP have also been identified, (IRA1 and IRA2). Figure 5 shows the locations of the catalytic and structural domains of p120-GAP. p120-GAP consists of an N-terminal region which contains two SH2 regions, one SH3 region and a pleckstrin homologuey (PH) region (Koch *et al*, 1991; Mayer *et al*, 1993; Musacchio *et al*, 1993), and a C-terminal GTPase-activating catalytic domain of approximately 340 amino acids which interacts with Ras (Vogel *et al*, 1988; Trahey *et al*, 1988; Marshall *et al*, 1989; Gideon *et al*, 1992). This domain is sufficient to

interact with Ras but its catalytic properties differ from those of full length p120-GAP (Gideon *et al*, 1992; Martin *et al*, 1990).

The N-terminal region has been suggested to have a regulatory role on the catalytic domain (Gideon *et al*, 1992). By virtue of its SH2 and SH3 domains, p120-GAP can also bind phosphoproteins such as activated epidermal growth factor and platelet derived growth factor receptors (Kaplan *et al*, 1990) and also to the tyrosine phosphorylated proteins, p62 and p190 (Settleman *et al*, 1992a). Since p190 possesses GAP activity towards small guanine nucleotide binding proteins in the Rho/Rac family and GAP can direct interactions with cellular phosphoproteins *in vivo*, GAP may function as an effector molecule which modulates the cytoskeleton and cell adhesion (McGlade *et al*, 1993). A differential expression event results in type II GAP, a protein of molecular weight 100,400 (Trahey *et al*, 1988), which lacks the hydrophobic amino terminus of p120-GAP. Type II GAP is highly expressed in the placenta and in several human cell lines, but not in adult tissues (Trahey *et al*, 1988). Al-Alawi *et al* (1993) suggested that types I and II GAP might differ in their downregulation of Ras.

1.2.1.2 Neurofibromin (NF1)

Neurofibromatosis type I (NF1), or Von Recklinghausen neurofibromatosis, is one of the most common genetic diseases that predisposes humans to cancer, affecting 1 in 3500 individuals worldwide (Seizinger, 1993). Patients with neurofibromatosis I (NF1) display characteristic multiple dermal neurofibromas, benign tumours that typically appear in early adolescence and increase in numbers throughout life. The pathogenesis of these tumours is not known.The gene responsible for the disease was recently identified on chromosome 17 and cloned by reverse genetics (Viskochil *et al*, 1990; Cawthon *et al*, 1990; Wallace *et al*, 1990; Marchuk *et al*, 1991).

Figure 5(a): The catalytic and structural domains of p120-GAP

The locations of the catalytic and structural domains are shown. SH2 and SH3 domains refer to src homology domains 2 and 3, thought to be involved in phosphotyrosine binding. Possible phosphorylation sites for tyrosine kinase and protein kinase A are shown.

[Taken from Grand and Owen (1991)]

Figure 5(b): Structural comparison of RasGAPs and RasGAP-related proteins

GAP-related catalytic domains are shown in black. The additional regions of homology between IRA and NF1 proteins are shaded. The location of SH2, SH3, Pleckstrin-homology (PH) and CalB (LB) domains in p120-GAP and Gap1 homologues is indicated. The C-terminal half of IQGAP1 and IQGAP2 shows homology to the entire *S.pombe* Sar1 protein. A region containing four tandem Iqmotifs and an upstream region harbouring a unique kind of repeat are indicated by different shading.

[Taken from Bernards (1995)]

(a)

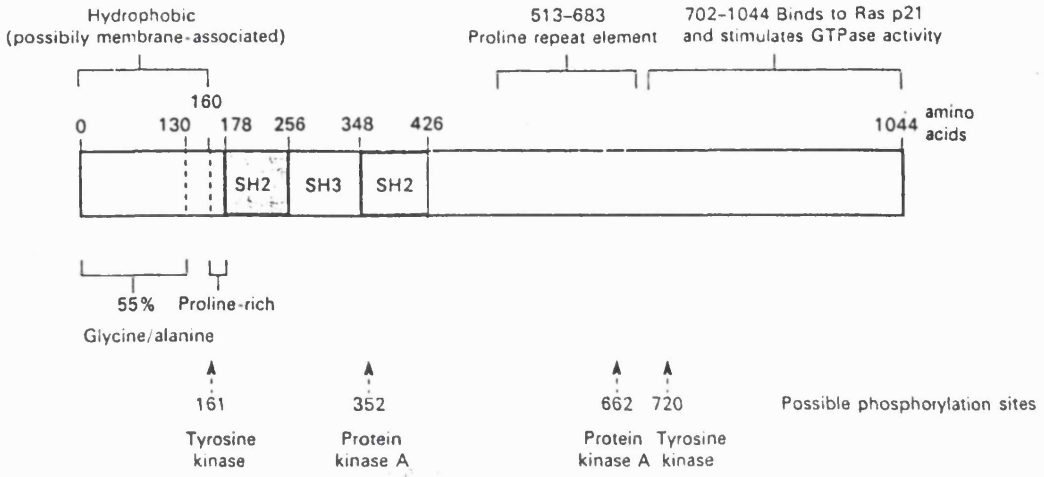
Hydrophobic
(possibily membrane-associated)
513–683
Proline repeat element
702–1044 Binds to Ras p21
and stimulates GTPase activity
160
0
130
178
256
348
426
1044
amino
acids
SH2
SH3
SH2
55%
Proline-rich
Glycine/alanine
161
Tyrosine
kinase
352
Protein
kinase A
662
Protein
kinase A
720
Tyrosine
kinase
Possible phosphorylation sites

(b)

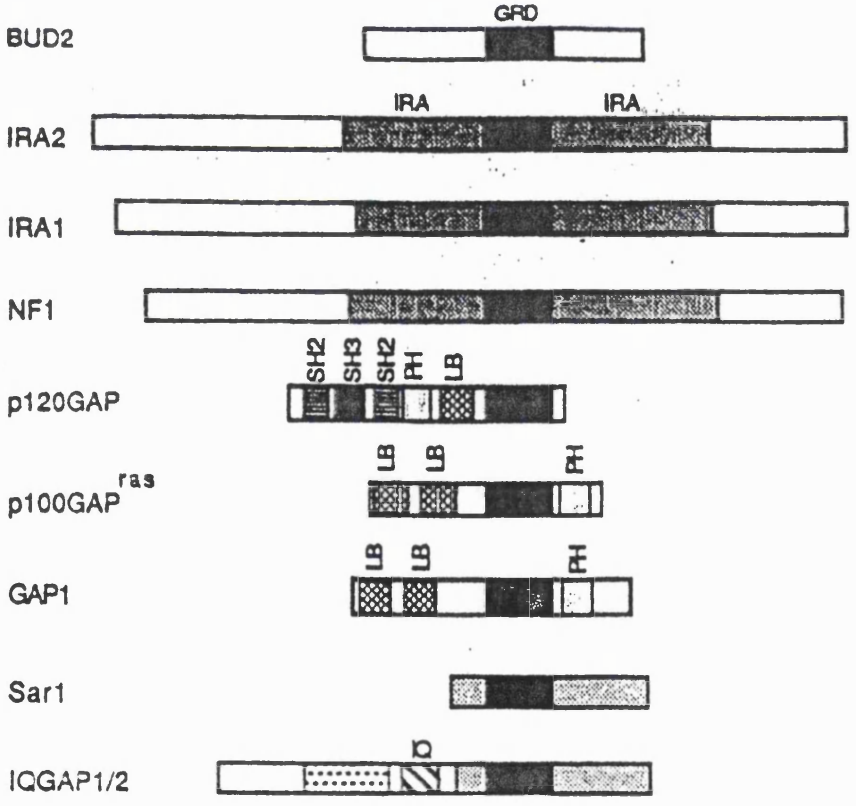
BUD2
GRD
IRA2
IRA
IRA
IRA1
NF1
p120GAP
SH2
SH3
SH2
PH
LB
p100GAP
ras
LB
LB
PH
GAP1
LB
LB
PH
Sar1
IQGAP1/2
D

It was found to encode a 2818 amino acid, 250-320 kDa protein (Declue *et al*, 1991; Gutmann *et al*, 1991; Hattori *et al*, 1991, 1992) with a central 360 residue domain which shared 30% amino acid homology with the Ras GTPase activating catalytic domains of p120-GAP, (Boguski and McCormick, 1993; Xu *et al*, 1990b; Martin *et al*, 1990) and IRA1 and IRA2, (Ballester *et al*, 1990; DeClue *et al*, 1991; Xu *et al*, 1990a; Martin *et al*, 1990). The regions of homology within the GAP proteins is shown in figure 5b.The common domain shared by NF1, p120-GAP and IRA possesses a GAP-like activity with specificity for Ras proteins. The suggestion that neurofibromin might be a second mammalian Ras GTPase activator protein was attractive since it implied that some tumour suppressors might be negative regulators of dominant oncogenes. The argument for the role of neurofibromin as a Ras-GAP was based on three observations. Firstly, NF1-GRD stimulated the GTPase of wild-type N-Ras but was inactive towards oncogenic (Asp12 and Val12) Ras mutants (Xu *et al*, 1990a; Buchberg *et al*, 1990). Secondly, the NF1-GRD rescued the heat shock sensitive phenotype of yeast *ira*$^-$ strains (Martin *et al*, 1990; Xu *et al*, 1990a; Ballester *et al*, 1990). Thirdly, neurofibromin deficient malignant neurofibrosarcoma lines contain 30-50% of Ras in the GTP-bound form, in contrast to the 10% in normal cells. This is consistent with a role for neurofibromin as a Ras GTPase activator. Neurofibromin is ubiquitously expressed during development (Daston and Ratner, 1993) and becomes a predominantly neuronal GTPase activating protein in the adult. Neurofibromin undergoes an alternative splicing event to produce the two splicing variants, types I and II NF1 (Anderson *et al*, 1993a; Suzuki *et al*, 1991; Nishi *et al*, 1991; Teinturier *et al*, 1992; Uchida *et al*, 1992). Type I NF1 appears to be more highly expressed in proliferative cells, whilst type II NF1 which contains a 63bp (21 amino acid) insert within the catalytic domain of the type I protein, is more prominantly expressed in differentiated cells.

p120-GAP and neurofibromin exhibit different biochemical properties. Both have different affinities for Ras, different catalytic efficiencies and different sensitivities to regulatory lipids. Both p120-GAP and neurofibromin interact with the same range of Ras proteins (H-Ras, K-Ras, N-Ras and R-Ras). They also bind to Rap proteins but fail to stimulate their GTPase activity. NF1-GRD has been demonstrated to bind to N-Ras with a 20-fold

higher affinity than p120-GAP (Martin *et al*, 1990). The full length neurofibromin and its truncated catalytic fragment (NF1-GRD) possess similar kinetic properties (Bollag *et al*, 1993). Whilst p120-GAP can interact with other cellular proteins, neurofibromin contains no motifs implicated in protein interactions and shares no similarity with other mammalian signalling proteins outside of its GRD.

However, catalytic activity is unlikely to be the only function of neurofibromin, since the protein is quite large with the catalytic domain forming only about 10% of the coding region in the central part of the molecule. Neurofibromin appears to co-localize with microtubules in all cell types examined, suggesting that neurofibromin is closely associated with cytoskeletal elements and might act as a GAP to direct cytoarchitectural changes in the cell in response to growth factors. There is evidence to suggest that NF1 is a tumour suppressor that is involved in the Ras signal transduction pathway. Tumour suppressor genes are thought to function as negative growth regulators such that their absence in tumour cells results in decreased downregulation of cell proliferation and a predisposition towards malignant transformation. Thus, if the NF1 tumour suppressor gene functions as a negative regulator in certain cells, one would predict a correlation between loss of NF1 expression and malignant transformation of these cells. Loss of NF1 expression has been observed in several sporadic tumours in individuals without NF1, such as neuroblastomas, malignant melanomas and pheochromocytomas (Anderson *et al*, 1993b; Johnson *et al*, 1993; The *et al,* 1993; Bollag *et al*, 1996). Inactivation of both NF1 alleles would be required for a tumour to develop from the resulting impaired regulation of Ras.GTP. Inactivation of both alleles has been demonstrated in specific benign (Sawada *et al*, 1996) and malignant tumours from patients with Von Recklinghausen neurofibromatosis (Declue *et al*, 1992; Legius *et al*, 1993; Anderson *et al*, 1993b). Several groups have demonstrated that NF1 is nearly absent in 3 neurofibrosarcomas from NF1 patients (Basu *et al*, 1992; Declue *et al*, 1992). Declue *et al* (1992) discovered increased levels of GTP-bound Ras which did not appear to be mutationally activated and low levels of NF1 in cell lines derived from malignant human schwannomas in NF1 patients. This increase in Ras.GTP was thought to be due to the diminished negative regulation by NF1. In support of such an inactivation mechanism, several groups have identified mutations within the

gene, such as translocations (Viskochil *et al*, 1990; Wallace *et al*, 1990; Reynolds *et al*, 1992), deletions (Upadhyaya *et al*, 1990; Viskochil *et al*, 1990; Menon *et al*, 1990), point mutations (Li *et al*, 1992) and insertions (Wallace *et al*, 1991). Gutmann and Collins (1993) suggested that phosphorylation of serine and threonine residues in neurofibromin might be responsible for inactivating neurofibromin as part of a signal transduction pathway leading to Ras activation and cell proliferation. Alternatively, neurofibromin may normally be constitutively active in whole cells and inhibition of its GAP activity may be acheived by interaction with tubulin (Bollag *et al*, 1993) or phospholipids (Bollag and McCormick, 1991). In tumours where NF1 mutations do not inactivate the NF1 gene such as astrocytic tumours, increased expression of neurofibromin has been observed (Gutmann *et al*, 1996). Such an upregulation of NF1 is postulated to involve positive feedback by activated Ras which is constitutively elevated in human astrocytomas and as such may represent a futile attempt of astrocytoma cells to downregulate Ras and reduce uncontrolled proliferation.

Two models have been proposed for the cellular role of GAPs. In the first model, the role of GAPs would be to downregulate Ras by inducing GTP hydrolysis (Zhang *et al*, 1990). In the second model, GAP would be the effector for Ras or part of an effector complex involved in transmitting the signal from activated Ras (Cales *et al*, 1988). Both p120-GAP and NF1 bind to the effector binding domain (residues 32-40) and the switch II region of Ras, (Adari *et al.*1988) and as such are candidates for the role of the elusive Ras effector in pathways downstream of Ras (McCormick, 1990; McCormick, 1995; Bernards, 1995). A third region of Ras located within the α3 helix (residues 101-103) has been recently identified as being required for efficient p120-GAP and neurofibromin-mediated hydrolysis (Yoder-Hill *et al*, 1995; Wood *et al*, 1994). p120-GAP is predominantly cytoplasmic and is translocated to the plasma membrane where it is thought to interact with Ras at the effector site (residues 30-40). The association of GAP with normal Ras.GTP leads to a conformational change in the Ras protein, increasing its intrinsic GTPase activity. GAP is also able to interact with mutant 'activated' forms of Ras, although there is no conformational change and the intrinsic GTPase is not stimulated. Evidence for and against the role of GAPs as Ras effectors is discussed in section 1.3.

1.2.2 Guanine nucleotide exchange factors (GEFs)

Ras proteins are rendered active through an exchange process in which GDP is released from Ras and replaced with GTP (reviewed by Feig, 1994). This process is extremely slow but can be accelerated by interaction with guanine nucleotide exchange factors (GEFs). The Ras-related proteins, Rab and Rho appear to be additionally regulated by guanine nucleotide dissociation inhibitors (GDIs) (Ueda *et al*, 1990; Sasaki *et al*, 1991). Many guanine nucleotide exchange factors have now been identified in both eukaryotic and mammalian systems (Martegani *et al*, 1992; Burton *et al*, 1993). The basic mechanism of interaction between Ras superfamily members and their GEFs appears to be conserved throughout the G-protein family. GEFs for Ras-related GTPases are thought to function by promoting the release of GDP, through stabilization of the nucleotide-free state of the protein (Mistou *et al*, 1992). The nucleotide-free protein is very transient and GTP rapidly re-binds to form the active protein. This results in the dissociation of the GEF which can activate further GTPase molecules. Certain exchange factors e.g. cdc25 (Mosteller *et al*, 1994) catalyze a more complex exchange mechanism involving a selective rather than a passive exchange of GTP for GDP. The first exchange factors to be identified were the products of the yeast CDC25 and *Drosophila Son-of-sevenless* genes (Broek *et al*, 1987; Robinson *et al*, 1987; Simon *et al*, 1991; Bonfini *et al*, 1992). Exchange factors such as RasGRF, Sos1 and Sos2 have subsequently been identified (Shou *et al*, 1992; Martegani *et al*, 1992; Cen *et al*, 1992; Bowtell *et al*, 1992; Wei *et al*, 1992). Later reports have suggested that the vav proto-oncogene product is a Ras exchange protein in haematopoietic cells (Gulbins *et al*, 1993) a finding which has been questioned more recently (Bustelo *et al*, 1994). It has previously been shown that the dbl oncogene product activates Rho subfamily GTP-binding proteins by catalyzing the dissociation of GDP from their nucleotide binding site. More recently the acidic phospholipid, phosphatidylinositol 4,5-biphosphate (PIP2) has been shown to provide an alternative mechanism for the activation of CDC42H, Rho and Arf (Zheng *et al*, 1996).

1.3 Downstream effectors for Ras

The last few years have seen a sudden surge in the number of proteins identified as candidates for Ras effectors (Marshall, 1996; McCormick and Wittinghofer, 1996;

Marshall, 1995; Wittinghofer and Herrmann, 1995). The proteins identified to date are shown in Table 1. Due to the similarity of the effector domains of Ras-related proteins, various approaches were taken to determine whether the Ras binding proteins identified were true effectors of Ras or whether they were effectors for other members of the Ras subfamily. These approaches were based on demonstrating the ability of Ras binding proteins to meet key criteria used in identifying Ras effectors.

Table 1: Potential effectors of Ras and of Ras subfamily members

Potential Effector	Protein Function
PI(3) Kinase P110 subunit α,β, γ	Lipid Kinase
Ral-GDS RGL/RGL2 RLF	GEF for Ral
Scd-1 (*S. pombe*)	Putative guanine nucleotide exchange factor for CDC42sp. Control of actin cytoskeleton.
Adenylyl cyclase (*S. cerevisiae*)	cAMP production
Rln AF6 canoe Rsbs 1, 2 and 4	Unknown
PKC-ζ MEKK-1 Byr-2 (*S. pombe*) c-raf A-raf B-Raf	Protein kinase
Lin45 (*C. elegans*) Draf (*D.melnogaster*) Raf-1	MAPKKK in ERK-dependant signalling from receptor tyrosine kinases.
$p120^{GAP}$ Neurofibromin	GAP for p21Ras

The first criterion, and the one by which most candidate Ras effectors were initially identified, is that Ras effectors preferentially bind to Ras.GTP. A Ras binding protein is unlikely to be an effector if it lacks this ability to differentially bind nucleotides. In addition, effector-Ras interactions might be expected to be high affinity, except in some signalling processes in which the effector may be required to rapidly dissociate from GTP-bound Ras and thus demonstrates a low apparent affinity. This approach is not definitive since such *in vitro* affinity measurements cannot easily be extrapolated to the situation *in vivo* in which Ras is localized to the plasma membrane and a number of other cellular components come into play, any number of which might affect effector-Ras interactions. In particular, the interaction between Ras.GTP and candidate effectors has been reported to be influenced by salt concentration. A second criterion which distinguishes a Ras effector from an effector involved in an alternative signalling pathway, is the appearance of a complex between Ras and the candidate effector upon activation of Ras to the GTP-bound state following a stimulus. The absence of such a complex following coimmunoprecipitation or colocalization in the cell signifies the unliklihood of the effector being involved in Ras signalling.

The third, and strongest criterion for a Ras effector is the ability of Ras to activate the candidate effector in a GTP-dependent manner, *in vitro*. Another useful approach for identifying Ras effectors is to express mutant effectors that are either constitutively activated or which act as interfering negatives to block Ras-dependent signalling. But by far the best approach to date to identify potential Ras effectors was devised by Wigler and colleagues and involves a yeast two hybrid system.

Initial studies identified two proteins, p120-GAP and neurofibromin, which fulfilled the primary criterion for a Ras effector in that they bound to Ras in a GTP-dependent manner (Trahey *et al*, 1988; Martin *et al*, 1990). There is much debate as to whether GAPs can function as effectors in some systems.

Evidence that GAP is a biological target for mammalian Ras has come from the following observations: Firstly, p120-GAP binds Ras via its effector domain (Adari *et al*, 1988).The

primary Ras binding site of GAP has been localized to the carboxy terminal 343 amino acids and is referred to as the GAP catalytic domain (Marshall *et al*, 1989). This region can be expressed as a stable independent domain capable of binding Ras.GTP and activating its GTPase. The Ras binding domain of GAP is conserved in other RasGAPs. It is currently unclear as to whether Ras binds a small region of GAP analogous to the Ras effector region or a larger area of the surface as is typical of most protein-protein interactions. The binding region for Ras on GAP has been proposed to map to within residues 715-753 (Molloy *et al*, 1995). Secondly, p120-GAP binds oncogenic Ras, but fails to stimulate its GTPase activity (Vogel *et al*, 1988). Thirdly, effector mutations that prevent signalling also blocked p120-GAP binding (Trahey *et al*, 1988; Cales *et al*, 1988). In addition, there is much evidence to suggest that the non-catalytic segment of p120-GAP, which contains several motifs that are widely shared amongst signalling proteins (see section 1.3), has 'effector-like' functions. For example, the amino terminus of p120-GAP which contains SH2 and SH3 domains can mimic some effects of Ras signalling (Martin *et al*, 1992; Medema *et al*, 1992). However, activation of Ras responsive genes by expression of the amino terminus of p120-GAP required endogenous Ras function. In addition, activation of *Xenopus laevis* p34 kinase (maturation promoting factor) by Ras has been suggested to be GAP-dependent (Dominguez *et al*, 1991) and antibodies against the SH3 domain of p120-GAP have been shown to block Ras-activated maturation in the Xenopus oocyte (Duschesne *et al*, 1993). The carboxy terminal GTPase-activating catalytic domain of p120-GAP was able to inhibit the oncogenic Ras-dependent transactivation of a polyoma enhancer sequence (Schweighoffer *et al*, 1992). Full length p120-GAP was able to restore function. Similarly, the non-catalytic segment of p120-GAP was responsible for the Ras-dependent inhibition of the coupling of muscarinic acetylcholine receptors to heterotrimeric G-proteins that regulate potassium channels in atrial membranes (Yatani *et al*, 1990; Martin *et al*, 1992), and blocked fibroblast transformation by muscarinic receptors (Xu *et al*, 1994). The most conclusive evidence for a signalling role for GAP was obtained from a series of experiments that showed involvement of the amino terminus of GAP in the regulation of cytoskeletal structure and cell adhesion to the extracellular matrix (McGlade *et al*, 1993). It is an attractive idea that some of these findings relate to the ability of this N-terminal segment to bind to two

phosphotyrosine proteins, p62 and p190 (Ellis *et al*, 1990; Settleman *et al*, 1992b). Because p190 is a GAP for Rho GTPases, it was proposed that its association with p120-GAP may serve to integrate Ras and Rho-mediated signalling. Signals relayed from p120-GAP to p190 may be responsible for cytoskeletal changes in growth factor stimulated cells (Nobes and Hall, 1994).

However, subsequent experiments suggested that p120-GAP was not an effector for Ras. This argument was based on observations that p120-GAP could suppress NIH3T3 cell transformation by over-expressed wild-type Ras (Zhang *et al*, 1990). In addition, experiments using effector mutants capable of differentiating between GAP and Raf-1 binding argued against p120-GAP as an effector (Stone *et al*, 1993). In *S. pombe*, disruption of the Sar1/Gap1 gene leads to sporulation defects characteristic of those of an activated Ras1 mutant, suggesting that Sar1/Gap1 acts as a negative regulator of Ras1 (Imai *et al*, 1991; Wang *et al*, 1991a). A *Drosophila* Gap1 loss of function mutation mimics activation of the sevenless protein tyrosine kinase (Gaul *et al*, 1992). In addition, in *S. cerevisiae*, ira mutants which resemble yeasts that harbour an activated Ras2 val19 protein, also suggested that IRA is primarily a negative regulator (Tanaka *et al*, 1990).

The role of neurofibromin as a downstream effector of Ras is an area which remains largely unexplored. Experimental evidence so far supports a purely negative regulatory role for neurofibromin and any functions tentatively ascribed to NF1 have remained speculative. Neurofibromin has been proposed to play a role in Ras-induced differentiation of neuronal cells (The *et al*, 1993). However, other studies have shown that *Drosophila* Gap1, not *Drosophila* NF1 is a downstream component in the signalling pathway that controls R7 photoreceptor cell differentiation (Gaul *et al*, 1992). Some of the pleiotropic symptoms of NF1 might be caused by disruptions of biological processes mediated by Ras relatives, such as R-Ras and Rap. This is supported by the fact that both NF1 and GAP stimulate the GTPase of R-Ras (Rey *et al*, 1994) and interact with but do not stimulate the GTPase of Rap. As such, neurofibromin has been proposed to play a role in R-Ras mediated apoptotic signalling pathways since R-Ras may associate with Bcl2 (Fernandez-Sarabla and Bisschoff, 1993). Finally, neurofibromin has been alleged to associate with

both microtubules (Gregory *et al*, 1993) and cell surface receptors (Boyer *et al*, 1994). These two functions could be incorporated into a model in which neurofibromin plays a role in the endocytic downregulation of receptors. Support for this purely speculative function of NF1 can be found in studies in which PDGF receptors, mutated in the phospatidyl inositol-3-kinase binding site, are defective in endocytosis (Joly *et al*, 1994). In addition, the microtubule associated GTPase dynamin, which plays a role in endocytosis, has been shown to interact with several SH3 domain containing signalling proteins, including Grb2 (Scaife *et al*, 1994; Miki *et al*, 1994; Seedorf *et al*, 1994).

The effector binding domain of GTP-bound Ras interacts not only with p120-GAP and neurofibromin, but also with the N-terminal regulatory domain of the cytosolic Raf family of serine/threonine kinases, c-Raf-1, A-raf and B-raf (McCormick, 1994; Marshall, 1995; Wittinghofer and Herrmann, 1995; McCormick and Wittinghofer, 1996). The best characterized Ras effector from mammalian cells in terms of biological relevance as well as structural detail is the c-Raf-1 serine/threonine kinase. c-Raf-1 was initially identified as transmitting a downstream signal from Ras in Ras-dependent signalling pathways in mammalian cells, *C.elegans* and *D.melanogaster* (Dickson and Hafen, 1994). The initial suggestion that Raf is downstream of Ras came from microinjection experiments in which the monoclonal anti-Ras antibody, Y13-259 was able to inhibit signaling via the PDGF receptor, the transforming activity of v-Src and v-Ras but not of v-Raf, but that an anti-Raf antibody could inhibit the transforming activity of v-Ras (Smith *et al*, 1986). In addition, antisense Raf RNA and dominant negative Raf mutants were demonstrated to inhibit Ras mediated signalling (Kolch *et al*, 1991). It was subsequently revealed that Raf was a direct target of Ras in yeast two hybrid experiments (Vojtek *et al*, 1993; Van Aelst *et al*, 1993; Zhang *et al*, 1993) *in vitro* (Moodie *et al*, 1993; Warne *et al*, 1993) and by coimmunoprecipitation in stimulated fibroblasts (Finney *et al*, 1993; Hallberg *et al*, 1994). These studies showed that the regulatory region of the c-Raf-1 protein kinase binds tightly to mammalian Ras in a GTP-dependent manner. A Ras binding site (RBS-1) of mammalian Raf-1 was mapped to an 81 amino acid segment (comprising residues 51-131) from the conserved region 1 (CR1) in its N-terminal regulatory domain (Vojtek *et al*, 1993; Chuang *et al*, 1994; Ghosh and Bell, 1994; Emerson *et al*, 1995; Herrmann *et al*,

1995; Pumiglia *et al*, 1995). This region forms an independent folding domain (Emerson *et al*, 1994; Chuang *et al*, 1994) known as the RBD (Ras Binding Domain) which is sufficient to bind to Ras in a GTP-dependent manner with reasonable affinity (Fridman *et al*, 1994; Marshall, 1995; Wittinghofer and Herrmann, 1995; Herrmann *et al*, 1995; Barnard *et al*, 1995; Gorman *et al*, 1996). The minimal Ras-binding domain has been suggested to consist of residues 77 to 101 (Niehof *et al*, 1995). The structure of the Raf-RBD and identification of the Ras interaction surface have recently been elucidated by NMR (Emerson *et al*, 1995). In addition, the structure of Raf-RBD in a complex with Rap-1A has been solved by X-ray crystallography (Nassar *et al*, 1995). Such structural analyses have proposed that the binding of the switch I region of Ras to the RBD is the major site of Ras GTP-dependent binding. However, other contacts are thought to contribute to binding and kinase activation (Yamamori *et al*, 1995; Okada *et al*, 1996). For example, mutations at residues 31, 57 and 59 of H-ras have been shown to inhibit binding to full length c-Raf-1 (Shirouzu *et al*, 1994). Mutations at residues 26, 29, 39, 40, 41, 44 and 45 have been suggested to be necessary for Ras-dependent Raf-activation (Shirouzu *et al*, 1994). In addition, post-translational modification of H-ras has been shown to be required for activation of B-Raf (Yamamori *et al*, 1995). As yet, attempts to co-crystallize full length c-Raf-1 with Ras or Ras-related proteins has been unsuccessful. Such a structure would shed light on the existence of contacts between Ras and c-Raf1 outside the RBD. The switch II region of Ras is not involved in binding Raf-RBD but may be involved in binding to the cysteine rich domain of Raf. Recently, a second Ras binding domain was identified in Raf-1 (RBS-2) corresponding to a region within the cysteine rich domain (CRD) in the N-terminal region of Raf-1 (Brtva *et al*, 1995; Drugan *et al*, 1996). Recently, the solution structure of the Raf-1 CRD encompassing residues 139-184, has been determined by NMR (Mott *et al*, 1996). Several other regions of the regulatory domain have been proposed to play a role in binding (Zhang *et al*, 1993; White *et al*, 1995). Recent studies have suggested that the RBS1 and RBS2 interact with distinct regions of Ras (Brtva *et al*, 1995; Hu *et al*, 1995a) and both interactions may be required for Raf-mediated transformation. In intact unstimulated Raf-1, the RBS-1 may be cryptic (Drugan *et al*, 1996). This interaction can be disrupted by mutations in the effector region, such as Asp38Ala, and a strong correlation exists between the biological activity of

effector mutants and their ability to bind to Raf. The interaction between Ras and Raf has been shown to be rapidly reversible (Gorman *et al*, 1996). The dissociation constant for the interaction between Ras.GTP and the RBD of Raf-1 is ca.10nM (Herrmann *et al*, 1995) and the affinity to the GDP-bound form is 1000-fold lower. The interaction of Raf kinase with Ras results in the translocation of the kinase to the plasma membrane where Raf is activated (discussed in section 1.4).

Since the discovery of Raf as an effector of Ras, other candidate effectors have been identifed by means of the yeast two-hybrid system or direct protein-protein interactions. The lipid kinase, phosphatidylinositol-3-kinase (PI-3-kinase) is composed of two subunits, p85 which contains SH2 domains involved in receptor interaction and the catalytic subunit, p110. Direct biochemical evidence for the interaction between the α- and β-type p110 subunits of PI-3-kinase and Ras (Rodriguez-Viciana *et al*, 1994; 1996; Kodaki *et al*, 1994; Stoyanov *et al*, 1995) suggest that PI-3-kinase is an effector for Ras. PI-3-kinase binds to Ras in a GTP-dependent manner with a dissociation constant of 500nM. The enzymatic activity of PI-3-kinase is enhanced as a result of its direct interaction with Ras.GTP. However, PI-3-kinase may not simply be a downstream target of Ras. Hu *et al* (1995b) have demonstrated that a constitutively activated form of PI-3-kinase acts upstream of Ras and that such an effect can be inhibited by N17Ras.

Further Ras effectors have been identified through observations that different effector site mutations block different Ras-effector interactions (White *et al*, 1995). In this way, a further six candidates for Ras effectors have been identified. These include Ral-GDS (Ral guanine nucleotide dissociation stimulator) an exchange factor for the Ras-related protein Ral (Hofer *et al*, 1994; Spaargaren and Bischoff, 1994), Ral-GDS like proteins (RGL and RGL2) of unknown function (Kikuchi *et al*, 1994; Peterson *et al*, 1996) and a novel protein designated RalGDS-like factor (RLF) (Wolthius *et al*, 1996). The Ras mutant Gly60Ala has a weak effect on the binding of Ras to Raf but the Ral-GDS interaction is more severely affected (Hwang *et al*, 1996). Ras has a 100-fold higher affinity for Raf-RBD than for Ral-GDS. In contrast Rap binds Ral-GDS with 100-fold higher affinity than Raf-RBD (Herrmann *et al*, 1996). The role of adenylyl cyclase (involved in cAMP

production) in *S. cerevisiae* as a Ras effector has been demonstrated by its ability to be activated *in vitro* by Ras.GTP (Toda *et al*, 1985; Marshall, 1995; Wittinghofer and Herrmann, 1995; McCormick and Wittinghofer, 1996). Interestingly, deletion of adenylyl cyclase is non-lethal suggesting the existence of a second Ras-dependent pathway in *S. cerevisiae* (Mulcahy *et al*, 1985).

At least two Ras effectors have been identified in *S. pombe*. Byr2 functions as a MAPK kinase kinase in the pheromone MAPK pathway (Wang *et al*, 1991b) and binds to Ras with nanomolar affinity in a GTP-dependent manner (Masuda *et al*, 1995; Marshall, 1995; McCormick, 1994; Wittinghofer and Hermann, 1995; McCormick and Wittinghofer, 1996). The Ras mutant Tyr32Phe is unable to bind to Raf but still binds Byr2 whereas mutations outside the effector region (Asp38Asn, Thr58Ala) show the opposite effect (Akasaka *et al*, 1996). In addition Scd1, a putative GEF for the GTPase Cdc42p involved in regulation of the actin cytoskeleton has been shown to interact with Ras (Chang *et al*, 1994). The mammalian homologue of Byr2, known as MEKK1 seems to be activated in a Ras-dependent manner (Lange-Carter *et al*, 1994) and Russell *et al* (1995) have demonstrated direct binding between MEKK1 and Ras.GTP. Kuriyama *et al* (1996) have identified a putative target for Ras known as AF-6 (Prasad *et al*, 1993) whose structure resembles that of *Drosophila* Canoe, which is involved in the notch signalling pathway (Miyamoto *et al*, 1995). The recombinant N-terminal domain of AF-6 and Canoe specifically interacted with GTPγS.GST-H-Ras, indicating that both proteins are putative targets for Ras. Diaz-Meco *et al* (1994) have demonstrated that Ras interacts *in vitro* with the regulatory domain of ζ-protein kinase C (ζPKC). They have also shown that this association *in vivo* is triggered by PDGF. Finally, Rsbs 1,2 and 4 have been identified using the two-hybrid screen (Van Aelst *et al*, 1994) and Rin1 (Ras interaction/interference) was identified from its direct interaction with Ras and its ability to compete with Raf-1 for the binding site on Ras (Han and Colicelli, 1995).

1.3.1 Signal transduction through Ras

Our knowledge of signalling pathways activated by receptor protein tyrosine kinases has

been advancing rapidly (figure 6) and a number of SH2/SH3 adaptor proteins have now been identified which play critical roles in transducing such signals (Hunter, 1997; Lim *et al*, 1996; Post and Brown, 1996). There is strong evidence to indicate that Ras is a key component of mitogenic signalling pathways activated by both growth factor receptor tyrosine kinases such as the EGF receptor, the PDGF receptor (reviewed by Schlessinger and Ullrich, 1992; Schlessinger, 1993) and the insulin receptor (reviewed by White, 1994; White and Kahn, 1994). Activation of Ras by such receptors is thought to be predominantly due to an increase in the activity of guanine nucleotide exchange factors rather than by inhibition of GAP activity (Medema *et al*, 1993). Three proteins have been implicated in the activation of Ras via an increase in guanine nucleotide exchange.

A 23-kDa growth factor receptor-bound protein termed Grb2 (Lowenstein *et al*, 1992) or Ash (Matuoka *et al*, 1992) has been reported to play a role as an adapter molecule linking the upstream receptor tyrosine kinases to Ras (Downward, 1994; Gale *et al*, 1993), similar to its homologueue from *Caenorhabditis elegans*, Sem-5 (Clark *et al*, 1992) or from *Drosophila melanogaster*, Drk (Olivier *et al*, 1993; Simon *et al*, 1993). The Grb2 protein comprises a Src Homology 2 (SH2) domain, involved in the binding of tyrosine-phosphorylated protein domains (Pawson and Gish, 1992) flanked by two SH3 domains whose role is to mediate binding to proline-rich sequences (Ren *et al*, 1993). Recently, evidence to support the existence of a family of Grb-2-like proteins has come from the identification of a novel SH3-SH2-SH3 adaptor protein designated Grap, for Grb2-related adaptor protein (Feng *et al*, 1996). Grap shows 59% amino acid sequence identity with Grb2 and forms a complex with mSos1 primarily through its N-terminal SH3 domain.

Sos1m has been postulated to be the exchange factor activated by EGF in intact and permeabilized fibroblasts (Medema *et al*, 1993) and by the sevenless tyrosine kinase receptor in *Drosophila* (Simon *et al*, 1991; Bonfini *et al*, 1992).

Figure 6: Signal transduction pathways through Ras

Diagram showing the proteins involved in both Ras-dependent and Ras-independent signalling pathways from receptor tyrosine kinases (PTK) to the nucleus. The role of these proteins is discussed in section 1.3.1

[Taken from Hunter (1997)]

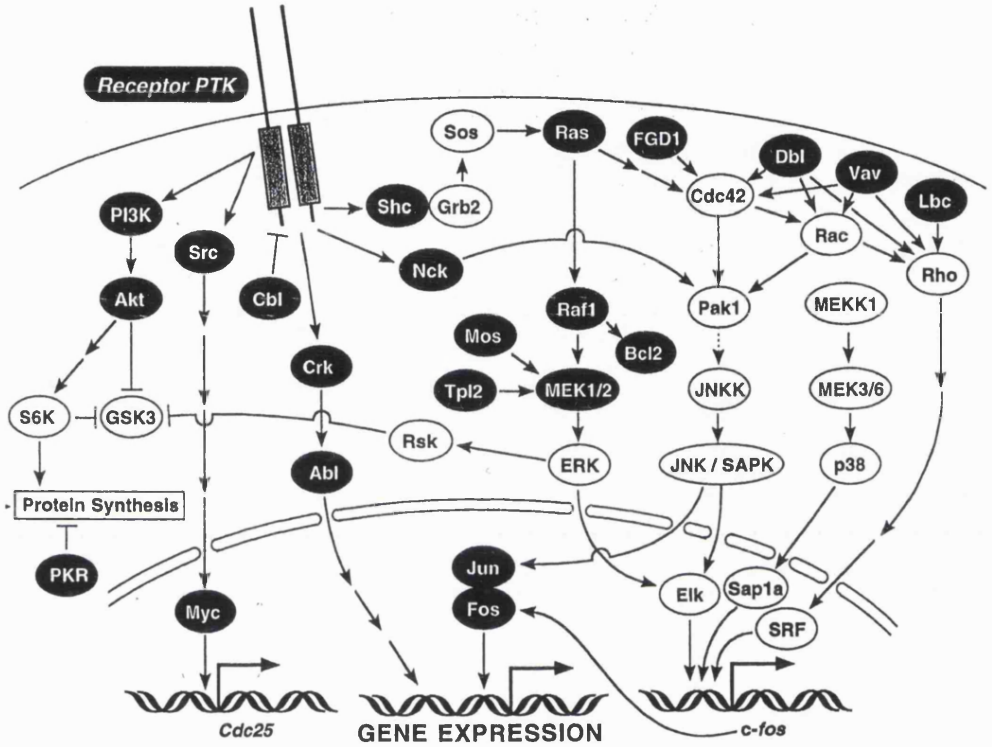
Receptor PTK
Sos
Ras
FGD1
Dbl
Vav
Lbc
Cdc42
Rac
Rho
Shc
Grb2
PI3K
Src
Nck
Cbl
Akt
Raf1
Pak1
MEKK1
Mos
Bcl2
Crk
Tpl2
MEK1/2
JNKK
MEK3/6
S6K
GSK3
Rsk
ERK
JNK / SAPK
p38
Abl
Protein Synthesis
PKR
Jun
Fos
Elk
Sap1a
SRF
Myc
Cdc25
GENE EXPRESSION
c-fos

Figure 7(a): Mechanism of Ras activation by the EGF receptor

The SH3 domains of Grb2 are bound to a proline-rich region in the carboxy-terminal tail of Sos. Upon EGF-receptor activation and autophosphorylation, the Grb2/Sos complex binds to Tyr1068 at the carboxy-terminal tail of the EGF receptor, thus relocating Sos to the plasma membrane. The interaction between the guanine nucleotide releasing activity of Sos and membrane-bound Ras leads to the exchange of GDP for GTP. Formation of GTP-bound Ras leads to activation of a kinase cascade including Raf, MAPKK, MAPK and other pleiotropic responses essential for cell growth and differentiation.

[Taken from Schlessinger (1993)]

Figure 7(b) Mechanism of Ras activation by the insulin receptor

Upon insulin receptor activation and autophosphorylation, the Grb2/Sos complex binds to phosphorylated tyrosine residues at the carboxy terminal tail of the insulin receptor, via the tyrosine phosphorylated adaptor proteins, Shc and IRS.

[Taken fron White (1996)]

(a)

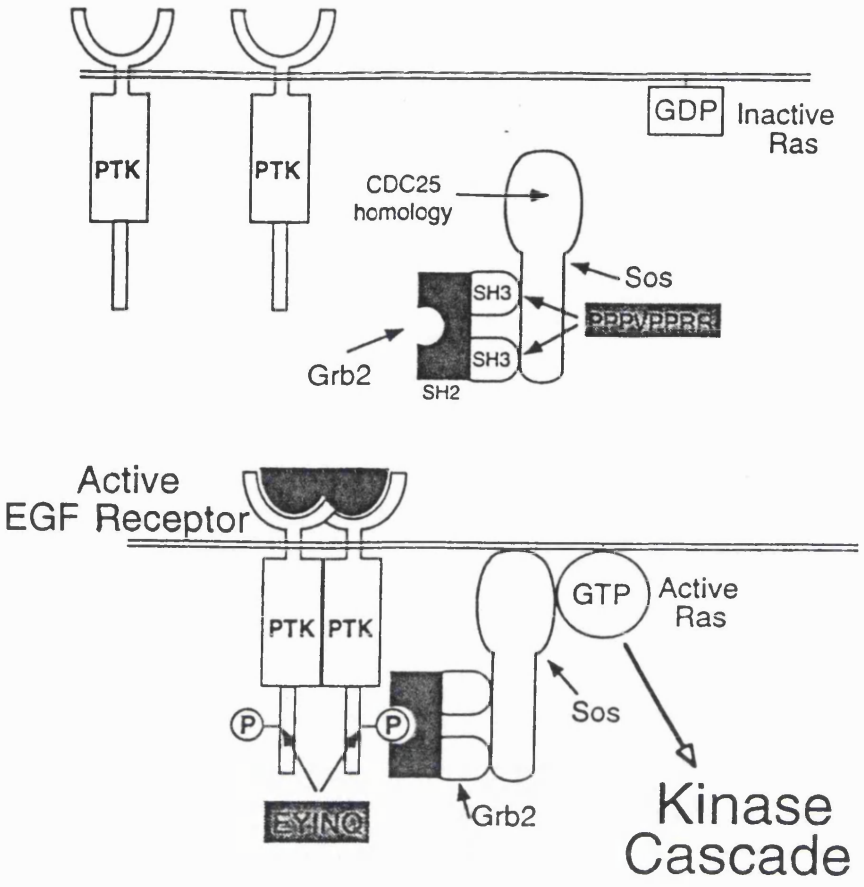
PTK
PTK
GDP
Inactive
Ras
CDC25
homology
Sos
SH3
PPPVPPRR
SH3
Grb2
SH2
Active
EGF Receptor
PTK
PTK
GTP
Active
Ras
P
P
Sos
EYINQ
Grb2
Kinase
Cascade

(b)

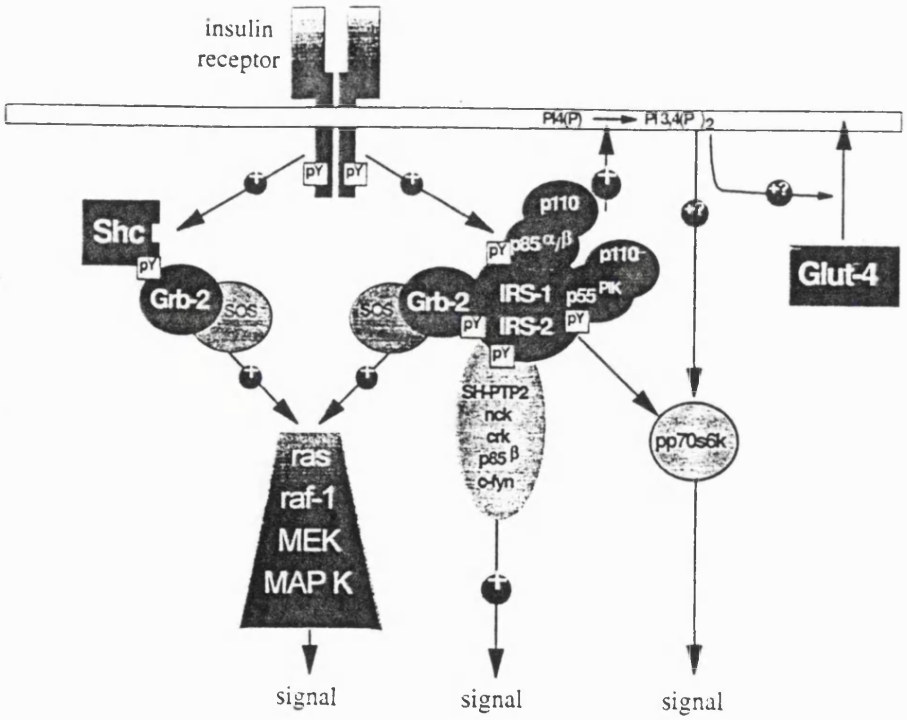
insulin
receptor
PI4(P)
PI3,4(P)2
pY
pY
Shc
pY
Grb-2
SOS
SOS
Grb-2
p110
p85α/β
pY
p110-
IRS-1
p55PIK
IRS-2
pY
pY
pY
SH-PTP2
nck
crk
p85β
c-fyn
Glut-4
ras
raf-1
MEK
MAP K
pp70s6k
signal
signal
signal

Activation of the EGF, insulin and PDGF receptors leads to the phosphorylation of a third protein important in Ras activation (i.e the Shc protein), which contains a single SH2 domain in addition to a glycine/proline-rich domain (Pelicci *et al*, 1992; Pronk *et al*, 1994). Shc is thought to function as a bridge between Grb2/Sos1 complexes and tyrosine kinases (such as the insulin receptor tyrosine kinase) in situations where the receptor is unable to associate with the Grb2/Sos1 complex directly. A novel SH2 protein called Shb has been cloned (Welsh *et al*, 1994) which has also been suggested to function as an adaptor protein linking SH3 domain proteins to tyrosine kinases or other tyrosine phosphorylated proteins (Karlsson *et al*, 1995).

Ligand binding to the extracellular domain of receptor tyrosine kinases is followed by receptor dimerization (Lemmon and Schlessinger, 1994), stimulation of protein tyrosine kinase activity and autophosphorylation at intracellular tyrosine residues. In addition, tyrosine phosphorylation of Shc occurs. This process of autophosphorylation creates binding sites for intracellular signal transduction molecules containing one or two copies of SH2 domains (Schlessinger and Ullrich, 1992; Pawson and Schlessinger, 1993). The two SH2 containing adaptor proteins, Grb2 and Shc, can recruit Sos to the membrane, either by their direct association with the activated receptor tyrosine kinase, or by interaction with intermediate proteins, depending upon the particular receptor which is activated.

Upon stimulation of cells with a growth factor such as EGF, tyrosine phosphorylation of the receptor tyrosine kinase and Shc occurs. In EGF-stimulated signalling pathways, (illustrated in figure 7a) Grb2 associates with the autophosphorylated tail of the EGF receptor or Shc, via its SH2 domain (Pelicci *et al*, 1992; Rozakis-Adcock *et al*, 1992; Rojas *et al*, 1996). In addition, Grb2 interacts with the guanine nucleotide releasing factor, Sos, via its SH3 domains. Such a direct association of the Grb2/Sos1 complex with the activated EGF receptor is thought to trigger the activation of Ras (Egan *et al*, 1993; Gale *et al*, 1993, Li *et al*, 1993; Rozakis-Adcock *et al*, 1993; Buday and Downward, 1993). However, it has not yet been shown that the formation of the EGF receptor-mSos1 complex depends on Grb2 rather than another adaptor molecule with similar functions to

Grb2. In addition, it is not yet known how the formation of this signalling complex activates mSos1. Activation of Sos could occur upon binding of the Grb2-Sos complex to the EGF receptor, by phosphorylation or by induction of a conformational change. However, the association of Grb2 with Sos has been shown to be independent of receptor activation since the complex has been identified in non-activated cells. The binding of the Grb2-Sos complex to activated receptors has been shown to increase the affinity of Grb2 for Sos but not to activate Sos (Buday and Downward, 1993). Activation of Sos is most likely to occur as a result of SH2/SH3 mediated protein-protein interactions, since neither Grb2 nor mSos1 is significantly phosphorylated on tyrosines. Alternatively, Ras might be activated by the recruitment of Sos to the plasma membrane, which increases the local concentration of Sos at the membrane and brings Sos into close proximity with its target protein, Ras. Translocation of Sos to the plasma membrane by virtue of its association with Grb2 increases the effective concentration of Sos in contact with Ras at the plasma membrane and leads to the activation of Ras by promoting the release of GDP, enabling the accumulation of active Ras in EGF-stimulated cells (Egan *et al*, 1993; Buday and Downward, 1993).

In the insulin signalling pathway (illustrated in Figure 7b), the insulin receptor does not directly associate with SH2 proteins. Instead, the activated insulin receptor phosphorylates a docking molecule known as insulin receptor substrate 1 (IRS-1) (reviewed by White, 1994).This molecule subsequently forms an initial signalling complex with the downstream signal-transducing proteins such as PI-3-kinase, the protein tyrosine-specific phosphatase, Syp, and the small adaptor proteins Grb2 and Nck. In fact both IRS-1 and Shc can potentially link the activated insulin receptor with the Grb2-Sos complex and thus activate Ras, and both molecules are essential for the overall insulin-induced growth stimulus (Yonezawa *et al*, 1994). Yamauchi *et al* (1994) have suggested that IRS-1 and Shc compete for a limited pool of Grb2, resulting in a signalling pathway dependent upon the relative concentrations of the two complexes in the cell. Shc is considered to play a more important role than IRS-1 in insulin-stimulation of GNRF activity (Sasaoka *et al*, 1994) and Ras activation. Ras activation is transient and rapidly returns to its basal GDP-bound state. Insulin and EGF have been demonstrated to utilize different molecular pathways to

achieve Ras inactivation.

Inactivation of Ras following insulin stimulation is proposed to result from a feedback serine/threonine phosphorylation of Sos by the Ras/Raf/MEK/ERK pathway which directly correlates with a dissociation of the Grb-2-Sos complex and the return of Ras to its GDP-bound form (Cherniack *et al*, 1995; Waters *et al,* 1995; Holt *et al*, 1996a). EGF also induces a serine/threonine phosphorylation of Sos, but this phosphorylation is proposed to induce a dissociation of the Grb-2/Sos complex from Shc (Buday *et al*, 1995; Holt *et al*, 1996b) rather than a dissociation of the Grb-2/Sos complex itself. Waters *et al* (1996) have demonstrated that only a small fraction of the total cellular pool of Grb-2 was associated with Sos and that this fraction undergoes insulin-stimulated dissociation. EGF does not utilize this pool of Grb-2/Sos but recruits an alternative Grb2/Sos pool that undergoes a dissociation from Shc. However, direct evidence for the existence of alternative pathways to Grb2 which may contribute to Sos-mediated Ras activation has come from the identification of other small adaptor proteins such as Nck and CrkII (Hu *et al*, 1995c; Feller *et al*, 1995), which interact with Sos via their SH3 domains. Okada and Pessin (1996) have shown that different cellular pools of Sos associate with different adaptor proteins to form various signalling complexes which undergo distinct patterns of assembly/disassembly in response to growth factor stimulation.

Activation of Sos in EGF-stimulated cells, is linked to changes in gene expression by a series of serine/threonine phosphorylation events mediated by mitogen-activated protein kinases (MAPK) or extracellular signal-regulated kinases (ERK). Activation of MAP kinases occurs by phosphorylation of both threonine and tyrosine by a dual specificity protein kinase, MAP kinase kinase (MAPKK) (Anderson *et al*, 1990a). It emerged that MAPKK itself is activated by phosphorylation which led to the speculation that a MAP kinase kinase kinase (MAPKKK) existed. The first MAPKKK to be identified was Raf-1 p74, the product of the c-*raf-1* protooncogene (Kyriakis *et al*, 1992; Howe *et al*, 1992; Dent *et al*, 1992). Raf is thought to be located downstream from Ras in the signal transduction pathway (Smith *et al*, 1986; Kolch *et al*, 1991; Koide *et al*, 1993). Growth factor stimulation of certain receptors activates Raf in a Ras-dependent manner (Wood

et al, 1992), whereas other stimulii, such as the activation of PKC by phorbol esters, lead to the activation of Raf in a Ras-independent manner. Raf may be activated by an interaction with activated Ras. Indeed, Raf has been demonstrated to directly associate with Ras in its GTP-bound conformation, via its amino-terminal regulatory domain. There are two possible models for the activation of c-Raf-1 by Ras. Firstly, the interaction of c-Raf-1 with Ras results in the translocation of the c-Raf-1 to the plasma membrane where its kinase activity is switched on by events which remain to be identified (Traverse *et al*, 1993; Wartmann and Davis, 1994; Leevers *et al*, 1994; Stokoe *et al*, 1994; Marais *et al*, 1995). Such a membrane activation event has been postulated to involve tyrosine phosphorylation of c-Raf-1 (Marais *et al*, 1995). The second possibility is that activation is achieved through the direct binding of Ras and c-Raf-1 in the presence of 14-3-3 protein (Freed *et al*, 1994a,b; Burbelo and Hall, 1995; Yamamori *et al*, 1995; Rommel *et al*, 1996). Since post-translational modification of H-Ras was found to be essential to this process, it was suggested that H-Ras farnesylation may be involved in c-Raf-1 activation rather than membrane recruitment. Alternatively, Raf activation could be induced by a conformational change in Raf upon Ras binding resulting in elevated kinase activity. Ras binding would involve the switch I region of Ras binding to the c-Raf-1 Ras binding domain (RBD) in addition to the direct interaction of the farnesyl group with c-Raf-1 possibly at the Raf-N-terminal cysteine rich domain (CRD). There is much evidence to suggest the involvement of Raf-1 CRD in the activation process (Chow *et al*, 1995). The Raf-1 CRD has been demonstrated to bind to phospholipids (Ghosh *et al*, 1994) and possibly 14-3-3 proteins (Freed *et al*, 1994; Irie *et al*, 1994; Fu *et al*, 1994; Fantl *et al*, 1994; Li *et al*, 1995; Papin *et al*, 1996). Raf-1 CRD is able to simultaneously bind several ligands including Ras and the phospholipid phosphatidylserine (PS) (Ghosh *et al*, 1994a). The formation of a complex between Ras, PS and the N-terminus of Raf-1 is necessary for activation of the Raf-1 kinase (Ghosh *et al*, 1994; Drugan *et al*, 1996). Activated Raf is then able to phosphorylate and activate MAPKK (MEK1/2) which in turn activates the MAPK (ERK). MAPKK can also be activated by two other oncoproteins namely, Mos and Tpl2, underscoring the importance of the ERK MAPK pathway in transformation. Two other MAPKKK have been identified, namely, MEKK and Ras-dependent ERK-kinase stimulator (REKS) (Kuroda *et al*, 1995). It is possible that Raf, p120-GAP and

neurofibromin compete for Ras.GTP in the cell since they all interact with Ras at the effector region of loop2.

Over the years, our understanding of the role of Ras in signal transduction has improved to the point where it is now possible to draw a plausible scheme linking cell surface receptors, via Ras and cytoplasmic kinases to nuclear transcription factors. The next most important question will be how different receptors elicit distinct biological responses. The answer to this most likely lies in the fact that different responses require receptors to assemble different combinations of cytoplasmic signalling proteins. In addition to the signalling proteins mentioned above, there are other signal transduction components which are recruited into complexes with activated receptor tyrosine kinases, via their src-homology domains. These include phosphoinositide-specific phospholipase Cγ (PLCγ) (Wahl *et al*, 1989; Meisenhelder *et al*, 1989; Anderson *et al*, 1990b; Ronnstrand *et al*, 1992), members of the non-receptor Src family of tyrosine kinases (Kypta *et al*, 1990; Anderson *et al*, 1990b; Mori *et al*, 1993), Nck and Crk (Feller *et al*, 1994) and the phosphotyrosine phosphatase SHPTP-2 (Lechleider *et al*, 1993), the GTPase activating protein Ras-GAP (Kaplan *et al*, 1990; Kaslauskas *et al*, 1990; Anderson *et al*, 1990b), the transcription factor Stat 3 (Zhong *et al*, 1994) and phosphatidylinositol-3-OH kinase (PI-3-K) (Kaplan *et al*, 1987; Kaslauskas and Cooper, 1989; Levy-Toledano *et al*, 1994). A discussion of the possible effector roles for these proteins is presented in section 1.3. These large signalling complexes may mediate a number of independent signalling pathways downstream of Ras, via the activation of various effectors for Ras.

Downstream events independent of Raf such as specific transcriptional activation events, activation of p70 S6 kinase and membrane ruffling, might be mediated by the PI-3-K pathway. The downstream target of PI-3-K has been identified as the serine/threonine kinase, Akt (Bos, 1995). The critical targets for Akt phosphorylation are not known but it has been shown that Akt can phosphorylate and inhibit glycogen synthase kinase 3 (GSK3) in response to insulin. Akt may also be upstream of the 70K S6 kinase which can also phosphorylate and inhibit GSK3.

The Raf-independent morphological changes involving actin-based cellular structures are mediated by the Ras-related subfamily of Rho GTPases, including Rho, Rac and Cdc42. Among the direct targets for Cdc42 and Rac are several protein kinases, including PAK1 (Manser *et al*, 1994) and Rho kinase (ROK) (Leung *et al*, 1995). These kinases act as effectors since they can directly affect the reorganization of the relevant actin-containing structures. ROK promotes the formation of Rho-induced actin containing stress fibres and focal adhesion complexes. PAK stimulates the disassembly of stress fibres which has been shown to accompany the formation of Cdc42-induced peripheral actin containing structures such as filopodia. Adaptors such as Nck may be connected to the actin cytoskeleton and Rho family proteins, since Nck SH3 domains bind PAK1. An Nck/PAK1 complex is translocated to activated growth factor receptor tyrosine kinases via the Nck SH2 domain increasing PAK1 activity (Galisteo *et al*, 1996). Activated Rac and Cdc42 stimulate the JNK/SAPK (c-jun N-terminal kinase/stress activated protein kinase) of p38 MAPK pathways (Coso *et al*, 1995; Minden *et al*, 1995) possibly through binding or Rac/Cdc42 to PAK which leads to its activation (Bagrodia *et al*, 1995). However, PAK activation is not required for Rac/Cdc42-induced cytoskeletal changes. Cdc42, Rac and Rho are upregulated by interaction with exchange factors such as Dbl and Vav. FGD1 can only activate Cdc42 (Olson *et al*, 1996). Cdc42 is then able to activate Rac, which in turn can activate Rho, thus leading to activation of all three members. However, such a linear activation process may not always occur since Cdc42 and Rho activities may be competitive or even antagonistic.

1.3.1 Oncogenic transformation by Ras involves multiple effectors

There is substantial evidence to support a critical involvement of the Raf/MEK/MAPK cascade in mediating Ras transformation. Firstly, Ras-mediated signalling events and transformation can be blocked by the use of kinase-deficient mutants of Raf-1, MEKS and MAPKs (Kolch *et al*, 1991; Cowley *et al*, 1994; Westwick *et al*, 1994; Khosravi-Far *et al*, 1995; Qui *et al*, 1995a,b). Secondly, mutants of Raf-1 which are constitutively activated have been shown to exhibit strong transforming activities in rodent fibroblast transformation assays (Bonner *et al*, 1985; Stanton *et al*, 1989).In fact, the observation that plasma-membrane targeted Raf-1 exhibits the same potent transforming activity as

oncogenic Ras has led to suggestions that the primary role of Ras is to mediate translocation of Raf-1 to the plasma membrane where activation of Raf-1 is triggered by Ras-independent events (Leevers *et al*, 1994; Stokoe *et al*, 1994). Thus Raf-1 activation is sufficient to mediate full Ras-transforming activity. This theory is consistent with the finding that constitutively activated Raf-1 is sufficient to overcome the loss of Ras function caused by the Ras (17N) dominant negative or the Y13-259 anti-Ras neutralizing antibody (Feig and Cooper, 1988b; Smith *et al*, 1986). Thirdly, tumourigenic transformation of NIH3T3 cells can be induced by constitutively activated MEKS (Alessi *et al*, 1994; Mansour *et al*, 1994). Lastly gain of function mutations in Raf, MEK or MAPK homologues in *Drosophila melanogaster* have been demonstrated to overcome defects in Ras (Dickson *et al*, 1992; Tsuda *et al*, 1993).

However, there is increasing evidence that Ras may mediate its actions through the activation of multiple downstream effector-mediated pathways. Evidence for the existence of Raf-independent Ras-signalling pathways which may mediate Ras transforming activity has come from the identification of an increasing number of Ras effectors. The absence of structural conservation amongst the effectors at their Ras interaction sites suggest that significant differences exist in the recognition mechanisms by which effector molecules associate with Ras. The exact role of these effectors in mediating Ras downstream signal transduction and transformation is still unclear. It is now known that oncogenic Ras co-ordinately activates both Raf-dependent and Raf-independent pathways to mediate full Ras-induced transforming activity. There is increasing evidence to suggest that activation of the Raf-independent pathway(s) is sufficient to cause cellular transformation and requires the participation of Rho family proteins. It was discovered that Ras depends on the synergistic activaton of at least two pathways, the c-Raf-1/MEK/MAPK pathway and the Rac and Rho pathway, for full transforming activity (Qiu *et al*, 1995a,1995b; Joneson *et al*, 1996; Khosravi-Far *et al*, 1995, 1996). Figure 8 shows the involvement of Ras in the direct activation of multiple signalling pathways. Recently, a concensus Ras binding sequence has been identified which is shared among a subset of Ras effectors, namely, Raf-1 and NF1-GAP (Clark *et al*, 1996).

Figure 8: Direct activation of multiple signalling pathways by Ras

Diagram showing some of the putative effector molecules for Ras and the proteins involved in downstream signalling from these effectors

[Taken from Marshall (1995)]

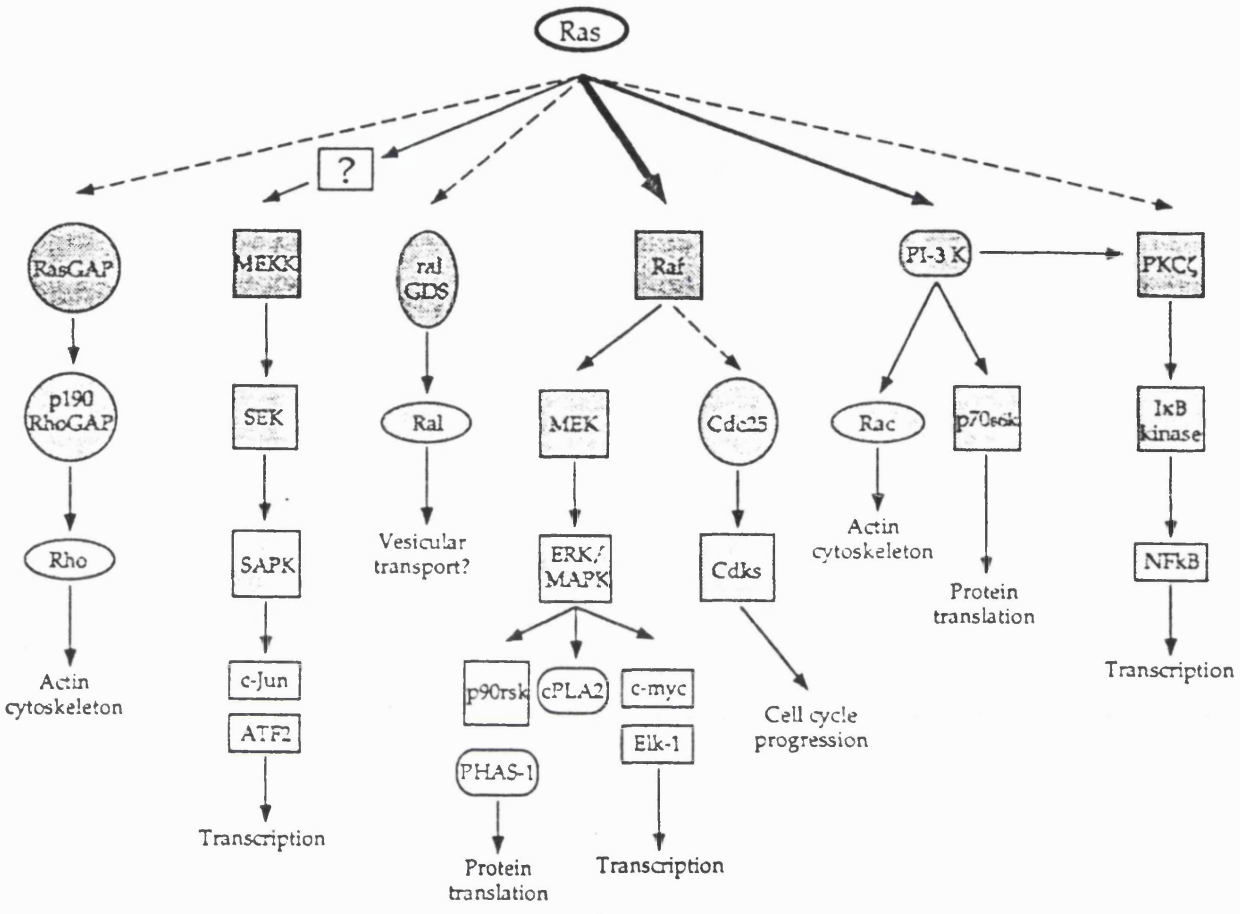
Ras
?
RasGAP
p190 RhoGAP
Rho
Actin cytoskeleton
MEKK
SEK
SAPK
c-Jun
ATF2
Transcription
ral GDS
Ral
Vesicular transport?
Raf
MEK
ERK/ MAPK
p90rsk
cPLA2
c-myc
PHAS-1
Elk-1
Protein translation
Transcription
Cdc25
Cdks
Cell cycle progression
PI-3 K
Rac
Actin cytoskeleton
p70sck
Protein translation
PKCζ
IκB kinase
NFkB
Transcription

Indeed, Raf and neurofibromin have been shown to compete for the effector binding site on Ras (Gorman *et al*, 1996; Mori *et al*, 1995). Bollag and McCormick (1991) proposed that the differential inhibition of neurofibromin by lipids

Recent evidence suggests that Ras may activate a second signalling pathway which may involve the functions of the Ras-related proteins Rac1 and RhoA for oncogenic Ras-mediated transformation. Khosravi-Far *et al* (1995) have evidence to support the possibility that oncogenic Ras-activation of Rac1 and RhoA, coupled with the activation of the Raf/MAPK pathway, is required to trigger the full morphogenic and mitogenic consequences of oncogenic Ras transformation (Qiu *et al*, 1995a,b). Additional experiments have suggested that Rac activation lies downstream of PI-3-K activation on a PDGF-stimulated signalling pathway (Wennstrom *et al*, 1994; Hawkins *et al*, 1995). Furthermore, Urano *et al* (1996) have found evidence to support the idea that Ras-induced activation of Ral-GDS and its substrate Ral, contributes to the growth regulatory effects of Ras.

In order for Ras to activate different signalling pathways, a certain level of effector selectivity must be in operation. For example, protein kinase A has been demonstrated to regulate the selectivity of Ras binding to either Ral-GDS or Raf-1 (Kikuchi and Williams, 1996). In addition, Ikeda *et al* (1995) have demonstrated that Rap1 regulates the interaction of Ras with RGL. Such an observation suggests that Rap1 and protein kinase A may co-operate to distinguish the signal of Ras to RGL from that to Raf-1.

Mitogenic lipids such as arachidonic acid, prostaglandins and phosphoinositides have been proposed to be involved in the signalling pathway selection process. Such lipids have been reported to either stimulate or inhibit the catalytic activities of p120-GAP and neurofibromin (Bollag and McCormick, 1991; Han *et al*, 1991; Golubic *et al*, 1991). The idea that p120-GAP and neurofibromin might be effectors of different Ras responses has come from the observation that p120-GAP forms complexes with some but not all protein tyrosine kinases (PTKs) whilst neurofibromin forms part of another signalling pathway by complexing with receptors such as B cell receptors (Boyer *et al*, 1994). Bollag and

McCormick (1991) suggested that the selective inactivation of either signalling pathway might be achieved by differentially inhibiting the GAPs via their interaction with lipids. In support of this, neurofibromin is more sensitive to some of these compounds than p120-GAP (Bollag and McCormick, 1991; Golubic *et al*, 1991). The interaction of lipids with GAPs has also been used in support of arguments both for and against the role of GAPs as effectors for Ras. This will be discussed further in chapter 3.

Chapter 2 - Materials and Methods

2.1 General molecular biology methods

2.1.1 Cloning materials

T4 DNA Polymerase, T4 DNA ligase and all restriction enzymes were from Boehringer Mannheim. Shrimp alkaline phosphatase and sequenase kits were from USB. Taq polymerase was from Perkin Elmer and dNTPs were from Pharmacia. Agarose powder was from Flowgen. L-broth and Terrific broth were prepared according to Maniatis *et al* (1982). The human $NF1_{334}$ cDNA construct in the *E. coli* expression vector pGEX-2T and the universal primers used in the mutagenesis procedure described in section 2.1.4, were obtained from Dr. Richard Skinner (GlaxoWellcome, Stevenage).

The expression vector for wild-type $NF1_{334}$, pGEX-2T (see Figure 9 for plasmid map) consisted of the $NF1_{334}$-EEF coding sequence (1038bp) inserted into the pGEX-2T vector as a *BglII* fragment (Figure 10). Residues 1195-1528, the catalytic domain of NF1 (using the numbering of Marchuck *et al* (1991)), were polymerase chain reaction-cloned into the pGEX-2T expression vector (Smith and Johnson, 1988) so that a glutathione transferase/$NF1_{334}$ fusion protein was encoded. The fusion region contains a thrombin cleavage site for the cleavage of GST from $NF1_{334}$ during purification. The two $NF1_{334}$ mutants, R1276A and R1391A generated by the PCR mutagenesis procedure described in section 2.1.4, were derived from this vector.Transformation of the pGEX-2T.$NF1_{334}$ expression vector into either *E. Coli* RR1ΔM15 or BL21 cells was performed by the heat-shock method according to Maniatis *et al* (1982).

2.1.2 Isolation of pGEX-2T.$NF1_{334}$ DNA

To prepare large scale amounts of the pGEX-2T.$NF1_{334}$ DNA, *E. coli* RR1ΔM15 cells containing the expression vector were inoculated into 250ml of L-Broth containing 50μg/ml ampicillin, and the cells were grown overnight at 37°C with shaking at 250rpm. The cells were pelleted in a Beckman centrifuge at 5000rpm for 10 minutes at 4°C and resuspended in 10ml of 50mM Tris/HCl pH8.0, 10mM EDTA, 100μg/ml RNase A. An equal volume of 200mM NaOH, 1% (w/v) SDS was added, and the solution incubated for 5 minutes at room temperature to lyse the cells. The SDS and chromosomal DNA was precipitated by addition of an equal volume of 2.55M potassium acetate, pH 4.8, with

gentle mixing. The precipitate was removed by centrifugation at 10,000rpm at 4°C for 30 minutes in a Sorvall SS-34 rotor. The supernatant was applied to a plasmid purification column (Qiagen) pre-equilibrated in 750mM NaCl, 50mM MOPS pH 7.0, 15% (v/v) ethanol, 0.15% (v/v) triton X-100. The column was then washed with 1M NaCl, 50mM MOPS pH 7.0, 15% (v/v) ethanol, and the plasmid DNA eluted with 1.25M NaCl, 50mM MOPS pH 8.2, 15% (v/v) ethanol. The DNA was pelleted by addition of 0.7 volumes of isopropanol and centrifugation at 10,000rpm for 30 minutes at 4°C. The pellet was then washed with 70% (v/v) ethanol and air dried, before being dissolved in a suitable volume of TE buffer (10mM Tris/HCl pH 8.0, 1mM EDTA).

To prepare small scale amounts of pGEX-2T-$NF1_{334}$ DNA, colonies were picked from the transformation plate using a toothpick and patched onto a gridded L-Agar plate containing 50µg/ml ampicillin. The toothpick was then dropped into 5ml of L-broth containing 50µg/ml ampicillin and the cultures grown up at 37°C overnight in a shaking incubator at 250rpm. 1.5ml of culture was spun down in a bench centrifuge at room temperature, at 13,000rpm for 30 seconds. The supernatant was decanted off and 350µl STET (+RNAase) (8% sucrose, 0.5% triton X-100, 50mM EDTA, 10mM Tris/HCl pH8.0, 20µg/ml RNAase A containing 1mg/ml lysozyme) added to resuspend the pellet. 15µl of lysozyme (20mg/ml) was then added and the resuspended pellet was heated to 100°C for 2 minutes and then spun for 5-6 minutes at 13,000rpm in a bench centrifuge at room temperature. The resultant pellet was removed with a toothpick. 350µl isopropanol was added to the supernatant and the DNA spun out at 13,000rpm for 30 minutes in a bench centrifuge at room temperature. The pellet was washed in 70 % ethanol, dried and resuspended in TE buffer.

2.1.3 Purification of DNA fragments from agarose gels

The Freeze-Squeeze method (Maniatis *et al*, 1982) was used for quantitative purification of DNA fragments from agarose gels. The band of interest was excised from the gel and placed in a 15ml tube with 5ml of 0.3M Sodium acetate, 1mM EDTA, for 15 minutes at room temperature. The gel piece was blotted dry and placed in a 0.5ml eppendorf with a small hole at the bottom, containing glass wool. The tube was placed in liquid nitrogen

for 2-5 minutes and then placed in a 1.5ml eppendorf and spun at room temperature in a bench centrifuge at 8000rpm for 8 minutes to extract the DNA from the gel. The eluted DNA was precipitated by adding 1/100 volume of a solution of 10% acetic acid, 1M $MgCl_2$, followed by 2-4 volumes of -20°C absolute ethanol. This solution was placed at -20°C for at least 15 minutes and then centrifuged in a bench centrifuge at 12,000rpm for 10 minutes at room temperature to pellet the precipitated DNA. The DNA was washed with 75% ethanol, dried under vacuum and resuspended in a suitable volume of TE.

2.1.4 PCR site-directed mutagenesis and amplification

Mutagenesis was performed in a two-step PCR, essentially as described in Landt *et al* (1990). The universal oligonucleotides (shown in Figure 10 and Table 1) 113, 130 and 115, were complementary to the 5' ends of the $NF1_{334}$ gene coding strand. Oligonucleotides 114 and 131 were complementary to the 5' ends of the $NF1_{334}$ gene non-coding strand. The universal primers were diluted to a concentration of 100pmol/µl. Mutagenic primers BS1 and BS2 were designed to introduce the mutation from arginine to alanine at positions 1391 and 1276 respectively. These primers, synthesised by A. Harris (NIMR, London) were supplied as a solution in ammonium hydroxide. The solution was then placed at 70°C for 1h. The primers were dried down in a speed-vac (Savant) for 1h and resuspended in 80µl of TE buffer. To introduce the R1391A mutation, 0.7ng of template DNA (pGEX-2T-$NF1_{334}$) was incubated with 10x buffer for Taq polymerase (40µl), dNTP (8µl), universal primer 131 (400pmoles), antisense mutant primer BS2 (1pmole), and 1 unit of Taq polymerase, in a reaction volume of 400µl. A similar amplification was performed to introduce the R1276A mutation, except that the 3' universal primer, 113 (400pmoles) and mutant primer BS1 were used. PCR amplification was performed in a Hybaid Omnigene cycler using the following cycling conditions:

92°C -1minute, 42°C -2 minutes, 72°C -2 minutes; 1 cycle
92°C -1minute, 48°C -2 minutes, 72°C -2 minutes; 10 cycles
92°C -1minute, 53°C -2 minutes, 72°C -2 minutes; 10 cycles
92°C -1minute, 57°C -2 minutes, 72°C -2 minutes; 10 cycles

Figure 9: Map of $NF1_{334}$ Expression Plasmid, pGEX-2T

The 5.98 Kb vector contains the 1Kb $NF1_{334}$ gene under the translational control of a tac promoter (ptac) and when transformed into *E. coli* confers ampicillin resistance, enabling the rapid selection of clones containing the plasmid. The $NF1_{334}$ gene consists of the coding region for residues 1195-1528 of full length neurofibromin. The sequence is preceded by the coding region for glutathione transferase and tagged at the 3' end with the coding sequence for Glu-Glu-Phe (Skinner *et al*, 1991) for recombinant protein purification purposes. Some restriction endonuclease sites are shown, including *XhoI* and *NdeI* used to obtain the mutant $NF1_{334}$ expression vectors. Also shown is the lacZ gene and the lacIq gene. The arrows indicate the $NF1_{334}$ gene binding sites for the universal primers used throughout the mutagenesis procedure. The direction of the arrow represents the direction in which the elongation reaction proceeds.

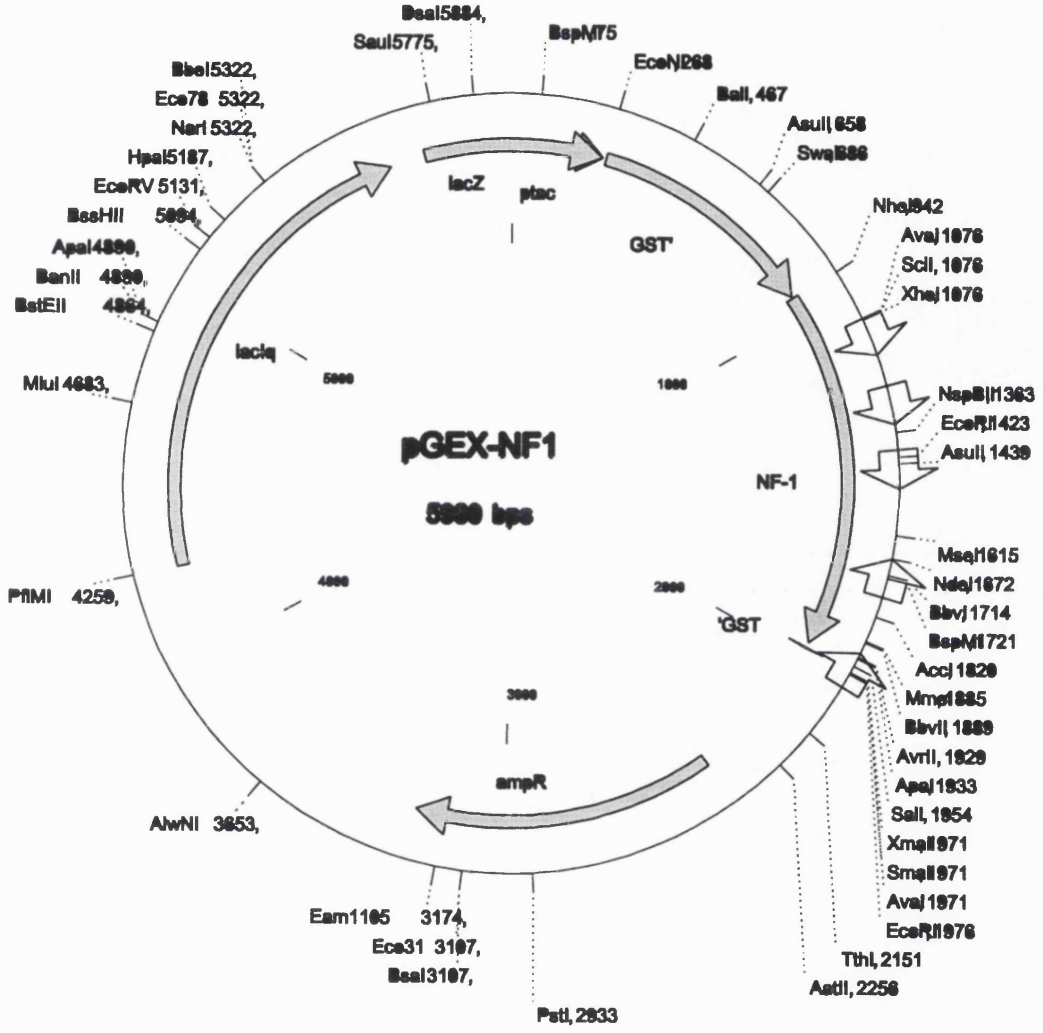
pGEX-NF1
5000 bps
lacZ
ptac
GST'
NF-1
'GST
ampR
lacIq
1000
2000
3000
4000
5000
BsaI5884,
SauI5775,
BspMI75
EcoNI268
BalI, 467
AsuII 658
SwaI886
NheI942
AvaI 1076
ScII, 1076
XhoI 1076
NspBII1363
EcoRII423
AsuII 1439
MseI1615
NdeI1672
BbvI 1714
BspMI721
AccI 1829
MmeI885
BbvII 1889
AvrII, 1829
ApaI 1933
SalI, 1954
XmaI971
SmaI971
AvaI 1971
EcoRII976
TthI, 2151
AatII, 2256
PstI, 2933
Eam1105 3174,
Eco31 3197,
BsaI3197,
AlwNI 3953,
PflMI 4259,
MluI 4683,
BstEII 4864,
BanII 4890,
ApaI4896,
BssHII 5064,
EcoRV 5131,
HpaI5187,
NarI 5322,
Eco78 5322,
BbeI5322,

Figure 10: Map of $NF1_{334}$ - EEF construct

Linear representation of the $NF1_{334}$ gene indicating the positions of restriction endonuclease sites within the gene. The arrows indicate the binding sites for the universal primers used in both the mutagenesis process and in the sequencing. The direction of the arrows represents the directionality of the primers.

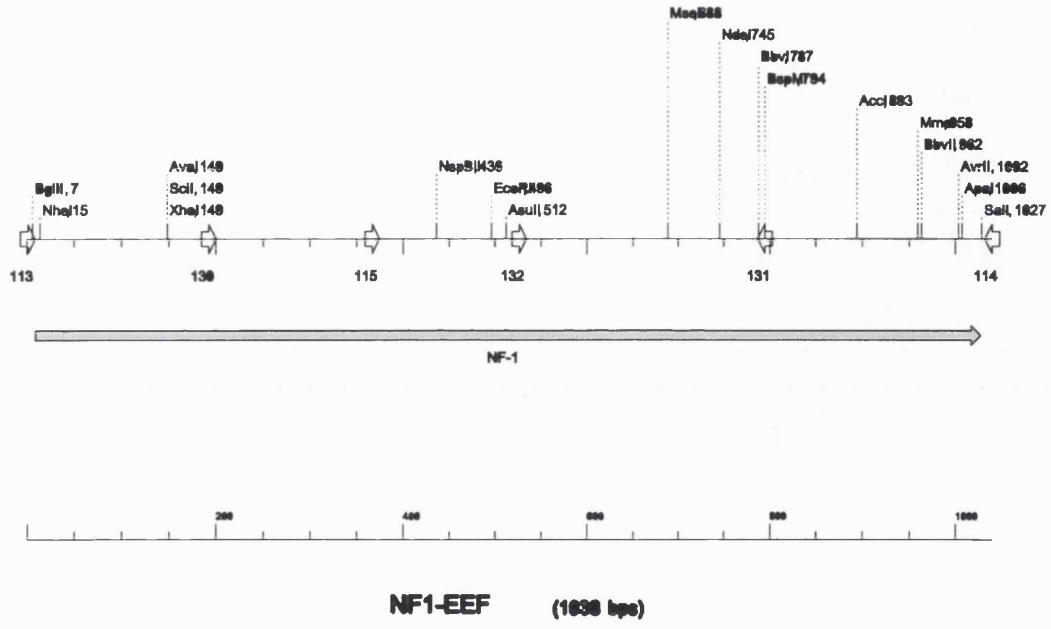

NF1-EEF (1038 bps)

Table 2: Sequences of oligonucleotides for PCR site directed mutagenesis of $NF1_{334}$

This figure shows the sequences of all the oligonucleotides used in this study, the position at which they anneal to the coding sequence. The base-pair mismatch sites designed within the mutagenic oligonucleotides are underlined.

Primer	Sequence	$NF1_{334}$ gene binding site	Function
113	5' TTT GAC AGA TCT ACG CTA GCA GAA ACA GTA TTG GCT 3'	1-37	Universal primer complementary to 5' end of $NF1_{334}$ gene coding strand
114	5' TTT GTG GTC GAC TTA GAA CTC CTC TGG GGG CCC TAG GTA TGC AAG 3'	994-1026	Universal primer complementary to 5' end of $NF1_{334}$ gene non-coding strand
115	5' GAT TGG CAA CAT GTT AGC 3'	366-384	Universal primer complementary to 5' end of $NF1_{334}$ gene coding strand
130	5' CAA CTG CTC TGG AAC AT 3'	193-209	Universal primer complementary to 5' end of $NF1_{334}$ gene coding strand
131	5' CGT GCT GCA TCA AAG TT 3'	778-794	Universal primer complementary to 5' end of $NF1_{334}$ gene non-coding strand
BS1	5' -CTG TTG CCT GCG AAG AGA GTC 3'	246-266	Mutagenic primer for R1276A mutation
BS2	5'-GTT CCT CGC ATT TAT CAA TCC 3'	594-614	Mutagenic primer for R1391A mutation

The double stranded mutant primers, BS1a and BS2a, products of the first round of PCR, containing the R1276A and R1391A mutations respectively, were ethanol precipitated and gel purified. To generate the full length R1391A fragment, 0.7ng of template vector DNA was incubated with the 3' universal primer, 114 (200pmol), excess amplified double stranded mutant fragment, BS1a, 10x Taq polymerase buffer (10µl), dNTP (2µl), and Taq polymerase (1µl), in a final reaction volume of 100µl. Amplification to generate the full length mutant R1276A fragment was essentially the same except that the 5' universal primer, 113 (200pmol) and the amplified double stranded mutant fragment BS2a, were used. PCR was performed as in the first PCR reaction. Both full length mutant fragments were phenol/chloroform treated and ethanol precipitated as described previously. Both DNA fragments were digested with *NdeI* and *XhoI* and gel purified. Digested vector DNA was treated with shrimp alkaline phosphatase (CIP) and 10x CIP buffer, to dephosphorylate the terminal 5' phosphate groups and prevent religation of the cut ends. Recombinant vectors were then prepared by ligation of the DNA fragments into the digested vector.

2.1.5 Other molecular biology techniques

All other molecular biology techniques, such as restriction digests, removal of phosphates with Shrimp Alkaline phosphatase, ligations with T4 DNA ligase, phenol/chloroform extractions, DNA precipitations and DNA concentration determinations, were carried out according to Maniatis *et al* (1982). Techniques such as DNA sequencing were performed using a sequenase kit according to protocols sent from the manufacturer.

2.2 Protein purification

2.2.1 H-Ras (1-166)

Normal truncated Harvey-Ras (residues 1-166) was expressed in *E. coli* and purified by procedures similar to those described in Skinner *et al* (1994). *E. coli* strain RR1ΔM15 containing plasmid ptacRas c' (John *et al*, 1989) was plated from a glycerol stock onto M9 minimal agar supplemented with the following components, autoclaved or filter sterilized

where appropriate: 2mM $MgSO_4$, 0.1mM $CaCl_2$, 0.2% glucose, 1μg/ml thiamine, 20μg/ml leucine and 200μg/ml ampicillin. The strain was grown up at 37°C overnight. A starter culture was prepared by inoculating 2ml TB medium containing 200μg/ml ampicillin, with a single colony from the M9 plate. The culture was incubated in a shaking incubator (250rpm) at 37°C until the A_{600} had reached ~ 0.8. The starter culture was diluted 1:5000 into fresh medium (100μl added to 500ml fresh TB medium containing 200μg/ml ampicillin) and the cultures were incubated overnight in a shaking incubator (250rpm) at 37°C. Cultures were harvested in a Sorvall RC-5B refrigerated superspeed centrifuge for 15 minutes at 6500rpm at 4°C. Pellets were stored at -70°C.

H-Ras was expressed in RR1ΔM15 cells to a high level, as shown in figure 11. The cell pellet was resuspended in an equivalent volume of buffer to the wet weight of cells harvested. The buffer used for resuspension was 10mM Tris/HCl pH 7.5, 50mM NaCl, 10mM $MgCl_2$, 5mM dithiothreitol and 20μM GDP known as buffer A. The Cell suspension was sonicated (Ultrasonics W-385, setting 7, ½" probe) twice for 30 seconds, with addition of PMSF (100mM stock in isopropanol) to 1mM before each sonication. Cell breakage was monitored by protein release. After each sonication, 20μl of the suspension was removed, spun for 1 minute at 12000rpm in a bench centrifuge at room temperature and 0.5μl of the supernatant assayed for total protein content using the Biorad assay (as described in section 2.3.5.1). This enabled the degree of cell lysis which was usually complete after 2 sonication procedures, to be monitored. Cell debris was removed by centrifugation at 40000rpm for 60 minutes at 4°C in a Beckman 70Ti rotor. The protein concentration of the supernatant was adjusted to 45mg/ml with buffer A.

The purification of H-Ras involved a separation process combining both ion exchange and gel filtration. The Ras protein was detected throughout the purification procedure by its electrophoretic mobility and its ability to bind [^{3}H]GDP.

Figure 11: SDS PAGE electrophoretic analysis of the induction of H-Ras

Samples from the induction of H-Ras were analyzed on a denaturing 19.5% SDS PAGE gel as described in section 2.3.1. *Lanes 1* and *6* contain the molecular weight markers. *Lanes 2* and *3* are uninduced samples. *Lanes 4* and *5* are induced samples. Proteins were visualized by staining with coomassie blue. H-Ras appears as a band which is approximately 19kD in size.

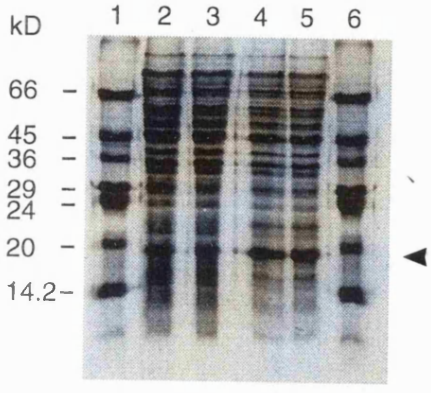
kD
1 2 3 4 5 6
66
45
36
29
24
20
14.2

Figure 12(a): SDS PAGE electrophoretic analysis of the elution of H-Ras from the Q-sepharose column

Fractions collected during the elution of H-Ras from the Q-sepharose column were analysed on a denaturing 19.5% SDS PAGE gel as described in section 2.3.1. MVII: molecular weight markers; 40KSn: supernatant from the high speed clarification spin. Proteins were visualized by staining with coomassie blue. H-Ras was eluted in fractions 92-101.

Figure 12(b): SDS PAGE electrophoretic analysis of the elution of H-Ras from the sephacryl S-200 column

Fractions collected during the elution of H-Ras from the Sephacryl S-200 column were analysed on a denaturing 19.5% SDS PAGE gel as described in section 2.3.1. Proteins were visualized by staining with coomassie blue. MVII: molecular weight markers; 40KSn: supernatant from the high speed clarification spin. H-Ras (ca. >95% pure) was eluted in fractions 50-58.

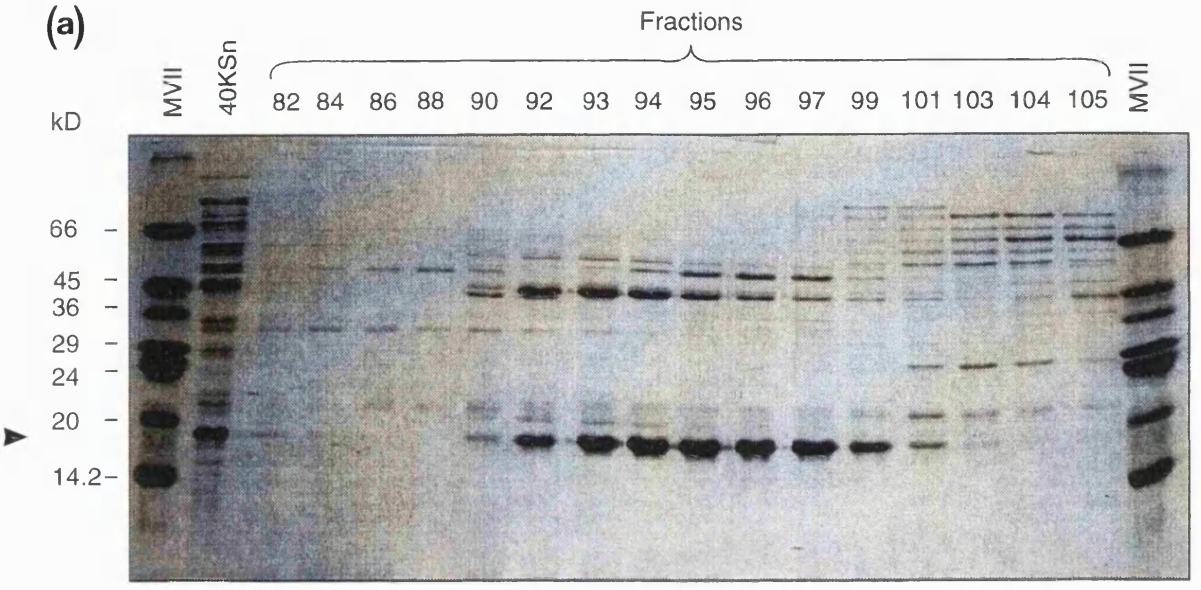
(a)
Fractions
MVII
40KSn
82 84 86 88 90 92 93 94 95 96 97 99 101 103 104 105
MVII
kD
66
45
36
29
24
20
14.2

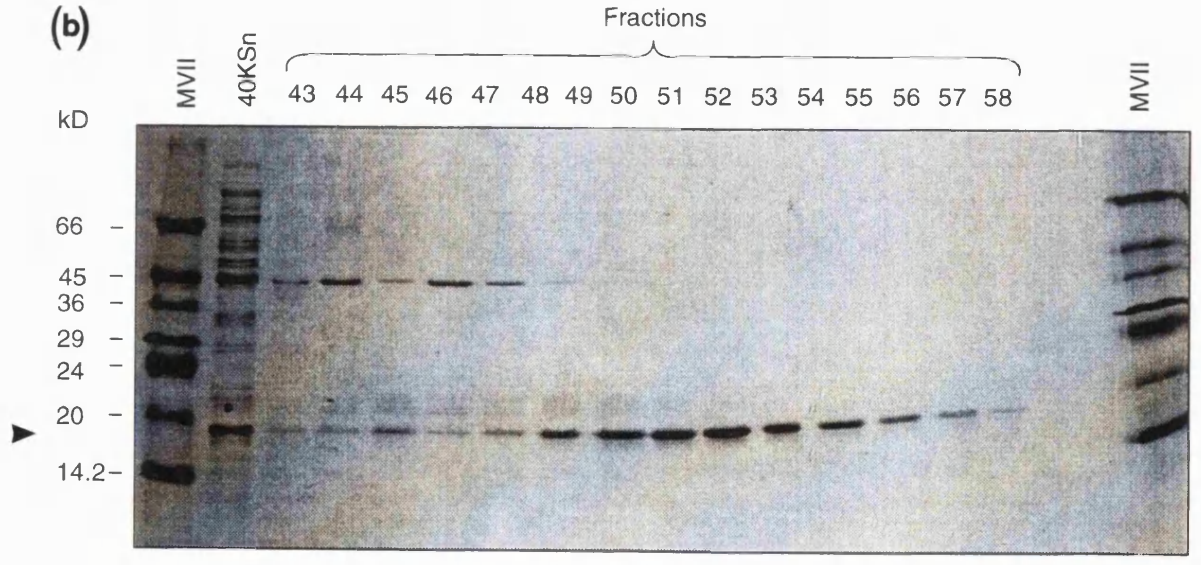
(b)
Fractions
MVII
40KSn
43 44 45 46 47 48 49 50 51 52 53 54 55 56 57 58
MVII
kD
66
45
36
29
24
20
14.2

An ion exchange Q-sepharose column (15 x 2.6cm; 80cm^3 packed gel bed) was pre-equilibrated prior to use in 10mM Tris/HCl pH 7.5, 10mM $MgCl_2$, 1M NaCl followed by 10mM Tris/HCl pH 7.5, 10mM $MgCl_2$, 50mM NaCl. On the day of use an A_{280} baseline was obtained on the chart recorder by washing the column with 1 column volume of 10mM Tris/HCl pH 7.5, 50mM NaCl, 10mM $MgCl_2$, 5mM dithiothreitol, 20μM GDP and 0.1mM PMSF, henceforth referred to as buffer B, at a flow rate of 0.1-4ml min^{-1}. The sephacryl S-200 high resolution (HR) gel filtration column (82 x 2.6cm; 435cm^3 packed gel bed) was pre-equilibrated in 10mM Tris/HCl pH 7.5, 100mM NaCl, 10mM $MgCl_2$ henceforth referred to as buffer C. On the day of use the column was washed in buffer C supplemented with 1mM dithiothreitol and 20μM GDP, at a flow rate of 22ml h^{-1}.

The supernatant was applied to the Q-sepharose column at a flow rate of 2ml min^{-1}, and fractions were collected every 6 minutes. The column was subsequently washed with buffer A at 4ml min^{-1}. Fractions were collected every 3 minutes, until the absorbance at 280nm had reached the baseline, at which point the flow rate was changed to 2ml min^{-1}. Electrophoretic analysis of flow-through fractions (1-30) from the Q-sepharose column demonstrated that Ras had bound to the column (data not shown). The Ras protein was eluted overnight from the Q-Sepharose column using a linear gradient (500ml buffer B and 500ml buffer B supplemented with 450mM NaCl) at a flow rate of 0.77ml min^{-1}, collecting fractions every 10 minutes. Fractions containing the Ras protein (92-101) were pooled on the basis of ability to bind [^{3}H]GDP, protein concentration (as determined using the Biorad assay) and purity (as assessed by SDS PAGE gel electrophoresis) (figure 12a). The contribution by Ras to the total protein content in these fractions was estimated to be approximately 50%. A protein which is known to co-express with Ras in this system is elongation factor-Tu, a GTP-binding protein which is eluted from the Q-sepharose column slightly ahead of Ras.

Pooled Ras, at concentrations >1mg/ml, was concentrated by ammonium sulphate precipitation. Ammonium sulphate (Ultra Pure) was added to the pooled protein with stirring at 4°C to achieve 78% saturation. The ammonium sulphate was allowed to

dissolve over 30 minutes and precipitated protein was collected by centrifugation at 4°C at 40000rpm for 8-10 minutes in a Beckman 70Ti rotor. The pellet was dissolved in a minimum amount of purification buffer B. At concentrations <1mg/ml, Ras was concentrated under pressure in an Amicon ultrafiltration unit, using a PM10 filter (Amicon). Protein solutions were dialyzed for approximately 10 minutes against purification buffer A.

The dialyzed protein was diluted to 45mg/ml in buffer A and loaded onto the sephacryl S-200 column at a flow rate of 22ml h^{-1}, collecting fractions every 20 minutes. Elution was carried out overnight using buffer C at the same flow rate. Again, gel electrophoresis (figure 12b) and [^{3}H]-GDP-binding assays (data not shown) revealed that the Ras protein had eluted into fractions 43-58. The Ras protein in fractions 50-58 was pooled and judged to be approximately 95% pure. Pooled Ras was concentrated by ammonium sulphate precipitation and dialyzed overnight against 10mM Tris/HCl pH 7.5, 50mM NaCl and 2mM $MgCl_2$. Protein samples were stored at -70°C until required. Final yields of H-Ras were in the region of 180mg of pure protein from 23g (wet weight) of cells grown from 4 litres of L-broth.

Truncated [Leu61]Harvey-Ras (residues 1-166) was purified as described by Skinner *et al* (1994). Full length [Leu61]Harvey-Ras was purified by Dr C. Jackson in Dr J. Ecclestons laboratory.

2.2.2 Catalytic domain of neurofibromin, $NF1_{334}$

$NF1_{334}$, the catalytic domain of neurofibromin was expressed in *E. coli* as a fusion protein with glutathione transferase, essentially as described by Skinner *et al* (1994). Purified $NF1_{334}$ was subsequently obtained by cleavage of the glutathione transferase from the $NF1_{334}$ in the final stages of the purification (Eccleston *et al*, 1993).

E.coli strain RR1ΔM15, (Brownbridge *et al*, 1993), containing plasmid pGEX2T-$NF1_{334}$ was plated onto Luria-Bertani agar supplemented with 200μg/ml ampicillin. A starter culture was prepared by inoculating 10ml of Luria-Bertani medium (L-broth), supplemented with 200μg/ml ampicillin, with several colonies from this plate. The culture was incubated overnight in a shaking incubator (200rpm) at 37°C. Subsequently, the starter culture was diluted 1:1000 into fresh medium (0.5-1ml, added to 8 flasks containing 500ml fresh medium supplemented with 200μg/ml ampicillin) and cultures were grown up in a shaking incubator (200rpm) until A_{600} reached ~ 0.8. Protein expression was induced by the addition of IPTG to the cultures from a 100mM stock, to a final concentration of 1mM. The cultures were incubated overnight at 37°C and cells were harvested at 4°C in a Sorvall RC-5B (DuPont Instruments) refrigerated superspeed centrifuge, for 20 minutes at 6500rpm. The resulting pellet was stored at -70°C. Figure 13 shows the induction of neurofibromin as a 65kDa fusion protein with glutathione transferase.

Cell breakage was essentially identical to that described for the purification of H-Ras, except that the buffer used for pellet resuspension and cell lysis was 10mM Tris/HCl pH 7.5 containing 50mM NaCl, 0.1mM EDTA and 1mM dithiothreitol, henceforth called purification buffer D. The final supernatant was diluted with purification buffer D, to achieve a protein concentration of 45mg/ml. The protein solution was then loaded onto a glutathione agarose column (S-linked; Sigma G-4510; 7 x 1.6cm: equilibrated in purification buffer D at 4°C) at a flow rate of 0.5ml min^{-1}, collecting fractions every 20 minutes. Unbound proteins were removed by washing the column with > 1 column volume of purification buffer D, initially at the same flow rate and then at 1ml min^{-1}, collecting fractions every 4 minutes.

For the latter stages of the purification i.e.: cleavage of glutathione transferase from $NF1_{334}$, the glutathione agarose column was attached to *p*-aminobenzamidine agarose (Sigma A-7155; 5cm^3 packed gel bed), and antithrombin III-agarose (Sigma A-8293; 1.2cm^3 packed gel bed) columns, in succession. The columns were equilibrated with

purification buffer E (purification buffer D supplemented with 2mM $CaCl_2$). Cleavage was achieved by passing 50ml of purification buffer F [purification buffer E containing 100µl thrombin (2.5mg/ml human plasma thrombin, Sigma T3010)] through the column overnight at a flow rate of 0.042ml min^{-1}. Fractions were collected every 60 minutes. Biorad assays were performed to assess the protein content of each fraction, and SDS PAGE gels run to determine the purity of the eluted $NF1_{334}$. Figure 14a shows the elution of cleaved neurofibromin as a 36kDa protein, from the glutathione agarose column. Glutathione transferase and uncleaved NF1.GST were eluted from the glutathione agarose column with purification buffer G (purification buffer D supplemented with 5mM glutathione, pH 8.0) at a flow rate of 0.65ml min^{-1}, collecting fractions every 6 minutes. For re-use, the columns were washed individually in 3M NaCl and reequilibrated in purification buffer D. Figure 14b shows the elution of free glutathione transferase and uncleaved NF1-GST from the glutathione agarose column.

Depending on concentration, pooled $NF1_{334}$ was concentrated by either ammonium sulphate precipitation or ultrafiltration as described for the H-Ras purification. The pellet from the ammonium sulphate precipitation was dissolved in a minimum amount of purification buffer D. Protein solutions were dialyzed overnight against purification buffer D. Purified protein was stored at -70°C. Cleaved $NF1_{334}$ was estimated to be approximately 95% pure and final yields were in the region of 15-20mg of protein per 20g of cells (wet weight) form 4 litres of LB broth. The expression and purification of R1276A and R1391A $NF1_{334}$ was essentially identical to that of wild-type $NF1_{334}$. However, care was taken to avoid cross-contamination of mutant $NF1_{334}$ preparations with wild-type $NF1_{334}$ by soaking the column apparatus in 10% formic acid and replacing the glutathione agarose matrix after each purification. Purified mutant proteins were desalted by dialyzing against 10mM Tris/HCl pH 7.5, 0.1mM EDTA and 1mM dithiothreitol.

The catalytic domain of p120-GAP, GAP_{344}, was purified as described by Skinner *et al* (1991).

Figure 13: SDS PAGE electrophoretic analysis of the induction of NF1.GST

Samples from the induction of NF1.GST were analyzed on a denaturing 19.5% SDS PAGE gel as described in section 2.3.1. *Lanes 1* and *7* contain the molecular weight markers; *Lanes 2* and *3* contain uninduced samples; *Lane 4* contains the induced sample; *Lane 5* contains the sonicated cell extract; *Lane 6* contains a supernatant from the high speed clarification spin. Proteins were visualized by staining with coomassie blue. NF1.GST appears as a band of approximately 65kD in size.

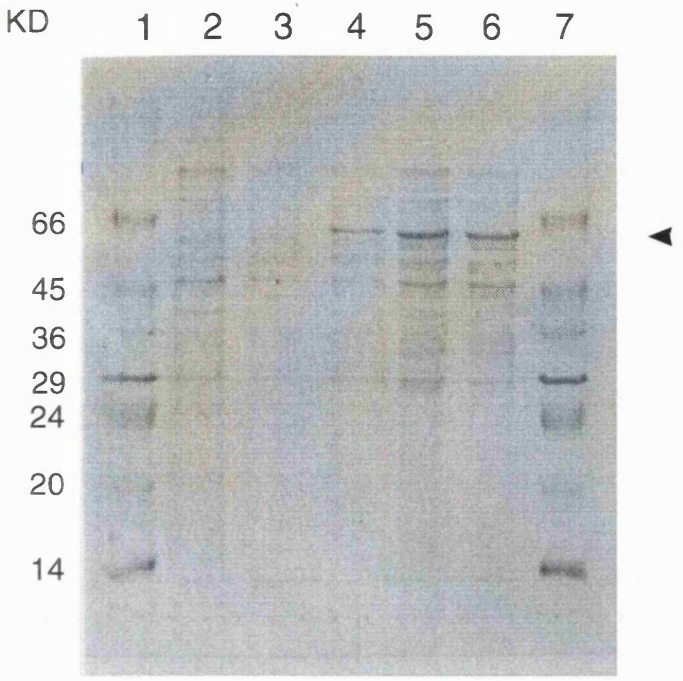
KD
1 2 3 4 5 6 7
66
45
36
29
24
20
14

Figure 14(a): SDS PAGE electrophoretic analysis of the elution of cleaved $NF1_{334}$ from the glutathione agarose column

Fractions collected during the elution of cleaved $NF1_{334}$ from the glutathione agarose column, were analyzed on a denaturing 19.5% SDS PAGE gel as described in section 2.3.1. Proteins were visualized by staining with coomassie blue. MVII: molecular weight markers; 40KSn: high speed clarification spin. $NF1_{334}$ was eluted in fravtions 40-54 and was judged to be ca. >95% pure.

Figure 14(b): SDS PAGE electrophoretic analysis of the elution of glutathione and NF1.GST from the glutathione column

Fractions collected during the elution of free glutathione and uncleaved NF1.GST from the glutathione agarose column, were analyzed on a denaturing 19.5% SDS PAGE gel as described in section 2.3.1. Proteins were visualized by staining with coomassie blue. MVII: molecular weight markers; 40KSn: supernatant from high speed clarification spin.

(a)

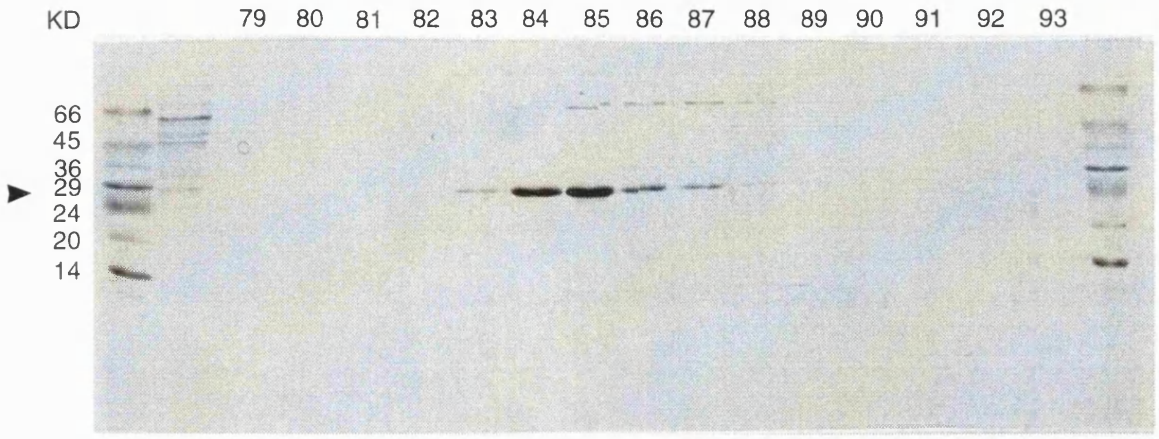
KD
79 80 81 82 83 84 85 86 87 88 89 90 91 92 93
66
45
36
29
24
20
14

(b)

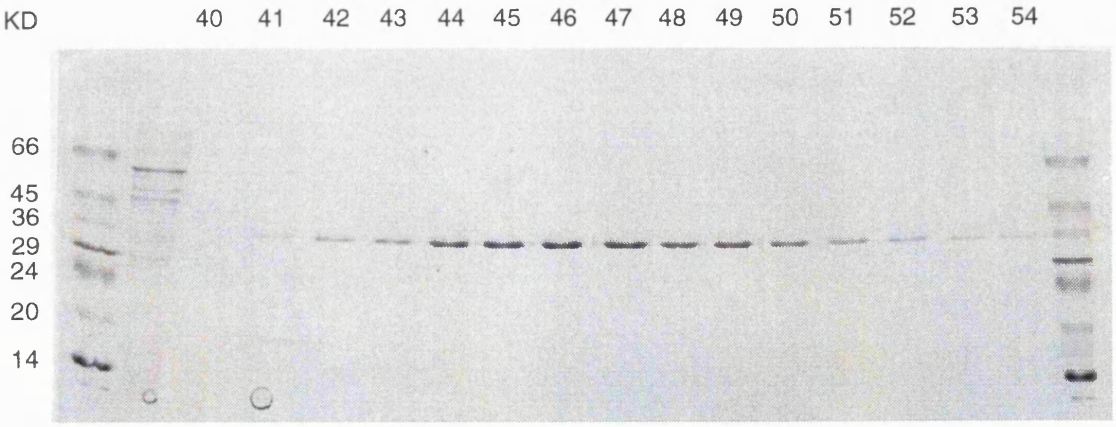
KD
40 41 42 43 44 45 46 47 48 49 50 51 52 53 54
66
45
36
29
24
20
14

2.2.3 Assay of [^{3}H]GDP binding

The assay medium was composed of 50mM Tris/HCl pH 7.5, 10mM EDTA, 50mM NaCl, 1mM dithiothreitol and 3μM [^{3}H]GDP (5000Ci/mol). The wash buffer was prepared from 50mM Tris/HCl, 50mM NaCl, 5mM $MgCl_2$, pH 7.5. For the assay, 50μl of assay medium was equilibrated in eppendorf tubes at 37°C. The Ras sample (<10μl) to be analyzed was added, mixed gently and incubated at 37°C for 10 minutes. The samples were then transferred to ice and 0.9ml ice-cold wash buffer added. The reaction mix was filtered through a nitrocellulose BA85 filter, washed with wash buffer and the filter placed in a scintillation vial with 8ml of filter count scintillant. The vials were shaken for approximately 10 minutes until the filters had dissolved. The amount of radioactivity bound to Ras was determined using a Beckman LS 3801 liquid scintillation counter.

2.3 Protein characterization

2.3.1 SDS polyacrylamide gel electrophoresis

19.5% separating polyacrylamide gels were prepared according to Laemmli (1970) using 10ml separating gel mix, 40μl 100mg/ml ammonium persulphate and 4μl TEMED. Separating gel mix consisted of 65ml Acrylagel (30% acrylamide), 4.4ml Bis-acrylagel (2% methylene bis-acrylamide) (both from National Diagnostics, Atlanta), 25ml 1.5M Tris/HCl, pH 8.8, 4.6ml water and 1ml of 10% (w/v) SDS. 5% stacking polyacrylamide gels were prepared using 5ml stacking gel mix, 40μl 100mg/ml ammonium persulphate, 4μl TEMED. Stacking gel mix consisted of 8.33ml Acrylagel, 3.25ml Bis-acrylagel, 6.25ml 1M Tris/HCl pH 6.8, 31.7ml water and 0.5ml of 10% SDS. Samples were prepared by addition of a suitable volume of SDS sample buffer (bromophenol blue containing 0.01% β-mercaptoethanol) to the sample material and heating the samples to 90°C for 2-3 minutes. 19.5% gels were run at 4°C under a continuous cooling system, at 40mA, until the bromophenol blue had reached the base of the gel. Gels were fixed in a solution of methanol: acetic acid: water, prepared in the ratio of 5:1:5, for 5 minutes, stained for a further 5 minutes in 0.1% coomassie blue R250 dissolved in the same mixture, and destained in a mixture of 7.5% acetic acid, 5% methanol.

2.3.2 Circular dichroism

Circular dichroism spectra were obtained in both the near-UV (340-250nm) and far-UV (260-180nm) ranges by Dr. Steve Martin at N.I.M.R. Wild type, R1276A and R1391A $NF1_{334}$, were diluted into 20mM Tris/HCl pH 7.5, 1mM $MgCl_2$, 0.1mM dithiothreitol, clarified and the absorption spectra recorded in 10mm cuvettes. Scatter corrected curves (Log(λ) versus Log(Abs) correction to 320nm) were used to determine concentrations; 2.04mg/ml, 1.17mg/ml, 1.07mg/ml for wild-type, R1276A and R1391A $NF1_{334}$ respectively. CD spectra were recorded at room temperature in 10mm cuvettes (near-UV) and demountable 0.1mm cuvettes (far-UV).

2.3.3 Intrinsic tryptophan fluorescence

Intrinsic tryptophan fluorescence was monitored using an excitation wavelength of 290nm. Tryptophan emission scans for wild-type, R1276A and R1391A $NF1_{334}$ were obtained from 290-420nm, using the SLM photon-counting spectrofluorimeter. Samples were diluted in 20mM Tris/HCl pH 7.5, 1mM $MgCl_2$, 0.1mM dithiothreitol, to a final concentration of 10μM. The spectra obtained from all three proteins were compared and the emission maxima noted.

2.3.4 Electrospray mass spectrometry

Electrospray mass spectrometry was carried out by Steve Howell at N.I.M.R. Samples to be analyzed were diluted into sterile distilled water to a concentration of approximately 30-50pmol/μl. Approximately 75pmol of material was injected into the mass spectrometer.

2.3.5 Total protein concentration determinations

2.3.5.1 Biorad protein assay

The Biorad protein assay (Biorad Laboratories, UK) is a modified version of the Bradford assay, (Bradford, 1976) and is suitable for measuring between 4 and 40μg of protein. Samples for analysis were prepared by mixing 0.8ml of water with up to 50μl of protein

(or for larger sample volumes, a total of 0.8ml of sample plus water) and 0.2ml Biorad dye reagent, in 1ml disposable plastic cuvettes. The components were allowed to equilibrate for 5 minutes before measuring the absorbance at 595nm using a Perkin-Elmer Lamda 7 UV/Vis spectrophotometer. A standard curve was prepared by monitoring the absorbance at 595nm of known concentrations of gamma globulin. Unknown protein concentrations were read directly from the standard curve. It was noted that the protein concentration of Ras as determined by the Biorad assay differed by a predetermined factor of 1.6 (Lowe *et al*, unpublished results) from that determined by an aminoacid analyzer. Therefore, any Ras concentration measurements determined using the Biorad assay were divided by 1.6 to obtain the absolute Ras concentration.

2.3.5.2 Absorbance at A_{280}

Absolute measurements of protein concentration were obtained by measuring the absorbance of a solution of purified protein at 280nm using the Perkin-Elmer Lambda 7 UV/Vis spectrophotometer. An initial background scan was obtained by placing 100µl of an appropriate buffer into a quartz cuvette and scanning the absorbance between 220 and 400nm. The buffer was then replaced with the protein of interest and a similar scan performed. The background absorbance at 280nm was subtracted from the sample absorbance at 280nm and the protein concentration calculated using the appropriate extinction coefficient (ϵ). $NF1_{334}$ and GAP_{344} concentrations were determined using the calculated extinction coefficients of these proteins at 280nm (Gill and Von Hippel, 1989; $32.32mM^{-1}\ cm^{-1}$ for $NF1_{334}$ and $15.1mM^{-1}\ cm^{-1}$ for GAP_{344}).

2.4 Preparation of lipids and DPH-carboxylic acid

All fatty acids and phospholipids were purchased from Sigma. Arachidonic acid was dissolved in ethanol (Spectrosol grade, BDH) to form a stock solution at 40mM. Appropriate dilutions were made in ethanol, and aliquots of these added to the experiments such that the final concentration of ethanol was not more than 2%, and in general was chosen to be 1%. All other fatty acids were prepared in the same manner.

Phospholipids, dissolved in chloroform, were evaporated to dryness in a glass vial under a stream of nitrogen gas. The thin layer of lipid was suspended in 20mM Tris/HCl pH 7.5 and sonicated at 4°C for 30 seconds at a final concentration of approximately 1mM. Stock solutions of DPH carboxylic acid (*p*-((6-phenyl)-1,3,5-hexatrienyl)benzoic acid) were obtained by dissolving in ethanol to a final concentration of 0.2mM, and thereafter stored in the dark to prevent degradation of the fluorophore.

2.5 Preparation of Ras.nucleotide complexes

Ras.GTP or Ras.[^{3}H]GTP complexes were prepared by nucleotide exchange in the presence of a GTP regenerating system (Skinner *et al*, 1994). This method essentially involves the use of pyruvate kinase which catalyzes the conversion of phosphoenolpyruvate to pyruvate with the consequent phosphorylation of GDP to GTP.

2.5.1 Ras.[^{3}H]GTP and Ras.GTP

A radiolabelled complex was prepared by incubating 100µl of H-Ras (166) or [Leu61] H-Ras (166) with the following components: 25µl [^{3}H]GTP (110µci); 10µl of 200mM phosphoenolpyruvate in water; 0.1µl of 1M KCl; 10µl of 3M ammonium sulphate dissolved in 10mM Tris/HCl pH 7.5. A Ras.GTP complex was prepared by incubating 100µl H-Ras (166) or [Leu61] H-Ras (166) with the following components: 5µl 200mM phosphoenolpyruvate in water; 5µl of 5mM GTP; 1.5µl [^{3}H]GDP (0.7µci); 0.1µl of 1M KCl; 8.5µl 3M ammonium sulphate in 10mM Tris/HCl pH 7.5. Oxidized dithiothreitol is a contaminant which absorbs at 280nm and obscures the GDP peak using HPLC methods. [^{3}H]GDP was incorporated into the reaction mixture to enable the GDP peak to be visualized on the radioactivity trace. The reaction components were gently mixed and upon addition of 7µl pyruvate kinase (Sigma type VII p7768 in glycerol) the reaction was transferred to 37°C and incubated for 30 minutes. The progress of the reaction was followed with time by the transferral of 1µl of reaction mix at 15 and 30 minute intervals into eppendorf tubes containing 50µl HPLC buffer (88% K_2HPO_4/KH_2PO_4 pH5.9 containing 2.25mM TBA). The extent of conversion of GDP to GTP was determined by

HPLC analysis (as detailed in section 2.6.1). Once the conversion was complete, usually after a total of 30 minutes, the reaction was stopped and all sample tubes were transferred to ice.

Unbound nucleotide was removed by centrifugal gel filtration using a sephadex G-25 (SF) column. The column was prepared by packing 2.5ml of a sephadex suspension (pre-swelled in equilibration buffer; 10mM Tris/HCl pH7.5, 1mM dithiothreitol, 0.1mM $MgCl_2$) into a 1ml disposable syringe supported by a polystyrene plug at the base. The packed column was equilibrated by spinning in a Hereaus refrigerated bench centrifuge at 2000rpm for 2 minutes at 4°C. 200µl of equilibration buffer was applied to the top of the column, which was then spun under exactly the same conditions. This procedure was repeated until the volume of buffer applied was equal to the volume eluted. The reaction mixture was applied to the top of the column and the column centrifuged as before. Approximately 90% of the applied protein was eluted at this stage at approximately 90% of the applied protein concentration. Addition of a further 50-100µl of equilibration buffer and respinning the column, resulted in the remainder of the protein being eluted in a diluted form. The concentration of Ras.GTP was determined by Biorad assay and absorbance at 280nm.

2.5.2 Ras.mantGTP

2.5.2.1 Synthesis of triethylammonium bicarbonate (TEAB)

$$(C_2H_5)_3N + CO_2 + H_2O \rightarrow (C_2H_5)_3NH^+ + HCO_3^-$$

The preparation of a 1M solution of TEAB requires 140ml of distilled triethylamine per litre of a final solution. Triethylamine (TE) was distilled, from which only the middle 80% of the distillate was subsequently used. To 140ml distilled triethylamine, 500ml cold distilled deionized water was added. CO_2 was bubbled through the solution at 4°C until the pH fell to between 7.5 and 7.6. The solution was made up to 1litre with cold distilled deionized water to give a 1M solution of TEAB. TEAB was stored at 4°C for no longer

than 1-2 months since the pH gradually rises with time, and it was used for the purification of mantGTP.

2.5.2.2 Preparation of 2' (3')-*O*-*N*-methylanthraniloylguanosine 5'-triphosphate, (MantGTP)

The methodology used to synthesise 2' (3')-*O*-*N*-methylanthraniloyl derivatives of GTP was essentially the same as that used by Hiratsuka (1983), with modifications described by Neal *et al* (1990).

Guanosine 5' triphosphate (0.27mmole), was dissolved in 4ml of water at 37°C. The pH was adjusted to 9.6 with 1M NaOH, and 0.54 mmole of methylisatoic anhydride added with continuous stirring. The reaction mixture was kept at a constant pH of 9.6 by titrating in 1M NaOH, until the reaction reached a point where the pH ceased to drop, and was therefore considered to be complete. Addition of 1M HCl enabled the pH of the reaction mixture to be reduced to 7.6, a prerequisite for the purification procedure. Purification of mantGTP involved dilution of the crude products to 50ml with 10mM triethylamine bicarbonate (TEAB), prior to loading onto a DEAE-bicarbonate column (36cm x 3cm). MantGTP, amongst other components, were eluted from the column at a flow rate of approximately 100ml h^{-1}, by means of a linear gradient which consisted of 3 litres of 10mM to 0.6M TEAB. Fractions were collected every 10 minutes. Detection of nucleotide and mant fluorophore was achieved by monitoring the eluant for absorbance at 254 and 350nm respectively. MantGTP was located in the fourth peak to be eluted from the column. Fractions from this peak were pooled in three batches and evaporated to dryness in a rotary evaporator at 37°C. Residual TEAB was removed by repeated additions of methanol and subsequent evaporation to dryness. MantGTP residue was then dissolved in a small volume of water, approximately 4ml, and the concentration determined using the extinction coefficient for mantGTP of 5.7mM^{-1} cm^{-1} at 350nm. Pools 1, 2 and 3 were calculated to be 6.9mM, 18.2mM and 2.6mM respectively. The final product was stored at -20°C. HPLC analysis (as detailed in section 2.6.1) of the mantGTP was carried out to determine the level of contamination by GDP and hence the purity.

Pools 2 and 3 were found to be 98% pure, however, pool 1 contained significant contamination by mantGDP, and hence was only 81% pure.

2.5.2.3 Preparation of Ras.mantGTP

Ras.mantGTP complexes were prepared for use in stopped-flow experiments as described by Eccleston *et al* (1993). For the reaction, 0.14μmoles H-Ras (166) was incubated at room temperature for 10 minutes with a 50-fold excess of mantGTP (7.0μmoles) and fast exchange buffer (FEB), consisting of 50mM Tris/HCl pH 7.5, 40mM EDTA and 200mM ammonium sulphate, so that the total volume did not exceed 1ml. The exchange reaction was quenched by addition of 40mM $MgCl_2$. Separation of Ras.mantGTP from unbound mantGTP was achieved by passing the reaction mix down a G25 sephadex PD10 column (Pharmacia) equilibrated in 20mM Tris/HCl pH 7.5, 1mM $MgCl_2$, 0.1mM dithiothreitol at 4°C. The progress of both components through the column was monitored by UV illumination. Pure Ras-bound mantGTP, present in the first fluorescent band, was eluted from the column with equilibration buffer. The concentration of the Ras.mantGTP complex was determined from the absorbance of the complex at 350nm ($\epsilon_{mantGTP}$ = 5.7 mM^{-1} cm^{-1}). Approximate concentrations of Ras.mantGTP were in the range of 40-50μM.

2.6 Analysis of nucleotide bound to Ras

2.6.1 GTP/GDP resolution by HPLC

HPLC separation of mantGTP and mantGDP was required in order to assess the extent of Ras.mantGTP hydrolysis in certain experiments. Separation of mantGDP and mantGTP was achieved by anion exchange HPLC on a Partisil-10 SAX column (Whatman) eluting with 0.6M ammonium dihydrogen phosphate buffer pH 4.0, containing 25% (v/v) methanol. Samples to be analyzed were diluted into this buffer to a final concentration of 10μM, of which 10μl was loaded onto the column at a flow rate of 1.5ml min^{-1}. Separation of nucleotides was followed by monitoring the fluorescence of the mant-moiety with excitation at 366nm and emission at 440nm. MantGDP was eluted from the column at approximately 4.5min followed by the mantGTP which is eluted from the column after

9-10min.

2.6.2 [^{3}H]GTP / [^{3}H]GDP resolution by HPLC

[^{3}H]GTP and [^{3}H]GDP were quantified by HPLC separation using ion-pair chromatography on a Lichrosorb RP18 (5-μm particle size; 250 x 4 mm) column eluting isocratically at 1ml min^{-1} with degassed HPLC running buffer (12% acetonitrile; 88% tetrabutylammonium hydroxide (TBA) (2.25mM) dissolved in 56mM potassium phosphate buffer, pH5.9) essentially as described by Pingoud *et al* (1988). Samples of Ras.[^{3}H]GTP and Ras.[^{3}H]GDP to be analyzed were diluted into HPLC running buffer and 50μl loaded onto the column using a hamilton syringe. Radionucleotides were detected and quantified by in-line mixing with scintillant using a Berthold radiochemical detector. The ratio of GDP to GTP was assessed by measuring the area under the GDP and GTP peaks observed on the radioactivity trace.

2.7 Fluorescence measurements

2.7.1 Steady state fluorescence

Measurements were performed on a Perkin-Elmer LS-50B spectrofluorimeter at 30°C. Experiments were performed in 20mM Tris/HCl pH 7.5, 1mM $MgCl_2$, 0.1mM dithiothreitol. A single position water thermostatted holder for 10mm quartz cuvettes was used in most experiments, but in cases where simultaneous data acquisition was required for a series of samples, the four-position, motor driven, water thermostatted cell holder was used in place of the single cell holder. Light source was supplied by a pulsed xenon discharge lamp. For experiments in which a large increase in fluorescence was expected, the excitation and emission wavelengths and the emission slit widths were chosen such that the increase in fluorescence observed was within the instruments fluorescence detection limits.

2.7.2 Critical micellar concentration (CMC) determination

CMC was determined by two independent procedures, one based on light scattering, the other based on fluorescence changes of DPH carboxylic acid. In both cases the experiments were performed in 20mM Tris/HCl, pH 7.5, 1mM $MgCl_2$, 0.1mM dithiothreitol at 30°C. The use of light scattering to measure the critical micellar concentration of lipids is based on the principle that as the particle size of a lipid suspension in a cuvette increases, the light scattering component increases proportionately. In theory, the light scattering component will be small in solutions of monomeric lipids, but as the lipid concentration increases and micelles are formed, the light scattering component will increase, giving rise to a sigmoidal plot, in which the point at which the light scattering rises steeply corresponds to the concentration at which micelles are formed. Fatty acids were disolved in ethanol and titrated into buffer such that a maximum of 2% ethanol was present. Light scattering was monitored in the Perkin-Elmer LS 50B fluorimeter at 500nm. The CMC was taken to be the concentration of lipid at which a sharp discontinuity occurred in the light scattering *versus* concentration graph.

Alternatively, CMC was determined by titrating the lipid in the concentration range 0-100μM, into a solution of 1μM DPH carboxylic acid and was taken to be the concentration of lipid at which a discontinuity occured in the graph of fluorescence intensity *versus* concentration of lipid added (Serth *et al*, 1991).

2.8 Catalytic activity measurements

2.8.1 Ras.GTP hydrolysis

The rates of GAP_{344} or $NF1_{334}$ stimulated Ras.GTPase were measured by incubating a stoichiometric normal Ras.[^{3}H]GTP complex with catalytic amounts of the appropriate GAP, in the presence and absence of lipid. Incubations were performed in 20mM Tris/HCl pH7.5, 1mM $MgCl_2$, 0.1mM dithiothreitol at 25°C for 10 minutes. The assay was started upon addition of 10μl Ras to all eppendorfs to give a final concentration of approximately 7μM. Final concentrations of GAP_{344} and $NF1_{334}$ were 0.040μM and 0.014μM. The concentrations of GAPs were chosen so that in the absence of inhibitor the maximum extent of Ras.GTP hydrolysis was 80% and generally was less and so gave a reasonable estimate of the true initial rate. The extent of hydrolysis in the absence of GAP_{344} or

$NF1_{334}$ was negligible as compared to that in its presence. At the end of the incubation, samples were transferred to ice and immediately quenched by addition of 50µl Stop buffer (3ml HPLC running buffer plus 7µl of 5M HCl). The reaction components were mixed, frozen in dry-ice and stored at -70°C prior to HPLC analysis to determine the extent of conversion of Ras.[^{3}H]GTP to Ras.[^{3}H]GDP.

Fatty acids were added from ethanolic stocks such that the final concentration of ethanol was less than 2%. Phospholipids were added from buffered stocks. Control experiments showed that 2% ethanol had no effect on the GTP hydrolysis reaction.

2.8.2 Ras.mantGTP hydrolysis

2.8.2.1 Intrinsic rate of hydrolysis of H-Ras

Fluorescence measurements of the Ras.mantGTPase were made using an SLM 8000 photon-counting spectrofluorimeter (SLM instruments, Urbana, IL) using the mant group as the source of fluorescence. Excitation of the mant fluorophore was at 366nm with a 0.5nm slit width and fluorescence emission was monitored at 440nm with a 16nm slit width. A solution of Ras.mantGTP in 20mM Tris/HCl pH 7.5, 1mM $MgCl_2$, 0.1mM dithiothreitol, ± 100mM NaCl, was placed in a 1cm path length quartz fluorescence cuvette, at 30°C. A solution of mantGDP in buffer was used as a reference sample to check the stability of the lamp. At timed intervals, manual fluorescence readings of both the Ras.mantGTP and mantGDP samples were taken, 100µl aliquots were removed and the extent of mantGTP hydrolysis was measured by HPLC analysis. The GTPase activity of Ras in each sample was quenched by the addition of 50µl of 10% perchloric acid followed by 50µl of 4M sodium acetate to neutralize the acid. Samples were then rapidly frozen in dry ice. The phosphorylation state of the nucleotide was analyzed by anion exchange HPLC as described in section 2.6.1.

2.8.2.2 $NF1_{334}$-activated Ras.mantGTP hydrolysis

Measurements of fluorescence changes associated with the interaction of Ras with $NF1_{334}$ are fast and has necessitated the use of a stopped-flow instrument. Hydrolysis was measured under single and multiple turnover conditions. Experiments were performed either on the home-built stopped flow fluorimeter (Eccleston *et al*, 1993) or on a Hi-Tech SF-61 instrument. Both instruments employed 100watt Hg arc lamps as the light source. For the home-built instrument, excitation of the mant fluorophore was through a 365nm interference filter and emission monitored through a Wratten 47B filter. For the Hi-Tech SF-61, excitation of the mant fluorophore was through a monochromator at 365nm and emission was monitored through a Wratten 47B filter. Approximately 35µl of each solution was used per reaction in the home-built apparatus whereas 135µl was used in the Hi-Tech SF-61 instrument. Stock solutions of Ras.mantGTP were diluted into 20mM Tris.HCl pH7.5; 1mM $MgCl_2$; 0.1mM dithiothreitol +/- 100mM NaCl buffer to which arachidonic acid was also added when required. This Ras solution was mixed in the instrument with an equal volume of a solution of $NF1_{334}$ in buffer, again containing arachidonic acid if required. All concentrations subsequently quoted are after mixing. Any deviations from these standard conditions are stated in the individual results chapters.

2.9 Scintillation proximity assay (SPA)

The Scintillation proximity assay enables direct measurements of interactions between proteins by monitoring the binding of the two components at equilibrium, (figure 15). The standard assay was performed in 96 well sample plates (Wallac Part No. 1450-401) as described by Skinner *et al* (1994), except that the buffer was altered to 20mM Tris/HCl, in order to maintain consistency with previous experimental work. The assay was performed by first adding 80µl of a solution of 0.2µM NF1-GST in 20mM Tris/HCl pH 7.5, 2mM dithiothreitol to each well, followed by 120µl of a mixture of 0.07µM Ras.[^{3}H]GTP, 0.031mg/ml of anti-glutathione transferase antibody and 4.2mg/ml of Protein A PVT SPA beads (Amersham) suspended in 20mM Tris/HCl pH 7.5, 2mM dithiothreitol, 2mM $MgCl_2$. Lipids were either added to 80µl of the solution of NF1-GST, followed by addition of 120µl of a mixture containing SPA beads, anti-GST and radiolabelled Ras, or were added directly to the complete mixture of 200µl of these two

components. Each of these reagents was prepared in a siliconized glass vial to reduce losses of proteins by adsorption. The plates were sealed, shaken for 1h at 22°C, centrifuged at 2000rpm for 2 minutes and counted in a Wallac 1450 Microbeta scintillation counter set up in SPA mode. Lipids were added from ethanol stocks such that the volume of ethanol added at no time exceeded 1% of the final assay volume.

Figure 15: Diagrammatic representation of the NF1/ Ras scintillation proximity assay

An anti-glutathione transferase antibody is bound to protein A-coated fluoromicrosphere beads. The NF1-GST fusion protein binds to the antibody through the GST domain and in addition interacts through the neurofibromin catalytic domain with the Ras.[^{3}H]GTP complex. Scintillation occurs when the Ras is brought into close proximity with the beads. Binding of Ras to NF1-GST is monitored by an increase in light emission.

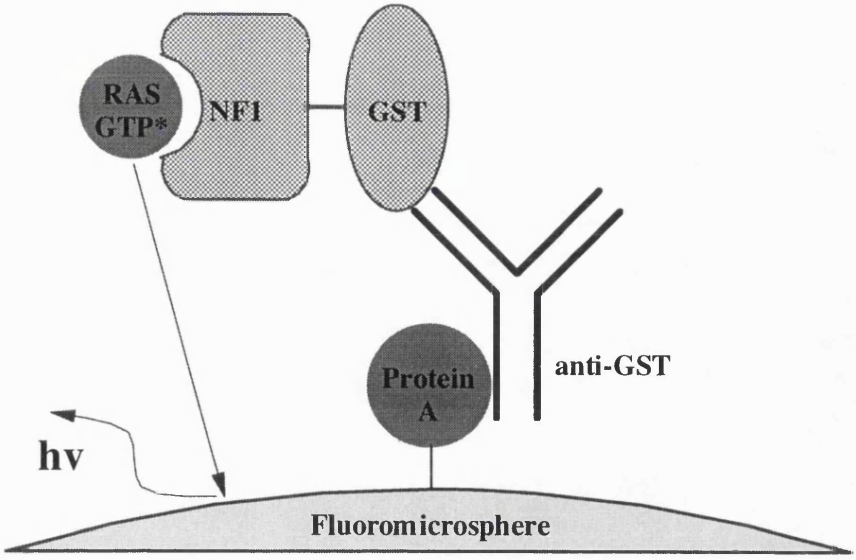
RAS
GTP*
NF1
GST
anti-GST
Protein
A
hv
Fluoromicrosphere

Chapter 3 - Mechanism of Inhibition by Arachidonic Acid of the Catalytic Activity of Ras GTPase-Activating Proteins

3.1 Introduction to the experiments

An increasingly large number of proteins have now been identified as effectors for Ras signalling pathways. Both p120-GAP and neurofibromin have many properties expected from a Ras effector, in that they bind preferentially to Ras.GTP rather than Ras.GDP, and interact with Ras at the effector binding region (Boguski and McCormick, 1993; Marshall, 1994; Lowe and Skinner, 1994). Evidence both for and against roles for p120-GAP and NF1 in downstream signalling pathways has been discussed in section 1.3. Although there is much experimental data to support a role of p120-GAP in signalling, other than just to downregulate Ras, most of the data for NF1 is consistent purely with a negative regulatory role (Lowe and Skinner, 1994). However, an effector role for both p120-GAP and NF1 was suggested by Bollag and McCormick (1991) based on their data on the differential inhibition of p120-GAP and NF1 by lipids.

An early response to mitogenic stimulation is a rapid alteration in levels of various lipids such as diacylglycerol, phosphatidic acid, arachidonic acid and metabolites of phosphatidylinositol (Fleischman *et al*, 1986; Tsai *et al*, 1989b; Yu *et al*, 1990; Rozengurt, 1991; Ferguson and Hanley, 1991; Sumida *et al*, 1993; ; Falasca and Corda, 1994). Phosphatidic acid itself has been demonstrated to act as a mitogen in specific cells (Yu *et al*, 1988). These mitogenic lipids (i.e produced in response to a mitogenic stimulus) have been shown to mediate their effects through the Ras signalling pathway. The signalling pathway involved in epidermal growth factor-stimulated arachidonic acid release was found to be similar to the signalling pathway for mitogenic responses to epidermal growth factor, and requires Ras activation, (Warner *et al*,1993). In addition, binding of lysophosphatidic acid to its LPA receptor has been observed to activate MAP kinases by a G-protein coupled pathway that requires both Ras and p74Raf-1, (Howe and Marshall, 1993). The mitogenic activity of phosphatidic acid, is reported to be Ras-dependent, in as much as it is blocked by microinjection of the neutralizing anti-Ras antibody, Y13-259, (Yu *et al*,1988). This was a key observation since it indicated that Ras proteins were infact controlled by phospholipid metabolites. Subsequent data on the inhibition of p120-GAP and NF1 by lipids *in vitro*, suggested that the mitogenic effects of these lipids might

be mediated by the inhibition of either GAP, leading to an increase in Ras.GTP and hence an activation of Ras.

Arachidonic acid, has been shown to inhibit the Ras GTPase-stimulating activity of the catalytic domain of NF1 (Bollag and McCormick, 1991; Golubic *et al*, 1991; Han *et al*,1991; Golubic *et al*, 1992; Bollag *et al*, 1993), the catalytic domain of p120-GAP (Serth *et al*, 1991; Golubic *et al*, 1992) and full length p120-GAP (Tsai *et al*, 1989a; Tsai *et al*, 1989b; Bollag and McCormick, 1991; Serth *et al*, 1991; Han *et al*, 1991). Arachidonic acid was observed to differentially inhibit types I and II NF1, (Uchida *et al*, 1992), with type II inhibited to a greater extent than type I. Inhibition of GAP activity in a cytosolic extract by arachidonic acid is reportedly antagonized by the presence of diacylglycerol, (Homayoun *et al*, 1993), potentially providing a means for diacylglycerol to indirectly modulate the interaction between Ras and GAP.

Phosphatidic acid, phosphatidylinositol, phosphatidylinositol-4-monophosphate and phosphatidylinositol-4,5-diphosphate, have been reported to inhibit the activity of the catalytic domain of NF1, (Tsai *et al*, 1989a; Tsai *et al*, 1989b; Bollag and McCormick, 1991), but were unable to inhibit full length p120-GAP. In particular, Bollag and McCormick (1991) reported that phosphatidic acid inhibited NF1 catalytic activity but did not block binding of Ras to NF1. This led to an hypothesis in which NF1 was a Ras effector, modulated by lipid inhibition.

Unsaturated fatty acids with different chain lengths such as linoleic, elaidic and palmitoleic acids, have been reported to inhibit the GTPase-stimulating activity of full-length p120-GAP and the catalytic domain of p120-GAP, (Serth *et al*, 1991). Saturated fatty acids such as palmitic, arachidic and stearic acids, were unable to inhibit the activity of full length p120-GAP and the catalytic domain of NF1, (Serth *et al*, 1991; Bollag and McCormick, 1991).

Prostaglandins, the eicosanoid metabolites of arachidonic acid, have also been reported to modulate the activity of full length p120-GAP, (Han *et al*, 1991). $PGF_{2\alpha}$ and PGA_2 were found to stimulate GAP activity, whereas PGI_2 was inhibitory. This suggested that Ras may be controlled by the relative concentrations of eicosanoids, generated by the lipoxygenase and cyclooxygenase pathways. Stimulation of phospholipaseA2 by growth factors would produce an immediate rise in arachidonic acid and lipoxygenase metabolites that could inhibit RasGAP and activate Ras. Induction of the cyclooxygenase pathway at a later stage would lead to the production of prostaglandins that could stimulate RasGAP and inactivate Ras.

Furthermore, mitogenic lipids such as arachidonic acid, (Serth *et al*, 1991) and phosphatidic acid, have been shown to physically associate with the GAP molecule, (Yu *et al*, 1990; Tsai *et al*, 1990; Tsai *et al*, 1991; Serth *et al*, 1991).

Large differences in potency and specificity of inhibition of GAPs by lipids have been observed by the various researchers in this field. For example, Bollag and McCormick (1991) reported that arachidonic acid inhibits p120-GAP with an I_{50} of approximately 200μM, and the catalytic domain of NF1 (NF1-GRD) with an I_{50} of approximately 30μM, whereas Golubic *et al* (1991) reported that the catalytic domains of NF1 and p120-GAP were both inhibited by arachidonic acid with I_{50}s between 8 and 16μM. With phosphatidic acid, Bollag and McCormick (1991) found no inhibition of p120-GAP, but an I_{50} of approximately 10μM with NF1-GRD. In contrast, Golubic *et al* (1991) found little or no inhibition by phosphatidic acid of the catalytic domains of either NF1 or p120-GAP. This diversity appears to be a reflection of the different experimental procedures, conditions and components utilized. Thus, there are reports showing that the inhibitory potency differs dependent upon whether full length or catalytic domains are expressed (Golubic *et al*, 1991; Serth *et al*, 1991; Bollag *et al*, 1993). Also the assay conditions and the procedure by which the lipids are solubilized appear to be important factors. Lipids have been introduced either as pure micelles or as mixed micelles with apparently differing results (Tsai *et al*, 1989b; Serth *et al*, 1991). Furthermore, some assays have been

performed in the presence of detergents (Bollag and McCormick, 1991; Serth *et al*, 1991) whereas others have not (Golubic *et al*, 1991; Serth *et al*, 1991). In this study, it was decided to keep the experimental system as simple as possible by performing experiments with pure lipids in the absence of detergents.

The aim of these studies was to investigate the mechanism of arachidonic acid inhibition of both p120-GAP and NF1 to see if it was different from that reported for phosphatidic acid. It was hoped that these studies would alleviate many of the inconsistencies in the literature, which in the past have led to a confusing overall picture of the role of lipids in regulation of Ras activity. Consistent analysis of the inhibition of GAP stimulatory activity by lipids using detergent-free assay conditions and pure lipid micelles, enabled the factors which cause the most experimental variability i.e. the presence of detergents and the formation of micelles by lipids, to be controlled, thus allowing salient observations to be made about the mechanism of inhibition by arachidonic acid.

3.2 Results

3.2.1 Inhibition of GAP_{344} and $NF1_{334}$-activated Ras.GTPase by arachidonic acid

The effect of arachidonic acid on the GTPase-stimulating activities associated with the catalytic domains of both p120-GAP (GAP_{344}) and neurofibromin ($NF1_{334}$) was investigated. The rates of GAP_{344} or $NF1_{334}$-stimulated Ras.GTPase were measured as described in detail in section 2.8.1. Arachidonic acid was added to these standard GAP activity assays from an ethanolic stock. Under these conditions, arachidonic acid (C20:4) inhibited $NF1_{334}$ and GAP_{344} activities with I_{50} values of 5 and 10μM respectively (figure 16). The inhibitory potency was much higher than that reported by Bollag and McCormick (1991). One experimental difference was noted, which was that these workers did not use pure lipid, but included the detergent Nonidet P40 in all assays so that presumably mixed micelles were formed. The inhibitory potency of arachidonic acid on p120-GAP has been previously assayed (Lowe *et al*, unpublished data) in the presence of 0.1% Nonidet P40. Only 18% inhibition of p120-GAP activity by 30μM arachidonic acid was observed,

whereas in the absence of Nonidet P40 nearly complete inhibition was obtained at that concentration. This suggested that partitioning of arachidonic acid into detergent micelles, reduced its inhibitory potency. All subsequent experiments were performed with lipids in the absence of detergent.

With GAP_{344}, the relationship between inhibitor concentration and inhibition achieved was not strictly hyperbolic, but rather was sigmoid (figure 16a), but with $NF1_{334}$ the data was more variable. More pronounced sigmoid curves had been observed with GAP by Serth *et al* (1991). In those experiments the steep phase occurred at approximately 40-50μM, which was the same as their experimentally determined critical micellar concentration (CMC) (i.e the concentration at which lipids form micellar structures). In my experiments, the CMC for arachidonic acid was determined either by light scattering of arachidonic acid itself (figure 17) or by the use of DPH fluorescence enhancement (data not shown), and found to be around 40μM. However, this concentration was clearly much higher than the I_{50}'s seen under my experimental conditions, demonstrating that micelle formation is not required for inhibition.

These studies have demonstrated that arachidonic acid is a potent inhibitor of $NF1_{334}$ and GAP_{344}-stimulated Ras.GTPase activity under steady state conditions. However, the method itself is limiting since the initial rate is estimated from only a single time point after 10 minutes. A continuous record of the hydrolysis process was obtained by replacing GTP by its close analogue mantGTP, as Ras.mantGTP hydrolysis is accompanied by a 10% decrease in fluorescence (Neal *et al*, 1990). Thus, nucleotide hydrolysis was readily followed by monitoring a rate of change in fluorescence of a stoichiometric complex of the fluorescent nucleotide analogue, 2'(3')*O*-*N*-methylanthraniloyl-GTP (mantGTP) bound to H-Ras, using a stopped-flow spectrofluorimeter. Using this approach, the mechanism of inhibition by arachidonic acid was investigated further by examining how the inhibitor affected the affinity of H-Ras.mantGTP for $NF1_{334}$ (K_d or K_m) and the maximal rate of hydrolysis (k_{cat}) under single and multiple turnover conditions.

Figure 16: Inhibition of the GAP_{344} and $NF1_{334}$ -stimulated Ras.GTPase by arachidonic acid

A solution containing 7μM Ras.[^{3}H]GTP was incubated with either 0.040μM GAP_{344} (Panel A) or 0.014μM $NF1_{334}$ (Panel B) in 20mM Tris/HCl, pH 7.5, 1mM $MgCl_2$, 0.1mM dithiothreitol at 25°C. Arachidonic acid (●) was added to the mixture from a stock solution in ethanol. After 10 minutes, the extent of [^{3}H]GTP hydrolysis was measured by HPLC separation of [^{3}H]GTP from [^{3}H]GDP. Inhibition of GTPase activity was calculated as a percentage relative to incubations without arachidonic acid.

(a)

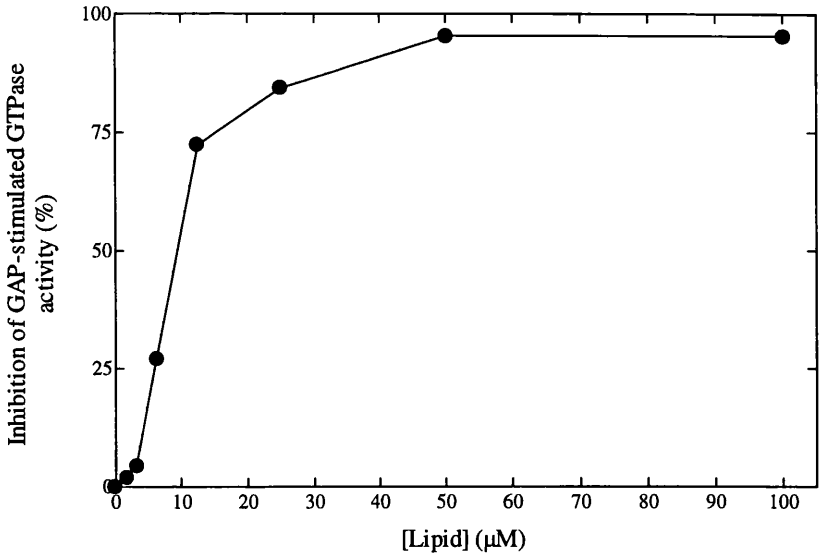
Inhibition of GAP-stimulated GTPase activity (%)
100
75
50
25
0
0
10
20
30
40
50
60
70
80
90
100
[Lipid] (μM)

(b)

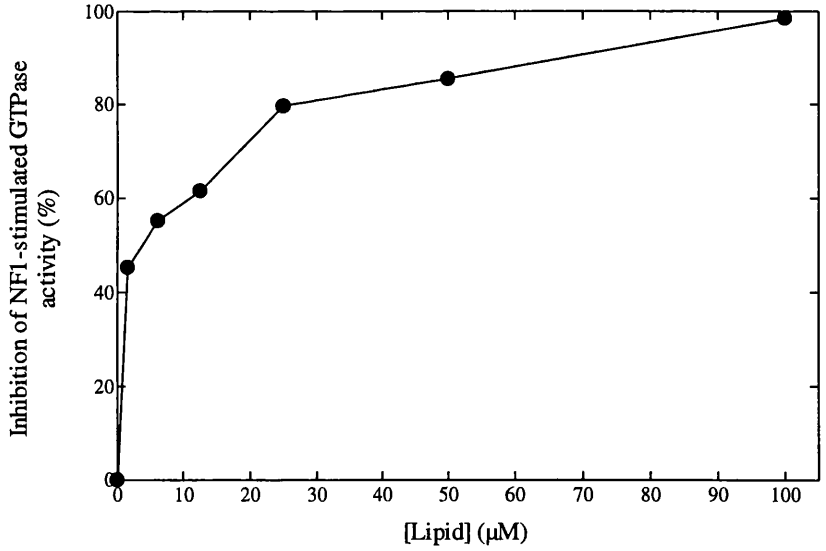
Inhibition of NF1-stimulated GTPase activity (%)
100
80
60
40
20
0
0
10
20
30
40
50
60
70
80
90
100
[Lipid] (μM)

Figure 17: Determination of the critical micellar concentration (CMC) of arachidonic acid by light scattering

Arachidonic acid, was added to a solution of 20mM Tris/HCl pH 7.5 containing 1mM $MgCl_2$ and 0.1mM dithiothreitol, prewarmed to 30°C in a 1cm path length quartz cuvette. 5μM increments were added from an ethanol stock, so as to produce a volume change of <2%. Light scattering was monitored at an excitation wavelength of 500nm, in the LS-50B fluorimeter. The point at which a sharp discontinuity occurred in the light scattering versus concentration graph was taken to be the CMC.

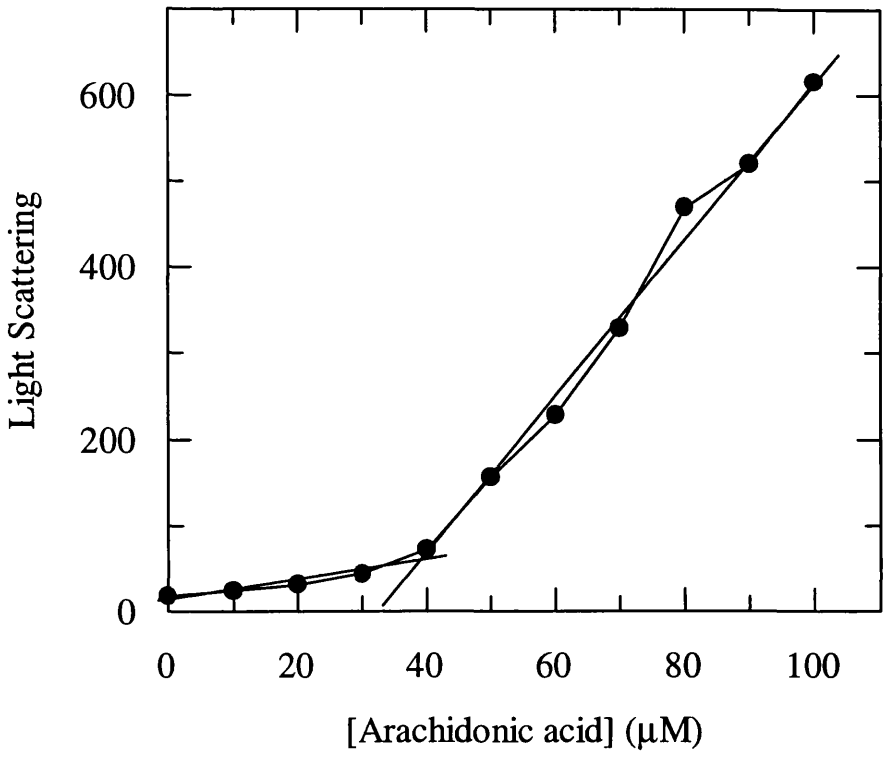
Light Scattering
600
400
200
0
0
20
40
60
80
100
[Arachidonic acid] (μM)

3.2.2 Single turnover kinetic analysis of the inhibition of $NF1_{334}$-activated Ras.mantGTPase by arachidonic acid

The affinity of interaction between Ras and GAPs and the maximal turnover rate of GAP can be directly determined under single enzyme turnover conditions, created by using a large excess of $NF1_{334}$ over Ras.GTP. The experimental procedures are greatly simplified by using mantGTP as a close analogue of GTP. This method has previously been successfully employed in other GTPase and ATPase mechanisms such as myosin ATPase, (Trentham *et al*, 1976) and the elongation factor Tu GTPase, (Eccleston *et al*, 1985), in addition to the Ras GTPase, (Eccleston *et al*,1993; Moore *et al*.1993). Mant derivatives of guanine nucleotides have been reported to behave as close analogues of the parent nucleotides, (Eccleston *et al*,1993) and the modification of the ribose moiety has little effect on the binding affinity of Ras with nucleotide (Eccleston *et al*,1989).

Experiments were performed as described by Eccleston *et al* (1993) except that H-Ras rather than N-Ras was used. H-Ras.mantGTP (1μM) was mixed with 5μM $NF1_{334}$ in 20mM Tris/HCl pH7.5, 1mM $MgCl_2$, 0.1mM dithiothreitol and the fluorescence monitored with time. A biphasic fluorescence change was observed (figure 18).The stopped-flow traces were similar to those obtained with N-Ras (Eccleston *et al*, 1993) in that they showed an initial rapid increase in fluorescence proposed to represent initial complex formation between Ras and $NF1_{334}$ (Jenkins, 1996) followed by an exponential decrease in fluorescence with a rate constant of 7.5 s^{-1}, representing the hydrolysis reaction.This rate was not increased by higher concentrations of $NF1_{334}$ indicating that the concentration of $NF1_{334}$ employed was high relative to the K_d for binding of Ras to $NF1_{334}$. This was further substantiated by the observation that the amplitude of the fluorescence intensity decrease remained relatively constant throughout the experiments. No reduction in the rate constant of Ras.mantGTP hydrolysis was observed when 20μM arachidonic acid was included in the reaction mixture, suggesting that arachidonic acid is not a purely non-competitive inhibitor.

If arachidonic acid is a competitive inhibitor of Ras binding to $NF1_{334}$, it would be

anticipated that the level of inhibition would depend upon the concentrations of Ras and NF1 and the affinity of interaction. In order to maintain pseudo-first order kinetics it was decided not to alter the concentrations of proteins, but rather to alter the affinity of interaction. It has previously been shown that the K_d for Ras binding to $NF1_{334}$ is 0.2μM at low ionic strength (Brownbridge *et al*, 1993) but it can be raised by addition of NaCl (Eccleston *et al*, 1993; Brownbridge *et al*, 1993). I therefore examined the effect of NaCl on the interaction of Ras with $NF1_{334}$ and the inhibition by arachidonic acid.The effect of NaCl on the observed pseudo-first order rate constant was qualitatively and quantitatively very similar to that observed with N-Ras (Eccleston *et al*, 1993), showing an increase in the observed rate constant (k_{obs}) up to around 100-150mM NaCl, at which it was approximately $17s^{-1}$, followed by a decrease such that at 500mM NaCl it was around $3s^{-1}$ (figure 19). This is consistent with NaCl increasing the K_d (weakening affinity) of Ras binding to $NF1_{334}$ and also increasing the rate constant of the cleavage step causing an overall weakening of the interaction between $NF1_{334}$ and Ras.mantGTP (Eccleston *et al*,1993). The effect of 20μM arachidonic acid on the observed rate constant at 100, 150, 300, 500 or 1000mM NaCl was examined. With 100 and 150mM NaCl, again no inhibition was observed. However, at 300mM NaCl, 24% inhibition was obtained. With higher concentrations of NaCl, the inhibition declined so that at 500mM and 1000mM NaCl, it was 20% and 15% respectively. At 500mM NaCl, the dependence of k_{obs} on the concentration of $NF1_{334}$ was linear in the range 5-20μM, suggesting that at this salt concentration, the K_d for binding of Ras to $NF1_{334}$ was >>10μM, such that the Ras was not saturated with $NF1_{334}$ under these experimental conditions.

It was possible that the lack of inhibition by arachidonic acid in the single turnover experiments, as compared to the initial multiple turnover experiments outlined previously (section 3.2.1), might have been as a result of the different procedures used to monitor hydrolysis i.e. conversion of [^{3}H]GTP to [^{3}H]GDP versus decrease in fluorescence of the Ras.mantGTP complex. Alternatively, the inhibitory effects of arachidonic acid might be mediated at a point further on in the hydrolysis cycle, such as the phosphate release step, or the point at which the Ras.mantGDP is released from the $NF1_{334}$.

Figure 18: Effect of arachidonic acid on the rate of $NF1_{334}$-catalyzed Ras.mantGTP hydrolysis, under single turnover conditions

Stopped-flow fluorescence experiments were performed in which 1μM H-Ras.mantGTP was mixed with 5μM $NF1_{334}$ at 30°C in the home-built stopped-flow instrument. Both sets of data were fitted to single exponentials to yield observed first order rate constants. All proteins were in 20mM Tris/HCl pH 7.5, 1mM $MgCl_2$, 0.1mM dithiothreitol. Fluorescence recordings are shown for experiments in the absence of arachidonic acid (trace a) and with 20μM arachidonic acid added to the $NF1_{334}$ solution (trace b).The solid lines indicate the best fits to single exponentials with rate constants of $7.5s^{-1}$.

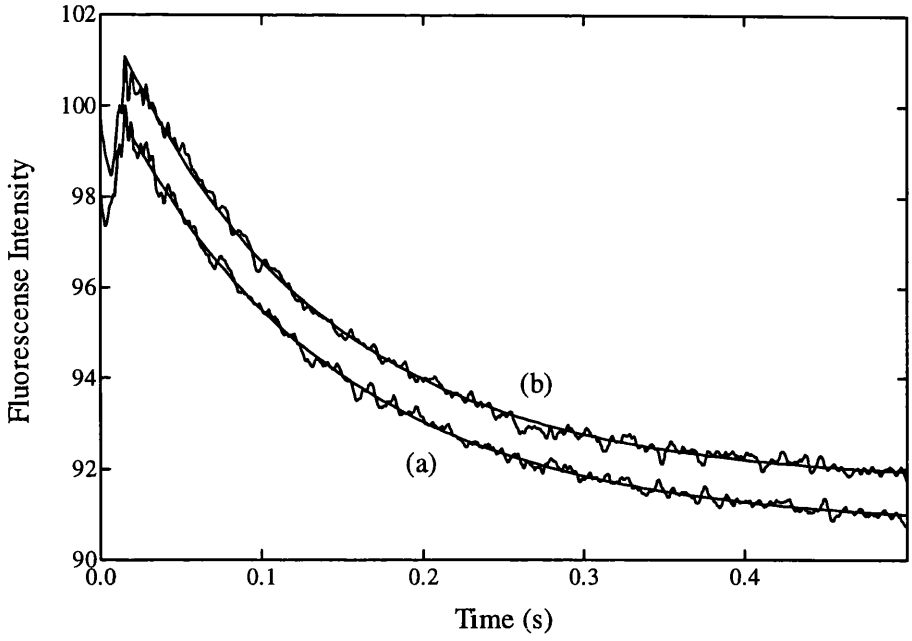
Fluorescense Intensity
102
100
98
96
94
92
90
0.0
0.1
0.2
0.3
0.4
Time (s)
(b)
(a)

Figure 19: The effect of NaCl concentration upon the rate of $NF1_{334}$ -stimulated H-Ras.mantGTP hydrolysis under single turnover conditions

H-Ras.mantGTP (1μM) was rapidly mixed with 5μM $NF1_{334}$ at 30°C in a home-built stopped- flow fluorimeter, in 20mM Tris/HCl pH 7.5, 1mM $MgCl_2$, 0.1mM dithiothreitol, supplemented with increasing concentrations of NaCl. The change in fluorescence intensity decreased exponentially over time and could be analyzed as single exponentials and the observed pseudo-first order rate constants plotted against [NaCl]. Data points are derived from the average of 5 separate traces ± standard errors.

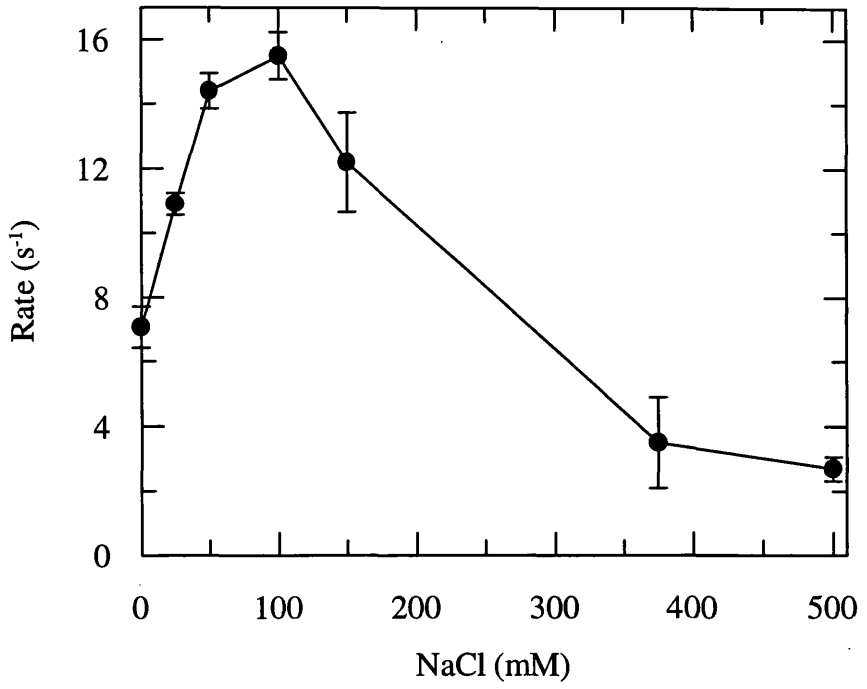
16
12
8
4
0
Rate (s^{-1})
0
100
200
300
400
500
NaCl (mM)

Therefore, the effects of arachidonic acid on the $NF1_{334}$-induced decrease in Ras.mantGTP fluorescence was measured under multiple turnover (steady state) conditions, i.e. with the concentration of $NF1_{334}$ well below the concentrations of Ras.mantGTP.

3.2.3 Steady-state kinetic analysis of the inhibition of $NF1_{334}$-activated Ras.mantGTPase by arachidonic acid

Hydrolysis was measured under multiple turnover conditions in which catalytic amounts of $NF1_{334}$ ($\leq$ 10% the molar concentration of Ras) were mixed with H-Ras.mantGTP. In these experiments, the initial rate of fluorescence change was measured directly from the photomultiplier output *versus* time plot in units of volts s^{-1}.To compensate for changes made in the applied photomultiplier voltage to allow measurements over a wide range of concentrations of Ras.mantGTP, it was neccessary to establish the relationship between volts and molar concentration of Ras.mantGTP. This was done in parallel experiments in which the Ras.mantGTP solution of known concentration was mixed in the stopped-flow fluorimeter with a solution consisting of 500μM GDP, 40mM EDTA and 400mM ammonium sulphate. This caused complete displacement of bound mantGTP from the Ras within 20 seconds and the amplitude of the resultant fluorescence decrease was measured. This allowed the relationship between total Ras.mantGTP and photomultiplier output to be established. The conversion of Ras.mantGTP to Ras.mantGDP results in about a 10% decrease in fluorescence. Although this was not precisely determined in our experiments we used a figure of 10% to allow us to calculate rates in units of molar concentration.

The initial rate as a function of concentration, (k_{init} μM s^{-1}) was obtained by multiplying the rate in volts s^{-1}, by the substrate concentration. The procedure for acquiring data traces was aimed at minimizing the effects of photobleaching on the sample and obtaining an accurate measurement of the amplitude of the fluorescence change. Initially, 3 pushes of H-Ras.mantGTP against 20mM Tris/HCl pH7.5, 1mM $MgCl_2$, 0.1mM dithiothreitol were carried out, with the shutter allowing light to pass into the sample chamber, closed. With H-Ras.mantGTP flushed through the system, the shutter was opened momentarily to enable a 4 volt signal to be set, so that the starting fluorescence was at 4 volts. With

the shutter closed, the syringe containing the buffer was replaced with one containing $NF1_{334}$ and 2 pushes of H-Ras.mantGTP against $NF1_{334}$ were carried out to waste. Immediately, 3 x 20 second pushes were carried out, with the shutter open, and the data collected. The $NF1_{334}$ syringe was then replaced with one containing a solution of 500μM GDP, 40mM EDTA and 400mM ammonium sulphate. With the shutter closed, one push to waste was carried out. The shutter was then opened and 3 x 20 second pushes were carried out and the data collected (shown in figure 20-trace c). Both syringes and the sample chamber were then flushed through with buffer prior to the following run. Arachidonic acid was added to both syringes since higher final concentrations of the fatty acid could be achieved without exceeding the CMC at any time during the experiment.

Using 1μM H-Ras.mantGTP and 0.1μM $NF1_{334}$, the initial rate of H-Ras.mantGTP hydrolysis was calculated from figure 20-trace a to be 1.1 μM s^{-1}. This corresponds to a turnover rate of $11s^{-1}$, similar to that seen under single turnover conditions, and consistent with the Ras.mantGTP concentration being well above the K_m and the $NF1_{334}$ being fully active. Inclusion of 20μM arachidonic acid reduced the initial rate of H-Ras.mantGTP hydrolysis by 45% (figure 20-trace b). This contrasted with the complete absence of inhibition under single turnover conditions, but was still lower than that obtained using Ras.[^{3}H]GTP (figure 16). The shape of the reaction progress curves in the absence of arachidonic acid (figure 20-trace a) was typical for the substrate concentration being higher than the K_m, i.e. a K_m of $<<1\mu M$, (linear phase followed by a sharp decrease in rate), whereas with arachidonic acid, the progress curve (figure 20-trace b) fitted a single exponential consistent with arachidonic acid increasing the value of the K_m.

The inhibitory potency of arachidonic acid was influenced by ionic strength. The effect of NaCl on the inhibition induced by 20μM arachidonic acid is shown in figure 21. In the absence of arachidonic acid, a bell-shaped curve, of initial rates against [NaCl] in which the initial rate increased from 1.1μM s^{-1} to 1.3μM s^{-1} at 100mM NaCl and decreased at higher concentrations of NaCl, (100mM-1000mM), was obtained, (figure 21). With increasing concentrations of NaCl, up to 300mM NaCl, an increase in inhibition by

arachidonic acid was seen, shown in figure 21, as an inset, but further increases in NaCl concentration resulted in a decrease in the level of inhibition. At 150mM NaCl, arachidonic acid inhibited with an I_{50} of approximately 20μM. Thus, 20μM arachidonic acid inhibited by 45% with no added NaCl, 80% with 300mM NaCl and 41% with 1000mM NaCl. With 300mM NaCl, the progress curves fitted single exponentials as expected when the substrate concentration was at or below the K_m, consistent with NaCl raising the K_m for Ras.

The biphasic effect on inhibition with increasing ionic strength is likely to be caused by an increase in the K_m for Ras.mantGTP resulting in more potent inhibition countered by a reduction in the affinity for arachidonic acid.

To measure values of K_m and k_{cat}, initial rates of hydrolysis were measured varying both the concentrations of H-Ras.mantGTP and of arachidonic acid. The experiments were performed in the presence of 50mM NaCl such that the K_m was around 1μM, low enough so that it was possible to saturate with the amounts of Ras available and high enough so that substrate concentrations at least 5-fold above the concentration of $NF1_{334}$ could be used.

Increasing concentrations of H-Ras.mantGTP were incubated with 0.1μM $NF1_{334}$ in 20mM Tris/HCl pH7.5, 1mM $MgCl_2$, 0.1mM dithiothreitol, supplemented with 50mM NaCl. Experiments were performed in the presence of 0, 12, 18, or 24 μM final concentrations of arachidonic acid, (figure 22). The data at each concentration of arachidonic acid were fitted by non-linear regression to the michaelis-menten equation to obtain values for K_m and k_{cat}.

Figure 20: Effect of arachidonic acid on the rate of $NF1_{334}$-catalyzed H-Ras.mantGTP hydrolysis, under multiple turnover conditions

Stopped-flow fluorescence experiments were performed in which 1μM H-Ras.mantGTP was mixed with 0.1μM $NF1_{334}$ at 30°C. Both proteins were in 20mM Tris/HCl, pH 7.5, 1mM $MgCl_2$, 0.1mM dithiothreitol. Fluorescence recordings are shown for experiments in the absence of arachidonic acid (trace a) and with 20μM arachidonic acid added to both the $NF1_{334}$ and Ras.mantGTP solutions (trace b). To convert fluorescence changes into molar concentrations, in separate experiments 1μM H-Ras.mantGTP was mixed with 500μM GDP dissolved in 20mM Tris/HCl, pH 7.5, 1mM $MgCl_2$, 0.1mM dithiothreitol, containing additionally 40mM EDTA and 400mM ammonium sulphate to promote rapid nucleotide exchange (trace c) (as described in section 3.2.3). The inset shows the initial phases of traces a and b on a larger scale.

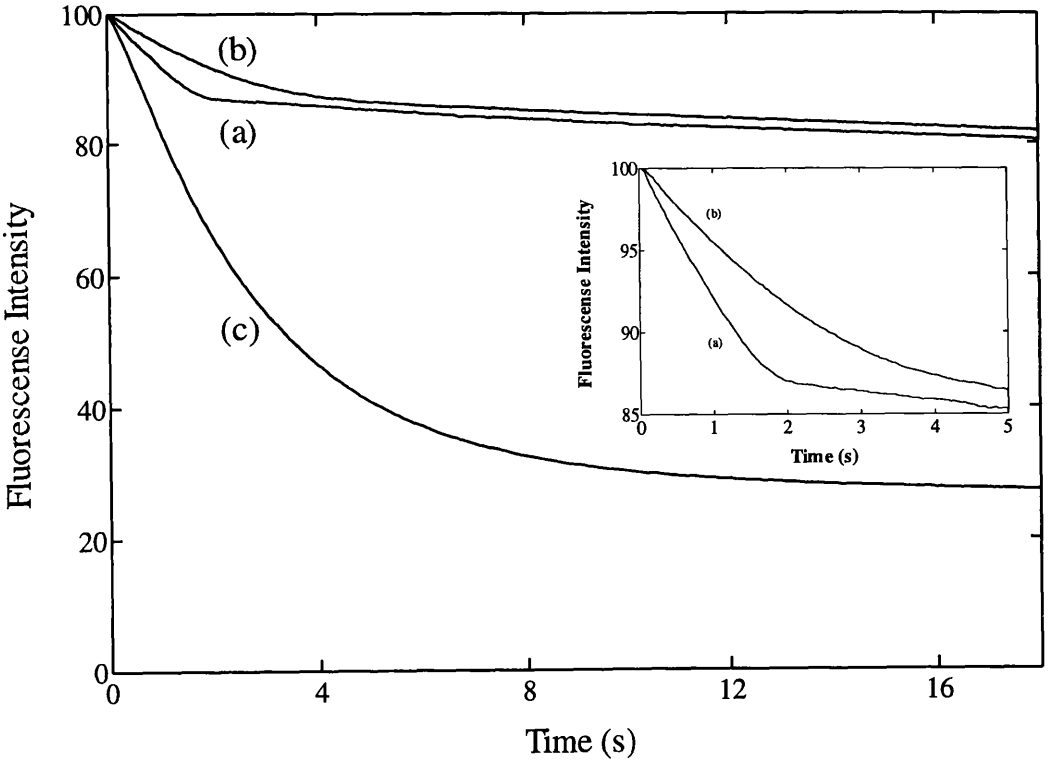
Fluorescense Intensity
100
80
60
40
20
0
0
4
8
12
16
Time (s)
(b)
(a)
(c)
Fluorescense Intensity
100
95
90
85
0
1
2
3
4
5
Time (s)
(b)
(a)

Figure 21: The effect of NaCl on the inhibition of $NF1_{334}$-catalyzed Ras.mantGTPase by arachidonic acid

Experiments similar to those described in figure 20 were performed in the presence of the indicated concentrations of NaCl and initial rates (k_{init}) of Ras.mantGTPase were measured, both in the absence (●) and presence (○) of 20μM arachidonic acid, which was added to both syringes. The inset shows the effect of NaCl on the percentage reduction in initial rates caused by arachidonic acid

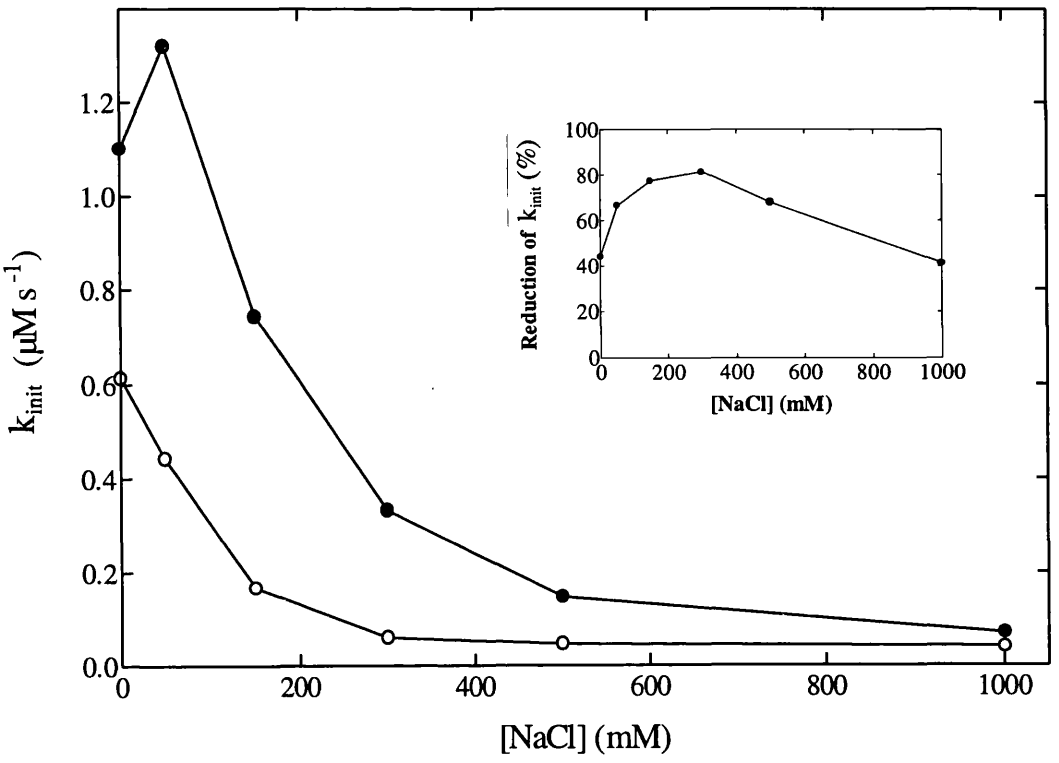
1.2
1.0
0.8
0.6
0.4
0.2
0.0
k_{init} ($\mu M\ s^{-1}$)
0
200
400
600
800
1000
[NaCl] (mM)
100
80
60
40
20
0
Reduction of k_{init} (%)
0
200
400
600
800
1000
[NaCl] (mM)

Figure 22: Steady state kinetic analysis of the inhibition of $NF1_{334}$ -catalyzed H-Ras.mantGTPase by arachidonic acid

Initial rates (k_{init}) of $NF1_{334}$-catalyzed H-Ras.mantGTP hydrolysis were measured in experiments similar to those shown in figure 20. Increasing concentrations of H-Ras.mant GTP were added into 0.1μM $NF1_{334}$ in 20mM Tris/HCl pH 7.5, 1mM $MgCl_2$, 0.1mM dithiothreitol, supplemented with 50mM NaCl at 30°C. Experiments were performed with 0μM (●), 12μM (○), 18μM (■), or 24μM (▲) arachidonic acid. The data at each concentration of arachidonic acid was fitted by non-linear regression to the Michaelis-Menten equation to obtain values of K_m and k_{cat}. In (a) and (b) the solid lines are based on these constants. K_m at 0, 12, 18 and 24μM arachidonic acid were 1.1, 1.3, 1.8 and 3.8μM, respectively. k_{cat} at 0, 12, 18 and 24μM arachidonic acid were 2.6, 2.3, 1.7 and 1.1μM.s^{-1}, respectively. In (c) the ratio of K_m to k_{cat} obtained from this curve-fitting has been plotted against the concentration of arachidonic acid used.

(a)

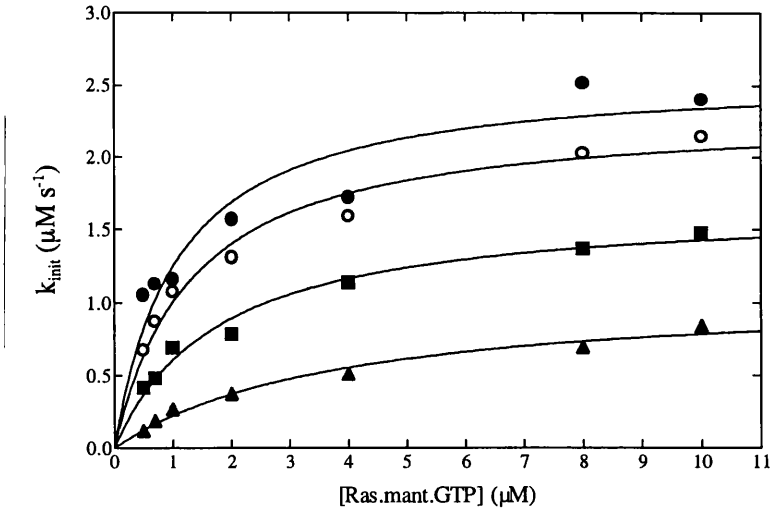
3.0
2.5
2.0
1.5
1.0
0.5
0.0
0 1 2 3 4 5 6 7 8 9 10 11
k_{init} ($\mu M\ s^{-1}$)
[Ras.mant.GTP] (μM)

(b)

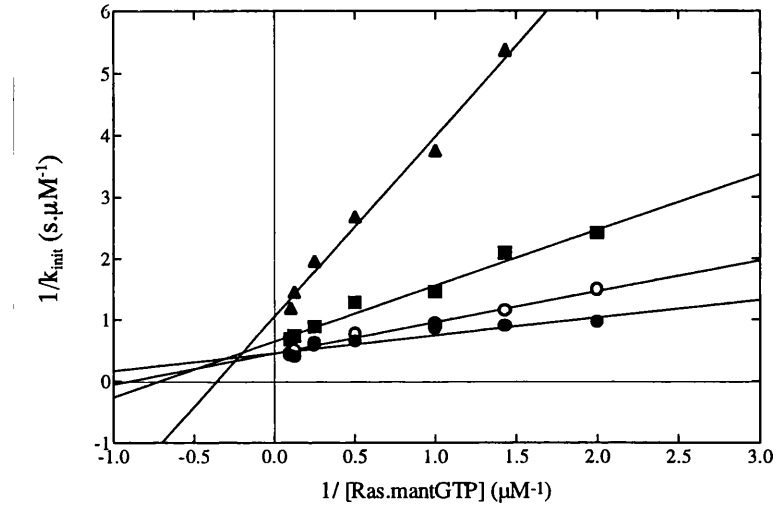
6
5
4
3
2
1
0
-1
-1.0 -0.5 0.0 0.5 1.0 1.5 2.0 2.5 3.0
$1/k_{init}$ ($s.\mu M^{-1}$)
1/ [Ras.mantGTP] (μM^{-1})

(c)

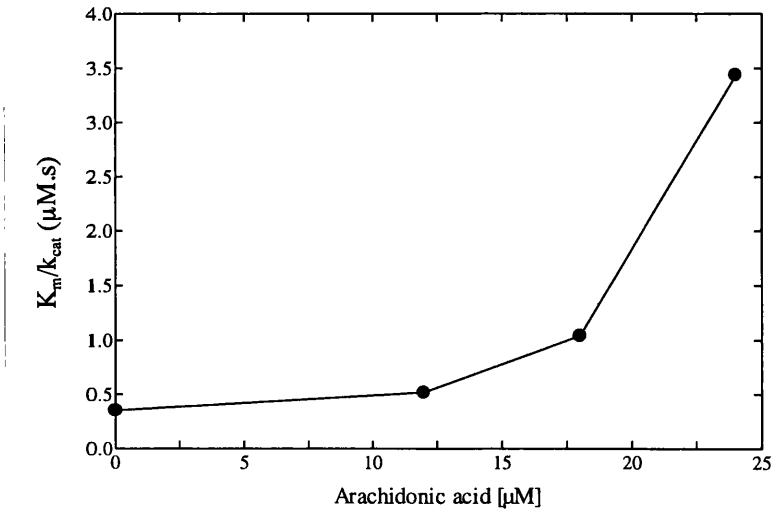
4.0
3.5
3.0
2.5
2.0
1.5
1.0
0.5
0.0
0 5 10 15 20 25
K_m/k_{cat} ($\mu M.s$)
Arachidonic acid [μM]

Table 3: Kinetic characterization of the effect of arachidonic acid on the hydrolysis of H-Ras.mantGTP under steady state conditions

Table showing the effect of arachidonic acid on the hydrolysis of Ras.mantGTP under steady state conditions, ie: 1μM H-Ras.mantGTP and 0.1μM $NF1_{334}$. Values for K_m and k_{cat} ± standard errors were obtained by fitting the data obtained at each concentration of arachidonic acid to the Michaelis-Menten equation, as shown in figure 22.

[AA] (μM)	V_{max} (μM s^{-1})	K_m (μM)
0	2.6 (± 0.2)	1.1 (± 0.3)
12	2.3 (± 0.1)	1.3 (± 0.2)
18	1.7 (± 0.08)	1.8 (± 0.3)
24	1.1 (± 0.09)	3.8 (± 0.8)

The pattern of inhibition displayed in the lineweaver-burk double reciprocal plot (figure 22b) is typical of mixed inhibition in which the inhibitor both decreases k_{cat} and increases K_m. If the data are interpreted as fitting a mixed inhibition model (Segel, 1975) then it can be calculated from the intersection point of the lines, that the K_m (or K_s if the components are in rapid equilibrium) was around 1μM and the αK_m, was approximately 5, where α represents the ratio of K_{iu} to K_{ic} shown in the scheme below.

$$\begin{array}{ccccc} & & K_s & & k_{cat} \\ NF1 + Ras\cdot mantGTP & & \rightleftharpoons & NF1\cdot Ras\cdot mantGTP & \rightarrow NF1 + Ras\cdot mantGDP \\ + & & & + & \\ Lipid & & & Lipid & \\ \updownarrow & K_{ic} & & \updownarrow & K_{iu} \\ NF1\cdot lipid + Ras\cdot mantGTP & & \rightleftharpoons & NF1\cdot lipid\cdot Ras\cdot mantGTP & \\ & & \alpha K_s & & \end{array}$$

This value of α suggests that the mixed inhibition is predominantly of a competitive character, but the uncompetitive component is still significant. In a 'mixed' inhibition system, (Dixon and Webb, 1979) both the k_{cat} and K_m are altered by the inhibitor so that the inhibitor binds both to the enzyme and to the enzyme-substrate complex with unequal affinity. Non-competitive inhibition occurs when $\alpha K_m = K_m$, ie: $\alpha = 1$. Therefore, an α value of ~ 5.0 suggests that inhibition by arachidonic acid is five fold more competitive than uncompetitive, in a 'mixed' inhibition model.

However, the data clearly does not fit this simple model in that the relationship between inhibition and the concentration of arachidonic acid at any fixed concentration of Ras is distinctly sigmoid and plots of either K_m/k_{cat} (figure 22c) or $1/k_{cat}$ against arachidonic acid concentration are non-linear parabolic upwards. A plot of percentage inhibition against

[Substrate] demonstrated that inhibition decreased with increasing substrate concentration, but at no point reached a level of zero inhibition, suggesting that more than one type of inhibition is in operation in this particular system.

3.2.4 Characterization of the interaction of arachidonic acid with $NF1_{334}$ and GAP_{344} using the fluorescent probe DPH-carboxylic acid

As the kinetic mechanism of inhibition of GAP activity by arachidonic acid is complex, other methods were examined to show whether arachidonic acid binds at the Ras binding site, or at some other site, on GAPs. It was postulated that *p*((6-phenyl)-1,3,5-hexatrienyl)benzoic acid (DPH-carboxylic acid), the structure of which is shown in figure 23, might be a sufficiently close analogue of arachidonic acid that it would act as a fluorescent probe of the lipid-binding site.

DPH-carboxylic acid was demonstrated to be an environment-sensitive probe since it exhibited substantial fluorescence enhancement in hydrophobic solvents such as chloroform as compared to that in water. Initial experiments demonstrated an increase in fluorescence of DPH-carboxylic acid (1μM) when mixed with $NF1_{334}$, GAP_{344} or bovine serum albumin (figure 24). At 10μM of each protein, the increase was 16-, 1.6- and 25-fold respectively. The data could be fitted to a simple binding equation, ($A + B \rightleftharpoons AB$) relating fluorescence to the total concentration of added ligand, from which the relevant binding affinities (K_d) could be extracted. The K_d values for the interactions of DPH-carboxylic acid with $NF1_{334}$, GAP_{344} and Bovine Serum Albumin, were calculated to be 2.6μM, 62μM and 0.55μM respectively.

For experiments in which arachidonic acid was included, bovine serum albumin, $NF1_{334}$ and GAP_{344} were used at concentrations below their K_d values to enable arachidonic acid to displace DPH-carboxylic acid from the fatty acid binding site. Arachidonic acid (10μM) abolished the enhancement of fluorescence of DPH-carboxylic acid caused by mixture with albumin, as expected if arachidonic acid competed with DPH-carboxylic acid for

binding to albumin (figure 25). However, at concentrations of arachidonic acid up to 40μM there was no significant reduction in the fluorescence of DPH-carboxylic acid mixed with either $NF1_{334}$ (figure 25) or GAP_{344}. Indeed with GAP_{344}, an increase was seen (discussed later, figure 27). As a control, DPH-carboxylic acid showed a negligible increase in fluorescence upon addition of up to 20μM arachidonic acid. This suggested that with the latter two proteins, the probe was binding at a site distinct from the arachidonic acid-binding site. However, I was still able to use DPH-carboxylic acid as a probe for ligands interacting with GAPs since the fluorescence of the protein-bound probe was sensitive to the addition of ligands.

The fluorescence of a solution containing 1μM DPH-carboxylic acid and 2μM $NF1_{334}$ was dramatically reduced by the addition of Harvey-Ras [Leu61].GTP protein (figure 26a). The reduction in fluorescence was nearly proportional to the concentration of added Ras, with half-maximal effect occurring at about 1μM [Leu61]H-Ras.GTP. This is consistent with a relatively high affinity of interaction of Ras with $NF1_{334}$, as expected for the binding of $NF1_{334}$ to the [Leu61]H-Ras mutant. Since several species were present in this experiment, it was neccessary to determine whether Ras.GTP was binding to $NF1_{334}$ or to the probe. Therefore, Ras.GTP was titrated into a mixture of 2μM DPH-carboxylic acid and 1μM $NF1_{334}$. In this experiment, the curve was shifted to the left with half-maximal reduction occurring at 0.5μM Ras.GTP. This data is consistent with Ras binding to $NF1_{334}$ rather than to DPH-carboxylic acid. As a further control, normal Ras.GDP was titrated into the mixture of DPH-carboxylic acid and $NF1_{334}$, but only 20% reduction in fluorescence occurred at 4μM Ras, consistent with the known weaker affinity of $NF1_{334}$ for Ras.GDP as compared with Ras.GTP. Kirsten-Ras [Val12].GTP, which binds to $NF1_{334}$ with a K_d of approximately 1μM, and is therefore, consistent with an intermediate affinity, gave a shallower curve (data not shown).

Figure 23: Comparison of the structures of (a) arachidonic acid and (b) DPH-carboxylic acid

(a)

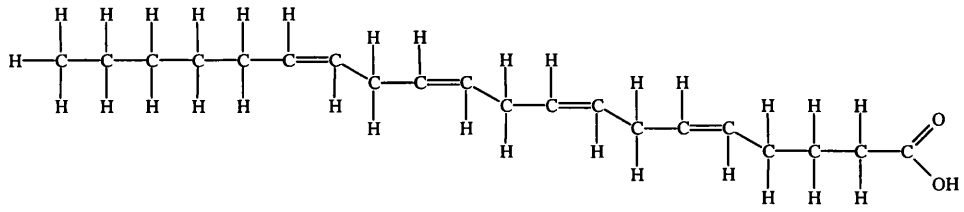

(b)

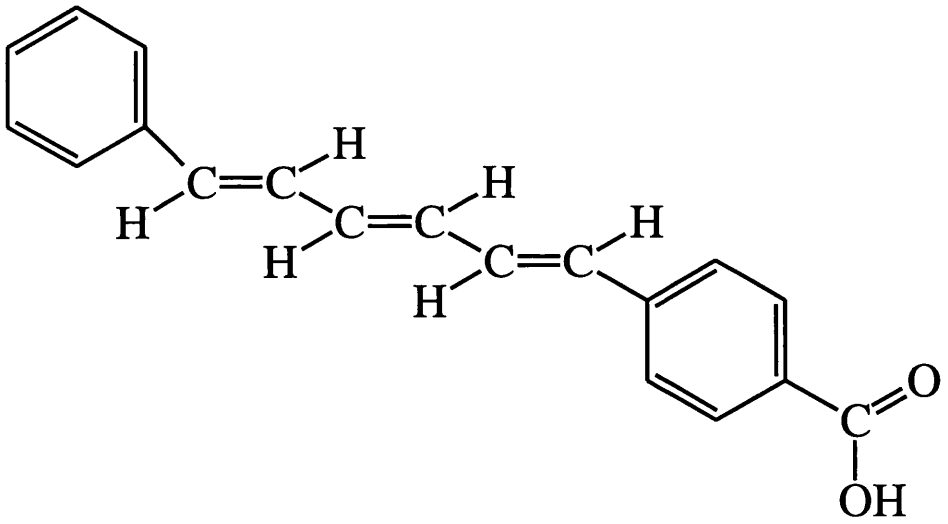

Figure 24: The effect of GAP_{344}, $NF1_{334}$ or bovine serum albumin on the fluorescence of DPH-carboxylic acid

GAP_{344} (■), $NF1_{334}$ (○) or bovine serum albumin (●) was titrated into a solution of 1μM DPH- carboxylic acid dissolved in 20mM Tris/HCl, pH 7.5 such that the concentration of DPH- carboxylic acid was not reduced significantly. Fluorescence was recorded with excitation at 357nm and with emission at 435nm. The data has been normalized on the initial fluorescence so that the fluorescence increases on addition of proteins, are directly comparable. The solid lines through the data shows the best fit to a binding isotherm for simple association of two molecules, with K_d = 2.6, 0.55 and 62μM with $NF1_{334}$, albumin and GAP_{344}, respectively. Data at concentrations of GAP_{344} up to 120μM was obtained but is not shown on this scale for clarity.

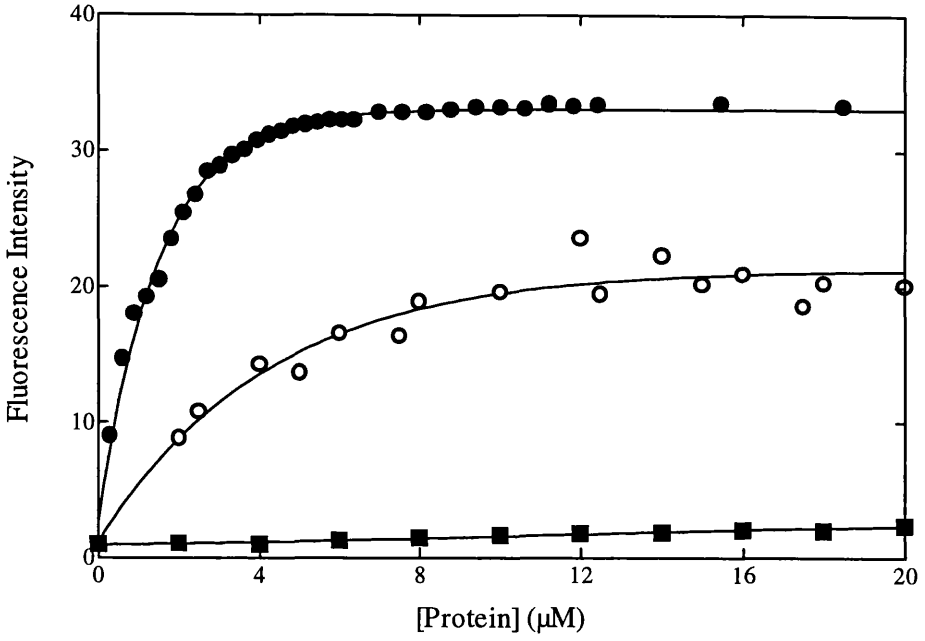
Fluorescence Intensity
40
30
20
10
0
0
4
8
12
16
20
[Protein] (μM)

Figure 25: Effect of arachidonic acid on the fluorescence of a mixture of DPH-carboxylic acid with $NF1_{334}$ or serum albumin

Arachidonic acid, from a stock solution in ethanol, was added to a solution of 1μM DPH-carboxylic acid in 20mM Tris/HCl, pH 7.5, containing either 0.5μM bovine serum albumin (●) or 2μM $NF1_{334}$ (○). The final concentration of ethanol was <1%. Fluorescence was recorded with excitation at 357nm and emission at 435nm. Data was corrected for light scattering caused by proteins and arachidonic acid, and for the fluorescence of 1μM DPH-carboxylic acid in the absence of added protein. The maximum correction was 3.7% and 11.6% of the maximum fluorescence with albumin and $NF1_{334}$ respectively. The corrected fluorescence in the absence of arachidonic acid was taken to be 100. With albumin, this represented 2.9-fold more fluorescence than with $NF1_{334}$.

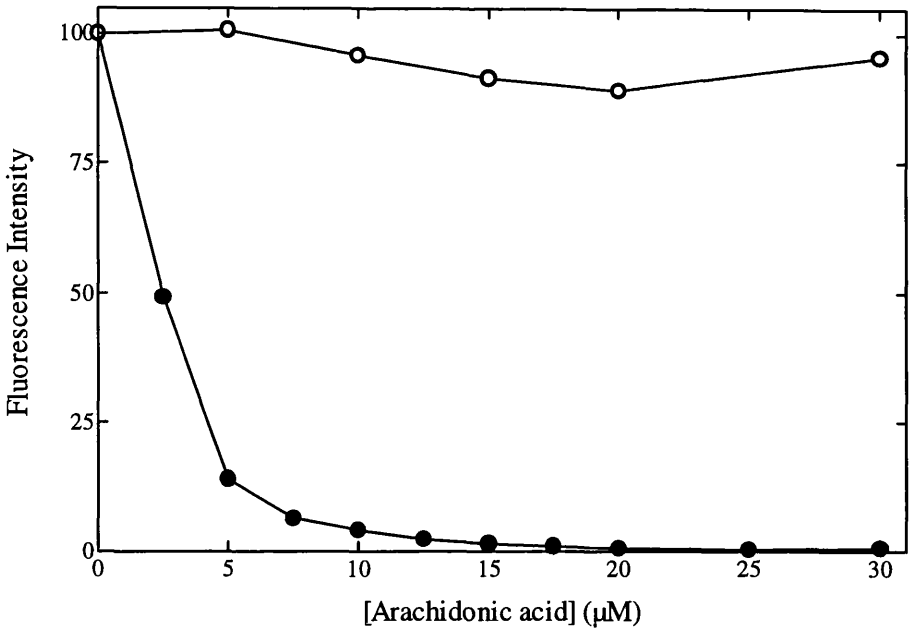
Fluorescence Intensity
100
75
50
25
0
0
5
10
15
20
25
30
[Arachidonic acid] (μM)

These data suggested that the probe was able to monitor the interacton between Ras and NF1. Therefore, the effect of arachidonic acid on the fluorescence changes induced by Ras was examined (figure 26a).

The decrease in fluorescence caused by addition of Ras to the mixture of DPH-carboxylic acid and $NF1_{334}$ was largely abolished by 20μM arachidonic acid, strongly suggesting competition between Ras and the lipid for binding to NF1. However, the dependence of the inhibition on the concentration of arachidonic acid was not hyperbolic (figure 26b). By plotting the reduction in fluorescence at 8μM [Leu61] Ras.GTP in the presence of all concentrations of arachidonic acid, a sigmoidal shaped curve was produced (figure 26b) indicating <10% inhibition of the fluorescence decrease at 5μM arachidonic acid and up to 70% inhibition at 20μM.

Addition of up to 8μM [Leu61]H-Ras.GTP to a mixture of DPH-carboxylic acid and GAP_{344} resulted in no change in fluorescence, and so effects of arachidonic acid could not be monitored. However, as noted above, arachidonic acid caused an increase in the fluorescence of a mixture of DPH-carboxylic acid and GAP_{344} (figure 27-trace a). This increase occurred in two phases both of similar magnitude, one rapid (<<30sec) the other slow. When 20μM arachidonic acid was added to a mixture of 2μM GAP_{344} and 1μM DPH-carboxylic acid, the slow phase could be fitted to a first order rate equation to yield a rate constant of 1×10^{-3} s^{-1} (figure 27-trace a). The magnitude of the fast phase was decreased about 50% by addition of 20μM Ras.GTP (figure 27-trace b). The rate constant of the slow phase was decreased by 80% by 20μM Ras, with no change in its amplitude (figure 27b). Higher concentrations of Ras.GTP did not result in any further reduction suggesting that there were both Ras-dependent and Ras-independent effects.

Figure 26: Effects of [Leu61]Ras.GTP and arachidonic acid on the fluorescence of a mixture of DPH-carboxylic acid and $NF1_{334}$

[Leu61]Ras.GTP was added to a solution of 1μM DPH-carboxylic acid in 20mM Tris/HCl, pH 7.5 and 2μM $NF1_{334}$ containing 0μM (♦), 5μM (○), 10μM (■), 15μM (▲) or 20μM (□) arachidonic acid. Fluorescence was recorded with excitation at 357nm and emission at 435nm. Data was corrected for light scattering caused by proteins and arachidonic acid, and for the fluorescence of 1μM DPH-carboxylic acid in the absence of added protein. The maximum correction was 12.8% of the maximum fluorescence. The corrected fluorescence in the absence of Ras.GTP was taken to be 100. In (b), the effect of arachidonic acid on the observed fluorescence in the presence of 8μM Ras.GTP is shown.

(a)

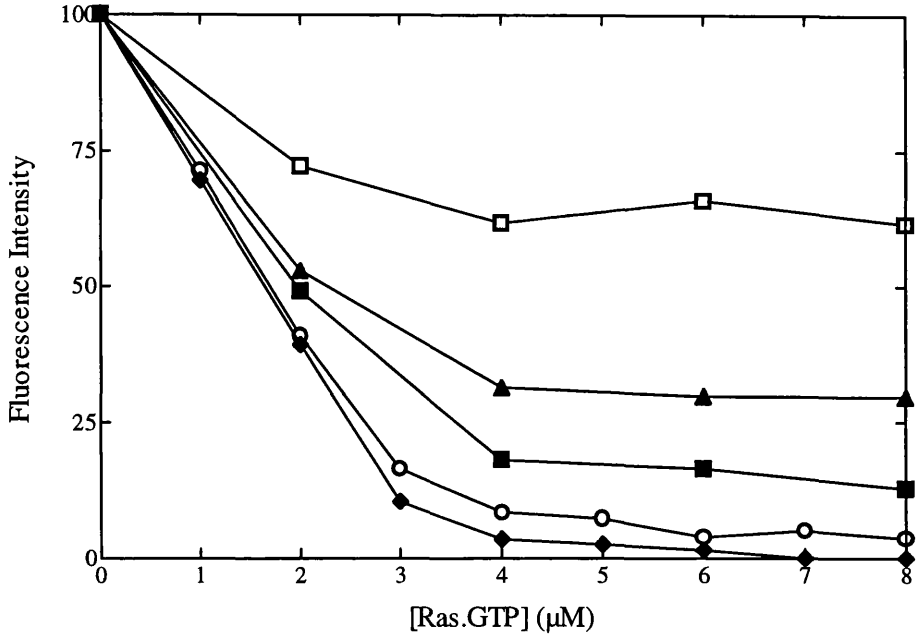
Fluorescence Intensity
100
75
50
25
0
0
1
2
3
4
5
6
7
8
[Ras.GTP] (μM)

(b)

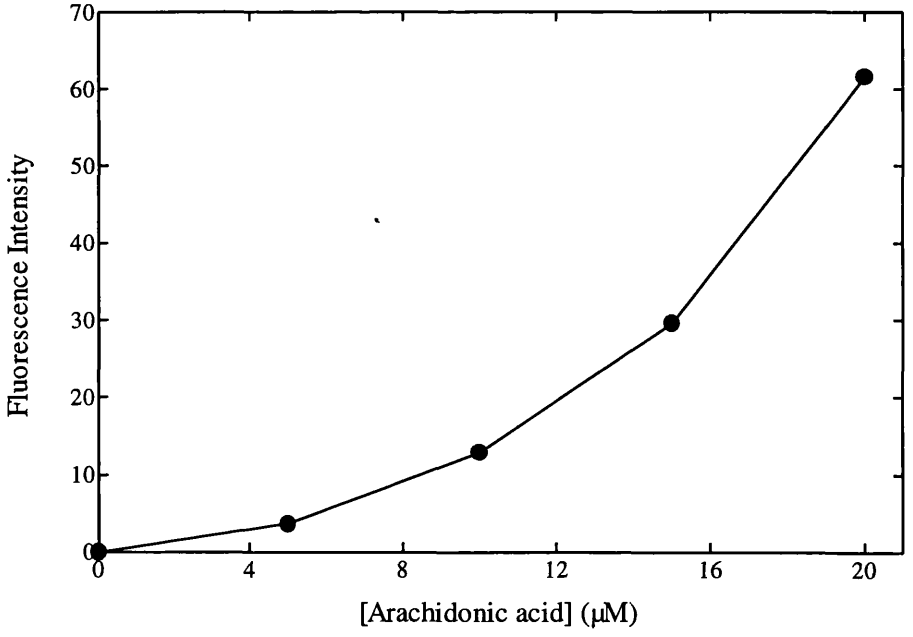
Fluorescence Intensity
70
60
50
40
30
20
10
0
0
4
8
12
16
20
[Arachidonic acid] (μM)

Figure 27: Effect of [Leu61]Ras.GTP on the fluorescence change induced by addition of arachidonic acid to a mixture of DPH-carboxylic acid and GAP_{344}

Arachidonic acid (20μM) was added to a mixture of GAP_{344} (2μM) and DPH-carboxylic acid (1μM) in 20mM Tris/HCl pH 7.5, 1mM $MgCl_2$, 0.1mM dithiothreitol, in the absence (trace a), or presence (trace b) of 20μM [Leu61]Ras.GTP. Fluorescence was recorded with excitation at 357nm and emission at 435nm.

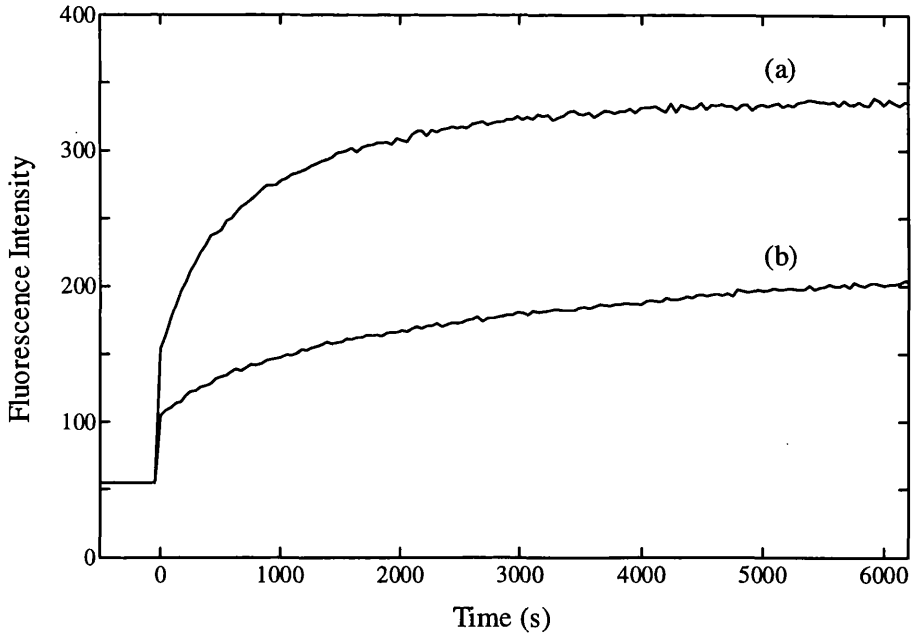
400
300
200
100
0
Fluorescence Intensity
(a)
(b)
0
1000
2000
3000
4000
5000
6000
Time (s)

Therefore, the presence of Ras appeared to prevent the slow increase in the fluorescence of the DPH-carboxylic acid-GAP_{344} mixture, mediated by arachidonic acid. This preventative effect was dependent upon the type and amount of Ras present. As with $NF1_{334}$, the experiments with DPH-carboxylic acid suggested that with GAP_{344} there was some competitive element in the binding of Ras and arachidonic acid to the GAP proteins. However to obtain a more definitive answer to this question, experiments to directly measure the binding of Ras and $NF1_{334}$ were needed.

3.2.5 NF1 / Ras binding scintillation proximity assay

3.2.5.1 Inhibition by arachidonic acid

The data from the kinetic characterization and use of the fluorescent probe suggested that arachidonic acid might, at least in part, be competing with Ras for binding to NF1 or GAP. We therefore, tested by a more direct method, whether arachidonic acid might block binding of Ras to NF1. Using a fluorescence anisotropy assay (Brownbridge *et al*, 1993) to monitor binding of $NF1_{334}$ to Ras.mantGTP, it was found that arachidonic acid reduced the anisotropy of the $NF1_{334}$/tagged Ras mixture back to that of Ras.mantGDP alone. (Brownbridge, G.G., Webb, M.R. and Lowe, P.N., unpublished data). Although this strongly suggested that arachidonic acid was blocking the binding of Ras with NF1, it could not be excluded that arachidonic acid was altering the anisotropy by some other mechanism, such as increasing the local motion of the bound fluorophore.

Therefore, I utilized the recently described scintillation proximity assay procedure (Skinner *et al*, 1994) to monitor directly the binding of Ras.GTP to $NF1_{334}$ and to test the effects of arachidonic acid on this interaction. This assay enables direct measurements of interactions between proteins by monitoring the binding of the two components at equilibrium. The assay involves the use of scintillant beads coated with an acceptor molecule, suspended in aqueous buffer, which are incubated with a ligand labelled with a radioisotope emitting weak beta radiation. When the emitter is in very close proximity to the acceptor molecule, light is produced, otherwise the energy is dissipated to the

solvent and scintillation does not occur. In practice, GST-$NF1_{334}$ fusion protein bound via an anti-GST antibody to protein A coated fluoromicrosphere beads, interacts with a Ras.[^{3}H]GTP complex. When the Ras is in close proximity to the beads i.e. when bound to $NF1_{334}$, scintillation occurs, whereas Ras in free solution does not cause any light emission. A key feature of this system is that it allows direct measurements of binding at equilibrium as there is no separation step. The assay has been used here to quantitate the effect of arachidonic acid on the binding of Ras to neurofibromin.

Arachidonic acid completely abolished the signal produced in this assay, with 50% inhibition occurring at 5-10μM arachidonic acid (figure 28a). As a control that the reduction in signal truly represented disruption of binding between Ras and NF1, arachidonic acid was added to a mixture of SPA beads, anti-GST and GST-Ras.[^{3}H]GTP complex (figure 28a). In this case, at concentrations of arachidonic acid up to 50μM, negligible inhibition was observed. This control demonstrated that arachidonic acid was not affecting binding of nucleotide to Ras, or binding between protein A and antibody or between antibody and GST. In most experiments there was a non-hyperbolic dependence of inhibition on concentration of arachidonic acid, with a distinct lag at low inhibitor concentrations.

Since the kinetic characterizations had been carried out in 50mM NaCl, the same concentration of NaCl was incorporated into the SPA assay. This decreased the counts to approximately half their original number as expected, (Skinner *et al*, 1994), however, since the original counts in the presence of $NF1_{334}$ were high, >1500cpm, the window between the background counts in the absence of $NF1_{334}$ and the sample counts in the presence of NaCl, was still large enough to determine the extent of inhibition by arachidonic acid. In the presence of 50mM NaCl, the titration curve was shifted to the left indicating that arachidonic acid was slightly more potent in the presence of salt. Figure 29 shows the inhibition of binding between $NF1_{334}$ and Ras.GTP by arachidonic acid in the absence and presence of 50mM NaCl.

Figure 28: Inhibition of binding of GST-$NF1_{334}$ to Ras.GTP by arachidonic acid and phosphatidic acid as monitored by SPA

In (a), arachidonic acid was added at the indicated concentrations to SPAs containing protein A SPA beads, anti-GST and either 0.04μM [Leu61] Ras.[^{3}H]GTP and 0.09μM GST-$NF1_{334}$ (●) or 0.04μM GST-[Leu61] Ras.[^{3}H]GTP (○). In (b), phosphatidic acid was added at the indicated concentrations to SPAs containing protein A SPA beads, anti-GST, 0.04μM [Leu61] Ras.[^{3}H]GTP and 0.09μM GST-$NF1_{334}$. Assays were performed by adding phosphatidic acid either prior to addition of Ras (●) or after addition of Ras (▲), as detailed in section 2.9.

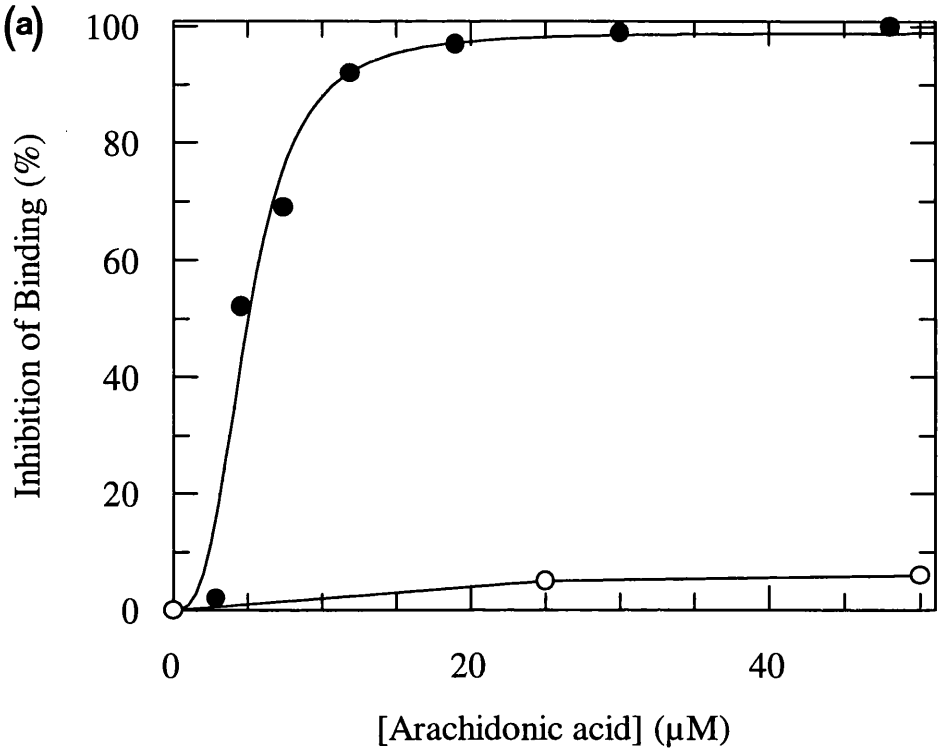
(a)
100
80
60
40
20
0
Inhibition of Binding (%)
0
20
40
[Arachidonic acid] (μM)

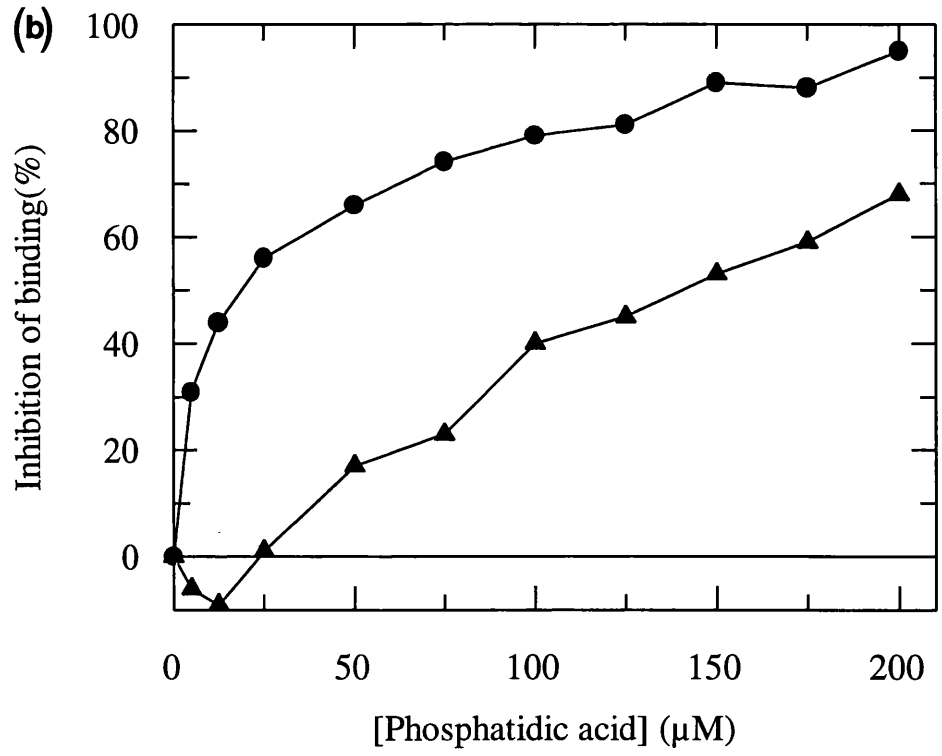
(b)
100
80
60
40
20
0
Inhibition of binding(%)
0
50
100
150
200
[Phosphatidic acid] (μM)

Figure 29: Inhibition of binding of GST-$NF1_{334}$ to Ras.GTP by arachidonic acid in the SPA assay, in the presence and absence of 50mM NaCl

Arachidonic acid was added at the indicated concentrations to SPAs containing protein A SPA beads, anti-GST, 0.04μM [Leu61] Ras.[^{3}H]GTP and 0.09μM GST-$NF1_{334}$. Experiments were carried out in the absence (●) or presence (○) of 50mM NaCl.

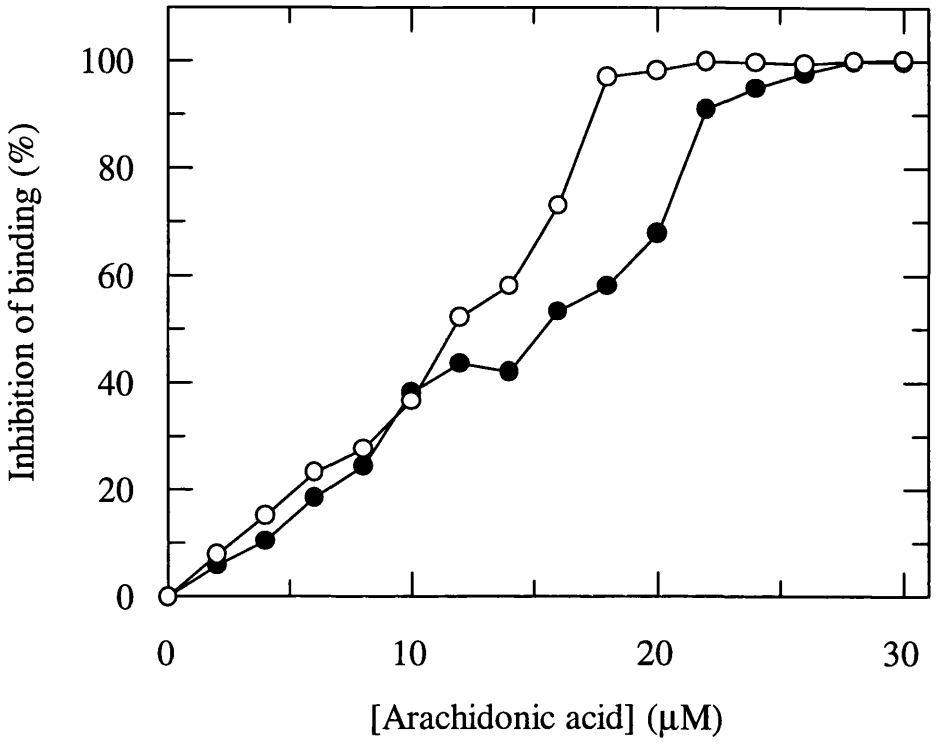
Inhibition of binding (%)
100
80
60
40
20
0
0
10
20
30
[Arachidonic acid] (μM)

3.2.6 Inhibition by other lipids

3.2.6.1 NF1 / Ras binding scintillation proximity assay

In the SPA, phosphatidic acid had distinct effects dependent upon the order of addition of components suggestive of an interaction which was not reversible on the time-scale of the experiments (figure 28b). Thus when phosphatidic acid was added as the last component i.e. to a mix of beads, antibody, GST-NF1 and Ras, it was a very weak inhibitor of binding with an I_{50} of approximately 150μM.

In contrast, when phosphatidic acid was added to GST-NF1 and then subsequently beads, antibody and Ras were added, it was a more potent inhibitor (I_{50} of approximately 20μM). The latter resulted in a transient exposure of NF1-GST to twice the final concentration of lipid in the absence of Ras. Inhibition was found to be dependent upon the order of addition, with in general, a much greater level of inhibition being seen when lipid was added to the assay prior to the addition of Ras. Such higher levels of inhibition could be explained by the absence of Ras during the addition of lipids to the assay. In the standard order of addition, Ras might serve to protect the $NF1_{334}$ against the denaturing effects exerted by the lipids. Similar behaviour was seen with arachidic acid, in that no more than 20% inhibition was seen at concentratons up to 100μM when added as the last component, but complete inhibition with an I_{50} of 10μM, was obtained when the compound was added to GST-NF1 prior to subsequent addition of beads, antibody and Ras. In contrast, the potency of arachidonic acid as an inhibitor of Ras binding to GST-NF1 was independent of the order of addition.

Upon addition of 100μM concentrations of the unsaturated fatty acids, palmitoleic (C16:1) and elaidic (C18:1trans), in the standard order, 45% and 25% inhibition was observed respectively, however addition of these lipids such that a transient higher concentration was produced, resulted in 80% inhibition for palmitoleic acid and 75% for elaidic acid. The unsaturated fatty acids, oleic, (C18:1), and linoleic, (C18:2) gave complete inhibition at 100μM with either order of addition, (figure 30a). The dependence

upon the order of addition was also observed for the saturated fatty acids, arachidic, (C20:0), stearic, (C18:0), and palmitic, (C16:0) when tested at 100μM, with <40% inhibition observed with the standard order of addition and, >80% inhibition at the transient 'high' concentration, with the exception of palmitic acid where only 50% inhibition was observed, (figure 30a). Other types of phosphatidic acid (i.e dilauroyl, dipalmitoyl, dioleoyl, distearoyl and dimyristoyl) were unable to inhibit the interaction between NF1-GST and Ras in the standard order of addition at 100μM, but showed high levels of inhibition, >80%, when added to the assay prior to the addition of Ras (figure 30b).

Titrations were subsequently carried out between the concentration range 0 and 200μM for all lipids, to examine both orders of addition in greater detail. The unsaturated fatty acids observed to inhibit the interaction between NF1-GST and Ras when added in the standard order, namely, oleic acid and linoleic acid, gave I_{50} values of 10μM and 15μM respectively. Other unsaturated fatty acids such as elaidic, palmitoleic and retinoic acids which gave greater inhibition at transient 'high' concentrations, produced I_{50} values of 20μM, 15μM, and 5μM respectively when titrated into the assay. In addition, saturated fatty acids such as arachidic, palmitic and stearic, were able to inhibit the Ras-NF1-GST interaction to a greater extent when added to the assay in this order, giving I_{50} values of 10μM, 100μM and 10μM. Finally, phosphatidic acids, titrated into the assay to create transient 'high' concentrations, resulted in the following I_{50} values: arachidonoyl, stearoyl, 20μM; dilauroyl, 30μM; dipalmitoyl, 15μM; dioleoyl, 40μM; distearoyl, 25μM and dimyristoyl, 15μM.

3.2.6.2 Inhibition of GAP_{344} and $NF1_{334}$-activated Ras.GTPase by lipids

The effect of fatty acids on the GAP_{344} and $NF1_{334}$-activated GTPase was studied an the results are shown in figure 31a. At 100μM, all fatty acids tested inhibited both GAPs to >80%. Bollag and McCormick (1991) presented data to show that phosphatidic acid was a non-competitive inhibitor of NF1 activity, and NF1 inhibited by phosphatidic acid was

Figure 30: Inhibition of binding of GST-$NF1_{334}$ to Ras.GTP by fatty acids and phospholipids as monitored by SPA

In (a), unsaturated and saturated fatty acids were added to SPAs containing protein A SPA beads, anti-GST and either 0.04μM [Leu61] Ras.[^{3}H]GTP and 0.09μM GST-$NF1_{334}$ to achieve final concentrations of 100μM. In (b), phosphatidic acids and phospholipids were added to SPAs containing protein A SPA beads, anti-GST, 0.04μM [Leu61] Ras.[^{3}H]GTP and 0.09μM GST-$NF1_{334}$ to achieve final concentrations of 100μM. Assays were performed by adding fatty acids and phospholipids either prior to addition of Ras or after addition of Ras as detailed in section 2.9. Fatty acids are represented by the total number of carbon atoms : number of double bonds. (C16:0, palmitic acid; C16:1, palmitoleic acid; C18:0, stearic acid; C18:1c, oleic acid; C18:1t, elaidic acid; C18:2, linoleic acid; C20:4, arachidonic acid; C20:0, arachidic acid; C14:0, myristic acid; C18:0/C20:4, arachidonyl-stearoyl phosphatidic acid; C12:0, lauric acid; LPA, lysophosphatidic acid).

(a)

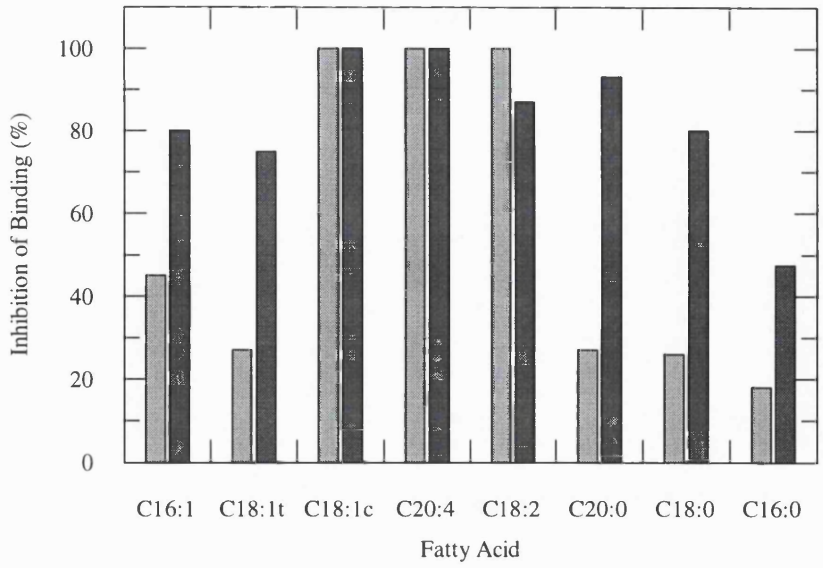
Inhibition of Binding (%)
100
80
60
40
20
0
C16:1
C18:1t
C18:1c
C20:4
C18:2
C20:0
C18:0
C16:0
Fatty Acid

(b)

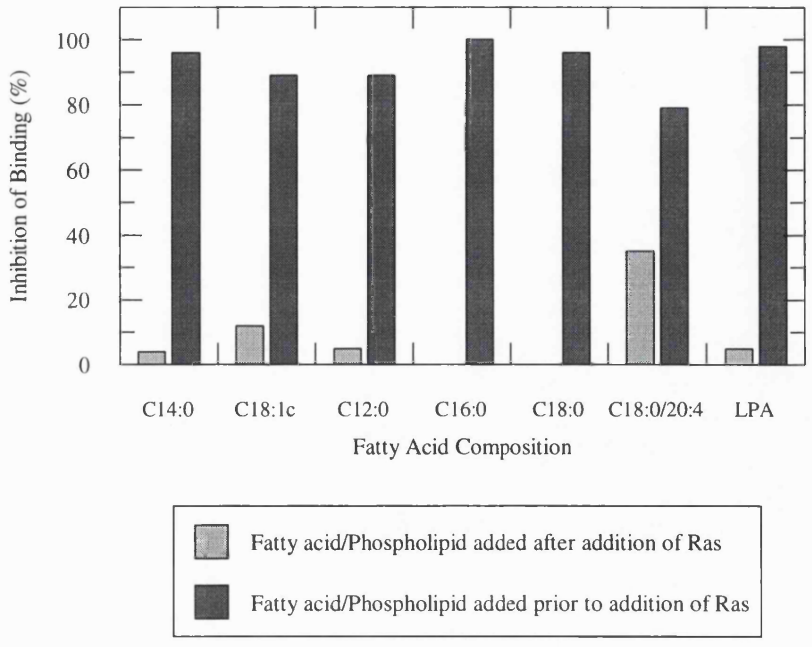
Inhibition of Binding (%)
100
80
60
40
20
0
C14:0
C18:1c
C12:0
C16:0
C18:0
C18:0/20:4
LPA
Fatty Acid Composition
Fatty acid/Phospholipid added after addition of Ras
Fatty acid/Phospholipid added prior to addition of Ras

Figure 31: Inhibition of the GAP_{344} and $NF1_{334}$-stimulated Ras.GTPase by fatty acids and phospholipids

A solution containing 7μM Ras.[^{3}H]GTP was incubated with either 0.040μM GAP_{344} or 0.014μM $NF1_{334}$ in 20mM Tris/HCl, pH 7.5, 1mM $MgCl_2$, 0.1mM dithiothreitol at 25°C. Fatty acids (a) and phospholipids (b) were added to the mixture to achieve final concentrations of 100μM. After 10 minutes, the extent of [^{3}H]GTP hydrolysis was measured by HPLC separation of [^{3}H]GTP from [^{3}H]GDP. Inhibition of GTPase activity was calculated as a percentage relative to incubations without lipids. Fatty acids are represented by total number of carbon atoms : number of double bonds. (C16:0, palmitic acid; C16:1, palmitoleic acid; C18:0, stearic acid; C18:1c, oleic acid; C18:1t, elaidic acid; C18:2, linoleic acid; C20:4, arachidonic acid; C20:0, arachidic acid; C14:0, myristic acid; C12:0, lauric acid; Ret, retinoic acid; C18:0/C20:4, arachidonyl-stearoyl phosphatidic acid; LPA, lysophosphatidic acid; PS, phosphatidylserine; PE, phosphatidylethanolamine; PIP, Phosphatidyl-4-monophosphate).

(a)

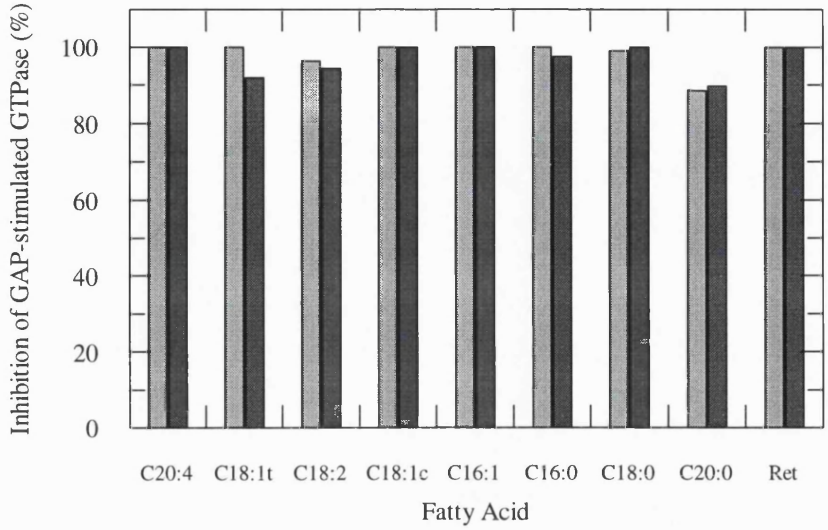
Inhibition of GAP-stimulated GTPase (%)
100
80
60
40
20
0
C20:4
C18:1t
C18:2
C18:1c
C16:1
C16:0
C18:0
C20:0
Ret
Fatty Acid

(b)

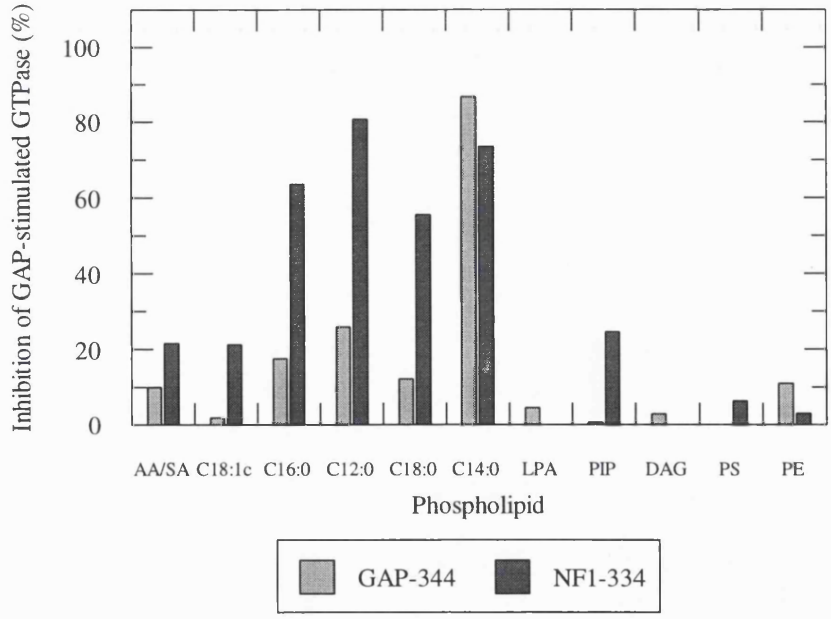
Inhibition of GAP-stimulated GTPase (%)
100
80
60
40
20
0
AA/SA
C18:1c
C16:0
C12:0
C18:0
C14:0
LPA
PIP
DAG
PS
PE
Phospholipid
GAP-344
NF1-334

still capable of binding Ras. As this differed from our findings with arachidonic acid, we examined the effect of phosphatidic acid in some of our own systems (figure 31a). Under our experimental conditions, up to 70μM phosphatidic acid gave no significant inhibition of either GAP_{344} or $NF1_{334}$ catalytic activity. In addition, phosphatidic acids containing the following fatty acyl components, distearoyl, dipalmitoyl, dioleoyl and arachidonoyl-stearoyl, showed less than 30% inhibition towards both GAP_{344} and $NF1_{334}$ when tested at 100μM, with the exception of phosphatidic acid, dimyristoyl and dilauroyl which were observed to differentially inhibit $NF1_{334}$ by 70% at 100μM.

3.3 Discussion

There are conflicting literature reports on the potency of arachidonic acid and phosphatidic acid, on their ability to differentially inhibit NF1 and p120-GAP activation of Ras.GTPase, and the mechanism by which this is achieved. Diversity in the reported inhibitory activities of lipids may be a reflection of the variability between different groups in, the way in which lipids were prepared, the assay conditions under which the inhibition by lipids is measured, the proteins upon which the inhibition is exerted, and the ability of lipids to form micelles. Arachidonic acid, as well as other unsaturated fatty acids, were prepared by some groups as mixed micelles, and by others as pure micelles. Pure micelles were prepared using methanol or chloroform: methanol solutions of fatty acids, dried, and dissolved in either 20mM HEPES, pH 7.6 (Serth *et al.*1991), 20mM Tris/HCl pH 7.5 (Yu *et al*, 1990; Homayoun *et al*, 1993) or 0.1M Tris/HCl pH 7.5 (Tsai *et al*, 1989a; Tsai *et al*, 1989b; Golubic *et al*, 1991; Tsai *et al*, 1991; Golubic *et al*, 1992). Mixed micelles were also produced by solubilization of dried fatty acids in detergents, such as 5mM Triton X-100, (Serth *et al*, 1991), 1% n-octylglucopyranoside (Tsai *et al*, 1989a; Tsai *et al*, 1989b) or Nonidet P-40 (Bollag and McCormick, 1991). I therefore investigated the effect of arachidonic acid on the interaction of Ras and GAPs using three different techniques in the simplest system possible.

Kinetic methods showed that in the absence of detergent, arachidonic acid inhibited the NF1- and p120-GAP activated activity of Ras.GTPase to similar extents with I_{50} values

of ca. 5-15μM (figure 16). These potencies are similar to those observed by Golubic *et al* (1991). It was noted that the inhibitory potency of arachidonic acid on GAP activity was markedly reduced by the presence of Nonidet detergent, to levels reported by Bollag and McCormick (1991) when they also used this detergent. Bollag and McCormick (1991) showed that mixed detergent-containing micelles of arachidonic acid inhibited the Ras.GTPase activity stimulated by the catalytic domain of NF1, with an I_{50} of 50μM. Uchida *et al* (1992) observed inhibition of the catalytic domain of type I NF1 by arachidonic acid with an I_{50} of 156μM. All subsequent experiments were performed in the absence of detergent. Under these conditions, phosphatidic acid was found to be only a weak reversible inhibitor of either GAP_{344} or $NF1_{334}$ catalytic activity (data not shown), as Golubic *et al* (1991) had concluded, and in contrast to the more potent inhibition seen by other groups. These data suggested that some of the reported differential inhibition effects of NF1 and p120-GAP by lipids might be artifactual.

The mechanism of the inhibition of the NF1-activated Ras.GTPase was investigated in more detail by using the fluorescent analogue of GTP, mantGTP. The fluorescence decrease that occurs between Ras.mantGTP and Ras.mantGDP allowed the hydrolysis to be monitored continuously (figure 20). This has many advantages over the use of radiolabelled GTP, which requires analysis of many single time points.

Under single turnover conditions, a biphasic effect of increasing ionic strength on inhibition of the $NF1_{334}$-catalyzed Ras.GTPase by arachidonic acid was observed (data not shown) i.e at concentrations of NaCl up to 300mM an increase in inhibition was seen (24% at 300mM) but further increases in NaCl resulted in a decrease in the level of inhibition (20% at 500mM and 15% at 1M). With certain assumptions, namely that the affinity of H-Ras.mantGTP for $NF1_{334}$ is 0.2μM (as reported by Brownbridge *et al*, 199 for the interaction of H-Ras.GDP-[NH]P with NF1-GRD) and that the affinity of arachidonic acid for $NF1_{334}$ is 10μM, one can calculate the level of inhibition expected in the single turnover experiments if the mechanism of inhibition is either non-competitive, i.e. arachidonic acid bound to both NF1 and NF1.Ras complex equally, or competitive,

i.e. binds only to free NF1. In the former, one would expect a level of inhibition of 60%, whereas in the latter model, the inhibition would be only 7% which would increase upon addition of NaCl, to 24%. Thus, the single turnover data is supportive of a competitive rather than a non-competitive character.

A similar biphasic effect was also observed under multiple turnover conditions (figure 21) except that a much higher level of inhibition was observed i.e at concentrations of NaCl up to 300mM an increase in inhibition was seen (80% at 300mM), but further increases in NaCl resulted in a decrease in the level of inhibition (60 % at 500mM NaCl and 40% at 1M NaCl). The reduction in the inhibitory potency of arachidonic acid at very high salt concentrations (>300mM) under single turnover and steady state conditions, could be explained by the effects of NaCl on the K_d's for binding of $NF1_{334}$ to both H-Ras.mantGTP and arachidonic acid. As the K_d for binding of NF1 to Ras is raised (done in these experiments by adding NaCl) arachidonic acid would be expected to be a more potent inhibitor if it competes with H-Ras.mantGTP for binding to $NF1_{334}$. However, at high salt concentrations, this increase in inhibition would be countered by a reduction in the affinity of $NF1_{334}$ for arachidonic acid, resulting in an overall reduction in inhibition. If arachidonic acid was able to bind to either $NF1_{334}$ or $NF1_{334}$ complexed to H-Ras.mantGTP with equal affinity in a non-competitive manner, addition of NaCl would not be expected to affect the inhibition, providing the conditions are non-saturating.

By varying the concentrations of both Ras.mantGTP and arachidonic acid, the effect of arachidonic acid on K_m and k_{cat} was established (figure 22). The inhibition was of a mixed character but predominantly competitive.

The second method to study the effect of arachidonic acid was to use the fluorescent probe DPH-carboxylic acid in equilibrium measurements of the interaction of Ras.GTP with NF1. Although DPH-carboxylic acid did not compete for the proposed arachidonic acid-binding site on NF1 (figure 25), as had been hoped, it still provided a probe on the

interaction of NF1 with Ras.GTP, since the fluorescence of bound DPH-carboxylic acid was reduced on the binding of Ras.GTP (figure 26), strongly suggesting competition between the Ras and lipid for binding to NF1. Alternatively, arachidonic acid might exert its effects by binding to the ternary complex and relieving a possible quenching effect exerted by Ras on $NF1_{334}$.

The third method to study the effect of arachidonic acid was to use a scintillation proximity assay (figure 28a). Arachidonic acid completely abolished the interaction between [Leu61]Ras.GTP and NF1, with 50% inhibition occurring at 5-10μM.

All of the data above support the argument that arachidonic acid competitively inhibits the interaction of Ras.GTP with NF1. Furthermore, the inhibitory effects occur well below the CMC for arachidonic acid under the conditions used, showing that the effect is not caused by micelle formation, as had been suggested by Serth *et al* (1991). Serth and colleagues suggested that the chemical structure of lipids per se is not responsible for their inhibitory effects, but rather it is their physical state of aggregation. In particular, it was observed that arachidonic acid inhibited GAP activity with a sharply sigmoid dose-response curve centred around its CMC and it was concluded that the arachidonic acid must be in a micellar form to exert its inhibitory effects. No data was presented on NF1, which would have been of particular interest as it might have been anticipated that arachidonic acid would inhibit NF1 at the same concentration (i.e. its CMC) as p120-GAP, in contrast to data reported by Bollag and McCormick (1991) showing a large selectivity in inhibition.

Despite this evidence for competitive inhibition, my results suggest that arachidonic acid can exert other effects on the interaction. For example, the inhibition of the GAP-activated Ras.GTPase (figures 16 and 22c) show a sigmoid or non-hyperbolic dose-response curve. In addition, the effect of arachidonic acid on the binding of Ras.GTP to NF1 as monitored by DPH-carboxylic acid (figure 26b) or by the scintillation proximity assay (figure 28a)

is not hyperbolic. I do not have an explanation for this phenomenon, but similar behaviour has been seen previously with arachidonic acid (Golubic *et al*, 1991; Serth *et al*, 1991). In particular, Golubic *et al* (1991) presented an unusual dose response for arachidonic acid in which 2.5mg/ml (8μM) arachidonic acid was not inhibitory but 5mg/ml (16μM) arachidonic acid gave 60% inhibition of GAP activity. Both concentrations were well below the CMC. It is possible that self-association of arachidonic acid to structures smaller than full micelles is required for maximal inhibitory effects. Arachidonic acid may also have more than one site for binding on GAP_{344} so that arachidonic acid binds in a co-operative manner. It is also possible that arachidonic acid, at low concentrations, is able to adsorb onto the plastic tubes or plates used in the assays. However, since the lowest concentration of arachidonic acid, prior to dilution into the assay, is 1μM, it is unlikely that significant adsorption of material would occur at this stage, such that the availability of arachidonic acid is sufficiently decreased to cause sigmoidal effects. However, adsorption to plastic surfaces may still occur upon 1000-fold dilution into the assay.

A further deviation from a simple competitive pattern was seen from the kinetic analysis (figure 22), which showed that arachidonic acid not only raised K_m but also reduced k_{cat}. The effect on k_{cat} is consistent with an irreversible inhibitory component for which some additional evidence has been obtained (data not shown). In the scintillation proximity assay, it was noted that when certain lipids (arachidic acid and phosphatidic acid, but not noticeably arachidonic acid) were added to NF1 before addition of Ras they were more potent inhibitors than when added after Ras, suggesting that the inhibitory mechanism was not always rapidly reversible on the time-scale of these experiments. Also, arachidonic acid caused slow time-dependent effects on the fluorescence of DPH-carboxylic acid bound to GAP, consistent with denaturation, which were significantly prevented by the inclusion of Ras (figure 27). The incomplete kinetic analyses previously presented by Serth *et al* (1991) and Bollag and McCormick (1991) could also be consistent with an irreversible effect. Bollag and colleagues (1991) reported that inhibition by phosphatidic acid is non-competitive, such that phosphatidic acid only acts to reduce V_{max} without affecting the K_m. For a reversible inhibitor of a single substrate reaction, this type of inhibition is rare, since it is difficult to modulate the active site catalysis without having

an effect on the binding. Alternatively such inhibition could be due to an irreversible inhibitor. Irreversible inhibition by arachidonic acid would give apparently non-competitive kinetics with respect to Ras as a substrate, since arachidonic acid would solely decrease the amount of active $NF1_{334}$ in solution.

The presence of Ras bound to a separate site from the arachidonic acid binding site on GAP_{344}, might protect against the possible denaturing effects of arachidonic acid and stabilize GAP_{344} against conformational changes. Interestingly, the Ras-induced reduction in the rate of the time-dependent fluorescence increase, was not complete, ie: maximum of 80% reduction in the rate at 10μM Ras, (Figure 27), which was not increased by addition of a further 10μM Ras, indicating that arachidonic acid has at least two effects on the GAP_{344} protein, one of which is prevented by Ras and the other which is unaffected by Ras. In addition, the Ras protein may bind to the same site as arachidonic acid, and prevent the slow time-dependent fluorescence change, thought to be caused by binding of arachidonic acid to GAP_{344} and subsequent denaturation of the protein. Similarly, a proportion of arachidonic acid will be able to bind to GAP_{344} and not be displaced by Ras.

Although these non-competitive effects occur, the predominantly competitive nature of the interaction leads to the conclusion that arachidonic acid does not act in the way that phosphatidic acid was reported to do by Bollag and McCormick (1991). They reported two main lines of evidence that phosphatidic acid does not block binding of Ras to NF1. Firstly, the inhibitor displayed non-competitive kinetics, in which the inhibitor reduced V_{max} without affecting K_m, typical of depletion of both substrate bound and free enzyme forms by inhibitor. However, such an inhibitory pattern is also seen with an irreversible or slowly reversible type of action. Secondly, they showed that phosphatidic acid did not block binding of Ras.GTP to NF1 immobilized on beads (Bollag and McCormick, 1991). No detailed quantitation (e.g. yield of bound proteins) or controls were given for this assay other than that SDS blocked binding. Previous experiments (Eccleston *et al*, 1993; Skinner *et al*, 1994) showed that the rate of dissociation of NF1 from Ras is very fast, such that no significant binding of Ras to NF1 should have been observed under the

experimental conditions of Bollag and McCormick (1991). Thus, the binding observed might not have been true reversible binding of NF1 to Ras. It has previously been shown that the detergent dodecylmaltoside blocks binding of Ras to NF1 (Skinner *et al*, 1994) again supporting the hypothesis that a primary mode of inhibition of amphipathic molecules such as lipids and detergents might be by preventing Ras binding to GAPs.

On the basis that certain lipids differentially inhibited p120-GAP and NF1 and on the assumption that one could extrapolate from data with phosphatidic acid that lipids in general do not block bindingof Ras to GAPs, Bollag and McCormick (1991) suggested a hypothesis with these key features: a) p120-GAP and NF1 are differentially regulated by lipids, b) lipids activate Ras signalling by inhibiting NF1 GTPase-stimulating activity, c) lipid-inhibited NF1 binds to Ras.GTP propagating a signal through NF1, d) NF1 and p120-GAP are alternative effectors for Ras and e) the mitogenic activity of certain lipids is through their modification of GAP activity in the cell. However, the data presented here is not in accordance with this hypothesis as a) no significant differential inhibition of activity was observed and b) lipid-inhibited GAPs do not bind to Ras. Two alternative hypotheses can be suggested which would be consistent with my data: If GAPs are indeed Ras effectors for a mitogenic pathway, the mitogenic activity of arachidonic acid cannot be accounted for through inhibition of GAP catalytic activities, since arachidonic acid also blocks binding between Ras and these putative effectors. Alternatively, the mitogenic activity of arachidonic acid may be accounted for by inhibition of GAP catalytic activity, but in this case GAPs are unlikely to be effectors for a mitogenic pathway.

While it is clear from my studies that *in vitro*, the GAP_{344} and $NF1_{334}$ stimulated Ras.GTPase can be inhibited by binding of arachidonic acid to GAPs and preventing Ras from binding, it remains to be demonstrated whether this has any physiological importance *in vivo*, in particular because it requires a high local concentration of lipid, to be effective. *In vivo*, arachidonic acid, liberated from membrane phospholipids, is rapidly metabolized to its eicosanoid counterparts upon mitogenic stimulation. Diacylglycerol has been shown to function as a regulator of stimulated arachidonic acid release, by regulating protein

kinase C (Whatley *et al*, 1993). For inhibition to be achieved, arachidonic acid must exert its effects almost immediately after mitogenic stimulation, during its transient existence as the fatty acid precursor, prior to its degradation to eicosanoid products such as prostaglandins and leukotrienes. However, although high concentrations of lipids are unlikely to be reached in the cytosolic compartment, such levels could be reached within the membrane. As such, GAPs may be sequestered to portions of the plasma membrane containing high concentrations of arachidonic acid as a means of regulating Ras activity

Alternatively, arachidonic acid may not enter the cyclooxygenase or lipoxygenase pathways but instead might act as a 'second messenger' by exerting direct effects on signal transduction (Naor, 1991; Liscovitch and Cantley, 1994). For example, arachidonic acid has been reported to increase the binding of GTP to a cytosolic GTP-binding protein and elicit superoxide anion generation in intact neutrophils (Abramson *et al*, 1991). In addition, Ligeti *et al* (1993) have shown that in intact HL-60 membranes, the interaction of Rap-1A with Rap-GAP is strongly enhanced by arachidonic acid. If this were the case, concentrations of arachidonic acid might reach high enough levels in the cytosol to be able to inhibit GAPs.

The proposed inhibition of GTPase-activating proteins by arachidonic acid will not only be dependent upon the relative concentrations of arachidonic acid in the cell but also on the concentrations of Ras and GAP proteins in the cell and on the affinity of interaction between Ras and GAPs. The catalytic domains of p120-GAP and neurofibromin bind to Ras with K_d's of approximately 20μM for p120-GAP and 1μM for neurofibromin, as measured at low ionic strength, (Brownbridge *et al*, 1993; Eccleston *et al*, 1993). However, at physiological ionic strength, which is reported to be approximately 150mM, the affinity of Ras for GAPs is reduced.

Hence it has been suggested that the activation state of Ras in the cell might be in part controlled by the relative concentrations of eicosanoids generated by the lipoxygenase and cyclooxygenase pathways, (Han *et al*, 1991). Metabolites of arachidonic acid, such as prostaglandins are known to antagonise the effects of arachidonic acid, by stimulating the

activity of GAPs. Therefore, stimulation of phospholipase A2 by growth factors would produce a rise in arachidonic acid and lipoxygenase products that could inhibit GAP and switch Ras on. The later induction of cyclooxygenase would lead to the production of GAP-stimulatory prostaglandins and hence inactivation of Ras.

3.4 Conclusions

The effect of arachidonic acid on the interaction between Ras and $NF1_{334}$ was investigated using three different techniques in the simplest system possible: by measuring catalytic activity under multiple turnover conditions, using *p*-((6-phenyl)-1,3,5-hexatrienyl)benzoic acid as a fluorescent probe for ligands binding to GAPs and using a scintillation proximity assay to measure direct binding of Ras to $NF1_{334}$.

(1) No significant differential inhibition of GAP_{344} or $NF1_{334}$ activity by arachidonic acid was observed. Arachidonic acid inhibited the $NF1_{334}$ and GAP_{344}-activated activity of Ras.GTPase with I_{50} values of 5-15μM. Furthermore, the inhibition by arachidonic acid included a major component that was competitive with Ras.GTP in addition to a non-competitive type effect consistent with protein denaturing activity.

(2) The fluorescence of DPH-carboxylic acid bound to $NF1_{334}$ was reduced upon binding of [Leu61]Ras.GTP. Arachidonic acid largely abolished this effect suggesting competition between Ras and lipid for binding to $NF1_{334}$.

(3) Arachidonic acid completely abolished the interaction between [Leu61]Ras.GTP and NF1-GST, with 50% inhibition occurring at 5-10μM.

(4) In my experiments, lipid-inhibited GAPs do not bind to Ras. Therefore, the mitogenic activity of arachidonic acid may only be accounted for by inhibition of GAP catalytic activity, if GAPs are not Ras effectors for such a mitogenic pathway.

3.5 Further work

(1) The inhibition of both the GAP-activated Ras.GTPase and the binding of Ras.GTP to NF1 by arachidonic acid showed sigmoidal effects which have yet to be explained. These effects may be due to multiple binding sites for arachidonic acid on NF1. It would be interesting to quantitate the number of binding sites for arachidonic acid on GAPs.

(2) Ultimately, it would be of interest to define the residues involved in binding lipids by X-ray crystallography of arachidonic acid bound to GAPs

Chapter 4 - The Importance of Two Conserved Arginine Residues in the Catalytic Mechanism of the Ras GTPase-Activating protein, Neurofibromin

4.1 Introduction to the Experiments

The Ras superfamily of guanine nucleotide binding proteins, comprising the Ras, Rho, Rab and Arf families, share common structural and biochemical properties. Each protein exists in a GTP-bound conformation which is converted into the GDP-bound conformation through hydrolysis of the bound GTP. The intrinsic GTPase rate of these proteins is quite slow (k_{cat} = 1.2 x 10^{-4} s^{-1}). This GTPase can be accelerated by up to five orders of magnitude in the presence of highly specific GTPase activating proteins (GAPs). GAPs have been characterized for members of all branches of the Ras superfamily. Since the first identification of p120-GAP as a RasGAP, many other RasGAPs have been cloned including neurofibromin, IRA1/2, p100GAP1m, IQGAP1/2, Sar1, Bud2, GAP^{celeg}, $GAP1^{IP4BP}$, dmGAP1 and $GAP^{R\text{-}Ras}$. These RasGAPs share a 360 amino acid region of sequence similarity referred to as the GAP catalytic domain or GAP-related domain (GRD). For NF1 and p120-GAP, this domain spans ca. residues 1175-1534 and 688-1047 respectively (according to the numbering of Wang *et al*, 1991a).

Mutagenesis studies have identified discrete sites of protein interaction on Ras involved in GAP binding and GAP induced GTPase activation (Schaber *et al*, 1989; Marshall, 1994). Ras interacts with GAP through its switch I and II regions, and probably through a third region centred around Asp92 referred to as the α3 domain (Marshall, 1994; Wood *et al*, 1994; Yoder-Hill *et al*, 1995). There is evidence to suggest that the catalytic domain of GAP is analogous to the effector region of Ras and is sufficient for Ras binding and GTPase activation. A number of groups have attempted to define the minimal regions of the catalytic domains of p120-GAP and NF1 sufficient for Ras interaction and catalytic activity. Martin *et al* (1990) suggested that a carboxy-terminal 483-residue fragment encompassing the GAP-related domain of neurofibromin was neccesary for full RasGAP activity. Further studies have suggested that the primary Ras binding site is localized to 334 (714-1047) or 344 (704-1047) residues of the GAP catalytic domain. Either region could be expressed as a stable truncated protein in *E. coli* which could bind Ras.GTP and was sufficient for full or almost full RasGAP activity (Marshall *et al*, 1989; Skinner *et al*, 1991; Gideon *et al*, 1992). Recently, Ahmadian *et al* (1996) have shown that fragments

of both p120-GAP and neurofibromin comprising residues 714-986 (GAP-273) and 1248-1477 (NF1-230) respectively, retain catalytic activity. Maruta and coworkers (Nur-E-Kamal *et al*, 1993) have reported that smaller fragments of NF1 (NF91, residues 1441-1532; NF78, residues 1441-1519) from outside the conserved RasGAP region can still stimulate the GTPase activity of Ras. They also demonstrated that a fragment of 56 amino acids from the same region was still able to bind Ras.GTP and a shorter 41-residue sequence (1441-1486) was able to suppress Ras-induced malignancy (Fridman *et al*, 1994). Attempts to identify individual amino acids from the GAP catalytic domain which might be involved in Ras binding or GTPase activation have focussed on conserved residues.

Comparative sequence analysis among mammalian and fungal RasGAPs (Wang *et al*, 1991a) have shown that the most highly conserved regions of the GRD can be divided into four blocks of homology shown in figure 32 (1, 2, 3A and 3B). These homologous regions contain 15 invariant residues that are conserved among the different RasGAP proteins such as NF1, p120-GAP, *S.cerevisiae* IRA1 and IRA2 proteins, *S.pombe* Sar1 protein (Ballester *et al*, 1990; Wang *et al*, 1991a) and *Drosophila* Gap1 (Gaul *et al*, 1992). Analysis of these invariant residues has mostly focussed on the residues within blocks 1, 3A and 3B, since a splicing variant of neurofibromin has been identified containing a 21-amino acid insertion which disrupts the integrity of block 2 without deleteriously affecting biological activity (Anderson *et al*, 1993a; Nishi *et al*, 1991). In addition, naturally occurring mutations in blocks 3A and 3B of NF1 have been identified in tumour cells (Li *et al*, 1992). Gutmann *et al* (1993) probed sequence databases for RasGAP catalytic domain motifs and pulled out three concensus motifs characteristic for RasGAPs. The motifs **EIE.....LLR**, **FLR...PA..P** and **K..Q..AN** and are located in blocks 1, 3A and 3B respectively. The sequence homology between different RasGAPs for blocks 1 and 3A are shown in figure 33. Four of the 13 invariant residues are proline (P1359, P1373, P1395 and P1400) and are likely to be of structural importance. Three are hydrophobic (F1389, L1390 and A1396) and unlikely to be directly involved in a catalytic mechanism. The remaining invariants are Q1426, N1430, E1264, R1276, R1391 and K1423. Several groups have previously investigated the role of some of these conserved residues by

making mutants in either the catalytic domain of p120-GAP (Skinner *et al*, 1991; Brownbridge *et al*, 1993; Hettich and Marshall, 1994; Miao *et al*, 1996) or neurofibromin (Weismuller and Wittinghofer, 1992; Gutmann *et al*, 1993; Poullet *et al*, 1994; Mori *et al*, 1995; Ishioka *et al*, 1995; Mittal *et al*, 1996; Morcos *et al*, 1996).

There are several models to describe the mechanism of the GAP-catalyzed Ras.GTPase. The first model proposes that the basic method of catalysis is the same as in Ras alone such that GAP stabilizes a certain catalytically active conformation of Ras or accelerates the isomerization step. In the second model, one or more side chains of residues within GAP could complement the active site of Ras and participate in catalysis possibly by stabilizing the transition state of the GTPase reaction. In this model the chemical mechanism of GTP hydrolysis by GAP-activated Ras is different from that in Ras alone. In support of the latter model, there is evidence to suggest that basic residues are involved in the GTPase reaction of the G_{alpha} subunit of heterotrimeric G proteins. Structural studies of $G_{i\alpha 1}$ (Coleman *et al*, 1994; Mixon *et al*, 1995) and transducin-α (G_t) (Noel *et al*, 1993; Sondek *et al*, 1994) have identified an arginine residue (Arg-174 in G_t; Arg-178 in $G_{i\alpha 1}$) in a key position to stabilize the transition state of the enzyme. This arginine residue is conserved in members of the G_α family including $G_{s\alpha}$ (Arg-187/188 or 201/202) and $G_{i\alpha 2}$ (Arg-179). The highly conserved region surrounding this basic residue is proposed to function as an 'inbuilt' activator of the GTPase activity of G_α proteins, analogous to the effect of GAP on Ras (Markby *et al*, 1993). Mutations of this conserved arginine, resulting in a loss of basicity, have been shown to impair GTPase activity both *in vitro* (Friessmuth and Gilman, 1989) and *in vivo* (Landis *et al*, 1989; Lyons *et al*, 1990). Furthermore, ADP-ribosylation of Arg-201 in $G_{s\alpha}$ and Arg-174 in G_t by cholera toxin also inhibits GTPase activity (Cassel and Selinger, 1977; Van Dop *et al*, 1984). Such studies have led to speculations that the conserved arginine residue may account for the higher hydrolytic rate of G_α proteins relative to those of the Ras family members. Although this arginine residue is missing in Ras, sequence comparisons between Ras and G_α proteins (Lambright *et al*, 1994) reveal that the equivalent residue in Ras would be Tyr-32 which lies within the effector loop. I was therefore interested in the hypothesis that GAPs might stimulate the Ras.GTPase by directly contributing basic residues to the active site on

Ras.GTP.There are three basic residues in GAPs: R1276, R1391 and K1423 (using the numbering of NF1).

Mutations at K1423 have shown effects on NF1-GRD stability, biological function and biochemical activity both *in vitro* and *in vivo*. These effects appear to be dependent upon the nature of the substitution rather than the methodology employed to analyze these effects, since independent groups working on the same mutation have obtained essentially similar results.

Two groups (Weismuller and Wittinghofer, 1992; Poullet *et al*, 1994) introduced a mutation into the catalytic domain of neurofibromin (NF1-GRD) converting the basic lysine residue at position 1423 into an uncharged methionine (K1423M). Weismuller and Wittinghofer performed a series of temperature inactivation and trypsin digestion experiments on the purified NF1-GRD and concluded that K1423 is involved in maintaining a stable structure and is unlikely to be a catalytic residue. In their hands the methionine substitution rendered the NF1-GRD more susceptible to trypsin digestion than the wild-type. In addition, the GAP activity of K1423M, measured using a filter binding assay, was considerably more sensitive to changes in temperature and salt concentration i.e. K1423M showed a 40°C shift (from 70°C to 30°C) in the temperature at which 50% of GAP activity is irreversibly lost and a 3-fold reduction (from 200mM to 60mM) in the concentration of NaCl required for 50% inhibition of GAP activity. Using an *in vivo* yeast complementation assay, Poullet and coworkers found that K1423M was unable to complement the heat shock sensitive phenotype of the yeast ira1 mutant, indicating a loss of biological function. The authors speculate that this loss of function might be caused by a reduction in the stability of the K1423M protein as had been previously observed (Weismuller and Wittinghofer, 1992), and although they could detect the protein from yeast cell lysates on a western blot, this data is not shown and no comment is made about the expression levels of K1423M compared to wild-type.

Certain tumours and patients with NF1 harbour mutations affecting residue 1423 (Li *et al*, 1992). The missense mutations K1423E and K1423Q within NF1-GRD have been detected in colon adenocarcinoma, myeloproliferative syndrome and anaplastic astrocytoma (Li *et al*, 1992). Poullet and coworkers (1994) also introduced a number of conservative (K1423R), non-conservative (K1423E, K1423Q, K1423S, K1423G) and random (K1423N) mutations into NF1-GRD. They found that lysine was the only amino acid to produce a functional NF1 in the yeast complementation assay. This is consistent with the previous results of Gutmann *et al* (1993) in which K1423S showed a reduced ability to complement the heat shock sensitive phenotype of either the yeast ira1- ira2- mutant or the pde2- mutant which expresses H-Ras. Furthermore, Ishioka and colleagues (1994) also showed that K1423S, K1423Q and K1423E disrupted NF1-GRD function *in vivo* using an assay for growth inhibition of a cdc25 temperature-sensitive mutant yeast strain expressing H-Ras.

Poullet *et al* (1994) noted that the GTPase activity of the purified NF1-GRD mutants, measured by an *in vitro* filter binding assay, were greatly reduced compared to the wild-type protein. Although the arginine mutant showed the highest activity, its GAP activity was still reduced by two-orders of magnitude (125-fold) demonstrating the absolute requirement for a lysine residue at this position. The GAP activity of the glutamic acid mutant was reduced by at least three orders of magnitude (1000-fold) as expected due to the charge inversion. The loss of charge accompanied by a decrease in the bulkiness of the side chain would account for the reduction in GAP activity observed for both the K1423Q (400-fold) and K1423S (600-fold) mutants. These results are consistent with the previous findings of Li *et al* (1992) who used a similar assay to show that the GAP activities of purified K1423E and K1423Q NF1-GRD proteins were reduced by 200- and 400-fold respectively. Gutmann and colleagues (1993) could not detect any GAP activity in K1423S cell lysates using an *in vitro* GAP assay, but an *in vivo* GAP assay revealed that yeast cells expressing the serine mutant had reduced levels of H-Ras bound GTP. This suggested that K1423S had reduced GAP activity compared to wild-type NF1-GRD.

Poullet *et al* (1994) obtained the affinities of Ras.GTP for purified mutant and wild-type NF1-GRD proteins by measuring the ability of H-Ras.GMPPCP to competitively inhibit NF1-GRD stimulated hydrolysis of ^{32}P-labelled Ras.GTP. The affinities of K1423R, K1423Q, K1423S and K1423E for Ras were reduced by at least two orders of magnitude. However, using the same method, Li and colleagues (1992) reported that the K1423E and K1423Q NF1-GRD mutations had no effect on Ras affinity. Gutmann *et al* (1993) showed no data on the affinity of K1423S for Ras.

Taken as a whole the data suggests that the basic lysine residue at position 1423 is essential for NF1-GRD function. Substitution of this lysine disrupts the biological function of NF1-GRD *in vivo* probably due to a reduced GAP activity or a reduction in stability. Evidence for the involvement of K1423 in binding is weak since effects of mutations on Ras affinity are variable, causing a reduction in some studies (Poullet *et al*, 1994) and no effect in others (Li *et al*, 1992).

Data from Skinner *et al* (1991) and Brownbridge *et al* (1993) strongly suggested that R903 of p120-GAP (equivalent to R1391) was important in catalysis. Subsequent experiments based on mutagenesis of R1276 and R1391 (or their equivalents in p120-GAP) gave conflicting data (Gutmann *et al*, 1993; Morcos *et al*, 1996; Miao *et al*, 1996; Mittal *et al*, 1996). This data will be discussed alongside my own in section 4.3. Confusion arising from mutation of these residues may have resulted because the fundamental parameters describing catalysis, the maximal rate (k_{cat}) and the affinity (either K_m or K_d) have not always been measured using purified wild-type and mutant proteins. Therefore, I decided to mutate R1276 and R1391 to alanine in the context of the catalytic domain of NF1 ($NF1_{334}$) and to precisely measure the effects on k_{cat} and K_d.

Figure 32: Sequence alignments of GAP-related domains

Residue numbers along the left margin identify the locations of the GAP-related domains within their parent sequences. Rectangles are drawn around the highly significant 'homology blocks' (Wang *et al*, 1991a); a dashed line is used for block 2 to indicate that this region is disrupted by a naturally occurring insertion (Anderson *et al*, 1993a; Nishi *et al*, 1991). Concensus sequences for these highly conserved blocks are given with bold-faced characters representing invariant residues and dots indicating the most variable positions. Mutations in NF1-GRD are indicated as italicized residues immediately below their wild-type counterparts.

[Taken from Gutmann *et al* (1993)]

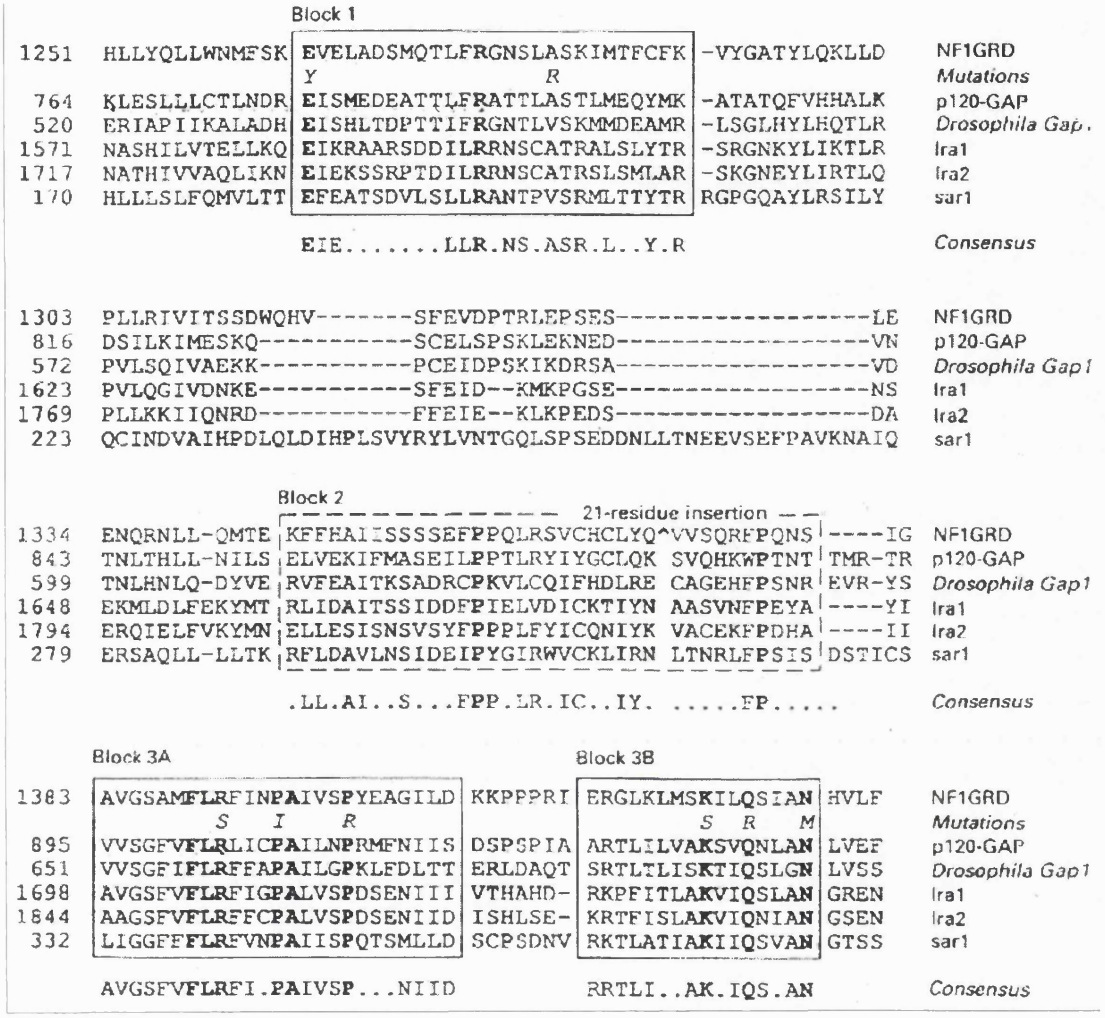
Block 1
1251 HLLYQLLWNMFSK EVELADSMQTLFRGNSLASKIMTFCFK -VYGATYLQKLLD NF1GRD
Y R
Mutations
764 KLESLLLCTLNDR EISMEDEATTLFRATTLASTLMEQYMK -ATATQFVHHALK p120-GAP
520 ERIAPIIKALADH EISHLTDPTTIFRGNTLVSKMMDEAMR -LSGLHYLHQTLR Drosophila Gap1
1571 NASHILVTELLKQ EIKRAARSDDILRRNSCATRALSLYTR -SRGNKYLIKTLR Ira1
1717 NATHIVVAQLIKN EIEKSSRPTDILRRNSCATRSLSMLAR -SKGNEYLIRTLQ Ira2
170 HLLLSLFQMVLTT EFEATSDVLSLLRANTPVSRMLTTYTR RGPGQAYLRSILY sar1
EIE.....LLR.NS.ASR.L..Y.R Consensus
1303 PLLRIVITSSDWQHV-------SFEVDPTRLEPSES----------LE NF1GRD
816 DSILKIMESKQ----------SCELSPSKLEKNED----------VN p120-GAP
572 PVLSQIVAEKK----------PCEIDPSKIKDRSA----------VD Drosophila Gap1
1623 PVLQGIVDNKE----------SFEID--KMKPGSE----------NS Ira1
1769 PLLKKIIQNRD----------FFEIE--KLKPEDS----------DA Ira2
223 QCINDVAIHPDLQLDIHPLSVYRYLVNTGQLSPSEDDNLLTNEEVSEFPAVKNAIQ sar1
Block 2
21-residue insertion
1334 ENQRNLL-QMTE KFFHAIISSSSEFPPQLRSVCHCLYQ^VVSQRFPQNS ----IG NF1GRD
843 TNLTHLL-NILS ELVEKIFMASEILPPTLRYIYGCLQK SVQHKWPTNT TMR-TR p120-GAP
599 TNLHNLQ-DYVE RVFEAITKSADRCPKVLCQIFHDLRE CAGEHFPSNR EVR-YS Drosophila Gap1
1648 EKMLDLFEKYMT RLIDAITSSIDDFPIELVDICKTIYN AASVNFPEYA ----YI Ira1
1794 ERQIELFVKYMN ELLESISNSVSYFPPPLFYICQNIYK VACEKFPDHA ----II Ira2
279 ERSAQLL-LLTK RFLDAVLNSIDEIPYGIRWVCKLIRN LTNRLFPSIS DSTICS sar1
.LL.AI..S...FPP.LR.IC..IY. .....FP..... Consensus
Block 3A
Block 3B
1383 AVGSAMFLRFINPAIVSPYEAGILD KKPPPRI ERGLKLMSKILQSIAN HVLF NF1GRD
S I R S R M
Mutations
895 VVSGFVFLRLICPAILNPRMFNIIS DSPSPIA ARTLILVAKSVQNLAN LVEF p120-GAP
651 VVSGFIFLRFFAPAILGPKLFDLTT ERLDAQT SRTLTLISKTIQSLGN LVSS Drosophila Gap1
1698 AVGSFVFLRFIGPALVSPDSENIII VTHAHD- RKPFITLAKVIQSLAN GREN Ira1
1844 AAGSFVFLRFFCPALVSPDSENIID ISHLSE- KRTFISLAKVIQNIAN GSEN Ira2
332 LIGGFFFLRFVNPAIISPQTSMLLD SCPSDNV RKTLATIAKIIQSVAN GTSS sar1
AVGSFVFLRFI.PAIVSP...NIID RRTLI..AK.IQS.AN Consensus

Figure 33(a): Sequence alignments of RasGAP-related domains

Sequence alignment of 12 members of the RasGAP family are shown. Concensus sequences for the highly conserved blocks 1 and 3A are given with bold-faced characters representing invariant residues. The sequence data was obtained from Ahmadian *et al* (1996) except for Sar1 (Gutmann *et al*, 1993; Hettich and Marshall, 1994), $GAP1^{IP4BP}$ (Cullen *et al*, 1995), IQGAP1 (Brill *et al*, 1996) and $GAP^{R\text{-}Ras}$ (Yamamoto *et al*, 1995).

NF1, p120-GAP (human), dmGAP1, Ira1/Ira2, Sar1, $GAP1^{IP4BP}$, GAP1m (human), $GAP^{R\text{-}Ras}$ (bovine), GAP^{celeg} (C.elegans), IQGAP1.

Figure 33(b): Sequence alignments of RhoGAP-related domains

Sequence alignment of 6 members of the RhoGAP family are shown. Concensus sequences for the highly conserved blocks 1 and 3A are given with bold-faced characters representing invariant residues. The sequence data was obtained from Barrett *et al* (1997).

(a)

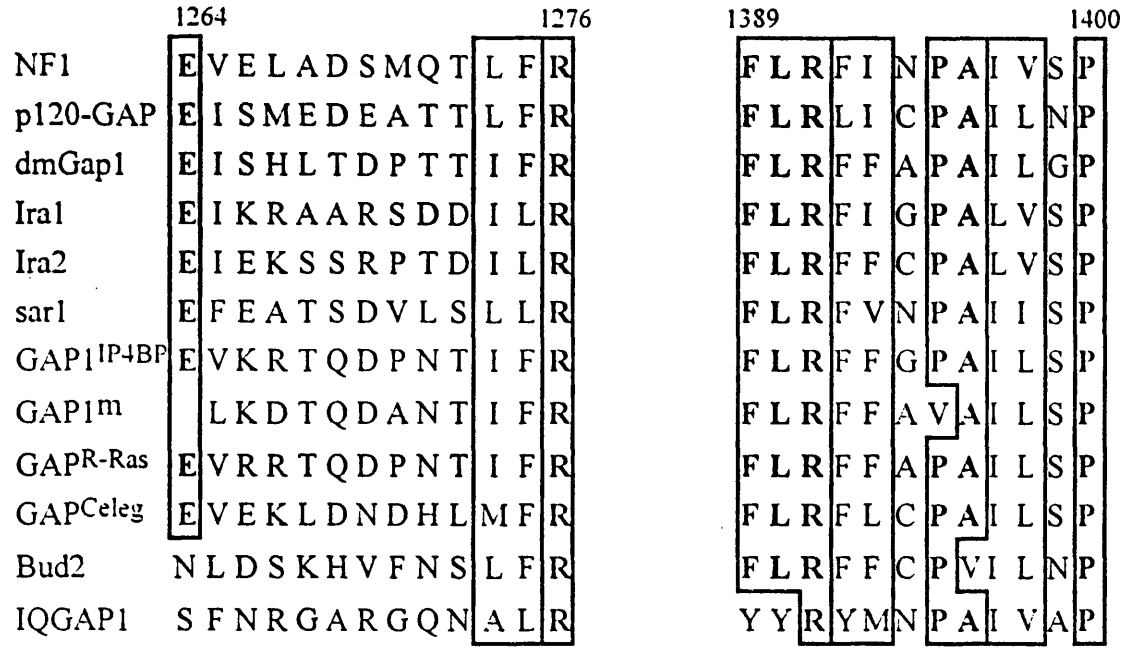
1264
1276
1389
1400
NF1 E V E L A D S M Q T L F R F L R F I N P A I V S P
p120-GAP E I S M E D E A T T L F R F L R L I C P A I L N P
dmGap1 E I S H L T D P T T I F R F L R F F A P A I L G P
Ira1 E I K R A A R S D D I L R F L R F I G P A L V S P
Ira2 E I E K S S R P T D I L R F L R F F C P A L V S P
sar1 E F E A T S D V L S L L R F L R F V N P A I I S P
GAP1IP4BP E V K R T Q D P N T I F R F L R F F G P A I L S P
GAP1m L K D T Q D A N T I F R F L R F F A V A I L S P
GAPR-Ras E V R R T Q D P N T I F R F L R F F A P A I L S P
GAPCeleg E V E K L D N D H L M F R F L R F L C P A I L S P
Bud2 N L D S K H V F N S L F R F L R F F C P V I L N P
IQGAP1 S F N R G A R G Q N A L R Y Y R Y M N P A I V A P

(b)

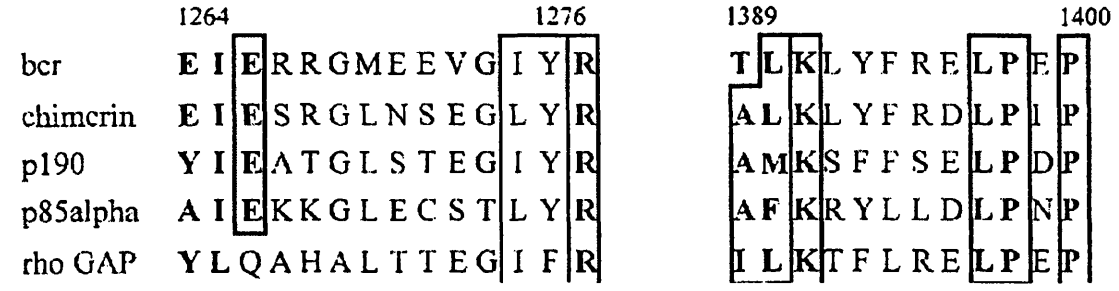
1264
1276
1389
1400
bcr E I E R R G M E E V G I Y R T L K L Y F R E L P E P
chimerin E I E S R G L N S E G L Y R A L K L Y F R D L P I P
p190 Y I E A T G L S T E G I Y R A M K S F F S E L P D P
p85alpha A I E K K G L E C S T L Y R A F K R Y L L D L P N P
rho GAP Y L Q A H A L T T E G I F R I L K T F L R E L P E P

4.2 Results

4.2.1 Characterization of wild-type, R1276A and R1391A $NF1_{334}$

The codons encoding for Arg1276 and Arg1391 of GST-$NF1_{334}$ were each mutated independently to those for Ala. Wild-type, R1276A and R1391A GST-$NF1_{334}$ were all expressed at the same levels and with the same solubility, producing 10-15mg of purified protein from 25g of induced cells. The proteins were purified as GST fusions and subsequently cleaved with thrombin as described in section 2.2.2. The thrombin-cleaved protein was used for all studies reported here All three purified proteins were nearly homogeneous as judged by SDS-PAGE (data not shown) and by electrospray mass spectrometry (described in section 2.3.4). Mass spectrometry gave molecular weights of 38554 ± 4, 38466 ± 4 and 38466 ± 3 for wild-type, R1276A and R1391A $NF1_{334}$ proteins respectively. These are within experimental error of the masses calculated from the anticipated protein sequences (38551, 38466, 38466). The difference in mass of 85 between the molecular weights of mutant and wild-type $NF1_{334}$ is consistent with the substitution of an arginine residue (molecular mass 174) for an alanine residue (molecular mass 89).

The effect of the mutations on the structure of $NF1_{334}$ was assessed by circular dichroism (CD) and intrinsic tryptophan emission studies. Circular dichroism spectra of wild-type, R1276A and R1391A $NF1_{334}$ were obtained in both the near-UV and far-UV by Dr Steve Martin as described in section 2.3.2. Spectra for all three proteins were obtained and plotted on the same graph. Both the near-UV and far-UV circular dichroism spectra for the two mutant proteins were indistinguishable from the wild-type protein, the difference between the samples being of the same order as the difference between different scans of the same sample. Spectra generated in the near and far-UV are shown in figures 34a and b respectively.The near-UV CD signal comes only from tyrosine, phenylalanine and tryptophan residues. The contribution from phenylalanine to the near UV spectra is represented by very small peaks at 262 and 267nm. Tyrosine probably accounts for most of the signal below 285nm and tryptophan gives rise to a positive peak at 290nm and perhaps some of the intensity at shorter wavelengths. The long wavelength negative signal

(>295nm) could also be due to tryptophan. These spectra show that the R1276A and R1391A mutations have no effect on the tertiary structure of $NF1_{334}$, at least as it is reflected by the environment of the aromatic residues. The far-UV CD signal comes almost entirely from the peptide bond. The calculated alpha-helical content of $NF1_{334}$ was 50-60%. These spectra show that the mutations do not affect the secondary structure of $NF1_{334}$.

Intrinsic tryptophan fluorescence was used to investigate whether the mutations had invoked any conformational changes in $NF1_{334}$. $NF1_{334}$ contains a total of 4 tryptophan residues. The emission maximum from these tryptophans is generally sensitive to the environment and as such can be used as a measure of the extent to which these residues are buried in the protein interior. An emission maximum of 355nm generally indicates that the tryptophans are very exposed on the surface of $NF1_{334}$, whereas an emission maximum of 322nm generally gives an indication that the tryptophan residues are highly buried in $NF1_{334}$. Intrinsic tryptophan emission spectra were recorded as decribed in section 2.3.3 on an SLM photon-counting spectrofluorimeter, thermostatted to 30°C. The emission maximum for all three proteins was estimated from the spectra to be ca. 337nm.The spectra shown in figure 35, are identical within the limits of experimental error supporting the hypothesis that the mutations have caused no gross structural rearrangements within $NF1_{334}$.

4.2.2 Kinetic characterization of the interaction of H-Ras.mantGTP with wild-type, R1391A and R1276A $NF1_{334}$

4.2.2.1 Intrinsic GTPase of H-Ras.mantGTP

The effect of the mutations of $NF1_{334}$ on their interaction with H-Ras was studied by the use of mantGTP and stopped-flow techniques as described in chapter 3. First, the intrinsic rate constant of the hydrolysis of H-Ras.mantGTP was determined since this was originally done with N-Ras.mantGTP (Neal *et al*, 1990).

Figure 34: Circular dichroism spectra of wild-type and mutant $NF1_{334}$

The secondary and tertiary structure composition of the wild-type and mutant $NF1_{334}$ was estimated using far-UV and near-UV circular dichroism spectropolarimetry respectively.

(a) Near UV spectra of wild-type, R1276A and R1391A $NF1_{334}$ were recorded as described in section 2.3.2 at room temperature in 10mm path length quartz cuvettes in the 250-340nm range. $NF1_{334}$ samples were diluted in 20mM Tris/HCl, pH7.5, 1mM $MgCl_2$, 0.1mM dithiothreitol, to a final concentration of 1-2mg/ml. The spectra shown are expressed as delta epsilon (molar) versus wavelength (nm).

(b) Far UV spectra of wild-type, R1276A and R1391A $NF1_{334}$ were recorded as described in section 2.3.2 at room temperature in 0.1mm path length quartz cuvettes in the 180-260nm range. $NF1_{334}$ samples were diluted in 20mM Tris/HCl, pH7.5, 1mM $MgCl_2$, 0.1mM dithiothreitol, to a final concentration of 1-2mg/ml. The spectra shown are expressed as delta epsilon (mrw) versus wavelength (nm).

(a)

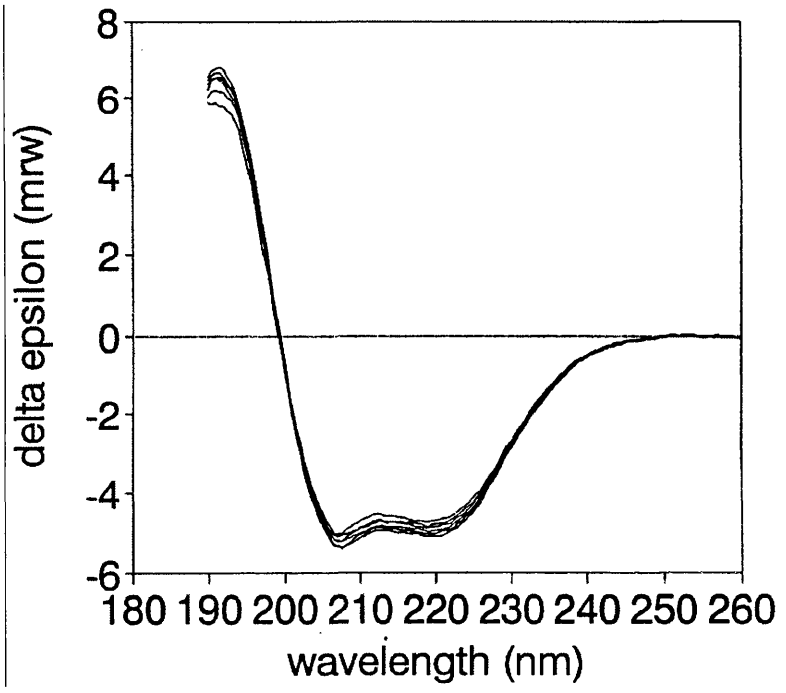
8
6
4
2
0
-2
-4
-6
delta epsilon (mrw)
180 190 200 210 220 230 240 250 260
wavelength (nm)

(b)

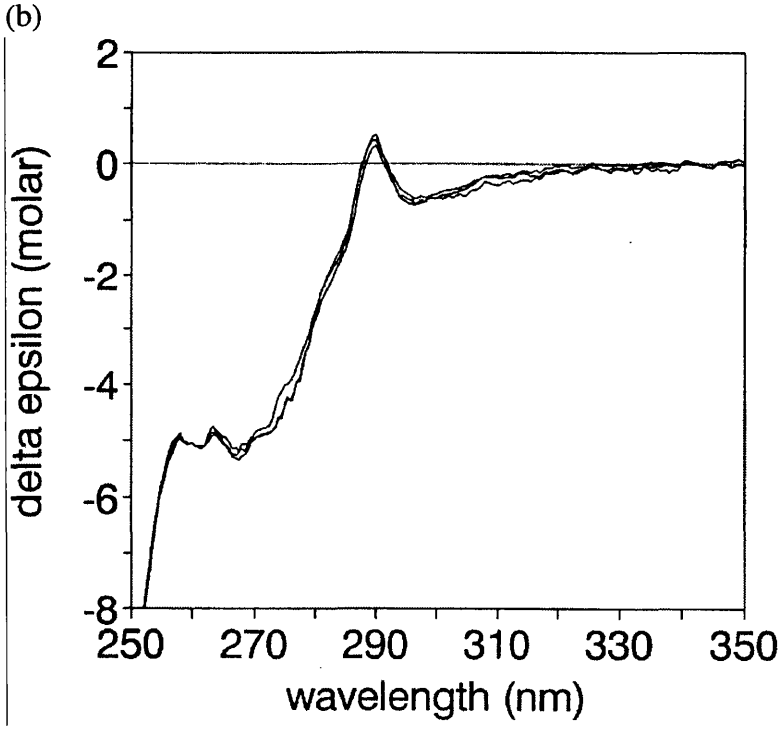
2
0
-2
-4
-6
-8
delta epsilon (molar)
250 270 290 310 330 350
wavelength (nm)

Figure 35: Intrinsic tryptophan emission spectra for wild-type, R1276A and R1391A $NF1_{334}$

Tryptophan emission for wild-type (—), R1276A (----), R1391A (– –) $NF1_{334}$ and buffer (——) was monitored from 290-420nm at an excitation wavelength of 290nm, using the SLM photon-counting spectrofluorimeter. Samples of $NF1_{334}$ were diluted to a final concentration of 10μM in 20mM Tris/HCl, pH 7.5, 1mM $MgCl_2$, 0.1mM dithiothreitol. Tryptophan emission spectra were recorded in 1cm path length quartz cuvettes at 30°C.

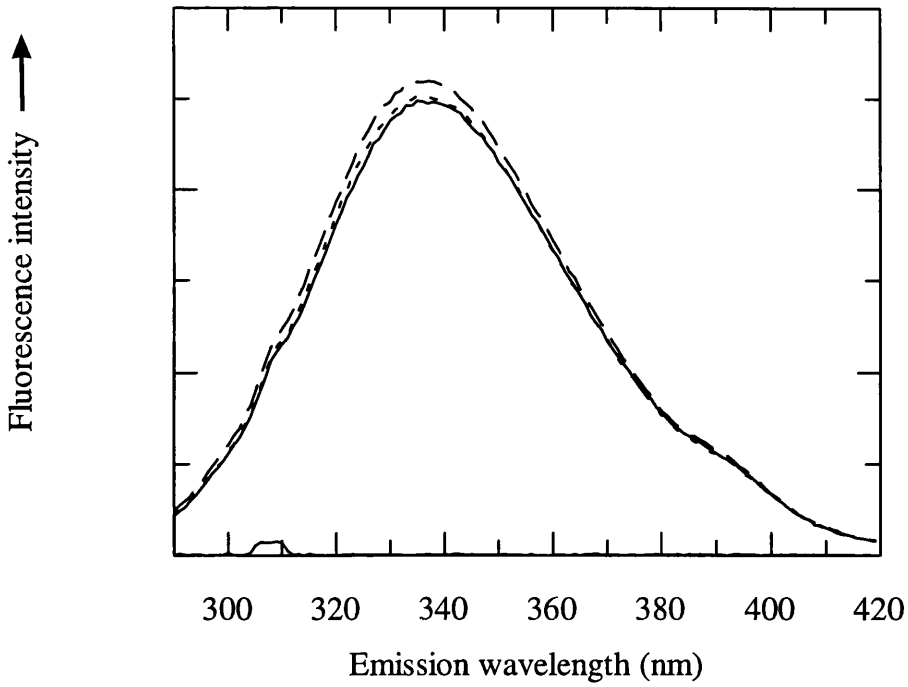
Fluorescence intensity
300
320
340
360
380
400
420
Emission wavelength (nm)

A solution of 3μM H-Ras.mantGTP in 20mM Tris/HCl pH 7.5, 1mM $MgCl_2$, 0.1mM dithiothreitol, was incubated at 30°C as described in section 2.8.2.1. Fluorescence intensity was measured with time and the results are shown in figure 36a. In addition, samples were taken at intervals and analysed by HPLC for the percentage of mantGTP and mantGDP. These results are shown as an inset in figure 36a. The fluorescence decreased by ca. 12% over 5 hours. The fluorescence data could be accurately fitted to a double exponential with rate constants of 5.3 x 10^{-3} s^{-1} (amplitude 2.7%) and 1.8 x 10^{-4} s^{-1}(amplitude 8.5%). The mantGTP/mantGDP percentage data could be fitted to a single exponential with a rate constant of 1.6 x 10^{-4} s^{-1}. These results are qualitatively similar to the results of Moore *et al* (1993) using N-Ras in that a small fast decrease was observed followed by a slower decrease which had a rate constant identical to the cleavage reaction within experimental error. The cause of the small fast phase is unknown.

The experiment was repeated in the presence of 100mM NaCl (figure 36b). The fluorescence data could best be fitted to a double exponential with rate constants of 3.5 x $10^{-3}s^{-1}$ (amplitude 3.9%) and 1.6 x $10^{-4}s^{-1}$ (amplitude 9.5%). The intrinsic rate of hydrolysis determined from the mantGTP/mantGDP percentage data (1.6 x $10^{-4}s^{-1}$) was unaffected by the inclusion of 100mM NaCl (1.45 x $10^{-4}s^{-1}$) (data shown as inset in figure 36b) and was similar to that obtained previously with N-Ras (Moore *et al*, 1993) under identical conditions.

Figure 36: Fluorescence changes and the rate of mantGTP cleavage associated with mantGTP hydrolysis by H-Ras

(a) H-Ras.mantGTP (48μM) at 4°C was diluted into 20mM Tris/HCl pH7.5, 1mM $MgCl_2$, 0.1mM dithiothreitol, at 30°C to a final concentration of 3μM. The fluorescence intensity of the solution was monitored with time using excitation and emission wavelengths of 366 and 440nm respectively (●). The solid line through the circles is a double exponential best fit to the Ras.mantGTP data with $k_{obs1} = 5.3 \times 10^{-3}$ s^{-1}, $A_1 =$ 2.75%, $k_{obs2} = 1.8 \times 10^{-4}$ s^{-1}, and $A_2 = 8.55\%$ (where A refers to the amplitude of each phase). The inset shows the rate of cleavage of mantGTP by H-Ras measured by HPLC as described in section 2.6.1. The data is fitted to a single exponential with $k_{obs} = 1.6 \times 10^{-4}$ s^{-1}.

(a) As in **(a)** except that the buffer also contained 100mM NaCl. The solid line through the circles is a double exponential best fit to the Ras.mantGTP data with $k_{obs1} = 3.5 \times 10^{-3}$ s^{-1}, $A_1 = 3.9\%$, $k_{obs2} = 1.6 \times 10^{-4}$ s^{-1}, and $A_2 = 9.5\%$. The inset shows the rate of cleavage of mantGTP by H-Ras and could be fitted to a single exponential with $k_{obs} = 1.45 \times 10^{-4}$ s^{-1}.

(a)

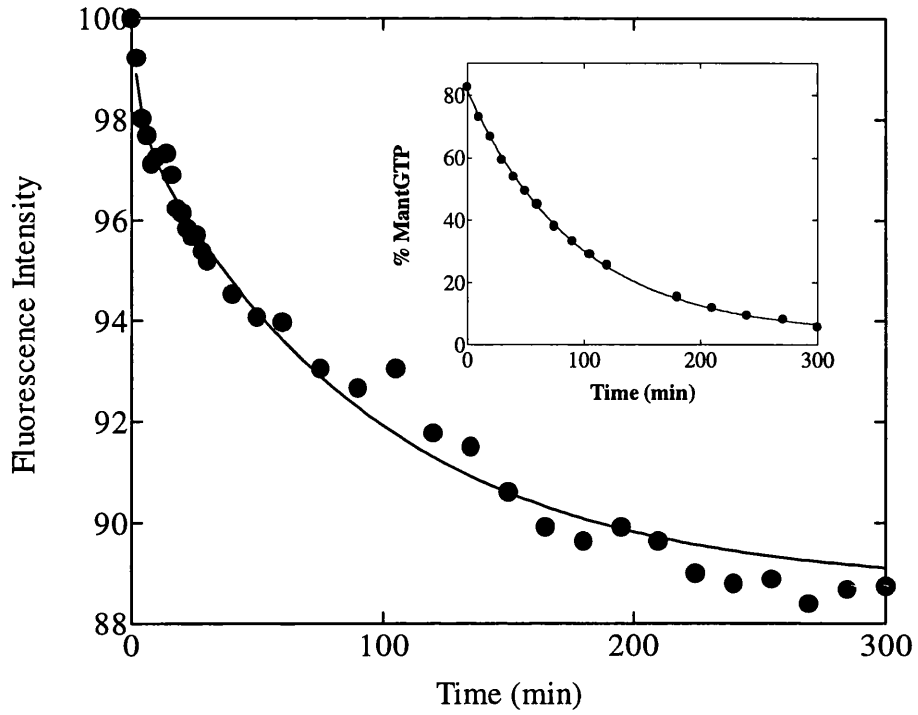
Fluorescence Intensity
100
98
96
94
92
90
88
0
100
200
300
Time (min)
% MantGTP
80
60
40
20
0
100
200
300
Time (min)

(b)

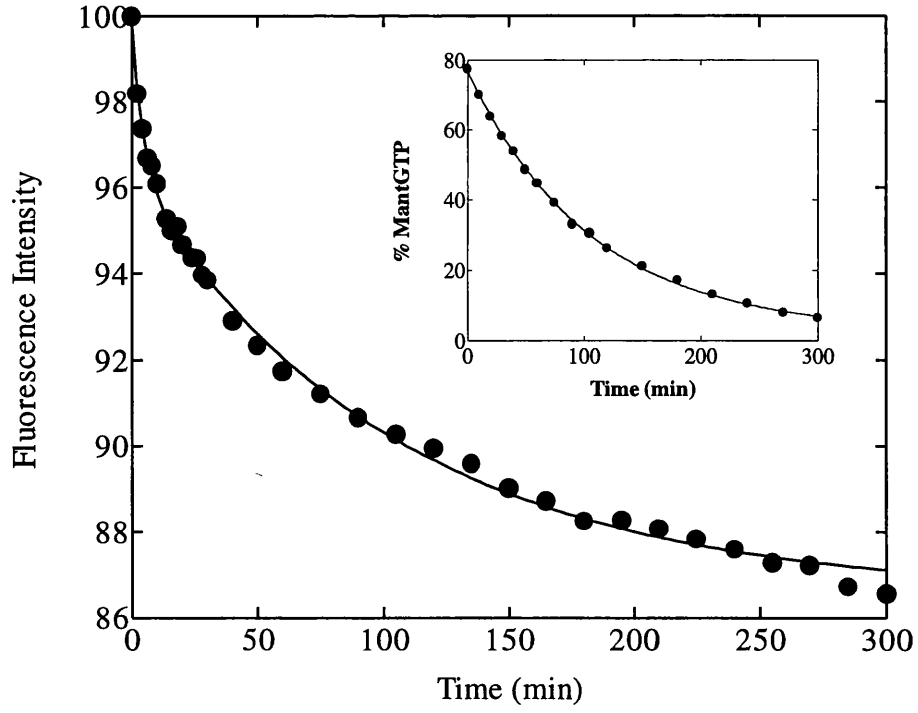
Fluorescence Intensity
100
98
96
94
92
90
88
86
0
50
100
150
200
250
300
Time (min)
% MantGTP
80
60
40
20
0
100
200
300
Time (min)

4.2.2.2 $NF1_{334}$-stimulated GTPase

Having established the intrinsic behaviour of H-Ras.mantGTP, the interaction of H-Ras.mantGTP with wild-type, R1276A and R1391A $NF1_{334}$ was investigated using single turnover conditions (i.e excess $NF1_{334}$) and monitoring mant fluorescence.

Upon mixing H-Ras.mantGTP with wild-type $NF1_{334}$ in a stopped-flow instrument (as shown in chapter 3) a biphasic fluorescence signal was obtained consisting of an initial second order increase in fluorescence followed by a slower first order exponential decrease in fluorescence which decreased to a final value approximately 12% below the starting value. This experiment was repeated in these studies to enable direct comparisons to be made between wild-type and mutant $NF1_{334}$ proteins. Therefore, 0.2μM H-Ras.mantGTP was mixed with 1-12μM wild-type $NF1_{334}$ in 20mM Tris/HCl, 1mM $MgCl_2$, 100mM NaCl, 0.1mM dithiothreitol and data for both processes collected. The time course of an example reaction at 2μM wild-type $NF1_{334}$ is shown over 80msec (figure 37a) and over 800msec (figure 37b). The second order increase in fluorescence shown in figure 37a is very rapid (<50msec) and is followed by the initial part of the fluorescence decrease. Therefore, the data was fitted to a double exponential with the second phase fixed at the value for the observed rate constant of the slow fluorescence change to give an observed rate constant of $22s^{-1}$. The exponential decrease in fluorescence shown in figure 37b had reached a stable endpoint within 500msec and the data was fitted to a single exponential with rate constant $12s^{-1}$. The dependence of these rate constants on the concentration of $NF1_{334}$ was investigated and the results are shown in figures 40a and 40b.

The above experiments were repeated using R1276A and R1391A $NF1_{334}$ instead of wild-type protein (figures 37c-f). With both mutant proteins, an initial rapid increase in fluorescence occurred (figure 37c and 37e) which was slower than that observed with wild-type $NF1_{334}$, reaching a stable endpoint within 200msec. Data for the fast phase obtained over 160msec for R1276A (figure 37c) and R1391A (figure 37e) could be fitted to single exponentials with rate constants of $26s^{-1}$ and $70s^{-1}$ respectively. In addition, with

both mutant proteins this process was followed by a decrease in fluorescence although these rates were about two orders of magnitude slower (>50sec) than the wild-type protein (figure 37d and 37f). Data for the slow phase obtained over 100sec for R1276A (figure 37d) and R1391A (figure 37f) could be fitted to single exponentials with rate constants of $0.02s^{-1}$. However, these slow processes did not reach stable endpoints but continued to slowly decrease. Control experiments in which a shutter on the exciting light was closed at various times during the reaction (data not shown) showed that this was due to photobleaching of the mant fluorescence because of the high intensity of the exciting light and long time course of these reactions. To overcome this problem, the slow time courses of the reactions with the mutant proteins were measured in a steady state fluorimeter where much less intense excitation light could be used (by using a narrow excitation slit) but the sensitivity of the instrument was sufficient to give a good signal to noise ratio. Therefore, measurements of the slow phase in the presence of R1276A or R1391A $NF1_{334}$ were obtained over 500sec using an SLM photon-counting spectrofluorimeter (SLM instruments, Urbana, IL). Excitation of the mant fluorophore was at 366nm using a 0.5nm excitation slit width and fluorescence emission was monitored through a KV399 cutoff filter (Schoff). H-Ras.mantGTP was diluted to a final concentration of 0.2μM by mixing with 20mM Tris/HCl pH 7.5, 1mM $MgCl_2$, 100mM NaCl, 0.1mM dithiothreitol prewarmed to 30°C in a 1cm path length quartz cuvette containing a micro-magnetic stirrer. 1-12μM R1276A or R1391A $NF1_{334}$ was manually injected into the solution of H-Ras.mantGTP and the fluorescence intensity monitored with time. The results are shown in figures 38a and 38b. It can be seen that the endpoint of the reaction is almost stable with only slight evidence of photobleaching. Since in these experiments the solutions are manually mixed which requires several seconds, the initial rapid increase in fluorescence is not seen. In these examples, at 4μM of either R1276A or R1391A $NF1_{334}$, the data were fitted to single exponentials with rate constants $0.02s^{-1}$ and $0.01s^{-1}$ respectively.

The effect of $NF1_{334}$ concentration on the observed rate constants of both the fast phase and slow phase of the reactions was studied for both mutant proteins and the results are shown in figures 40c-f. The slow nature of the exponential decrease in fluorescence

observed in reactions with mutant $NF1_{334}$ proteins enabled the relative proportions of mantGTP and mantGDP present at various times during the reaction to be determined by HPLC. This type of measurement could not be used for reactions involving wild-type $NF1_{334}$ due to the rapid nature of the fluorescence decrease. H-Ras.mantGTP (0.2μM) was mixed with 10μM R1276A $NF1_{334}$ in a stirred cell at 30°C in 20mM Tris/HCl pH 7.5, 1mM $MgCl_2$, 100mM NaCl, 0.1mM dithiothreitol. Samples were removed at timed intervals and the GTPase activity of Ras quenched by the addition of half the sample volume of both 10% perchloric acid and 4M sodium acetate. The extent of mantGTP hydrolysis was determined by HPLC as described in section 2.6.1. Figure 39 shows the results of this analysis. The percentage of mantGTP remaining was plotted against time. The data was fitted to a single exponential with an observed rate constant of $0.027s^{-1}$. This rate is identical within the limits of experimental error to the observed rate of the fluorescence decrease shown as an inset in figure 39, obtained under identical conditions ($0.022s^{-1}$). This suggested that for reactions involving R1276A, the slow fluorescence change corresponds to the rate limiting cleavage step.

4.2.3 Interpretation of the kinetic data on the interaction of H-Ras.mantGTP with wild-type, R1276A and R1391A $NF1_{334}$

Eccleston *et al* (1993) interpreted the fluorescence changes occurring on mixing N-Ras.mantGTP with excess wild-type $NF1_{334}$ as an initial second order binding step followed by a first order hydrolysis step.

$$\text{Ras.mantGTP} + \text{N} \rightleftharpoons \text{Ras.mantGTP.N} \rightleftharpoons \text{Ras.mantGDP.Pi.N} \qquad \text{(Scheme 1)}$$

Using a combination of stopped-flow fluorescence intensity, anisotropy and quenched-flow techniques over a range of ionic strength and temperature, Jenkins (1996) has proposed a more complex mechanism. However, for a comparison of the effects of mutations R1276A and R1391A on their interaction with Hras.mantGTP, scheme 1 is at present sufficient.

For a simple second order binding step the observed rate constant of the formation of Ras.mantGTP.N is given by

$$k_{obs} = k_1[N] + k_{-1} \qquad \text{(Equation 1)}$$

so that plotting k_{obs} against [N] gives a linear relationship where the slope is k_1 and the intercept of the Y-axis is k_{-1}. This analysis is suitable for the interaction of H-Ras.mantGTP with the two mutant $NF1_{334}$ proteins since the second step (scheme 1) is extremely slow.

Figures 40c and 40e show that there is indeed a linear relationship between k_{obs} and mutant $NF1_{334}$ concentration. Using the above relationship (eqn. 1), values for k_1 are 5.4 x 10^6 M^{-1} s^{-1} for R1276A and 3.8 x 10^6 M^{-1} s^{-1} for R1391A. Values of k_{-1} are $16s^{-1}$ and 50 s^{-1} for R1276A and R1391A respectively. By use of the relationship $K_d = k_{-1}/k_1$, values of K_d for the two mutant proteins can be calculated to be 3.0μM and 13.0μM for R1276A and R1391A respectively. An independent measurement of these K_d values can be obtained by examining the relationship between the amplitude of the fluorescence increase on mixing H-Ras.mantGTP with mutant $NF1_{334}$ (which is directly proportional to the concentration of H-Ras.mantGTP.N complex formed) and the initial concentration of mutant $NF1_{334}$. This gives a hyperbolic relationship (shown in figure 41) with values for the K_d^{app} of the interaction of H-Ras.mantGTP with R1276A and R1391A of 1.4μM and 7.8μM respectively. These values are similar to those obtained from the values derived from k_1 and k_{-1}.

For analysis of the interactions of H-Ras.mantGTP with wild-type $NF1_{334}$, the situation is more complex since the observed rate of binding is influenced by the subsequent hydrolysis step. In this case, the observed rate constant is given by:

$$k_{obs} = k_1[N] + k_{-1} + k_2 \qquad \text{(Equation 2)}$$

Plotting k_{obs} against [N] will therefore give a straight line of slope k_1 and intercept $k_{-1} + k_2$. It can be seen from figure 40a that there is a linear relationship which gives a second order binding constant of $7.9 \times 10^6\ M^{-1}\ s^{-1}$. The intercept is at $25s^{-1}$, which represents $k_{-1} + k_2$. k_2 is obtained from the observed rate constant of the subsequent slow phase (figure 37b) as discussed below and is found to be $23s^{-1}$. It is therefore difficult to calculate accurately a value of k_{-1} since it involves the difference between two relatively large numbers. However, if an upper limit of $5s^{-1}$ is placed on the difference between the intercept and k_2, an upper limit for $K_d = k_{-1}/k_1$, can be calculated as $< 0.6\mu M$. Since the initial binding step of the interaction between H-Ras.mantGTP and wild-type $NF1_{334}$ is very tight, no variation in the amplitude of the signal was seen with neurofibromin concentration over the range used (data not shown) unlike the situation with the mutant $NF1_{334}$ experiments where a hyperbolic relatioship was observed (figure 41).

The relationship between concentration of wild-type, R1276A and R1391A $NF1_{334}$ and the observed rate constant of the slow phase is shown in figures 40b, d and f respectively. In each case, a hyperbolic dependence of k_{obs} on $NF1_{334}$ concentration was observed. If this process is observing the formation of H-Ras.mantGDP.Pi.N (scheme 1) and the initial step is in rapid equilibrium, then fitting the data to a hyperbola gives a value for K_d and k_2. This assumption is valid for the mutant proteins where k_1 and k_{-1} are very fast compared to k_2. It is not valid in the case of wild-type $NF1_{334}$ where $k_{-1} < k_2$. However, kinetic simulation experiments show that this treatment gives values of K_d within a factor of 2 of the trace value. Using this approach values of K_d were calculated to be $1.1\mu M$, $1.0\mu M$ and ca. $2.5\mu M$ and values for k_2 were $23s^{-1}$, $0.02s^{-1}$ and $0.04s^{-1}$ for wild-type, R1276A and R1391A $NF1_{334}$ respectively. However, as can be seen in figures 37d and 37f, for the mutant proteins it is difficult to obtain as good a data for the very slow time course reactions as it is for the faster reactions of the wild-type proteins and there could be up to 50% errors in the values for mutant proteins.

The calculated equilibrium and kinetic rate constants for the interaction of H-Ras.mantGTP with wild-type, R1276A and R1391A $NF1_{334}$ are shown in table 4.

Figure 37: Stopped-flow fluorescence records of the interaction of H-Ras.mantGTP with $NF1_{334}$

Stopped flow fluorescence experiments were performed as described in section 2.8.2.2 in which 0.2μM H-Ras.mantGTP was mixed with 2μM (a, b) wild-type, (c, d) R1276A or (e, f) R1391A $NF1_{334}$ at 30°C in the Hi-Tech stopped-flow apparatus and the change in fluorescence intensity monitored with time, over 80msec (a), 160msec (c, e), 800msec (b) and 100sec (d, f). A representative trace for each timescale is shown for the interaction of H-Ras.mantGTP with wild-type (a, b), R1276A (c, d) and R1391A (e, f) $NF1_{334}$. All proteins were in 20mM Tris/HCl, pH 7.5, 1mM $MgCl_2$, 100mM NaCl, 0.1mM dithiothreitol. The smooth line through the data indicates the best fit to double (a) or single exponentials (b,c,d,e,f) with rate constants of (a) $22s^{-1}$ (b) $12s^{-1}$ (c) $26s^{-1}$ (d) $0.02s^{-1}$ (e) $70s^{-1}$ (f) $0.02s^{-1}$.

(a)

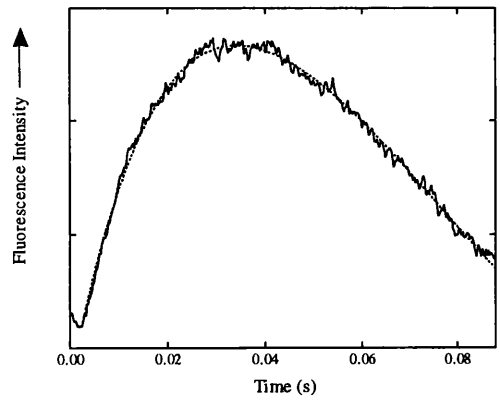
Fluorescence Intensity
0.00
0.02
0.04
0.06
0.08
Time (s)

(b)

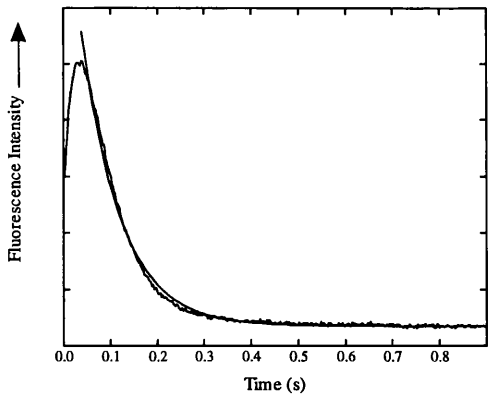
Fluorescence Intensity
0.0
0.1
0.2
0.3
0.4
0.5
0.6
0.7
0.8
Time (s)

(c)

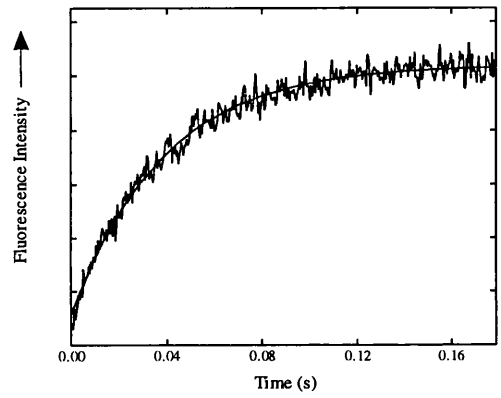
Fluorescence Intensity
0.00
0.04
0.08
0.12
0.16
Time (s)

(d)

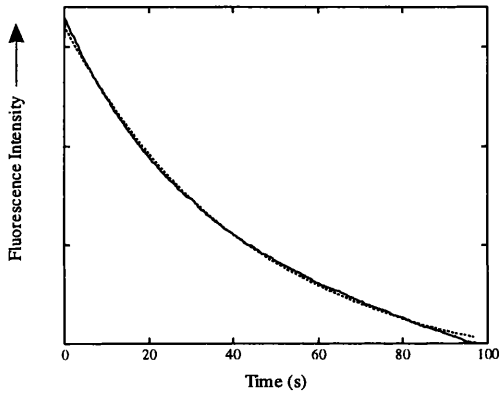
Fluorescence Intensity
0
20
40
60
80
100
Time (s)

(e)

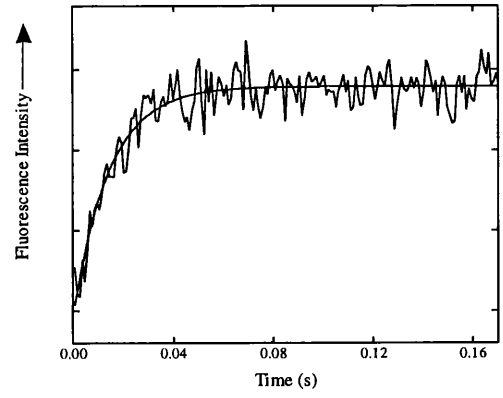
Fluorescence Intensity
0.00
0.04
0.08
0.12
0.16
Time (s)

(f)

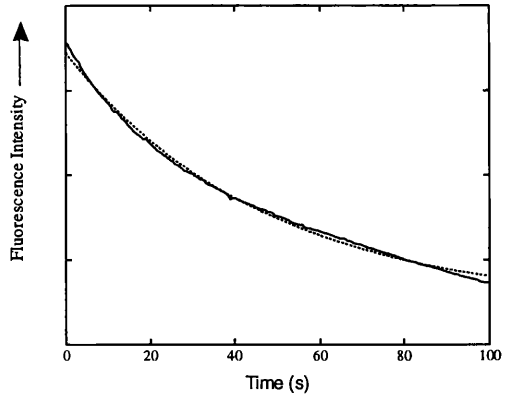
Fluorescence Intensity
0
20
40
60
80
100
Time (s)

Figure 38: Spectrofluorimeter data traces showing the slow phase of the interaction of H-Ras.mantGTP with R1276A and R1391A $NF1_{334}$

Fluorescence experiments were performed on an SLM photon-counting spectrofluorimeter, as described in section 4.2.2.2. For the reactions, 0.2μM H-Ras.mantGTP was mixed with 4μM (a) R1276A or (b) R1391A $NF1_{334}$, at 30°C. All proteins were in 20mM Tris/HCl pH,7.5, 1mM $MgCl_2$, 100mM NaCl, 0.1mM dithiothreitol. The arrows indicate the point at which $NF1_{334}$ was added to the reaction. The smooth line through the data indicate the best fit to single exponentials with rate constants of (a) $0.02s^{-1}$ (b) $0.01s^{-1}$.

(a)

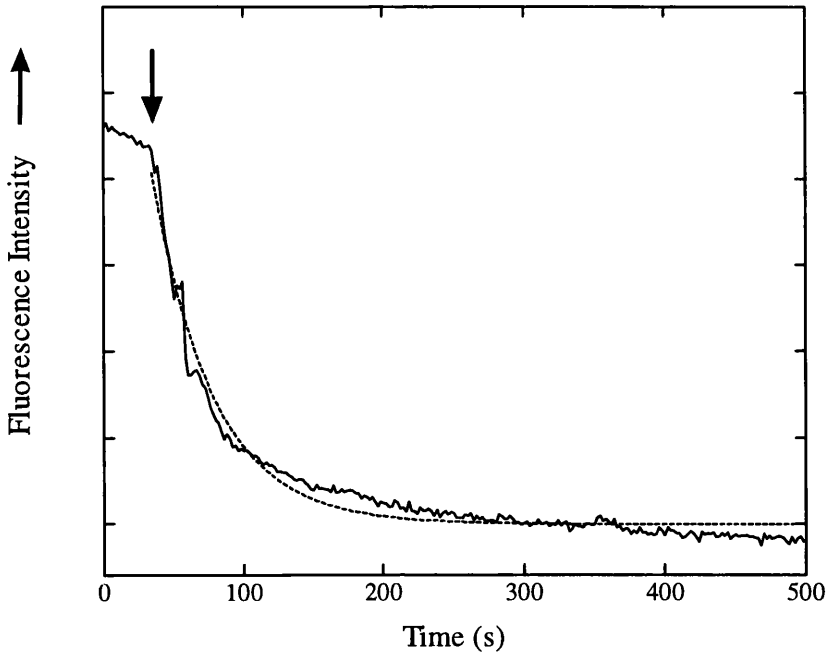
Fluorescence Intensity
0
100
200
300
400
500
Time (s)

(b)

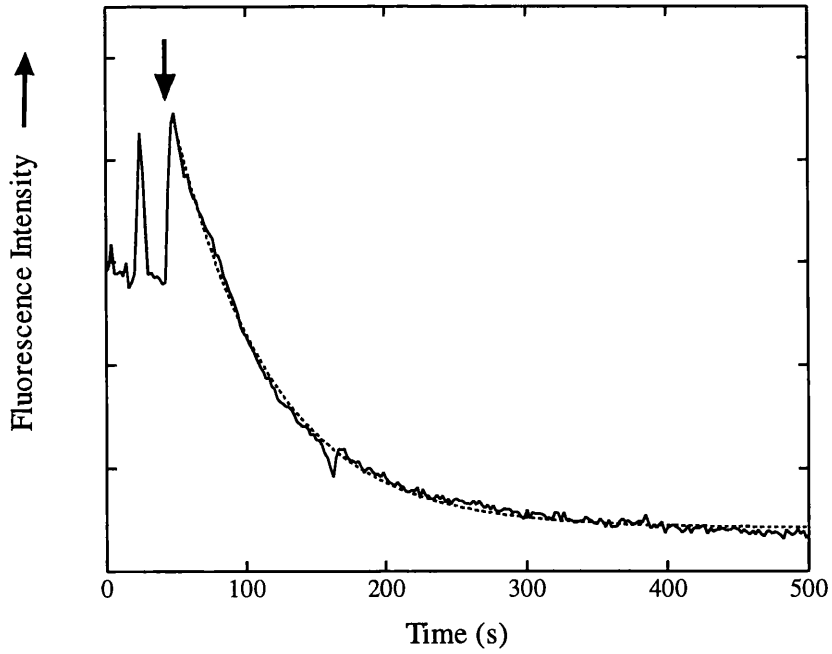
Fluorescence Intensity
0
100
200
300
400
500
Time (s)

Figure 39: R1276A-catalyzed cleavage of H-Ras.mantGTP

H-Ras.mantGTP (0.2μM) was mixed with 10μM R1276A $NF1_{334}$ in a stirred cell at 30°C. All proteins were in 20mM Tris/HCl pH 7.5, 1mM $MgCl_2$, 100mM NaCl, 0.1mM dithiothreitol. The extent of mantGTP hydrolysis was determined by HPLC as described in section 2.6.1. The percentage of mantGTP remaining was plotted against time. The smooth line through the data indicates the best fit to a single exponential with rate constant of $0.027s^{-1}$. The change in fluorescence intensity monitored over time under the same conditions is shown as an inset. The smooth line through the data indicates the best fit to a single exponential with rate constant of $0.022s^{-1}$.

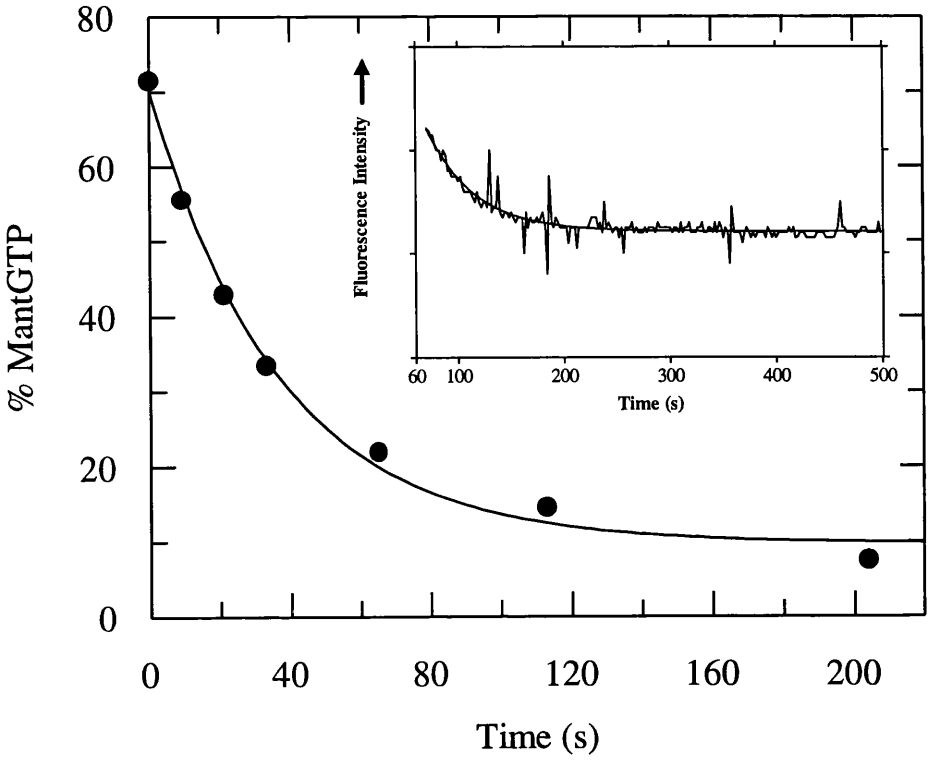
80
60
40
20
0
% MantGTP
0
40
80
120
160
200
Time (s)
Fluorescence Intensity
60
100
200
300
400
500
Time (s)

Figure 40: Dependence of observed rates of both fast and slow phases for the interaction of H-Ras.mantGTP with $NF1_{334}$, on $[NF1_{334}]$

In figures a, c and e, the observed rates of the fast phase obtained over 80msec (a) or 160msec (c, e) for the interaction of H-Ras.mantGTP with wild-type (a), R1276A (c) and R1391A (e) $NF1_{334}$ have been plotted against $[NF1_{334}]$ and shows a linear dependence over the concentrations of $NF1_{334}$ used. All proteins were in 20mM Tris/HCl pH 7.5, 1mM $MgCl_2$, 100mM NaCl, 0.1mM dithiothreitol. The smooth line through the data shows the best fit to a linear regression equation from which slopes of (a) $5.4 \times 10^6\ M^{-1}\ s^{-1}$ (c) $3.8 \times 10^6\ M^{-1}\ s^{-1}$ and (e) $7.9 \times 10^6\ M^{-1}\ s^{-1}$, and Y-axis intercepts of (a) $25s^{-1}$ (c) $16s^{-1}$ and (e) $50s^{-1}$ were determined.

In figures b, d and f, the observed rates of the slow phase, obtained over 800msec (b) or 500sec (d, f) for the interaction of H-Ras.mantGTP with wild-type (b), R1276A (d) and R1391A (f) $NF1_{334}$ have been plotted against $[NF1_{334}]$ and shows hyperbolic dependence over the concentrations of $NF1_{334}$ used. The smooth line through the data shows the best fit to a binding isotherm for simple association of two molecules (anisotropy S_0 = constant) with K_d's of (b) 1.1μM (d) 1.0μM (f) ca. 2.5μM, and k_2 of (b) $23s^{-1}$ (d) $0.02s^{-1}$ (f) $0.04s^{-1}$

(a)

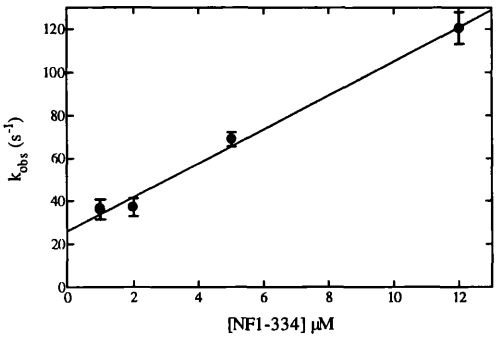
k_{obs} (s^{-1})
[NF1-334] μM

(b)

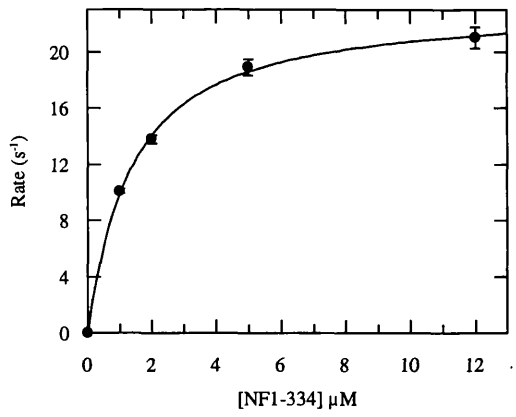
Rate (s^{-1})
[NF1-334] μM

(c)

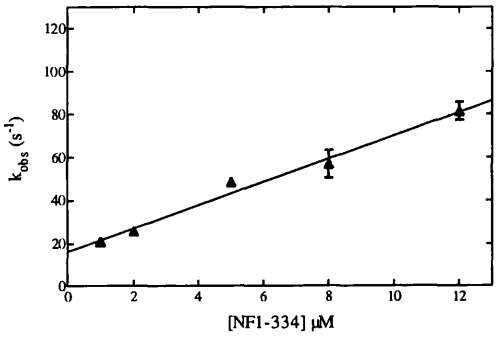
k_{obs} (s^{-1})
[NF1-334] μM

(d)

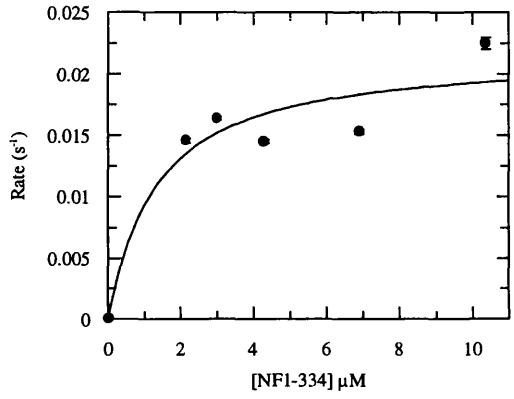
Rate (s^{-1})
[NF1-334] μM

(e)

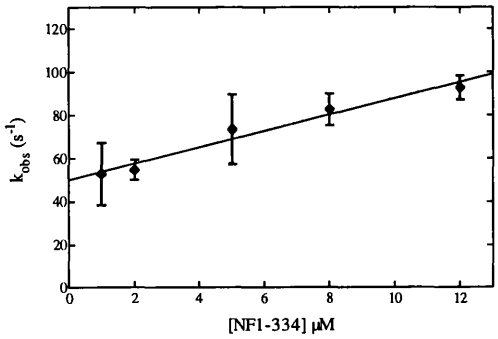
k_{obs} (s^{-1})
[NF1-334] μM

(f)

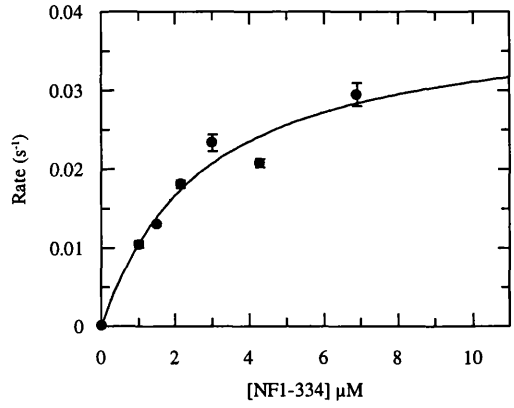
Rate (s^{-1})
[NF1-334] μM

Figure 41: Dependence of the amplitude of the fast phase for the interaction of H-Ras.mantGTP with R1276A and R1391A, on [$NF1_{334}$].

Absolute amplitudes of the fast phase of reactions from the stopped-flow fluorescence experiments shown in figure 37, were obtained by averaging the amplitudes from at least 5 data traces at each neurofibromin concentration. Amplitudes were plotted against R1276A (▲) and R1391A (♦) $NF1_{334}$. All proteins were in 20mM Tris/HCl pH 7.5, 1mM $MgCl_2$, 100mM NaCl, 0.1mM dithiothreitol. The solid line through each data set represents the best fit to a binding isotherm for simple association of two molecules (anisotropy S_0 = constant) with K_d^{app} of 1.4μM and 7.8μM respectvely.

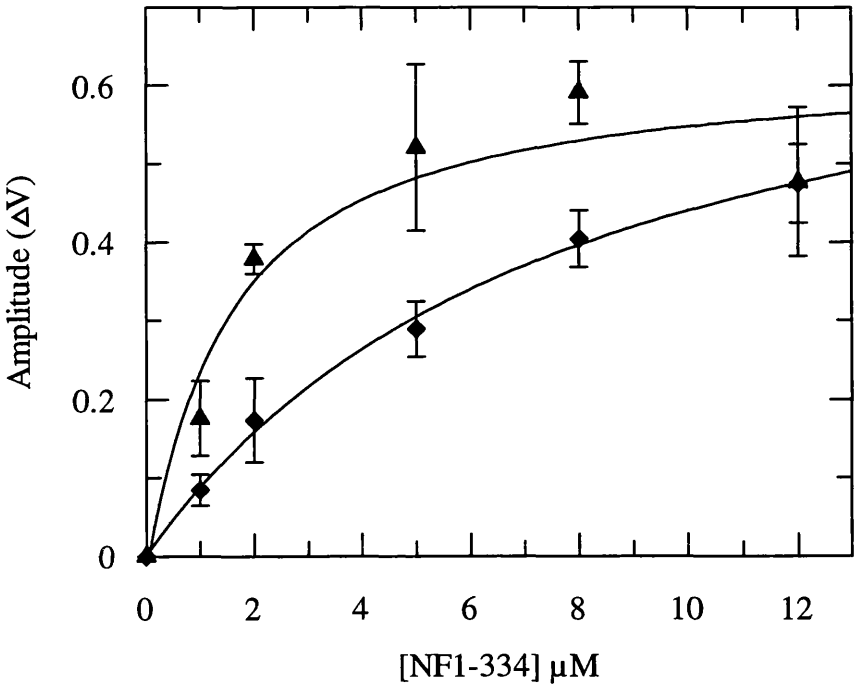
Amplitude (ΔV)
0.6
0.4
0.2
0
0
2
4
6
8
10
12
[NF1-334] μM

Table 4: Equilibrium and kinetic rate constants for the interaction of H-Ras.mantGTP with wild-type, R1276A and R1391A neurofibromin

$NF1_{334}$ variant	H-Ras.mantGTP				
	k_1 [1] ($M^{-1} s^{-1}$)	k_{-1} [2] (s^{-1})	K_d [3] (μM)	k_2 [4] (s^{-1})	Activation of Intrinsic GTPase
Wild-type	7.9×10^6	< 5	< 0.6	23	1.6×10^5
R1276A	5.4×10^6	16	3.0	0.02	130
R1391A	3.8×10^6	50	13.0	0.04	250

1 Obtained from slope of k_{obs} against $[NF1_{334}]$ in the association reaction (Fig 40a,c,e)

2 Obtained from intercept of k_{obs} against $[NF1_{334}]$ in the association reaction (Fig 40a,c,e)

3 Obtained from $K_d = k_{-1}/k_1$

4 Obtained from k_{obs} against $[NF1_{334}]$ in the hydrolysis reaction (Fig 40b,d,f)

4.2.4 Kinetic characterization of the interaction of [Leu61]H-Ras.mantGTP with wild-type, R1276A and R1391A $NF1_{334}$

By monitoring the binding of $NF1_{334}$ to Ras under conditions in which the rate constant for the hydrolysis step (k_2) is negligible, the derived dissociation rate constant (k_{-1}) will be a true reflection of the dissociation of Ras from $NF1_{334}$ rather than the sum of k_{-1} and k_2. Elimination of the hydrolysis step was achieved by the use of [Leu61]H-Ras.mantGTP. Brownbridge *et al*(1993) reported that the catalytic domain of p120-GAP, (GAP_{344}) causes a 27-fold activation of the GTPase activity of [Leu61]H-Ras compared to an activation of 10^5 of wild-type Ras proteins. By performing the reactions over a range of [$NF1_{334}$], k_{obs} can be plotted against [$NF1_{334}$] to give a straight line with the slope equal to k_1 and the intercept equal to k_{-1}.

On mixing 0.2μM [Leu61]H-Ras.mantGTP with excess (1-5μM) wild-type $NF1_{334}$, in 20mM Tris/HCl pH 7.5, 1mM $MgCl_2$, 100mM NaCl, 0.1mM dithiothreitol, a single exponential increase in fluorescence occurred. An example reaction at 2μM $NF1_{334}$ is given in figure 42a. The data could be fitted to a single exponential with an observed binding rate constant of $22s^{-1}$. When the experiment was repeated with R1276A and R1391A $NF1_{334}$, the amplitude of the signal was markedly reduced compared to the signal obtained in the wild-type $NF1_{334}$ reaction. Despite the reduction in the size of the signal, the data obtained with R1276A could still be fitted to a single exponential to obtain the observed rate of binding. In the example shown in figure 42c, at 2μM R1276A $NF1_{334}$, the observed rate of binding was $10s^{-1}$. However, the reduction in amplitude in reactions with R1391A was so severe that the data could not be fitted to single exponentials with any degree of accuracy. This suggested that the concentration of [Leu61]H-Ras.mantGTP.N complex at the start of the reaction was very low possibly as a result of a weaker binding of this mutant to [Leu61]H-Ras.mantGTP. Therefore, concentrations of all reactants were increased and the experiment was repeated. Upon mixing 1μM [Leu61]H-Ras.mantGTP with 4-12μM R1391A $NF1_{334}$ the overall amplitude of the signal was increased and the resultant increase in fluorescence could be fitted accurately to a single exponential. In the example shown in figure 42e, at 9μM R1391A $NF1_{334}$ the observed rate of binding was

$55s^{-1}$. Figure 43 shows the effect of $NF1_{334}$ concentration on the amplitude of the binding signal for all three $NF1_{334}$ proteins based on starting concentrations of [Leu61]H-Ras.mantGTP of 0.2μM (wild-type), 0.2μM (R1276A) and 1μM (R1391A). With all $NF1_{334}$ proteins, no subsequent decrease associated with the cleavage reaction was observed as occurred with H-Ras.mantGTP (figure 37b,d,f).

The effect of $NF1_{334}$ concentration on k_{obs} is shown in figures 42b,d and f. The data can be analysed according to a simple one step binding scheme:

$$[\text{Leu61}]\text{H-Ras.mantGTP} + N \underset{k_{-1}}{\overset{k_1}{\rightleftharpoons}} [\text{Leu61}]\text{H-Ras.mantGTP.N}$$

(Scheme 2)

where $k_{obs} = k_1[N] + k_{-1}$

so that a plot of k_{obs} against $NF1_{334}$ concentration gives a straight line of slope k_1 and intercept k_{-1}. Using this treatment values of k_1 of $1.1 \times 10^7\ M^{-1}\ s^{-1}$, $5.2 \times 10^6\ M^{-1}\ s^{-1}$ and $3.0 \times 10^6\ M^{-1}\ s^{-1}$ were obtained for wild-type, R1276A and R1391A $NF1_{334}$ respectively. Values of k_{-1} for wild-type and R1276A $NF1_{334}$ could not be obtained from this experiment because the intercept was too close to the origin and could only be assigned as $< 1\ s^{-1}$. A value of $40\ s^{-1}$ for k_{-1} for R1391A $NF1_{334}$ could be calculated by this method. However, this data was subject to large errors.

Values of k_{-1} were also determined by displacement experiments. A complex of [Leu61]H-Ras.mantGTP was initially prepared and this was rapidly mixed with excess [Leu61]H-Ras.GTP. The following process occurs:

$$\begin{array}{ccccc} & k_1 & & k_2 & \\ \text{[Leu61]Ras.mantGTP.N} & \rightleftharpoons & \text{N} + \text{[Leu61]Ras.GTP} & \rightleftharpoons & \text{[Leu61]Ras.GTP.N} \\ & k_{-1} & & k_{-2} & \end{array} \quad \text{(Scheme 3)}$$

$$+$$

$$\text{[Leu61]Ras.mantGTP}$$

If a sufficiently high enough concentration of [Leu61]H-Ras.GTP is used, all of the $NF1_{334}$ will be immediately sequestered by [Leu61]H-Ras.GTP after dissociating from [Leu61]H-Ras.mantGTP (i.e k_2 will be eliminated) and the observed rate constant of the fluorescence change following the dissociation of $NF1_{334}$ from [Leu61]H-Ras.mantGTP will be governed by k_{-1}. In these circumstances, the observed rate constant will be independent of [Leu61]H-Ras.GTP concentration.

A solution containing 0.1μM [Leu61]H-Ras.mantGTP and 0.2μM wild-type or R1276A $NF1_{334}$ was rapidly mixed with 18μM [Leu61]H-Ras.GTP in a stopped-flow apparatus (figures 44a,b). A decrease in fluorescence was observed which could be fitted to single exponentials with observed rate constants of 0.8 s^{-1} and 0.9 s^{-1} for wild-type and R1276A $NF1_{334}$ respectively. Although the concentration of [Leu61]H-Ras.GTP was not varied to determine if this represents the true rate constant of k_{-1}, Jenkins (1996) has done similar experiments with wild-type $NF1_{334}$ and shown that this is so.

Repeating this displacement experiment with R1391A $NF1_{334}$ gave a very small signal which was difficult to quantitate. This suggested that the concentration of [Leu61]H-Ras.mantGTP.N complex at the start of the reaction is very low presumably as a result of weaker binding of this mutant to [Leu61[Ras.mantGTP. Therefore, concentrations of all the reactants were increased. A solution containing 4μM [Leu61]H-Ras.mantGTP and 5μM R1391A $NF1_{334}$ was rapidly mixed with 46μM [Leu61]H-Ras.GTP (figure 44c). Under these conditions an exponential decrease in fluorescence was observed which gave

an observed rate constant of 39 s^{-1} from a fit to a single exponential.

The values of k_{-1} obtained from the intercept of the association reactions and from the displacement experiments are very consistent with each other. Using the relationship, $K_d = k_{-1}/k_1$, values of K_d for wild-type, R1276A and R1391A $NF1_{334}$ were calculated to be 0.07μM, 0.17μM and 13.0μM respectively. An independent measurement of these K_d values can be obtained by examining the relationship between the amplitude of the fluorescence increase on mixing [Leu61]H-Ras.mantGTP with all three $NF1_{334}$ proteins and the initial concentration of $NF1_{334}$ (figure 43). This gives a hyperbolic relationship with values for K_d^{app} for the interaction of [Leu61]H-Ras.mantGTP with wild-type, R1276A and R1391A $NF1_{334}$ of 0.29μM, 0.84μM and 19μM respectively. These values are similar to those obtained from the values derived from k_1 and k_{-1}. The values for equilibrium and kinetic constants for the interaction of [Leu61]H-Ras.mantGTP with wild-type, R1276A and R1391A $NF1_{334}$ are given in table 5.

Figure 42: Stopped-flow fluorescence records of the interaction of [Leu61]H-Ras.mantGTP with wild-type, R1276A and R1391A $NF1_{334}$

Figures a, c and e show stopped-flow fluorescence traces in which 0.2μM [Leu61]H-Ras.mantGTP was mixed with 2μM (a) wild-type, (b) R1276A, or 1μM [Leu61]H-Ras.mantGTP was mixed with 5μM (c) R1391A $NF1_{334}$ (concentrations after mixing) at 30°C in the Hi-Tech stopped flow apparatus, as described in section 2.8.2.2. The change in fluorescence intensity monitored with time. All proteins were in 20mM Tris/HCl, pH 7.5, 1mM $MgCl_2$, 100mM NaCl, 0.1mM dithiothreitol. The smooth lines through the data represent the best fit to a single exponential with rate constants of (a) $23s^{-1}$ (b) $10s^{-1}$ and (c) $55s^{-1}$.

In figures b, d and f, the observed rates of the fast phase have been plotted against [$NF1_{334}$] and show a linear dependence over the concentrations of $NF1_{334}$ used. The solid line shows the best fit to a linear equation with slope b) $1.1 \times 10^7 M^{-1} s^{-1}$ (d) $5.2 \times 10^6 M^{-1} s^{-1}$ (f) $3.0 \times 10^6 M^{-1} s^{-1}$ and Y-axis intercepts of (b) $<1s^{-1}$ (d) $<1s^{-1}$ (f) $40s^{-1}$.

(a)

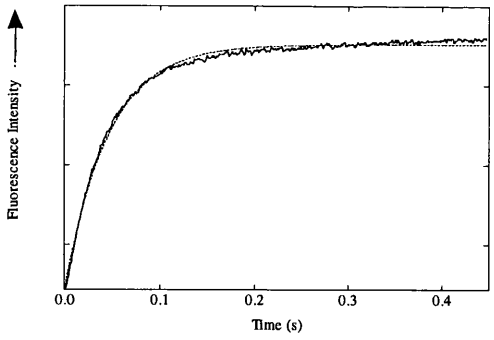
Fluorescence Intensity
0.0
0.1
0.2
0.3
0.4
Time (s)

(b)

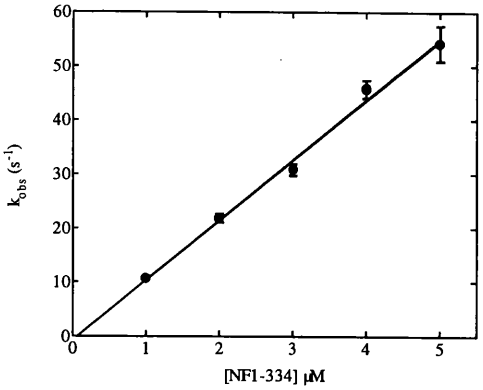
60
50
40
30
20
10
0
k_{obs} (s^{-1})
0
1
2
3
4
5
[NF1-334] μM

(c)

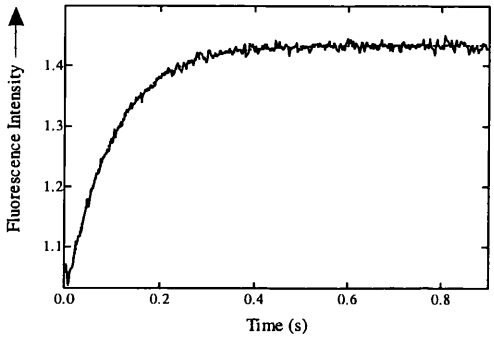
Fluorescence Intensity
1.4
1.3
1.2
1.1
0.0
0.2
0.4
0.6
0.8
Time (s)

(d)

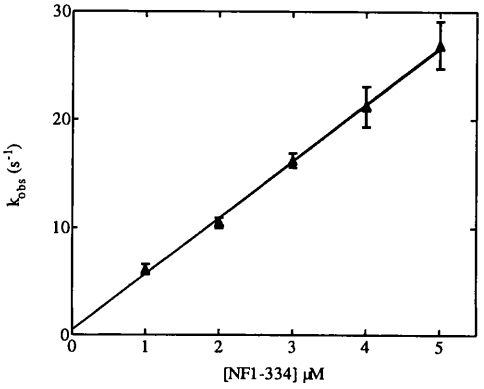
30
20
10
0
k_{obs} (s^{-1})
0
1
2
3
4
5
[NF1-334] μM

(e)

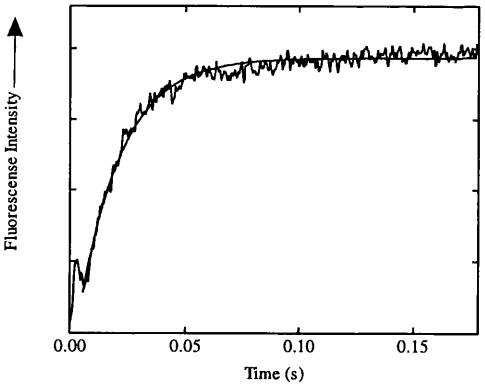
Fluorescense Intensity
0.00
0.05
0.10
0.15
Time (s)

(f)

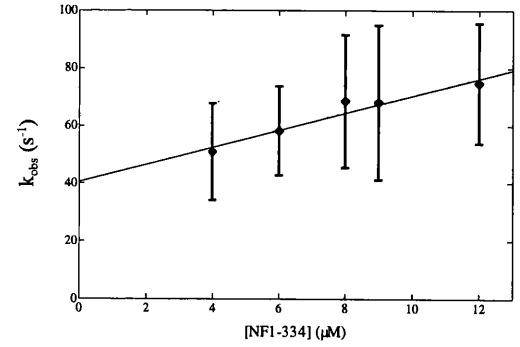
100
80
60
40
20
0
k_{obs} (s^{-1})
0
2
4
6
8
10
12
[NF1-334] (μM)

Figure 43: Dependence of the amplitude of the fast phase for the interaction of [Leu61]H-Ras.mantGTP with wild-type, R1276A or R1391A, on [$NF1_{334}$]

Absolute amplitudes of reactions from the stopped-flow fluorescence experiments shown in figure 42, were obtained by averaging the amplitudes from at least 5 data traces at each $NF1_{334}$ concentration. Amplitudes were plotted against concentration of wild-type (●), R1276A (▲) and R1391A (♦) $NF1_{334}$. All proteins were in 20mM Tris/HCl pH 7.5, 1mM $MgCl_2$, 100mM NaCl, 0.1mM dithiothreitol. The solid line through each data set represents the best fit to a binding isotherm for simple association of two molecules (anisotropy S_0 = constant) with K_d^{app} of 0.29μM, 0.84μM and 19μM for wild-type, R1276A and R1391A respectively.

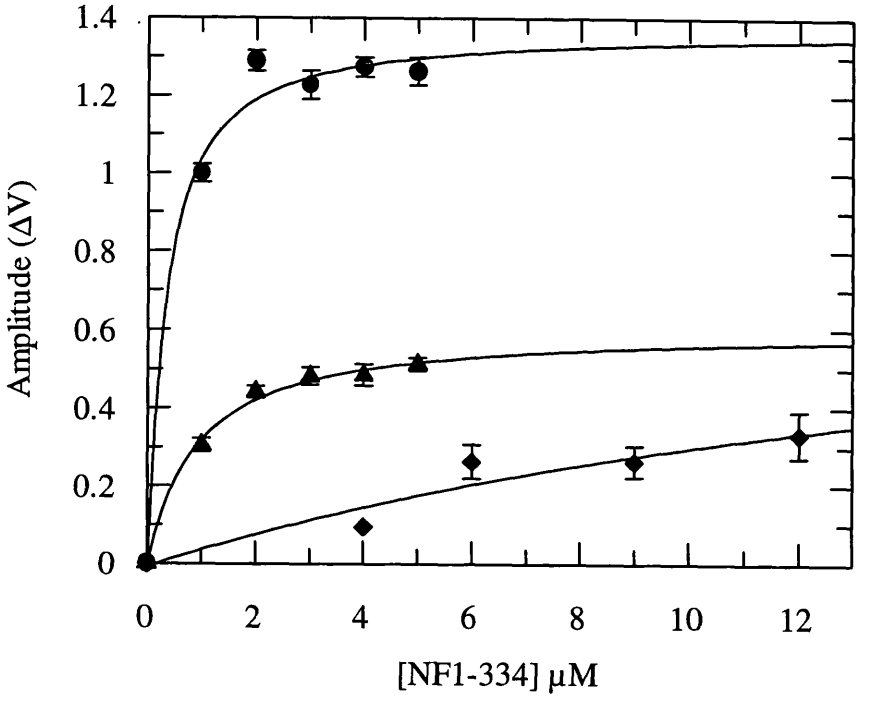
1.4
1.2
1
0.8
0.6
0.4
0.2
0
Amplitude (ΔV)
0
2
4
6
8
10
12
[NF1-334] μM

Figure 44: Displacement of [Leu61]H-Ras.mantGTP from its complex with $NF1_{334}$, by excess [Leu61]H-Ras.GTP

Displacement stopped-flow fluorescence experiments were performed in which (a), (b) 0.1μM [Leu61]H-Ras.mantGTP was mixed with 0.2μM of either wild-type or R1276A $NF1_{334}$, in the presence of 18μM [Leu61]H-Ras.GTP or (c) 4μM [Leu61]H-Ras.mantGTP was mixed with 5μM R1391A neurofibromin, in the presence of 46μM [Leu61]H-Ras.GTP, at 30°C in the Hi-Tech stopped-flow apparatus. All proteins were in 20mM Tris/HCl pH 7.5, 1mM $MgCl_2$, 100mM NaCl, 0.1mM dithiothreitol. Data traces were fitted to single exponentials with rate constants of $0.8s^{-1}$, $0.9s^{-1}$ and $39s^{-1}$ for wild-type, R1276A and R1391A $NF1_{334}$ respectively.

(a)

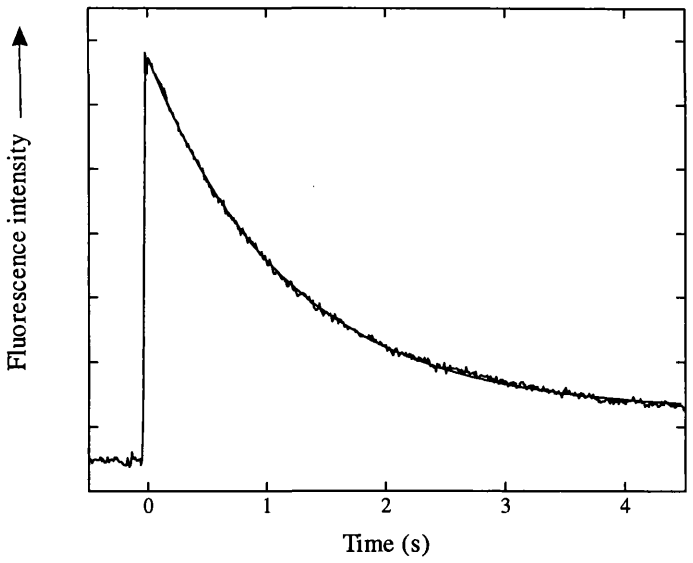
Fluorescence intensity
0
1
2
3
4
Time (s)

(b)

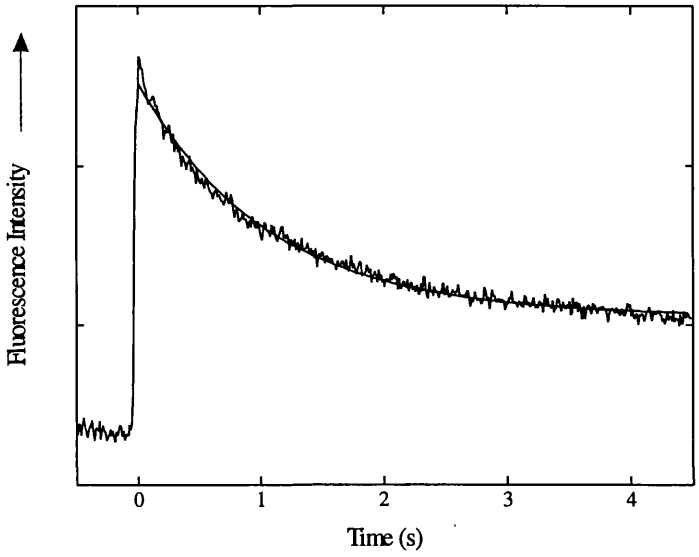
Fluorescence Intensity
0
1
2
3
4
Time (s)

(c)

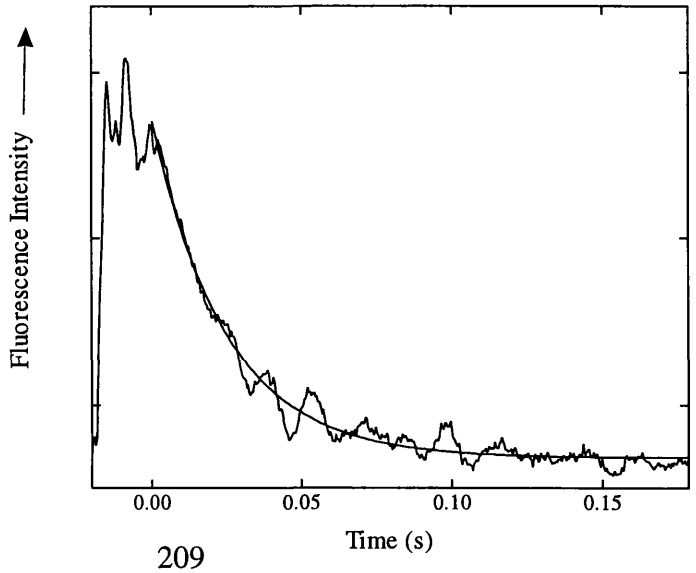
Fluorescence Intensity
0.00
0.05
0.10
0.15
Time (s)

Table 5: Equilibrium and kinetic rate constants for the interaction of [Leu61]H-Ras.mantGTP with wild-type, R1276A and R1391A neurofibromin

$NF1_{334}$ variant	[Leu61]H-Ras.mantGTP			
	k_1 [1] ($M^{-1} s^{-1}$)	k_{-1} [2] (s^{-1})	k_{-1} [3] (s^{-1})	K_d [4] (μM)
Wild-type	1.1×10^7	< 1	0.8	0.07
R1276A	5.2×10^6	< 1	0.9	0.17
R1391A	3.0×10^6	40	39	13.0

1 Obtained from slope of k_{obs} against $[NF1_{334}]$ in the association reaction (Fig 42b,d,f)

2 Obtained from intercept of k_{obs} against $[NF1_{334}]$ in the association reaction (Fig 40b,d,f)

3 Obtained from displacement reactions (Fig 44)

4 Obtained from $K_d = k_{-1}/k_1$

4.3 Discussion

There are several literature reports on mutations made at positions R1276 and R1391 within NF1-GRD and at the homologous residues of p120-GAP, R789 and R903. However the results and their interpretation have appeared to be conflicting. Gutmann *et al* (1993) replaced the basic arginine residue at position 1391 within the NF1-GRD with an uncharged serine. The resulting mutant (R1391S) showed a reduced ability to suppress the heat shock sensitive phenotypes of either ira1$^-$/ ira2$^-$ or pde2$^-$ mutant yeast strains, suggestive of a reduced stability or a reduced catalytic activity. However, the GAP activity of R1391S was indistinguishable from the wild-type protein both *in vitro* and *in vivo*. Gutmann and colleagues bridged this discrepancy by speculating that the *in vivo* yeast assay reflects binding of NF1-GRD to RAS and therefore interference with RAS effector function. Their conclusion from this data was that the R1391S mutation may diminish affinity for Ras without affecting hydrolysis activity. However, crude cell lysates rather than purified proteins were used and the defects, if any, on binding affinity or on hydrolysis were not quantified. Also no explanation was given as to how the mutation could reduce affinity without apparently affecting the ability to catalyze Ras.GTPase.

Morcos *et al* (1996) substituted the arginine residue at positions 1391 and 1276 in NF1-GRD with lysine and glycine respectively. Apparent affinity was measured in a quantitative yeast two hybrid screen measuring interaction with Ras. Expression of either R1391K or R1276G showed a striking increase in the two hybrid screen signal which was interpreted as being due to an increased affinity. In these experiments,the mutant proteins were not purified and the expression levels of mutant protein were not analyzed. Hence, an increase in signal could be either due to increased affinity or increased expression. The effect of the mutations on catalytic activity were also not determined.

In support of a role for R903 in catalysis, mutations at position 903, converting the arginine to lysine, isoleucine and glutamate, were introduced into the catalytic domain of p120-GAP. The mutant proteins were purified and analyzed for effects on their affinity for Ras (Brownbridge *et al*, 1993) and catalytic activity (Skinner *et al*, 1991). This

residue appeared to be important for catalysis as the conservative mutation R903K in GAP_{344} possessed 3% of the catalytic activity of wild-type GAP whereas the charge inversion mutant R903E had no detectable activity. In these experiments activity was measured at specific concentrations of reagents and k_{cat} itself was not measured (Skinner *et al*, 1991). However, K_d was measured showing that neither mutant resulted in more than an order of magnitude decrease (Brownbridge *et al*, 1993). In agreement with this data, Mittal *et al* (1996) have shown that the mutation R1391M binds to Ras with unchanged affinity but is catalytically impaired. Furthermore, Miao *et al* (1996) have reported that the mutation R786Q in bovine p120-GAP (equivalent to R789Q in human p120-GAP) has no detectable GAP activity, although the secondary structure was not measurably disrupted. An ELISA-based binding assay showed that R786Q bound to [Leu61]H-Ras 5-fold less than wild-type GAP (Miao *et al*, 1996). However, in view of the non-equilibrium nature of this assay and the rapid dissociation kinetics of Ras/GAP complexes (Eccleston *et al*, 1993), the quantitative effect of the mutation on affinity cannot be established from the published data.

The data presented in this chapter clearly shows that both R1276 and R1391 are required for efficient catalysis by NF1, as removal of either results in a 1000-fold loss of catalytic activity. One interpretation for the reduction in catalytic activity in these mutant $NF1_{334}$ proteins might have been that the presence of the mutations caused structural disruptions to the protein. The replacement of a positively charged hydrophobic arginine residue which has a branched side chain with an uncharged residue such as alanine which has a methyl group as its side chain, represents a non-conservative substitution within $NF1_{334}$. If the local structure surrounding residues 1276 and 1391 requires a charged residue such as arginine at these positions, then the loss of a positive charge and side chain by the introduction of alanine at these positions might be predicted to have a detrimental effect on the localized structure, ultimately disrupting the structural integrity of the protein. Such gross structural alterations might lead to insolubility of the protein, a problem previously encountered by Brownbridge *et al* (1993) with p120-GAP. However, this interpretation seemed unlikely since no such insolubility probems were encountered with the R1276A and R1391A $NF1_{334}$ mutants suggesting that their structure had not been totally disrupted.

Subsequent structural characterizations of both wild-type and mutant $NF1_{334}$ proteins using circular dichroism and tryptophan fluorescence studies confirmed that the loss of catalytic activity associated with the substitution of arginine for alanine at positions 1276 and 1391 within $NF1_{334}$, could be directly attributed to the specific mutation rather than to gross structural disruptions that might functionally inactivate the protein. Circular dichroism and tryptophan emission spectra for the mutant proteins were indistinguishable from those obtained for the wild-type protein.

R1276 contributes little to the binding energy as the affinity for either normal or [Leu61]H-Ras is only modestly increased (ca. 2-3 fold). R1391 appears to have some role in binding as mutation to alanine results in a 10-20-fold increase in K_d for interaction with normal Ras. Interestingly the effect of the mutation is much more marked on its interaction with [Leu61]H-Ras. Indeed, wild-type Ras binds wild-type NF1 10-fold weaker than [Leu61]H-Ras, whereas this differential is completely lost with the R1391A NF1. This suggests that the peculiarly high affinity of [Leu61]H-Ras for NF1 is related to an interaction with, or dependent upon, R1391 of NF1.

There has been much debate about the mechanism of both the intrinsic Ras.GTPase and the GAP-catalyzed GTPase reactions (Brownbridge *et al*, 1993; Schweins *et al*, 1994; Schweins *et al*, 1995; Schweins and Warshel, 1996; Schweins *et al*, 1996; Maegley *et al*, 1996; Geyer *et al*, 1996). The possible mechanisms for the intrinsic Ras.GTPase have been discussed in section 1.1.4.1. GAP could directly accelerate the cleavage rate of the Ras.GTPase by supplying one or more side chains to the active site of Ras. This would imply that the chemical mechanism of GTP hydrolysis by GAP-activated Ras is different from that in Ras alone. Alternatively, GAP could rearrange and stabilize the active site residues of Ras into a catalytically active conformation, implying that all the components neccessary for catalysis are held within the active site of Ras. My results are consistent with the first hypothesis that residues important for efficient catalysis are supplied by GAP. Possible roles for an active site arginine in the mechanism of catalysis include stabilizing the pentavalent phosphorous transition state, fixing residues which are highly

mobile such as Gln61 in the correct orientation for GTP hydrolysis, protonating the leaving group GDP, increasing the nucleophilicity of the attacking water, by-passing a proposed rate limiting conformatioal change or changing the chemical mechanism to include a phosphorylated enzyme intermediate. A recent proposal for the mechanism of the intrinsic and GAP-stimulated Ras.GTPase has come from model studies by Maegley *et al* (1996). Maegley and coworkers speculate that in the intrinsic Ras.GTPase, stabilization of the dissociative transition state is achieved through strengthening of a hydrogen bond between the backbone amide of Gly13 and the β-γ bridge oxygen of GTP. GAPs might accelerate the Ras.GTPase by further stabilizing the transition state. This could be achieved by either positioning the existing hydrogen bond to the β-γ bridge oxygen so as to achieve maximal rate enhancement, or by introducing a second stronger hydrogen bond donor (such as an arginine residue) for interaction with the β-γ bridge oxygen. In support of the latter interaction, the β-γ bridge oxygen was observed to interact with the conserved active site arginine of transducin (Arg-174) in the crystal structure (Noel *et al*, 1993). However, the large effect of GAP on the Ras.GTPase over the effect of the active site arginine within G_α proteins (10^5 versus 10^2) suggests that additional catalytic interactions remain to be identified. The latest experimental evidence (Schweins *et al*, 1996; Schweins and Warshel, 1996) suggests that the GAP-stimulated Ras.GTPase follows a similar chemical mechanism to that of the intrinsic GTPase. If this is correct, one would conclude that the role of the essential arginine(s) is to polarize the catalytic site thereby reducing the energy of the transition state, rather than by directly contributing residues involved in the catalytic mechanism. This is consistent with NMR data suggesting that in the ground state GAP does not interact directly with the nucleotide bound to Ras (Geyer *et al*, 1996).

Since this work was carried out, the X-ray structures of the catalytic domains of p120-GAP (Scheffzek *et al*, 1996) and Rho-GAP (Barrett *et al*, 1997) have been solved and published. The RasGAP structure shows that both R789 and R903 are in proximity both to each other and to the proposed location of the γ-phosphate of Ras.GTP in the Ras/GAP complex. As the guanidinium group of R903 contacts the main chain in the region of R789 the possibility was suggested that R789 is used for catalysis whereas R903

stabilizes the conformation of R789. This hypothesis is supported by the results of Skinner *et al* (1991), based on the properties of the conservative mutant L902I, showing that L902 is also essential for catalysis. Although both RhoGAP and RasGAP are predominantly α-helical, there is no clear secondary structure homology. However, it is interesting that RhoGAPs also have a conserved arginine residue in a similar sequence environment to that in RasGAPs (figure 33b). It is tempting to speculate that this arginine might also be involved in catalysis and that there is some similarity in the active site topology.

Figure 45: Details of the structure of GAP_{334}

A. Ribbon representation of the three-dimensional structure of GAP_{334} showing the arrangement of residues within the catalytic track. The totally invariant FLR motif is shown. The position of the invariant and highly conserved residues are shown as black and grey dots respectively.The residues marked participate in the formation of two different hydrophobic cores.

[Taken from Scheffzek *et al* (1996)]

B. Ribbon representation of the three-dimensional structures of both Ras and GAP334 showing the residues involved in the proposed docking mechanism of the two proteins.

[Taken from Scheffzek *et al* (1996)]

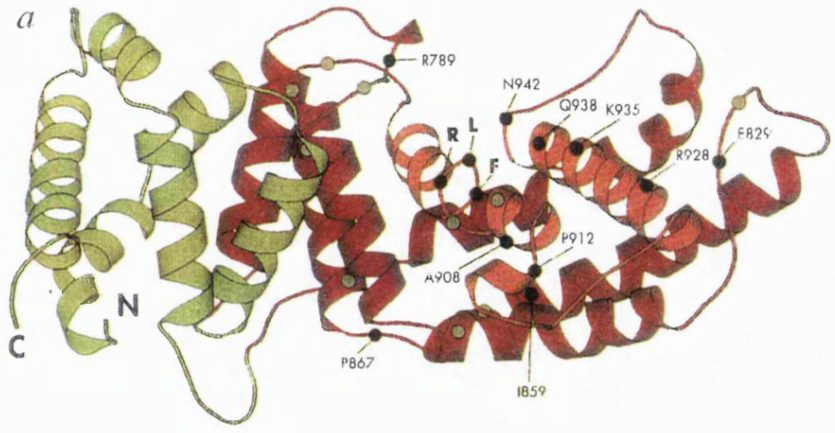
a
R789
N942
Q938
K935
R928
P912
A908
P867
I859
C
N

b

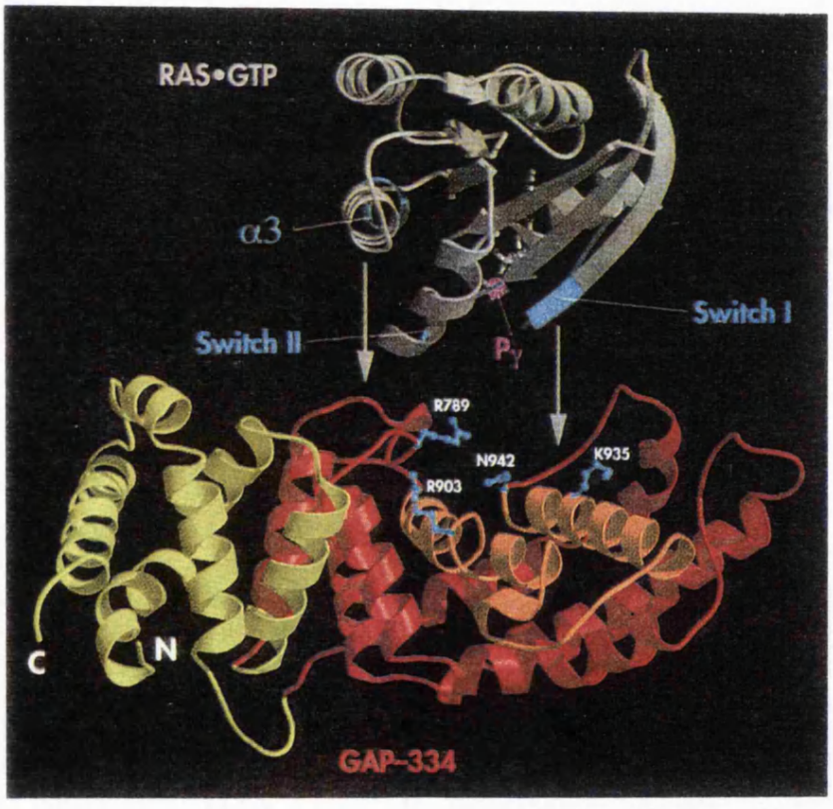
RAS•GTP
α3
Switch II
Switch I
R789
N942
K935
R903
C
N
GAP-334

4.4 Conclusions

(1) The contribution of two conserved arginine residues within $NF1_{334}$(R1276 and R1391) to both catalysis and binding affinity to Ras was studied by pre-steady state kinetic methods. Substitution of the arginine at both positions for alanine resulted in mutant proteins which were 1000-fold less active than wild-type $NF1_{334}$when catalytic activity was measured at saturating concentrations of $NF1_{334}$. These data are consistent with both arginine residues playing an important role in catalysis.

(2) R1391A reduced the affinity of $NF1_{334}$for both wild-type and [Leu61]H-Ras to a much greater extent than that observed for R1276A, suggesting that R1391 plays a greater role in binding to Ras.

(3) The high affinity of [Leu61]H-Ras for $NF1_{334}$ is completely lost with R1391A $NF1_{334}$, suggesting that the high affinity is related to an interaction with this arginine residue.

4.5 Further Work

(1) The reduction in activity for both R1276A and R1391A was calculated by comparing k_{cat} values obtained for R1276A and R1391A with the lower limit for k_{cat} obtained for wild-type $NF1_{334}$. The calculated reduction in activity will therefore be an underestimate of the maximum possible reduction in activity. Thus experiments aimed at obtaining a more accurate idea of the extent of reduction with mutant $NF1_{334}$ proteins might be a consideration for future work. This could be achieved by measuring an upper limit for k_{cat} with wild-type $NF1_{334}$ under our experimental conditions i.e 100mM NaCl, by determining whether the slow phase of the fluorescence change is monitoring the cleavage step or the dissociation of NF1 from Ras.mantGDP.Pi. Rate constants for both of these processes could be determined at 100mM NaCl using a combination of quenched flow and HPLC.

(2) An eventual goal would be to obtain the X-ray crystal structure of wild-type and

mutant $NF1_{334}$ in complex with Ras. This could be followed up by further mutagenesis of key residues identified from such an $NF1_{334}$/Ras X-ray structure.

Acknowledgements

I would like to take this opportunity to thank my supervisors, Dr P. N Lowe at GlaxoWellcome research laboratories and Dr J.F Eccleston at the National Institute for medical Research, for their help and invaluable advice throughout these studies and during the preparation of my thesis. Thanks must also go to Dr R. Skinner for his encouragement and kind donation of oligonucleotides for the site-directed mutagenesis, Dr Molly Strom for her invaluable assistance with the site-directed mutagenesis and Dr Steve Martin and steve Howell at N.I.M.R for the circular dichroism and mass spectrometry results. I would like to extend a special thankyou to my parents and my husband, Trevor, for all their support and to Chris Gorman for her valuable friendship. Finally, a big thankyou to all at Strangeways Research laboratory, especially Dr Gillian Murphy and the 'GGGs' for all their support but most of all for keeping me sane over the past year. Thanks George, I wont be needing the T-shirt anymore!

Chapter 5 - Bibliography

Abramson, S.B., Leszezynska-Piziak, J. and Weissmann, G. (1991) J. Immun **147** (1), 231-236

Adari, H., Lowy, D.R., Willumsen, B.M., Der, C.J. and McCormick, F. (1988) Science **240**, 518-521

Ahmadian, M.R., Weismuller, L., Lautwein, A., Bischoff, F.R. and Wittinghofer, A. (1996) J. Biol. Chem. **271** (27), 16409-16415

Akasaka, K., Tamada, M., Wang, F., Kariya, K-I., Shima, F., Kikuchi, A., Yamamoto, M., Shirouzu, M., Yokoyama, S. and Kataoka, T. (1996) J. Biol. Chem. **271** (10), 5353-5360

Al-Alawi, N., Xu, G., White, R., Clark, R., McCormick, F. and Feramisco, J.R. (1993) Mol. Cell. Biol. **13** (4), 2497-2503

Alessi, D.R., Saito, Y., Campbell, D.G., Cohen, P., Sithanandam, G., Rapp, U., Ashworth, A., Marshall, C.J. and Cowley, S. (1994) The EMBO J. **13** (7), 1610-1619

Anderson, N.G., Maller, J.L., Tonks, N.K. and Sturgill, T.W. (1990a) Nature **343**, 651-653

Anderson, D., Koch, C.A., Grey, L., Ellis, C., Moran, M.F. and Pawson, T. (1990b) Science **250**, 979-982

Andersen, L.B., Ballester, R., Marchuk, D.A., Chang, E., Gutmann, D.H., Saulino, A.M., Camonis, J., Wigler, M. and Collins, F.S. (1993a) Mol. Cell. Biol. **13** (1), 487-495

Anderson, L.B., Fountain, J.W., Gutmann, D.H., Tarle, S.A., Glover, T.W., Dracopoli, N.C., Housman, D.E. and Collins, F.S. (1993b) Nature Genetics **3**, 118-121

Antonny, B., Chardin, P., Roux, M. and Chabre, M. (1991) Biochemistry **30**, 8287-8295

Bagrodia, S., Derijard, B., Davis, R.J. and Cerione, R-A. (1995) J. Biol. Chem. **270**, 27995-27998

Bagshaw, C.R., Eccleston, J.F., Eckstein, F., Goody, R.S., Gutfreund, H. and Trentham, D.R. (1974) Biochem. J. **141**, 351-364

Ballester, R., Marchuk, D., Boguski, M., Saulino, A., Letcher, R., Wigler, M. and Collins, F. (1990) Cell **63**, 851-859

Barbacid, M. (1987) Annu. Rev. Biochem. **56**, 779-827

Barnard, D., Diaz, B., Hettich, L., Chuang, E., Zhang, X-F., Avruch, J. and Marshall, M. (1995) Oncogene **10**, 1283-1290

Barrett, T., Xiao, B., Dodson, E.J., Dodson, G., Ludbrook, S.B., Nurmahomed, K., Gamblin, S.J., Musacchio, A., Smerdon, S.J. and Eccleston, J.F. (1997) Nature **385**, 458-461

Basu, T.N., Gutmann, D.H., Fletcher, J.A., Glover, T.W., Collins, F.S. and Downward, J. (1992) Nature **356**, 713-715

Bellew, B.F., Halkides, C.J., Gerfen, G.J., Griffin, R.G. and Singel, D.J. (1996) Biochemistry **35**, 12186-12193

Bernards, A. (1995) Biochimica et Biophysica Acta **1242**, 43-59

Boguski, M.S. and McCormick, F. (1993) Nature **366**, 643-654

Bokoch, G.M. (1994) Curr. Opin. Cell Biol. **6**, 212-218

Bollag, G. and McCormick, F. (1991) Nature **351**, 576-579

Bollag, G., McCormick, F. and Clark, R. (1993) The EMBO J. **12** (5), 1923-1927

Bollag, G., Clapp, D.W., Shih, S., Adler, F., Zhang, Y-Y., Thompson, P., Lange, B.J., Freedman, M.H., McCormick, F., Jacks, T. and Shannon, K. (1996) Nature Genet. **12**, 144-148

Boman, A.L. and Kahn, R.A. (1995) Trends Biochem. Sci. **20**, 147-150

Bonfini, L., Karlovich, C.A., Dasgupta, C. and Banerjee, U. (1992) Science **255**, 603-606

Bonner, T.L., Kerby, S.B., Sutrave, P., Gunnell, G. and Rapp, U.R. (1985) Mol. Cell. Biol. **5** (6), 1400-1407

Bos, J.L. (1989) Cancer Res. **49**, 4682-4689

Bos, J.L. (1995) Trends Biochem. Sci. **20**, 441-442

Bourne, H.R., Sanders, D.A. and McCormick, F. (1991) Nature **349**, 117-127

Bourne, H.R., Sanders, D.A. and McCormick, F. (1990) Nature **348**, 125-131

Bowtell, D., Fu, P., Simon, M. and Senior, P. (1992) Proc. Natl. Acad. Sci. USA **89**, 6511-6515

Boyer, M.J., Gutmann, D.H., Collins, F.S. and Bar-Sagi, D. (1994) Oncogene **9**, 349-357

Bradford, M. (1976) Anal. Biochem. **72**, 248

Brill, S., Li, S., Lyman, C.W., Church, D.M., Wasmuth, J.J., Weissbach, L., Bernards, A. and Snijders, A.J. (1996) Mol. Cell. Biol. **16** (9), 4869-4878

Broek, D., Toda, T., Michaeli, T., Levin, L., Birchmeier, C., Zoller, M., Powers, S. and Wigler, M. (1987) Cell **48**, 789-799

Brownbridge, G.G., Lowe, P.N., Moore, K.J.M., Skinner, R.H. and Webb, M.R. (1993) J. Biol. Chem. **268**, 10914-10919

Brtva, T.R., Drugan, J.K., Ghosh, S., Terrell, R.S., Campbell-Burk, S., Bell, R.M. and Der, C.J. (1995) J. Biol. Chem. **270** (17), 9809-9812

Brunger, A.T., Milburn, M.V., Tong, L., DeVos, A.M., Jancarik, J., Yamaizumi, Z., Nishimura, S., Ohtsuka, E. and Kim, S.H. (1990) Proc. Natl. Acad. Sci. USA **87**, 4849-4853

Buchberg, A.M., Cleveland, L.S., Jenkins, N.A. and Copeland, N.G. (1990) Nature **347**, 291-294

Buday, L. and Downward, J. (1993) Cell **73**, 611-620

Buday, L., Warne, P.H. and Downward, J. (1995) Oncogene **11**, 1327-1331

Burbelo, P.D. and Hall, A. (1995) Curr. Biol. **5** (2), 95-96

Burton, J., Roberts, D., Montaldi, M., Novick, P. and de Camilli, P. (1993) Nature **361**, 464-467

Bustelo, X.R., Suen, K-L., Leftheris, K., Meyers, C.A. and Barbacid, M. (1994) Oncogene **9**, 2405-2413

Cai, H., Szeberenyi, J. and Cooper, G.M. (1990) Mol. Cell. Biol. **10** (10), 5314-5323

Cales, C., Hancock, J.F., Marshall, C.J. and Hall, A. (1988) Nature **332**, 548-551

Cassel, D. and Selinger, Z. (1977) Proc. Natl. Acad. Sci. USA **74**, 3307

Cawthon, R.M., Weiss, R., Xu, G., Viskochil, D., Culver, M., Stevens, J., Robertson, M., Dunn, D., Gesteland, R., O'Connell, P. and White, R. (1990) Cell **62**, 193-201

Cen, H., Papageorge, A.G., Zippel, R., Lowy, D.R. and Zhang, K. (1992) The EMBO J. **11** (11), 4007-4015

Chang, E.C., Barr, M., Wang, Y., Jung, V., Xu, H-P. and Wigler, M.H. (1994) Cell **79**, 131-141

Cherniack, A.D., Klarlund, J.K., Conway, B.R. and Czech, M.P. (1995) J. Biol. Chem. **270** (4), 1485-1488

Chow, Y-H., Pulmiglia, K., Jun, T.H., Dent, P., Sturgill, T.W. and Jove, R. (1995) J. Biol. Chem. **270** (23), 14100-14106

Chuang, E., Barnard, D., Hettich, L., Zhang, X-F., Avruch, J and Marshall, M.S. (1994) Mol. Cell. Biol. **14** (8), 5318-5325

Chung, H-H., Benson, D.R. and Schultz, P.G. (1993) Science **259**, 806-809

Clark, S.G., Stern, M.J. and Horvitz, H.R. (1992) Nature **356**, 340-344

Clark, G.J., Drugan, J.K., Terrell, R.S., Bradham, C., Der, C.J., Bell, R.M. and Campbell, S. (1996) Proc. Natl. Acad. Sci. USA **93**, 1577-1581

Cohen, L., Mohr, R., Chen, Y-Y., Huang, M., Kato, R., Dorin, D., Tamanoi, F., Goga, A., Afar, D., Rosenberg, N. and Witte, O. (1994) Proc. Natl. Acad. Sci. USA **91**, 12448-12452

Colby, W.W., Hayflick, J.S., Clark, S.G. and Levinson, A.D. (1986) Mol. Cell. Biol. **6** (2), 730-734

Coleman, D.E., Berghuis, A.M., Lee, E., Linder, M.E., Gilman, A.G. and Sprang, S.R. (1994) Science **265**, 1405-1412

Coso, O.A., Chiariello, M., Yu, J.C., Teramoto, H., Crespo, P., Xu, N., Miki, T. and Gutkind, J.S. (1995) Cell **81**, 1137-1146

Cowley, S., Paterson, H., Kemp, P. and Marshall, C.J. (1994) Cell **77**, 841-852

Cox, A.D., Brtva, T.R., Lowe, D.G. and Der, C.J. (1994) Oncogene **9**, 3281-3288

Cremo, C.R., Neuron, J.M. and Yount, R.G. (1990) Biochemistry **29**, 3309-3319

Cullen, P.J., Hsuan, J.J., Truong, O., Letcher, A.J., Jackson, T.R., Dawson, A.P. and Irvine, R.F. (1995) Nature **376**, 527-530

Daston, M.M. and Ratner, N. (1992) Developmental Dynamics **195**, 216-226

DeClue, J.E., Papageorge, A.G., Fletcher, J.A., Diehl, S.R., Ratner, N., Vass, W.C. and Lowy, D.R. (1992) Cell **69**, 265-273

DeClue, J.E., Cohen, B.D. and Lowy, D.R. (1991) Proc. Natl. Acad. Sci. U. S. A. **88**, 9914-9918

Dent, P., Haser, W., Haystead, T.A.J., Vincent, L.A., Roberts, T.M. and Sturgill, T.W. (1992) Science **257**, 1404-1407

Der, C.J., Pan, B-T. and Cooper, G.M. (1986a) Mol. Cell. Biol. **6** (9), 3291-3294

Der, C.J., Finkel, T. and Cooper, G.M. (1986b) Cell **44**, 167-176

DeVos, A.M., Tong, L., Milburn, M.V., Matlas, P.M., Jancarik, J., Noguchi, S., Nishimura, S., Miura, K., Ohtsuka, E. and Kim, S.H. (1988) Science **239**, 888-893

Diaz-Meco, M.T., Lozano, J., Municio, M.M., Berra, E., Frutos, S., Sanz, L. and Moscat, J. (1994) J. Biol. Chem. **269** (50), 31706-31710

DiBattiste, D., Golubic, M.,Stacey, D. and Wolfman, A. (1993) Oncogene **8**, 637-643

Dickson, B. and Hafen, E. (1994) Curr. Opin. Genet. Dev. **4**, 64-70

Dickson, B., Sprenger, F., Morrison, D. and Hafen, E. (1992) Nature **360**, 600-603

Dixon, M. and Webb, E.C. (1979) Enzymes 332-380, Academic Press Inc., New York

Dominguez, I., Marshall, M.S., Gibbs, J.B., Garcia de Herreros, A., Cornet, M.E., Graziani, G., Diaz-Meco, M.T., Johansen, T., McCormick, F. and Moscat, J., (1991) The EMBO J. **10** (11), 3215-3220

Dorin, D., Cohen, L., Del Villar, K., Poullet, P., Mohr, R., Whiteway, M., Witte, O. and Tamanoi, F. (1995) Oncogene **11**, 2267-2271

Downward, J. (1994) FEBS Lett. **338**, 113-117

Drugan, J.K., Khosravi-Far, R., White, M.A., Der, C.J., Sung, Y-J., Hwang, Y-W. and Campbell, S.L. (1996) J. Biol. Chem. **271** (1), 233-237

Duchesne, M., Schweighoffer, F., Parker, F., Clerc, F., Frobert, Y., Thang, M.N. and Tocque, B. (1993) Science **259**, 525-528

Eccleston, J.F. (1981) Biochemistry **20**, 6265-6272

Eccleston, J.F. and Webb, M.R. (1982) J. Biol. Chem. **257** (9), 5046-5049

Eccleston, J.F., Dix, D.B., Thompson, R.C. (1985) J. Biol. Chem. **260** (30), 16237-16241

Eccleston, J.F., Kanagasabai, T.F., Molloy, D.P., Neal, S.E. and Webb, M.R. (1989) NATO ASI Ser. **165**, 87-97

Eccleston, J.F., Moore, K.J.M., Brownbridge, G.G., Webb, M.R. and Lowe, P.N. (1991) Biochem. Soc. Trans. **19**, 432-437

Eccleston, J.F., Moore, K.J.M., Morgan, L., Skinner, R.H. and Lowe, P.N. (1993) J. Biol. Chem. **268** (36), 27012-27019

Egan, S.E., Giddings, B.W., Brooks, M.W., Buday, L., Sizeland, A.M. and Weinberg, R.A. (1993) Nature **363**, 45-51

Ellis, C., Moran, M., McCormick, F. and Pawson, T. (1990) Nature **343**, 377-381

Emerson, S.D., Waugh, D.S., Scheffler, J.E., Tsao, K-L., Prinzo, K.M. and Fry, D.C. (1994) Biochemistry **33** (25), 7745-7752

Emerson, S.D., Madison, V.S., Palermo, R.E., Waugh, D.S., Scheffler, J.E., Tsao, K-L., Kiefer, S.E., Liu, S.P. and Fry, D.C. (1995) Biochemistry **34** (21), 6911-6918

Faix, J. and Dittrich, W. (1996) FEBS Lett. **394** (3), 251-257

Falasca, M. And Corda, D. (1994) Eur. J. Biochem. **221**, 383-389

Fantl, W.J., Muslin, A.J., Kikuchi, A., Martin, J.A., MacNicol, A.M., Gross, R.W. and Williams, L.T. (1994) Nature **371**, 612-614

Farnsworth, C.L. and Feig, L.A. (1991) Mol. Cell. Biol. **11** (10), 4822-4829

Fasano, O., Bruns, W., Crechet, J., Sander, G. and Parmeggiani, A. (1978) Eur. J. Biochem. **89**, 557-565

Fasano, O., Aldrich, T., Tamanoi, F., Taparowsky, E., Furth, M. and Wigler, M. (1984) Proc. Natl. Acad. Sci. USA **81**, 4008-4012

Feig, L.A., Pan, B-T., Roberts, T.M. and Cooper, G.M. (1986) Proc. Natl. Acad. Sci. USA **83**, 4607-4611

Feig, L.A. and Cooper, G.M. (1988a) Mol. Cell. Biol. **8** (6), 2472-2478

Feig, L.A. and Cooper, G.M. (1988b) Mol. Cell. Biol. **8** (8), 3235-3243

Feig, L.A. (1994) Curr. Opin. Cell Biol. **6**, 204-211

Feller, S.M., Ren, R., Hanafusa, H. and Baltimore, D. (1994) Trends Biochem. Sci. **19**, 453-458

Feller, S.M., Knudsen, B. and Hanafusa, H. (1995) Oncogene **10**, 1465-1473

Feng, G-S., Ouyang, Y-B., Hu, D-P., Shi, Z-Q., Gentz, R. and Ni, J. (1996) J. Biol. Chem. **271** (21), 12129-12132

Ferguson, J.E. and Hanley, M.R. (1991) Curr. Opin. Cell. Biol. **3**, 206-212

Fernandez-Sarabia, M.J. and Bischoff, J.R. (1993) Nature **366**, 274-275

Fernando Diaz, J., Wroblowski, B. and Engelborghs, Y. (1995) Biochemistry **34**, 12038-12047

Feuerstein, J., Goody, R.S. and Wittinghofer, A. (1987) J. Biol. Chem. **262** (18), 8455-8458

Feuerstein, J., Goody, R.S. and Webb, M.R. (1989) J. Biol. Chem. **264** (11), 6188-6190

Finney, R.E., Robbins, S.M. and Bishop, J.M. (1993) Curr. Biol. **3**, 805-811

Fischer von Mollard, G., Stahl, B., Li, C., Sudhof, T.C. and Jahn, R. (1994) Trends Biochem. Sci. **19**, 164-168

Fischer, R., Wei, Y., Anagli, J. and Berchtold, M.W. (1996) J. Biol. Chem. **271** (41), 25067-25070

Fleischman, L.F., Chahwala, S.B. and Cantley, L. (1986) Science **231**, 407-410

Foley, C.K., Pederson, L.G., Charifson, P.S., Darden, T.A., Wittinghofer, A., Pai, E.F. and Anderson, M.W. (1992) Biochemistry **31**, 4951-4959

Forrester, K., Almoguera, C., Han, K., Grizzle, W.E. and Perucho, M. (1987) Nature **327**, 298-303

Foster, R., Hu, K-Q., Lu, Y., Nolan, K.M., Thissen, J. and Settleman, J. (1996) Mol. Cell. Biol. **16** (6), 2689-2699

Franken, S.M., Scheidig, A.J., Krengel, U., Rensland, H., Lautwein, A., Geyer, M., Scheffzek, K., Goody, R.S., Kalbitzer, H.R., Pai, E.F. and Wittinghofer, A. (1993) Biochemistry **32**, 8411-8420

Frech, M., Darden, T.A., Pederson, L.G., Foley, C.K., Charifson, P.S., Anderson, M.W. and Wittinghofer, A. (1994) Biochemistry **33**, 3237-3244

Frech, M., John, J., Pizon, V., Chardin, P., Tavitian, A., Clark, R., McCormick, F. and Wittinghofer, A. (1990) Science **249**, 169-171

Freed, E., McCormick, F. and Ruggieri, R. (1994a) Cold Spring Harbour Symp. Quant. Biol. **59**, 187-193

Freed, E., Symons, M., MacDonald, S.G., McCormick, F. and Ruggieri, R. (1994b) Science **265**, 1713-1716

Freissmuth, M. and Gilman, A.G. (1989) J. Biol. Chem. **264** (36), 21907-21914

Fridman, M., Tikoo, A., Varga, M., Murphy, A., Nur-E-Kamal, M.S.A. and Maruta, H. (1994) J. Biol. Chem. **269** (48), 30105-30108

Fu, H., Xia, K., Pallas, D.C., Cui, C., Conroy, K., Narsimhan, R.P., Mamon, H., Collier, R.J. and Roberts, T.M. (1994) Science **266**, 126-129

Gale, N.W., Kaplan, S, Lowenstein, E.J., Schlessinger, J. and Bar-Sagi, D. (1993) Nature **363**, 88-92

Galisteo, M.L., Chernoff, J., Su, Y.C., Skolnik, E.Y. and Schlessinger, J. (1996) J. Biol. Chem. **271**, 20997-21000

Gaul, U., Mardon, G. and Rubin, G.M. (1992) Cell **68**, 1007-1019

Geyer, M., Schweins, T., Herrmann, C., Prisner, T., Wittinghofer, A. and Kalbitzer, H.R. (1996) Biochemistry **35**, 10308-10320

Ghosh, S., Qin Xie, W., Quest, F.G., Mabrouk, G.M., Strum, J.C. and Bell, R.M. (1994) J. Biol. Chem. **269** (13), 10000-10007

Ghosh, S. and Bell, R.M. (1994) J. Biol. Chem. **269** (49), 30785-30788

Gibbs, J.B., Sigal, I.S. and Scolnick, E.M. (1985) Trends Biochem. Sci. 350-353

Gibbs, J.B., Schaber, M.D., Allard, W.J., Sigal, I.S. and Scolnick, E.M. (1988) Proc. Natl. Acad. Sci. USA **85**, 5026-5030

Gibbs, J.B., Schaber, M.D., Schofield, T.L., Scolnick, E.M. and Sigal, I.S. (1989) Proc. Natl. Acad. Sci. USA **86**, 6630-6634

Gideon, P., John, J., Frech, M., Lautwein, A., Clark, R., Scheffler, J.E. and Wittinghofer, A. (1992) Mol. Cell. Biol. **12** (5), 2050-2056

Gill, S.C. and Von Hippel, P.H. (1989) Anal. Biochem. **182**, 319-326

Golubic, M., Tanaka, K., Dobrowolski, S., Wood, D., Tsai, M.H., Marshall, M., Tamanoi, F. and Stacey, D.W. (1991) The EMBO J. **10**, 2897-2903

Golubic, M., Roudebush, M., Dobrowolski, S., Wolfman, A. and Stacey, D.W. (1992) Oncogene **7**, 2151-2159

Gorman, C., Skinner, R.H., Skelly, J.V., Neidle, S. and Lowe, P.N. (1996) J. Biol. Chem. **271** (12), 6713-6719

Graham, S.M., Cox, A.D., Drivas, G., Rush, M.G., D'Eustachio, P. and Der, C.J. (1994) Mol. Cell. Biol. **14** (6), 4108-4115

Grand, R.J.A. and Owen, D. (1991) Biochem. J. **279**, 609-631

Graziano, M.P. and Gilman, A.G. (1989) J. Biol. Chem. **264**, 15475-15482

Gregory, P.E., Gutmann, D.H., Mitchell, A., Park, S., Boguski, M., Lacks, T., Wood, D.L., Jove, R. and Collins, F.S. (1993) Somat. Cell. Mol. Genet. **19**, 265-274

Gruenberg, J. and Maxfield, F.R. (1995) Curr. Opin. Cell Biol. **7**, 552-563

Gulbins, E., Coggeshall, M., Baier, G., Katzav, S., Burn, P. and Altman, A. (1993) Science **260**, 822-825

Gutmann, D.H., Wood, D.L. and Collins, F.S. (1991) Proc. Natl. Acad. Sci. USA **88**, 9658-9662

Gutmann, D.H. and Collins, F.S (1993) Neuron **10**, 335-343

Gutmann, D.H., Boguski, M., Marchuk, D., Wigler, M., Collins, F.S. and Ballester, R. (1993) Oncogene **8**, 761-769

Gutmann, D.H., Giordano, M.J., Mahadeo, D.K., Lau, N., Silbergeld, D. and Guha, A. (1996) Oncogene **12**, 2121-2127

Halkides, C.J., Farrar, C.T., Larsen, R.G., Redfield, A.G. and Singel, D.J. (1994) Biochemistry **33**, 4019-4035

Halkides, C.J., Bellew, B.F., Gerfen, G.J., Farrar, C.T., Carter, P.H., Ruo, B., Evans, D.A., Griffin, R.G. and Singel, D.J. (1996) Biochemistry **35**, 12194-12200

Hall, A., Marshall, C.J., Spurr, N.K. and Weiss, R.A. (1983) Nature **303**, 396-400

Hall, A. (1993) Curr. Opin. Cell Biol. **5**, 265-268

Hall, A. (1994) Annu. Rev. Cell Biol. **10**, 31-54

Hallberg, B., Rayter, S.I. and Downward, J. (1994) J. Biol. Chem. **269** (6), 3913-3916

Han, L. and Colicelli, J. (1995) Mol. Cell. Biol. **15** (3), 1318-1323

Han, J.W., McCormick, F. and Macara, I.G. (1991) Science **252**, 576-579

Harvey, J.J. (1964) Nature **204**, 1104-1105

Hattori, S., Ohmi, N., Maekawa, M., Hoshino, M., Kawakita, M. and Nakamura, S. (1991) Biochem. Biophys. Res. Comm. **177** (1), 83-89

Hattori, S., Maekawa, M. and Nakamura, S. (1992) Oncogene **7**, 481-485

Hawkins, P.T., Eguinoa, A., Qiu, R., Stokoe, D., Cooke, F.T., Walters, R., Wennstrom, S., Claesson-Welsh, L., Evans, T., Symons, M. and Stephens, L. (1995) Curr. Biol. **5** (4), 393-403

Herrmann, C., Martin, G.A. and Wittinghofer, A. (1995) J. Biol. Chem. **270** (7), 2901-2905

Herrmann, C., Horn, G., Spaargaren, M. and Wittinghofer, A. (1996) J. Biol. Chem. **271** (12), 6794-6800

Hettich, L. and Marshall, M. (1994) Cancer Res. **54**, 5438-5444

Hiratsuka, T. (1983) Biochem. Biophys. Acta **742**, 496-508

Hofer, F., Fields, S., Schneider, C. and Martin, G.S. (1994) Proc. Natl. Acad. Sci. USA **91**, 11089-11093

Holt, K.H., Kasson, B.G. and Pessin, J.E. (1996a) Mol. Cell. Biol. **16** (2), 577-583

Holt, K.H., Waters, S.B., Okada, S., Yamauchi, K., Decker, S.J., Saltiel, A.R., Motto, D.G., Koretzky, G.A. and Pessin, J.E. (1996b) J. Biol. Chem. **271**, 8300-8306

Homayoun, P. and Stacey, D.W. (1993) Biochem. Biophys. Res. Commun. **195**, 144-150

Howe, L.R. and Marshall, C.J. (1993) J. Biol. Chem. **268** (28), 20717-20720

Howe, L.R., Leevers, S.J., Gomez, N., Nakielney, S., Cohen, P. and Marshall, C.J. (1992) Cell **71**, 335-342

Hu, C.D., Kariya, K-i., Tamada, M., Akasaka, K., Shirouzu, M., Yokoyama, S. and Kataoka, T. (1995a) J. Biol. Chem. **270** (51), 30274-30277

Hu, Q., Klippel, A., Muslin, A.J., Fantl, W.J. and Williams, L.T. (1995b) Science **268**, 100-102

Hu, Q., Milfay, D. and Williams, L.T. (1995c) Mol. Cell. Biol. **15**, 1169-1174

Hunter, T. (1997) Cell **88**, 333-346

Hwang, M-C.C., Sung, Y-J. and Hwang, Y-W. (1996) J. Biol. Chem. **271** (14), 8196-8202

Ikeda, M., Koyama, S., Okazaki, M., Dohi, K. and Kikuchi, A. (1995) FEBS Lett. **375**, 37-40

Imai, Y., Miyake, S., Hughes, D.A. and Yamamoto, M. (1991) Mol. Cell. Biol. **11**, 3088-3094

Irie, K., Gotoh, Y., Yashar, B.M., Errede, B., Nishida, E. and Matsumoto, K. (1994) Science **265**. 1716-1719

Ishioka, C., Ballester, R., Engelstein, M., Vidal, M., Kassel, J., The, I., Bernards, A., Gusella, J.F. and Friend, S.H. (1995) Oncogene **10**, 841-847

Jenkins, T. (1996) Ph.D thesis, University of London

Jimenez, B., Arends, M., Esteve, P., Perona, R., Sanchez, R., Ramon, C., Wyllie, A. and Lacal, J.C. (1995) Oncogene **10**, 811-816

John, J., Frech, M. and Wittinghofer, A. (1988) J. Biol. Chem. **263** (24), 11792-11799

John, J., Schlichting, I., Schiltz, E., Rosch, P., Wittinghofer, A. (1989) J. Biol. Chem. **264** (22), 13086-13092

John, J., Sohmen, R., Feuerstein, J., Linke, R., Wittinghofer, A. and Goody, R.S (1990) Biochemistry **29**, 6058-6065

Johnson, M.R., Look, A.T., DeClue, J.E., Valentine, M.B. and lowy, D.R. (1993) Proc. Natl. Acad. Sci. USA **90**, 5539-5543

Joly, M., Kazlauskas, A., Fay, F.S. and Corvera, S. (1994) Science **263**, 684-687

Joneson, T., White, M.A., Wigler, M.H. and Bar-Sagi, D. (1996) Science **271**, 810-812

Jurnak, F. (1985) Science **230**, 32-36

Kaplan, D.R., Whitman, M., Schaffhausen, B., Pallas, D.C., White, M., Cantley, L.and Roberts, T.M. (1987) Cell **50**, 1021-1029

Kaplan, D.R., Morrison, D.K., Wong, G., McCormick, F. and Williams, L.T. (1990) Cell **61**, 125-133

Karlsson, T., Songyang, Z., Landgren, E., Lavergne, C., Paolo Di Fiore, P., Anafi, M., Pawson, T., Cantley, L.C., Claesson-Welsh, L. and Welsh, M. (1995) Oncogene **10**, 1475-1483

Kazlauskas, A. and Cooper, J.A. (1989) Cell **58**, 1121-1133

Kazlauskas, A., Ellis, C., Pawson, T. and Cooper, J.A. (1990) Science **247**, 1578-1587

Khosravi-Far, R. and Der, C.J. (1994) Cancer Metastasis Rev. **13**, 67-89

Khosravi-Far, R., Solski, P.A., Clark, G.J., Kinch, M.S. and Der, C.J. (1995) Mol. Cell. Biol. **15** (11), 6443-6453

Khosravi-Far, R., White, M.A., Westwick, J.K., Solski, P.A., Chrzanowska-Wodnicka, M., Van Aelst, L., Wigler, M.H. and Der, C.J. (1996) Mol. Cell Biol. **16** (7), 3923-3933

Kikuchi, A., Demo, S.D., Ye, Z-H., Chen, Y-W. and Williams, L.T. (1994) Mol. Cell. Biol. **14** (11), 7483-7491

Kikuchi, A. and Williams, L.T. (1996) J. Biol. Chem. **271** (1), 588-594

Kirsten, W.H. and Mayer, L.A. (1967) J. Nat. Cancer Inst. **39**, 311-335

Kitayama,H., Sugimoto, Y., Matsuzaki, T., Ikawa, Y. and Noda, M. (1989) Cell **56**, 77-84

Koch, C.A., Anderson, D., Moran, M.F., Ellis, C. and Pawson, T. (1991) Science **252**, 668-674

Kodaki, T., Woscholski, R., Hallberg, B., Rodriguez-Viciana, P., Downward, J. and Parker, P.J. (1994) Current Biology **4** (9), 798-806

Koepp, D.M. and Silver, P.A. (1996) Cell **87**, 1-4

Koide, H., Satoh, T., Nakafuku, M. And Kaziro, Y. (1993) Proc. Natl. Acad. Sci. USA **90**, 8683-8686

Kolch, W., Heidecker, G., Kochs, G., Hummel, R., Vahidi, H., Mischak, H., Finkenzeller, G., Marme, D. and Rapp, U.R. (1993) Nature **364**, 249-252

Kolch, W., Heidecker, G., Lloyd, P. and Rapp, U.R. (1991) Nature **358**, 417-421

Krengel, U., Schlichting, I., Scherer, A., Schumann, R., Frech, M., John, J., Kabsch, W., Pai, E.F. and Wittinghofer, A. (1990) Cell **62**, 539-548

Kuriyama, M., Harada, N., Kuroda, S., Yamamoto, T., Nakafuku, M., Iwamatsu, A., Yamamoto, D., Prasad, R., Croce, C., Canaani, E. and Kaibuchi, K. (1996) J. Biol. Chem. **271** (2), 607-610

Kuroda, S., Shimizu, K., Yamamori, B., Matsuda, S., Imazumi, K., Kaibuchi, K. and Takai, Y. (1995) J. Biol. Chem. **270** (6), 2460-2465

Kuroda, Y., Suzuki, N. and Kataoka, T. (1993) Science **259**, 683-686

Kypta, R.M., Goldberg, Y., Ulug, E.T. and Courtneidge, S.A. (1990) Cell **62**, 481-492

Kyriakis, J.M., App, H., Zhang, X-F., Banerjee, P., Brautigan, D.L., Rapp, U.R. and Avruch, J. (1992) Nature **358**, 417-421

Laemmli, U.K. (1970) Nature **227**, 680-685

Lambright, D.G., Noel, J.P., Hamm, H.E. and Sigler, P.B. (1994) Nature **369**, 621-628

Landis, C.A., Masters, S.B., Spada, A., Pace, A.M., Bourne, H.R. and Vallar, L. (1989) Nature **340**, 692-698

Landt, O., Grunert, H. and Hahn, U. (1990) Gene **96**, 125-128

Lange-Carter, C.A., Pleiman, C.M., Gardner, A.M., Blumer, K.J. and Johnson, G.L. (1994) Science **260**, 315-319

Langen, R., Schweins, T. and Warshel, A. (1992) Biochemistry **31**, 8691-8696

Lechleider, R.J., Sugimoto, S., Bennett, A.M., Kashishian, A.S., Cooper, J.A., Shoelson, S.E., Walsh, C.T. and Neel, B.G. (1993) J. Biol. Chem. **268** (29), 21478-21481

Lee, C.H.J., Della, N.G., Chew, C.E. and Zack, D.J. (1996) J. Neurosci. **16** (21), 6784-6794

Leevers, S.J., Paterson, H.F. and Marshall, C.J. (1994) Nature **369**, 411-414

Legius, E., Marchuk, D.A., Collins, F.S. and Glover, T.W. (1993) Nature Genet. **3**, 122-126

Lemmon, M.A. and Schlessinger, J. (1994) Trends Biochem. Sci. **19**, 459-463

Leung, T., Manser, E., Tan, L. and Lim, L. (1995) J. Biol. Chem. **270** (49), 29051-29054

Levy-Toledano, R., Taouis, M., Blaettler, D.H., Gorden, P. and Taylor, S.I. (1994) J. Biol. Chem. **269** (49), 31178-31182

Li, Y., Bollag, G., Clark, R., Stevens, J., Conroy, L., Fults, D., Ward, K., Friedman, E., Samowitz, W., Robertson, M., Bradley, P., McCormick, F., White, R. and Cawthon, R. (1992) Cell **69**, 275-281

Li, N., Batzer, A., Daly, R., Yajnik, V., Skolnik, E., Chardin, P., Bar-Sagi, D., Margolis, B. and Schlessinger, J. (1993) Nature **363**, 85-92

Li, S., Janosch, P., Tanji, M., Rosenfeld, G.C., Waymire, J.C., Mischak, H., Kolch, W. and Sedivy, J.M. (1995) The EMBO J. **14** (4), 685-696

Ligeti, E., Pizon, V., Wittinghofer, A., Gierschik, P., Jakobs, K.H. (1993) Eur. J. Biochem. **216**, 813-820

Lim, L., Manser, E., Leung, T. and Hall, C. (1996) Eur. J. Biochem. **242**, 171-185

Liscovitch, M. And Cantley, L.C. (1994) Cell **77**, 329-334

Lowe, P.N., Page, M.J., Bradley, S., Rhodes, S., Sydenham, M., Paterson, H. And Skinner, R.H. (1991) J. Biol. Chem. **266** (3), 1672-1678

Lowe, P.N. and Skinner, R.H. (1994) Cellular Signalling **6** (2), 109-123

Lowenstein, E.J., Daly, R.J., Batzer, A.G., Li, W., Margolis, B., Lammers, R., Ullrich, A., Skolnik, E.Y., Bar-Sagi, D. and Schlessinger, J. (1992) Cell **70**, 431-442

Lowy, D.R., Zhang, K., Declue, J.E. and Willumsen, B.M. (1991) Trends Genet. **7**, 346-350

Lowy, D.R. and Willumsen, B.M. (1993) Annu. Rev. Biochem. **62**, 851-891

Lyons, J., Landis, C., Harsh, G., Vallar, L., Grunewald, K., Feichtinger, H., Duh, Q., Clark, O., Kawasaki, E. and Bourne, H. (1990) Science **249**, 655-659

Macara, I.G., Lounsbury, K.M., Richards, S.A., McKiernan, C. and Bar-Sagi, D. (1996) FASEB J. **10**, 625-630

Maegley, K.A., Admiraal, S.J. and Herschlag, D. (1996) Proc. Natl. Acad. Sci. USA **93**, 8160-8166

Maekawa, M., Nakamura, S. and Hattori, S. (1993) J. Biol. Chem. **268** (30), 22948-22952

Maekawa, M., Li, S., Iwamatsu, A., Morishita, T., Yokota, K., Imai, Y., Kohsaka, S., Nakamura, S. and Hattori, S. (1994) Mol. Cell. Biol. **14**, 6879-6885

Maguire, J., Santoro, T., Jensen, P., Siebenlist, U., Yewdell, J. and Kelly, K. (1994) Science **265**, 241-244

Maniatis, T., Fritsch, E.F. and Sambrook, J. (1982) Molecular Cloning: A Laboratory Manual, Cold Spring Harbour Laboratory, New York.

Manne, V., Bekesi, E. and Kung, H-F. (1985) Proc. Natl. Acad. Sci. USA **82**, 376-380

Manser, E., Leung, T., Salihuddin, H., Zhao, Z-S. and Lim, L. (1994) Nature **367**, 40-46

Mansour, S.J., Matten, W.T., Hermann, A.S., Candia, J.M., Rong, S., Fukasawa, K., Vande Woude, G.F. and Ahn, N.G. (1994) Science **265**, 966-970

Marais, R., Light, Y., Paterson, H.F. and Marshall, C.J. (1995) The EMBO J. **14** (13), 3136-3145

Marchuk, D.A., Saulino, A.M., Tavakkol, R., Swaroop, M., Wallace, M.R., Anderson, L.B., Mitchell, A.L., Gutmann, D.H., Boguski, M. and Collins, F.S. (1991) Genomics **11**, 931-940

Markby, D.W., Onrust, R. And Bourne, H.R. (1993) Science **262**, 1895-1901

Marshall, M.S., Hill, W.S., Assunta, S.N., Vogel, U.S., Schaber, M.D., Scolnick, E.M., Dixon, R.A.F., Sigal, I.S. and Gibbs, J.B. (1989) The EMBO J. **8**, 1105-1110

Marshall, M.S. and Hettich, L.A. (1993) Oncogene **8**, 425-431

Marshall, M.S. (1994) Trends Biochem. Sci. **18**, 250-254

Marshall, M.S. (1995) FASEB J. **9**, 1311-1318

Marshall, C.J. (1996) Curr. Opin. Cell Biol. **8**, 197-204

Martegani, E., Vanoni, M., Zippel, R., Coccetti, P., Brambilla, R., Ferrari, C., Sturani, E. and Alberghina, L. (1992) The EMBO J. **11** (6), 2151-2157

Martin, G.A., Yatani, A., Clark, R., Conroy, L., Polakis, P., Brown, A.M. and

McCormick, F. (1992) Science **255**, 192-194

Martin, G.A., Viskochil, D., Bollag, G., McCabe, P.C., Crosier, W.J., Haubruck, H., Conroy, L., Clark, R., O'Connell, P., Cawthon, R.M., Innis, M.A. and McCormick, F. (1990) Cell **63**, 843-849

Masuda, T., Kariya, K-I., Shinkai, M., Okada, T. and Kataoka, T. (1995) J. Biol. Chem. **270** (5), 1979-1982

Matuoka, K., Shibata, M., Yamakawa, A. and Takenawa, T. (1992) Proc. Natl. Acad. Sci. USA **89**, 9015-9019

Mayer, B.J., Ren, R., Clark, K.L. and Baltimore, D. (1993) Cell **73**, 629-630

McCormick, F. (1990) Mol. Carcinog. **3**, 185-187

McCormick, F., Martin, G.A., Clark, R., Bollag, G. and Polakis, P. (1991) Cold Spring Harb. Symp. Quant. Biol. **56**, 237-241

McCormick, F. (1992) Phil. Trans. R. Soc. Lond. B **336**, 43-48

McCormick, F. (1994) Trends Cell Biol. **4**, 347-350

McCormick, F. (1995) Curr. Opin. Genet. Dev. **5**, 51-55

McCormick, F. and Wittinghofer, A. (1996) Curr. Opin. Biotech. **7**, 449-456

McGlade, J., Brunkhorst, B., Anderson, D., Mbamalu, G., Settleman, J., Dedhar, S., Rozakis-Adcock, M., Chen, L.B. and Pawson, T. (1993) The EMBO J. **12**, 3073-3081

Medema, R.H., De Laat, W.L., Martin, G.A., McCormick, F. and Bos, J.L. (1992) Mol. Cell. Biol. **12** (8), 3425-3430

Medema, R.H., De Vries-Smits, A.M.M., Van Der Zon, G.C.M., Maassen, J.A. and Bos, J.L. (1993) Mol. Cell. Biol. **13** (1), 155-162

Meisenhelder, J., Suh, P-G., Rhee, S.G. and Hunter, T. (1989) Cell **57**, 1109-1122

Melchior, F. and Gerace, L. (1995) Curr. Opin. Cell Biol. **7**, 310-318

Menon, A.G., Anderson, K.M., Riccardi, V.M., Chung, R-Y., Whaley, J.M., Yandell, D.W., Farmer, G.E., Freiman, R.N., Lee, J.K., Li, F.P., Barker, D.F., Ledbetter, D.H., Kleider, A., Martuza, R.L., Gusella, J.F. and Seizinger, B.R. (1990) Proc. Natl. Acad. Sci. USA **87**, 5435-5439

Miao, W., Eichelberger, L., Baker, L. and Marshall, M.S. (1996) J. Biol. Chem. **271** (26), 15322-15329

Miki, H., Miura, K., Matuoka, K., Nakata, T., Hirokawa, N., Orita, S., Kaibuchi, K., Takai, Y. And Takenawa, T. (1994) J. Biol. Chem. **269** (8), 5489-5492

Milburn, M.V., Tong, L., DeVos, A.M., Brunger, A., Yamaizumi, Z., Nishimura, S. and Kim, S-H. (1990) Science **247**, 939-945

Miller, A-F., Papastavros, M.Z. and Redfield, A.G. (1992) Biochemistry **31**, 10208-10216

Miller, A-F., Halkides, C.J. and Redfield, A.G. (1993) Biochemistry **32**, 7367-7376

Minden, A., Lin, A., Claret, F.X., Abo, A. and Karin, M. (1995) Cell **81**, 1147-1157

Mistou, M., Jacquet, E., Poullet, P., Rensland, H., Gideon, P., Schlichting, I., Wittinghofer, A. and Parmeggiani, A. (1992) The EMBO J. **11** (7), 2391-2397

Mittal, R., Ahmadian, M.R., Goody, R.S. and Wittinghofer, A. (1996) Science **273**, 115-117

Mixon, M.B., Lee, E., Coleman, D.E., Berghuis, A.M., Gilman, A.G., Sprang, S.R. (1995) Science **270**, 954-960

Miyamoto, H., Nihonmatsu, I., Kondo, S., Ueda, R., Togashi, S., Hirata, K., Ikegami, Y. and Yamamoto, D. (1995) Genes and Dev. **9**, 612-625

Molloy, D.P., Owen, D. and Grand, R.J.A. (1995) FEBS Lett. **368**, 297-303

Moodie, S.A., Willumsen, B.M., Weber, M.J. and Wolfman, A. (1993) Science **260**,

1658-1661

Moodie, S.A., Paris, M., Villafranca, E., Kirshmeier, P., Willumsen, B.M. and Wolfman, A. (1995) Oncogene **11**, 447-454

Moore, K.J.M., Lowe, P.N. and Eccleston, J.F. (1992) Phil. Trans. R. Soc. Lond. B **336**, 49-54

Moore, K.J.M., Webb, M.R. and Eccleston, J.F. (1993) Biochemistry **32**, 7451-7459

Moore, M.S. and Blobel, G. (1993) Nature **365**, 661-663

Morcos, P., Thapar, N., Tusneem, N., Stacey, D. and Tamanoi, F. (1996) Mol. Cell. Biol. **16** (5), 2496-2503

Mori, S., Ronnstrand, L., Yokote, K., Engstrom, A., Courtneidge, S.A., Claesson-Welsh, L. and Heldin, C-H. (1993) The EMBO J. **12** (6), 2257-2264

Mori, S., Satoh, T., Koide, H., Nakafuku, M., Villafranca, E. and Kaziro, Y. (1995) J. Biol. Chem. **270** (48), 28834-28838

Mosteller, R.D., Han, J. and Broek, D. (1994) Mol. Cell. Biol. **14** (2), 1104-1112

Mott, H.R., Carpenter, J.W., Zhong, S., Ghosh, S., Bell, R.M. and Campbell, S.L. (1996) Proc. Natl. Acad. Sci. USA **93**, 8312-8317

Mulcahy, L.S., Smith, M.R. and Stacey, D.W. (1985) Nature **313**, 241-243

Musacchio, A., Gibson, T., Rice, P., Thompson, J. and Saraste, M. (1993) Trends Biochem. Sci. **18**, 343-348

Naor, Z. (1991) Mol. Cell. Endocrin. **80**, 181-186

Nassar, N., Horn, G., Herrmann, C., Scherer, A., McCormick, F. and Wittinghofer, A. (1995) Nature **375**, 554-560

Neal, S.E., Eccleston, J.F., Hall, A. and Webb, M.R. (1988) J. Biol. Chem. **263** (36),

19718-19722

Neal, S.E., Eccleston, J.F. and Webb, M.R. (1990) Proc. Natl. Acad. Sci. USA **87**, 3562-3565

Niehof, M., Radziwill, G., Klauser, S. and Moelling, K. (1995) Biochem. Biophys. Res. Com. **206** (1), 46-50

Nishi, T., Lee, P.S.Y., Oka, K., Levin, V.A., Tanase, S., Morino, Y. and Saya, H. (1991) Oncogene **6**, 1555-1559

Nobes, C. and Hall, A. (1994) Curr. Opin. Genet. Dev. **4**, 77-81

Nobes, C.D. and Hall, A. (1995) Cell **81**, 53-62

Noel, J.P., Hamm, H.E. and Sigler, P.B. (1993) Nature **366**, 654-663

Nur-E-Kamal, M.S.A., Varga, M., Maruta, H. (1993) J. Biol. Chem. **268** (30), 22331-22337

Okada, S. and Pessin, J.E. (1996) J. Biol. Chem. **271** (41), 25533-25538

Okada, T., Masuda, T., Shinkai, M., Kariya, K-I. and Kataoka, T. (1996) J. Biol. Chem. **271** (9), 4671-4678

Olivier, J.P., Raabe, T., Henkemeyer, M., Dickson, B., Mbamalu, G., Margolis, B., Schlessinger, J., Hafen, E. and Pawson, T. (1993) Cell **73**, 179-191

Olson, M.F., Ashworth, A. and Hall, A. (1995) Science **269**, 1270-1272

Olson, M.F., Pasteris, N.G., Gorski, J.L. and Hall, A. (1996) Curr. Biol. **6**, 1628-1633

Pai, E.F., Kabsch, W., Krengel, U., Holmes, K.C., John, J. and Wittinghofer, A. (1989) Nature **341**, 209-214

Pai, E.F., Krengel, U., Petsko, G.A., Goody, R.S., Kabsch, W. and Wittinghofer, A. (1990) The EMBO J. **9** (8), 2351-2359

Papin, C., Denouel, A., Calothy, G. And Eychene, A. (1996) Oncogene **12**, 2213-2221

Paterson, H.F., Self, A.J., Garrett, M.D., Just, I., Aktories, K. and Hall, A. (1990) J. Cell Biol. **111**, 1001-1007

Pawson, T. and Gish, G.D. (1992) Cell **71**, 359-362

Pawson, T. and Schlessinger, J. (1993) Current Biology **3** (7), 434-442

Pelicci, G., Lanfrancone, L., Grignani, F., McGlade, J., Cavallo, F., Forni, G., Nicoletti, I., Grignani, F., Pawson, T. and Pelicci, P.G. (1992) Cell **70**, 93-104

Peterson, S.N., Trabalzini, L., Brtva, T.R., Fischer, T., Altschuler, D.L., Martelli, P., Lapetina, E.G., Der, C.J. and White, G.C. (1996) J. Biol. Chem. **271** (47), 29903-29908

Pingoud, A., Wehrmann, M., Pieper, U., Gast, F.U., Urbanke, C., Alves, J., Feuerstein, J. and Wittinghofer, A. (1988) Biochemistry **27**, 4735-4740

Pizon, V., Chardin, P., Lerosey, I., Olofsson, B. and Tavitian, A. (1988) Oncogene **3**, 201-204

Polakis, P. and McCormick, F. (1992) Cancer Surv. **12**, 25-42

Polakis, P. and McCormick, F. (1993) J. Biol. Chem. **268** (13), 9157-9160

Post, G.R. and Brown, J.H. (1996) FASEB J. **10**, 741-749

Poullet, P., Lin, B., Esson, K. and Tamanoi, F. (1994) Mol. Cell. Biol. **14** (1), 815-821

Prasad, R., Gu, Y., Alder, H., Nakamura, T., Canaani, O., Saito, H., Huebner, K., Gale, R.P., Nowell, P.C., Kuriyama, K., Miyazaki, Y., Croce, C.M. and Canaani, E. (1993) Cancer Res. **53**, 5624-5628

Prendergast, G.C. and Gibbs, J.B. (1993) Adv. Cancer Res. **62**, 19-53

Prendergast, G.C., Khosravi-Far, R., Solski, P.A., Kurzawa, H., Lebowitz, P.F. and Der, C.J. (1995) Oncogene **10**, 2289-2296

Prive, G.G., Milburn, M.V., Tong, L., DeVos, A.M., Yamaizumi, Z., Nishimura, S. and Kim, S-H. (1992) Proc. Natl. Acad. Sci USA **89**, 3649-3653

Pronk, G.J., De Vries-Smits, A.M.M., Buday, L., Downward, J., Maassen, J.A., Medema, R.H. and Bos, J.L. (1994) Mol. Cell. Biol. **14** (3), 1575-1581

Pumiglia, K., Chow, Y-H., Fabian, J., Morrison, D., Decker, S. and Jove, R. (1995) Mol. Cell. Biol. **15** (1), 398-406

Qiu, R., Chen, J., Kirn, D., McCormick, F. and Symons, M. (1995a) Nature **374**, 457-459

Qiu, R., Chen, J., McCormick, F. and Symons, M. (1995b) Proc. Natl. Acad. Sci. USA **92**, 11781-11785

Reinstein, J., Schlichting, I., Frech, M., Goody, R.S. and Wittinghofer, A. (1991) J. Biol. Chem. **266** (26), 17700-17706

Ren, R., Mayer, B.J., Cicchetti, P. and Baltimore, D. (1993) Science **259**,1157-1161

Rensland, H., Lautwein, A., Wittinghofer, A. and Goody, R.S. (1991) Biochemistry **30**, 11181-11185

Rey, I., Taylor-Harris, P., Van Erp, H. and Hall, A. (1994) Oncogene **9**, 685-692

Reynet, C. and Kahn, C.R. (1993) Science **262**, 1441-1444

Reynolds, J.E., Fletcher, J.A., Lytle, C.H., Nie, L., Morton, C.C. and Diehl, S.R. (1992) Hum. Genet. **90**, 450-456

Rhodenhuis, S. (1992) Semin. Cancer Biol. **3**, 241-247

Ridley, A.J. and Hall, A. (1992) Cell **70**, 389-399

Ridley, A.J., Paterson, H.F., Johnston, C.L., Diekmann, D. and Hall, A. (1992) Cell **70**, 401-410

Ridley, A.J. (1994) BioEssays **16** (5), 321-327

Ridley, A.J. (1995) Curr. Opin. Genet. Dev. **5**, 24-30

Robinson, L.C., Gibbs, J.B., Marshall, M.S., Sigal, I.S. and Tatchell, K. (1987) Science **235**, 1218-1221

Rodriguez-Viciana, P., Warne, P.H., Dhand, R., Vanhaesebroeck, B., Gout, I., Fry, M.J., Waterfield, M.D. and Downward, J. (1994) Nature **370**, 527-532

Rodriguez-Viciana, P., Marte, B.M., Warne, P.H. and Downward, J. (1996) Phil. Trans. R. Soc. Lond. B. **351**, 225-232

Rojas, M., Yao, S. and Lin, Y-Z. (1996) J. Biol. Chem. **271** (44), 27456-27461

Rommel, C., Radziwill, G., Lovric, J., Noeldeke, J., Heinicke, T., Jones, D., Aitken, A. and Moelling, K. (1996) Oncogene **12**, 609-619

Ronnstrand, L., Mori, S., Arridsson, A-K., Eriksson, A., Wernstedt, C., Hellman, U., Claesson-Welsh, L. and Heldin, C-H. (1992) The EMBO J. **11** (11), 3911-3919

Rozakis-Adcock, M., Fernley, R., Wade, J., Pawson, T. and Bowtell, D. (1993) Nature **363**, 83-84

Rozakis-Adcock, M., McGlade, J., Mbamalu, G., Pellici, G., Daly, R., Li, W., Batzer, A., Thomas, S., Brugge, J., Pelicci, P.G., Schlessinger, J. and Pawson, T. (1992) Nature **360**, 689-692

Rozengurt, E. (1991) Cancer Cells **3**, 397-398

Rush, M.G., Drivas, G. and D'Eustachio, P. (1996) BioEssays **18** (2), 103-112

Russell, M., Lange-Carter, C.A. and Johnson, G.L. (1995) J. Biol. Chem. **270** (20), 11757-11760

Sasaki, T., Kaibuchi, K., Kabceneli, A.K., Novick, P.J. and Takai, Y. (1991) Mol. Cell. Biol. **11**, 2909-2912

Sasaoka, T., Draznin, B., Leitner, J.W., Langlois, W.J. and Olefsky, J.M. (1994) J. Biol. Chem. **269**, 10734-10738

Sawada, S., Florell, S., Purandare, S.M., Ota, M., Stephens, K. and Viskochil, D. (1996) Nature Genetics **14**, 110-112

Scaife, R., Gout, I., Waterfield, M.D. and Margolis, R.L. (1994) The EMBO J. **13** (11), 2574-2582

Schaber, M.D., Garsky, V.M., Boylan, D., Hill, W.S., Scolnick, E.M., Marshall, M.S., Sigal, I.S. and Gibbs, J.B. (1989) Proteins: Structure, Function and Genetics **6**, 306-315

Scheffzek, K., Lautwein, A., Kabsch, W., Ahmadian, M.R. and Wittinghofer, A. (1996) Nature **384**, 591-596

Scheidig, A.J., Franken, S.M., Corrie, J.E.T., Reid, G.P., Wittinghofer, A., Pai, E.F. and Goody, R.S. (1995) J. Mol. Biol. **253**, 132-150

Schlessinger, J. and Ullrich, A. (1992) Neuron **9**, 383-391

Schlessinger, J. (1993) Trends Biochem. Sci. **18**, 273-275

Schlichting, I., Almo, S.C., Rapp, G., Wilson, K., Petratos, K., Lentfer, A., Wittinghofer, A., Kabsch, W., Pai, E.F., Petsko, G.A. and Goody, R.S. (1990) Nature **345**, 309-315

Schweighoffer, F., Barlat, I., Chevallier-Multon, M-C., Tocque, B. (1992) Science **256**, 825-827

Schweins, T., Langen, R. and Warshel, A. (1994) Structural Biology **1**, 476-484

Schweins, T., Geyer, M., Scheffzek, K., Warshel, A., Robert, K. and Wittinghofer, A. (1995) Structural Biology **2**, 36-44

Schweins, T., Geyer, M., Kalbitzer, H.R., Wittinghofer, A. and Warshel, A. (1996) Biochemistry **35** (45), 14225-14231

Schweins, T. and Warshel, A. (1996) Biochemistry **35**, 14232-14243

Seedorf, K., Kostka, G., Lammers, R., Bashkin, P., Daly, R., Burgess, W.H., van der Bliek, A.M., Schlessinger, J. and Ullrich, A. (1994) J. Biol. Chem. **269** (23), 16009-16014

Segal, A.W. and Abo, A. (1993) Trends Biochem. Sci. **18**, 43-47

Segel, I.H. (1975) Enzyme Kinetics 170-204 Wiley-Interscience, New York

Seizinger, B.R. (1993) Nature Genet. **3**, 97-99

Serth, J., Lautwein, A., Frech, M., Wittinghofer, A. and Pingoud, A. (1991) The EMBO J. **10**, 1325-1330

Settleman, J., Narasimhan, V., Foster, L.C. and Weinberg, R.A. (1992a) Cell **69**, 539-549

Settleman, J., Albright, C.F., Foster, L.C. and Weinberg, R.A. (1992b) Nature **359**, 153-154

Shirouzu, M., Koide, H., Fujita-Yoshigaki, J., Oshio, H., Toyama, Y., Yamasaki, K., Furhman, S.A., Villafranca, E., Kaziro, Y. and Yokoyama, S. (1994) Oncogene **9**, 2153-2157

Shou, C., Farnsworth, C.L., Neel, B.G. and Feig, L.A. (1992) Nature **358**, 351-354

Simon, M.A., Bowtell, D.D.L., Dodson, G.S., Laverty, T.R. and Rubin, G.M. (1991) Cell **67**, 701-716

Simon, M.A., Dodson, G.S. and Rubin, G.M. (1993) Cell **73**, 169-177

Skelly, J.V., Suter, D.A., Kuroda, R., Neidle, S., Hancock, J.F. and Drake, A. (1990) FEBS Lett. **262** (1), 127-130

Skinner, R.H., Bradley, S., Brown, A.L., Johnson, N.J.E., Rhodes, S., Stammers, D.K. and Lowe, P.N. (1991) J. Biol. Chem. **266**, 14163-14166

Skinner, R.H., Picardo, M., Gane, N.M., Cook, N.D., Morgan, L., Rowedder, J., Lowe, P.N. (1994) Anal. Biochem **223**, 1-7

Smith, M.R., DeGudicibus, S.J. and Stacey, D.W. (1986) Nature **320**, 540-543

Smith, D.B. and Johnson, K.S. (1988) Gene **67**, 31-40

Sondek, J., Lambright, D.G., Noel, J.P., Hamm, H.E. and Sigler, P.B. (1994) Nature **372**, 276-279

Spaargaren, M. and Bischoff, J.R. (1994) Proc. Natl. Acad. Sci. USA **91**, 12609-12613

Stacey, D.W., Tsai, M.H., Yu, C.L. and Smith, J.K. (1988) Cold Spring Harb. Symp. Quant. Biol. **53**, 871-881

Stacey, D.W., Feig, L.A. and Gibbs, J.B. (1991) Mol. Cell. Biol. **11** (8), 4053-4064

Stanton, V.P., Nichols, D.W., Laudano, A.P and Cooper, A.P. (1989) Mol. Cell. Biol. **9** (2), 639-647

Stokoe, D., Macdonald, S.G., Cadwallader, K., Symons, M. and Hancock, J.F. (1994) Science **264**, 1463-1467

Stone, J.C., Colleton, M. and Bottorff, D. (1993) Mol. Cell. Biol. **13** (12), 7311-7320

Stouten, P.F.W., Sander, C., Wittinghofer, A. and Valencia, A. (1993) FEBS Lett. **320** (1), 1-6

Stoyanov, B., Volinia, S., Hanck, T., Rubio, I., Loubtchenkov, M., Malek, D., Stoyanova, S., Vanhaesebroeck, B., Dhand, R., Nurnberg, B., Gierschik, P., Seedorf, K., Hsuan, J.J., Waterfield, M.D. and Wetzker, R. (1995) Science **269**, 690-693

Sumida, C., Graber, R. and Nunez, E. (1993) Prostaglandins Leukotrienes Essent. Fatty Acids **48**, 117-122

Suzuki, Y., Suzuki, H., Kayama, T., Yoshimoto, T. and Shibahara, S. (1991) Biochem. Biophys. Res. Com. **181** (3), 955-961

Symons, M. (1996) Trends Biochem. Sci. **21**, 178-181

Takai, Y., Sasaki, T., Tanaka, K. and Nakanishi, H. (1995) Trends Biochem. Sci. **20**, 227-231

Tanaka, K., Nakafuku, M., Tamanoi, F., Kaziro, Y., Matsumoto, K. and Toh-e, A. (1990) Mol. Cell. Biol. **10** (8), 4303-4313

Tapon, N. and Hall, A. (1997) Curr. Opin. Cell Biol. **9**, 86-92

Teinturier, C., Danglot, G., Slim, R., Pruliere, D., Launay, J.M. and Bernheim, A. (1992) Biochem. Biophys. Res. Com. **188** (2), 851-857

The, I., Murthy, A.E., Hannigan, G.E., Jacoby, L.B., Menon, A.G., Gusella, J.F. and Bernards, A. (1993) Nature Genet. **3**, 62-66

Toda, T., Uno, I., Ishikawa, T., Powers, S., Kataoka, T., Broek, D., Cameron, S., Broach, J., Matsumoto, K. and Wigler, M. (1985) Cell **40**, 27-36

Tong, L., DeVos, A.M., Milburn, M.V. and Kim, S-H. (1991) J. Mol. Biol. **217**, 503-516

Trahey, M. and McCormick, F. (1987) Science **238**, 542-545

Trahey, M., Wong, G., Halenbeck, R., Rubinfeld, B., Martin, G.A., Ladner, M., Long, C.M., Crosier, W.J., Watt, K., Koths, K. and McCormick, F. (1988) Science **242**, 1697-1700

Traverse, S., Cohen, P., Paterson, H., Marshall, C., Rapp, U. and Grand, R.J.A. (1993) Oncogene **8**, 3175-3181

Trentham, D.R., Eccleston, J.F., Bagshaw, C. R. (1976) Q. Rev. Biophys. **9**, 217-281

Tsai, M.H., Hall, A. and Stacey, D.W. (1989a) Mol. Cell Biol. **9**, 5260-5264

Tsai, M.H., Yu, C.L., Wei, F.S. and Stacey, D.W. (1989b) Science **243**, 522-526

Tsai, M.H., Yu, C.L. and Stacey, D.W. (1990) Science **250**, 982-985

Tsai, M.H., Roudebush, M., Dobrowolski, S., Yu, C.L., Gibbs, J.B. and Stacey, D.W. (1991) Mol. Cell. Biol. **11**, 2785-2793

Tsuda, L., Inoue, Y.H., Yoa, M-A., Mizuno, M., Hata, M., Lim, Y-M., Adachi-Yamada, T., Ryo, H., Masamune, Y. and Nishida, Y. (1993) Cell **72**, 407-414

Uchida, T., Matozaki, T., Suzuki, T., Matsuda, K., Wada, K., Nakano, O., Konda, Y., Nishisaki, H., Nagao, M., Sakamoto, C. and Kasuga, M. (1992) Biochem. Biophys. Res. Com. **187**, 332-339

Ueda, T., Kikuchi, A., Ohga, N., Yamamoto, J. and Takai, Y. (1990) J. Biol. Chem. **265** (16), 9373-9380

Upadhyaya, M., Shen, M., Cherryson, A., Farnham, J., Maynard, J., Huson, S.M. and Harper, P.S. (1992) Human Mol. Gen. **1** (9), 735-740

Urano, T., Emkey, R. and Feig, L.A. (1996) The EMBO J. **15** (4), 810-816

Van Aelst, L., Barr, M., Marcus, S., Polverino, A. and Wigler, M. (1993) Proc. Natl. Acad. Sci. USA **90**, 6213-6217

Van Aelst, L., White, M.A. and Wigler, M.H. (1994) Cold Spring Harb. Symp. Quant. Biol. **59**, 181-186

Van Dop, C., Tsubokawa, M., Bourne, H.R. and Rama Chandran, J. (1984) J. Biol. Chem. **259** (2), 696-698

Viskochil, D., Buchberg, A.M., Xu, G., Cawthon, R.M., Stevens, J., Wolff, R.K., Culver, M., Carey, J.C., Copeland, N.G., Jenkins, N.A., White, R. and O'Connell, P. (1990) Cell **62**, 187-192

Vogel, U.S., Dixon, R.A.F., Schaber, M.D., Diehl, R.E., Marshall, M.S., Scolnick, E.M., Sigal, I.S. and Gibbs, J.B. (1988) Nature **335**, 90-93

Vojtek, A.B., Hollenberg, S.M. and Cooper, J.A. (1993) Cell **74**, 205-214

Wahl, M.I., Nishibe, S., Suh, P-G., Rhee, S.G. and Carpenter, G. (1989) Proc. Natl. Acad. Sci. USA **86**, 1568-1572

Wallace, M.R., Marchuk, D.A., Anderson, L.B., Letcher, R., Odeh, H.M., Saulino, A.M., Fountain, J.W., Brereton, A., Nicholson, J., Mitchell, A.L., Brownstein, B.H. and Collins, F.S. (1990) Science **249**, 181-186

Wallace, M.R., Anderson, L.B., Sulino, A.M., Gregory, P.E., Glover, T.W. and Collins, F.S. (1991) Nature **353**, 864-866

Wang, Y., Boguski, M., Riggs, M., Rodgers, L. and Wigler, M. (1991a) Cell. Reg. **2**, 453-465

Wang, Y., Xu, H-P., Riggs, M., Rodgers, L. and Wigler, M. (1991b) Mol. Cell. Biol. **11** (7), 3554-3563

Warne, P.H., Rodriguez-Viciana, P. and Downward, J. (1993) Nature **364**, 352-355

Warner, L.C., Hack, N., Egan, S.E., Goldberg, H.J., Weinberg, R.A. and Skorecki, K.L. (1993) Oncogene **8**, 3249-3255

Wartmann, M. and Davis, R.J. (1994) J. Biol. Chem. **269** (9), 6695-6701

Waters, S.B., Holt, K.H., Ross, S.E., Syu, L-J., Guan, K-L., Saltiel, A.R., Koretzky, G.A. and Pessin, J.E. (1995) J. Biol. Chem. **270** (36), 20883-20886

Waters, S.B., Chen, D., Kao, A.W., Okada, S., Holt, K.H. and Pessin, J.E. (1996) J. Biol. Chem. **271** (30), 18224-18230

Wei, W., Mosteller, R.D., Sanyal, P., Gonzales, E., McKinney, D., Dasgupta, C., Li, P., Liu, B-X. (1992) Proc. Natl. Acad. Sci. USA **89**, 7100-7104

Weissbach, L., Settleman, J., Kalady, M.F., Snijders, A.J., Murthy, A.E., Yan, Y-X. and Bernards, A. (1994) J. Biol. Chem. **269** (32), 20517-20521

Weismuller, L. and Wittinghofer, A. (1992) J. Biol. Chem. **267** (15), 10207-10210

Welsh, M., Mares, J., Karlsson, T., Lavergne, C., Breant, B. and Claesson-Welsh, L. (1994) Oncogene **9**, 19-27

Wennstrom, S., Hawkins, P., Cooke, F., Hara, K., Yonezawa, K., Kasuga, M., Jackson, T., Claesson-Welsh, L. and Stephens, L. (1994) Curr. Biol. **4** (5), 385-393

Westwick, J.K., Cox, A.D., Der, C.J., Cobb, M.H., Hibi, M., Karin, M. and Brenner, D.A. (1994) Proc. Natl. Acad. Sci. USA **91**, 6030-6034

Whatley, R.E., Stroud, E.D., Bunting, M., Zimmerman, G.A., McIntyre, T.M. and Prescott, S.M. (1993) J. Biol. Chem. **268** (22), 16130-16138

White, M.F. (1994) Curr. Opin. Genet. Dev. **4**, 47-54

White, M.F. and Kahn, C.R. (1994) J. Biol. Chem. **269** (1), 1-4

White, M.A., Nicolette, C., Minden, A., Polverino, A., Van Aelst, L., Karin, M. and Wigler, M.H. (1995) Cell **80**, 533-541

White, M.F. (1996) Phil. Trans. R. Soc. Lond. B **351**, 181-189

Willumsen, B.M., Norris, K., Papageorge, A.G., Hubbert, N.L. and Lowy, D.R. (1984) The EMBO J. **3** (11), 2581-2585

Wittinghofer, A. (1996) Structure **4**, 357-361

Wittinghofer, A. and Herrmann, C. (1995) FEBS Lett. **369**, 52-56

Wittinghofer, A. and Pai, E.F. (1991) Trends Biochem. Sci. **16**, 382-387

Wolthius, R.M.F., Bauer, B., Van't Veer, L.J., de Vries-Smits, A.M.M., Cool, R.H., Spaargaren, M., Wittinghofer, A., Burgering, B.M.T. and Bos, J.L. (1996) Oncogene **13**, 353-362

Wood, K.W., Sarnecki, C., Roberts, T.M. and Blenis, J. (1992) Cell **68**, 1041-1050

Wood, D.R., Poullet, P., Wilson, B.A., Khalil, M., Tanaka, K., Cannon, J.F. and Tamanoi, F. (1994) J. Biol. Chem. **269** (7), 5322-5327

Xu, G., Lin, B., Tanaka, K., Dunn, D., Wood, D., Gesteland, R., White, R., Weiss, R. and Tamanoi, F. (1990a) Cell **63**, 835-841

Xu, G., O'Connell, P., Viskochil, D., Cawthon, R., Robertson, M., Culver, M., Dunn, D., Stevens, J., Gesteland, R., White, R. and Weiss, R. (1990b) Cell **62**, 599-608

Xu, N., McCormick, F. and Gutkind, J.S. (1994) Oncogene **9**, 597-601

Yamamori, B., Kuroda, S., Shimizu, K., Fukui, K., Ohtsuka, T. and Takai, Y. (1995) J. Biol. Chem. **270** (20), 11723-11726

Yamasaki, K., Shirouzu, M., Muto, Y., Fujita-Yoshigaki, J., Koide, H., Ito, Y., Kawai, G., Hattori, S., Yokoyama, S., Nishimura, S. and Miyazawa, T. (1994) Biochemistry **33**, 65-73

Yamauchi, K. and Pessin, J.E. (1994) J. Biol. Chem. **269** (49), 31107-31114

Yatani, A., Okabe, K., Polakis, P., Halenbeck, R., McCormick, F. and Brown, A.M. (1990) Cell **61**, 769-776

Yoder-Hill, J., Golubic, M. and Stacey, D.W. (1995) J. Biol. Chem. **270** (46), 27615-27621

Yonezawa, K., Ando, A., Kaburagi, Y., Yamamoto-Honda, R., Kitamura, T., Hara, K., Nakafuku, M., Okabayashi, Y., Kadowaki, T., Kaziro, Y. and Kasuga, M. (1994) J. Biol. Chem. **269** (6), 4634-4640

Yu, C.L., Tsai, M.H. and Stacey, D.W. (1988) Cell **52**, 63-71

Yu, C.L., Tsai, M.H. and Stacey, D.W. (1990) Mol. Cell. Biol. **10**, 6683-6689

Zhang, K., DeClue, J.E., Vass, W.C., Papageorge, A.G., McCormick, F. and Lowy, D.R. (1990) Nature **346**, 754-756

Zhang, X.F., Settleman, J., Kyriakis, J.M., Takeuchi-Suzuki, E., Elledge, S.J., Marshall, M.S., Bruder, J.T., Rapp, U.R. and Uvruch, J. (1993) Nature **364**, 308-313

Zheng, Y., Glaven, J.A., Wu, W.J. and Cerione, R.A. (1996) J. Biol. Chem. **271**, 23815-23819

Zhong, Z., Wen, Z.L. and Darnell, J.E. (1994) Science **264**, 95-98

Zhu, J., Reynet, C., Caldwell, J.S. and Kahn, C.R. (1995) J. Biol. Chem. **270** (9), 4805-4812

Zhu, J., Bilan, P.J., Moyers, J.S., Antonetti, D.A. and Kahn, C.R. (1996) J. Biol. Chem. **271** (2), 768-773

THE JOURNAL OF BIOLOGICAL CHEMISTRY
Vol. 271, No. 3, Issue of January 19, pp. 1566–1572, 1996
Printed in U.S.A.

Mechanism of Inhibition by Arachidonic Acid of the Catalytic Activity of Ras GTPase-activating Proteins*

(Received for publication, June 6, 1995, and in revised form, August 29, 1995)

Beth A. Sermon, John F. Eccleston, Richard H. Skinner‡, and Peter N. Lowe‡§

From the Division of Physical Biochemistry, National Institute for Medical Research, The Ridgeway, Mill Hill, London NW7 1AA and the ‡Biology Division, Wellcome Research Laboratories, Langley Court, Beckenham, Kent BR3 3BS, United Kingdom

Ras is a guanine nucleotide-binding protein that acts as a molecular switch controlling cell growth. The Ras GTPase-activating proteins (GAPs) p120-GAP and neurofibromin are candidates as Ras effectors. The GTPase-activating activity of both proteins is inhibited by mitogenic lipids, such as arachidonic acid and phosphatidic acid, and differential inhibition of the two GAPs led to the hypothesis that both were effectors in a Ras-controlled mitogenic pathway (Bollag, G., and McCormick, F. (1991) *Nature* 351, 576–579). We have studied the mechanism of inhibition by arachidonic acid in three ways: first, by measurements of catalytic activity under multiple turnover conditions; second, using *p*-((6-phenyl)-1,3,5-hexatrienyl)benzoic acid as a fluorescent probe for ligands binding to GAPs; and third, by using a scintillation proximity assay to measure direct binding of Ras to neurofibromin. We found no significant differential inhibition between p120-GAP and neurofibromin by arachidonic acid. The inhibition by arachidonic acid included a major component that is competitive with Ras·GTP. These data suggest that insomuch as the mitogenic effects of lipids are mediated via inhibition of GAPs, GAPs are not Ras effector proteins. Additionally, lipids can exert a non-competitive type effect, consistent with a protein denaturing activity, making difficult extrapolations from *in vitro* data to the situation within cells, and possibly explaining the variability of literature data on inhibition by lipids.

The *ras* genes encode guanine nucleotide-binding proteins that act as molecular switches for signal transduction pathways controlling cell growth and differentiation (1–5). In the GTP-bound form, Ras is active and interacts with effector proteins to propagate a signal from the outside of the cell to the nucleus or cytoskeleton (6, 7). A region on Ras has been mapped out through mutagenesis and structural studies as the effector binding region (7). Ras has a low intrinsic GTPase activity, which is accelerated by the GTPase-activating proteins (GAPs)[1] p120-GAP and NF1 (6, 8). GAPs can thus act as negative regulators by converting Ras to the inactive GDP form. Activation of Ras to the GTP form occurs by nucleotide exchange, catalyzed by exchange factors (6).

Several candidate effector proteins have been proposed. Thus, very convincing evidence has emerged for the role of the serine-threonine kinase, c-Raf, as an effector controlling the activation pathway for MAP kinase (9–13). Phosphatidylinositol 3-OH-kinase interacts with the effector binding region of Ras and might well be an effector for a Ras signaling pathway controlling phosphoinositide metabolism (14). Ral-GDP dissociation stimulator also binds to the effector binding region of Ras, but is not known to have a biological activity associated with an effector function (15). Both p120-GAP and NF1 have many properties expected from a Ras effector, in that they bind preferentially to Ras·GTP rather than Ras·GDP and interact with Ras at the effector binding region (6–8). Evidence both for and against such a role has been presented. There is much experimental data to support a role of p120-GAP in signaling, other than just to down-regulate Ras, whereas with NF1 most data are consistent purely with a negative regulatory role (8). However, an effector role for both p120-GAP and NF1 was suggested by Bollag and McCormick (16) based on their data on the differential inhibition of p120-GAP and NF1 activity by lipids.

An early response to mitogenic stimulation is a rapid alteration in levels of various lipids such as diacylglycerol, phosphatidic acid, arachidonic acid, and metabolites of phosphatidylinositol (17–21). Phosphatidic acid itself acts as a mitogen in specific cells (22). Microinjection of a neutralizing anti-Ras antibody blocked the mitogenic activity of phosphatidic acid showing that its activity is completely Ras-dependent (22). Among other lipids, phosphatidic acid and arachidonic acid inhibit p120-GAP and NF1 *in vitro* (16, 19, 23–25). This suggested the possibility that the mitogenic effects of these lipids might be mediated by inhibition of p120-GAP, leading to an increase in Ras·GTP, and hence an activation of Ras. Bollag and McCormick (16) reported that phosphatidic acid inhibited NF1 catalytic activity but did not block binding of Ras to NF1. This led to an hypothesis in which NF1 was a Ras effector, modulated by lipid inhibition (16).

Large differences in potency and specificity of inhibition of GAPs by lipids have been observed by the various researchers in this field. For example, Bollag and McCormick (16) reported that arachidonic acid inhibits p120-GAP with an I_{50} of ~200 μM, and the catalytic domain of NF1 (NF1-GRD) with an I_{50} of ~30 μM, whereas Golubic *et al.* (23) reported that the catalytic domains of NF1 and of p120-GAP were both inhibited by arachidonic acid with I_{50} values between 8 and 16 μM. With

* The costs of publication of this article were defrayed in part by the payment of page charges. This article must therefore be hereby marked "*advertisement*" in accordance with 18 U.S.C. Section 1734 solely to indicate this fact.

§ To whom correspondence should be addressed. Tel.: 44-181-639-6370; Fax: 44-181-639-6877.

[1] The abbreviations used are: GAP, GTPase-activating protein; CMC, critical micellar concentration; mantGTP, 2′(3′)-*O*-*N*-methylanthraniloyl-GTP; mantGDP, 2′(3′)-*O*-*N*-methylanthraniloyl-GDP; phosphatidic acid, β-stearoyl-γ-arachidonyl-L-α-phosphatidic acid; NF1, neurofibromin; NF1–334 and GAP-344, the catalytic domains of NF1 and p120-GAP, respectively; DPH-carboxylic acid, *p*-((6-phenyl)-1,3,5-hexatrienyl)benzoic acid; DPH, 1,6-diphenyl-1,3,5-hexatriene; GST, glutathione *S*-transferase; HPLC, high performance liquid chromatography; Ras, protein product of the Harvey-*ras* gene (in all experiments, this refers to Ras truncated at residue 166, except where otherwise specified).

phosphatidic acid, Bollag and McCormick (16) found no inhibition of p120-GAP, but an I_{50} of ~10 μM with NF1-GRD. In contrast, Golubic *et al.* (23) found little or no inhibition by phosphatidic acid of the catalytic domains of either NF1 or p120-GAP. This diversity appears to be a reflection of different experimental procedures, conditions, and components utilized. Thus, there are reports showing that the inhibitory potency differs dependent upon whether full-length or catalytic domains are expressed (23, 24, 26). The assay conditions and the procedure by which the lipids are solubilized also appear to be important factors. Lipids have been introduced either as pure micelles or as mixed micelles with apparently differing results (19, 24). Furthermore, some assays have been performed in the presence of detergents (16, 24), whereas others have not (16, 23). In this study, we decided to keep the experimental system as simple as possible by performing experiments with arachidonic acid in the absence of detergents.

We report here an investigation into the mechanism of arachidonic acid inhibition of both p120-GAP and NF1 to see if it was different from that reported for phosphatidic acid. We show that there is a strong competitive element in the mechanism of arachidonic acid inhibition, such that arachidonic acid can block binding of NF1 to Ras. This has important implications for any hypothesis in which arachidonic acid, through interaction with GAPs, acts as a modulator of Ras signaling.

EXPERIMENTAL PROCEDURES

Proteins

NF1–334 was purified as described by Eccleston *et al.* (27) and GST-NF1–334 and [Leu^{61}]Harvey-Ras (residues 1–166) as described by Skinner *et al.* (28). Normal Harvey-Ras (residues 1–166) was expressed in *Escherichia coli* and purified by procedures similar to those in Ref. 28. GAP-344 was purified as described by Skinner *et al.* (29).

Arachidonic Acid

Arachidonic acid (Sigma) was dissolved in ethanol (Spectrosol grade, BDH) to form a stock solution at 40 mM. Appropriate dilutions were made in ethanol, and aliquots of these added to the experiments such that the final concentration of ethanol was not more than 2%, and in general was chosen to be 1%.

Nucleotide Complexes

Ras·GTP or Ras·[^{3}H]GTP complexes were prepared by nucleotide exchange in the presence of a GTP regenerating system (28). Ras·mantGTP complexes were prepared as described by Eccleston *et al.* (27).

CMC Determination

CMC was determined by two independent procedures, one based on light scattering and the other based on fluorescence changes of the probe DPH. In both cases the experiments were performed in 20 mM Tris/HCl, pH 7.5, 1 mM $MgCl_2$, 0.1 mM dithiothreitol. In the former procedure, fatty acids were dissolved in ethanol and titrated into buffer such that a maximum of 2% ethanol was present. Light scattering was monitored in a fluorimeter at 500 nm. The CMC was taken to be the concentration of lipid at which a sharp discontinuity occurred in the light scattering *versus* concentration graph. Alternatively, CMC was determined by titrating the lipid into a solution of DPH and was taken to be the concentration of lipid at which a discontinuity occurred in the graph of fluorescence intensity *versus* concentration of lipid added (24).

Steady-state Fluorescence

Measurements were performed on a Perkin-Elmer LS-50B spectrofluorimeter thermostatted at 30 °C. Experiments were performed in 20 mM Tris/HCl, pH 7.5, 1 mM $MgCl_2$, 0.1 mM dithiothreitol.

Scintillation Proximity Assay

This was performed basically as described by Skinner *et al.* (28), except that the buffer was 20 mM Tris/HCl, pH 7.5. The assay was performed by first adding 80 μl of a solution of 0.2 μM NF1-GST in 20 mM-Tris/HCl, pH 7.5, 2 mM dithiothreitol to each well, followed by 120 μl of a mixture of 0.07 μM Ras·[^{3}H]GTP, 0.031 mg/ml of anti-glutathione *S*-transferase antibody and 4.2 mg/ml of Protein A polyvinyltoluene scintillation proximity assay beads (Amersham) suspended in 20 mM Tris/HCl, pH 7.5, 2 mM dithiothreitol, 2 mM $MgCl_2$. Lipids were either added to 80 μl of the solution of NF1-GST, followed by addition of 120 μl of a mixture containing scintillation proximity assay beads, anti-GST, and radiolabeled Ras, or were added directly to the complete mixture of 200 μl of these two components.

HPLC Analysis

[^{3}H]GTP and [^{3}H]GDP were quantified by HPLC separation using ion-pair chromatography on a Lichrosorb RP18 (5-μm particle size; 250 × 4 mm) eluting isocratically at 1 ml·min^{-1} with 12% acetonitrile, 88% tetrabutylammonium hydroxide (2.25 mM) dissolved in 56 mM potassium phosphate buffer, pH 5.9, essentially as described by Pingoud *et al.* (30). Radionucleotides were detected and quantified by in-line mixing with scintillant, using a Berthold radiochemical detector.

Catalytic Activity Measurements

Ras·GTP Hydrolysis—The rates of GAP-344- or NF1–334-stimulated Ras·GTPase were measured by incubating a stoichiometric normal Ras·[^{3}H]GTP complex with the appropriate GAP, in the presence and absence of lipid. Incubations were performed in 20 mM Tris/HCl, pH 7.5, 1 mM $MgCl_2$, 0.1 mM dithiothreitol at 25 °C for 10 min. The concentration of Ras was about 7 μM. Final concentrations of GAP-344 and NF1–334 were 0.040 μM and 0.014 μM, respectively. The concentrations of GAPs were chosen so that in the absence of inhibitor the maximum extent of Ras·GTP hydrolysis was 80% and generally was less and so gave a reasonable estimate of the true initial rate. The extent of hydrolysis in the absence of GAP-344 or NF1–334 was negligible as compared to that in its presence. At the end of the incubation, samples were transferred to ice and immediately quenched by addition of an equal volume of HPLC running buffer. The samples were stored at −70 °C prior to HPLC analysis to determine the extent of conversion of Ras·[^{3}H]GTP to Ras·[^{3}H]GDP. Fatty acids were added from ethanolic stocks such that the final concentration of ethanol was less than 2%. Control experiments showed that 2% ethanol had no effect on the GTP hydrolysis reaction.

Ras·mantGTP Hydrolysis—Hydrolysis was measured under multiple turnover conditions in which catalytic amounts of NF1–334 (≤10% the molar concentration of Ras) were mixed with Ras·mantGTP. Experiments were performed either on the home-built stopped flow fluorimeter (27) or on a Hi-Tech SF-61 instrument with the excitation monochromator set at 365 nm and emission monitored through a Wratten 47B filter. In these experiments, stock solutions of Ras·mantGTP were diluted in buffer to which arachidonic acid was also added when required. This Ras solution was mixed in the instrument with an equal volume of a solution of NF1–334 in buffer, again containing arachidonic acid if required. All concentrations subsequently quoted are after mixing.

The initial rate of fluorescence change was measured directly from the photomultiplier output *versus* time plot in units of volts·s^{-1}. To compensate for changes made in the applied photomultiplier voltage to allow measurements over a wide range of concentration of Ras·mantGTP, it was necessary to establish the relationship between volts and molar concentration of Ras·mantGTP. This was done in parallel experiments in which the Ras·mantGTP solution of known concentration was mixed in the stopped flow fluorimeter with a solution consisting of 500 μM GDP, 40 mM EDTA, and 400 mM ammonium sulfate. This caused complete displacement of bound mantGTP from the Ras within 20 s (*cf.* Fig. 2, *trace c*), and the amplitude of the resultant fluorescence decrease was measured. This allowed the relationship between total Ras·mantGTP and photomultiplier output to be established. The conversion of Ras·mantGTP to Ras·mantGDP results in about a 10% decrease in fluorescence (31). Although this was not precisely determined in our experiments, we used a figure of 10% to allow us to to calculate rates in units of molar concentration.

RESULTS

Inhibition of GAP- and NF1-activated Ras·GTPase by Arachidonic Acid—Arachidonic acid was added to standard GAP activity assays from an ethanolic stock. Under these conditions, arachidonic acid inhibited GAP-344 and NF1–334 activities with I_{50} values of 10 and 5 μM, respectively (Fig. 1). The inhibitory potency was much higher than that reported by Bollag and McCormick (16). We noted one experimental difference, which was that these workers did not use pure lipid but

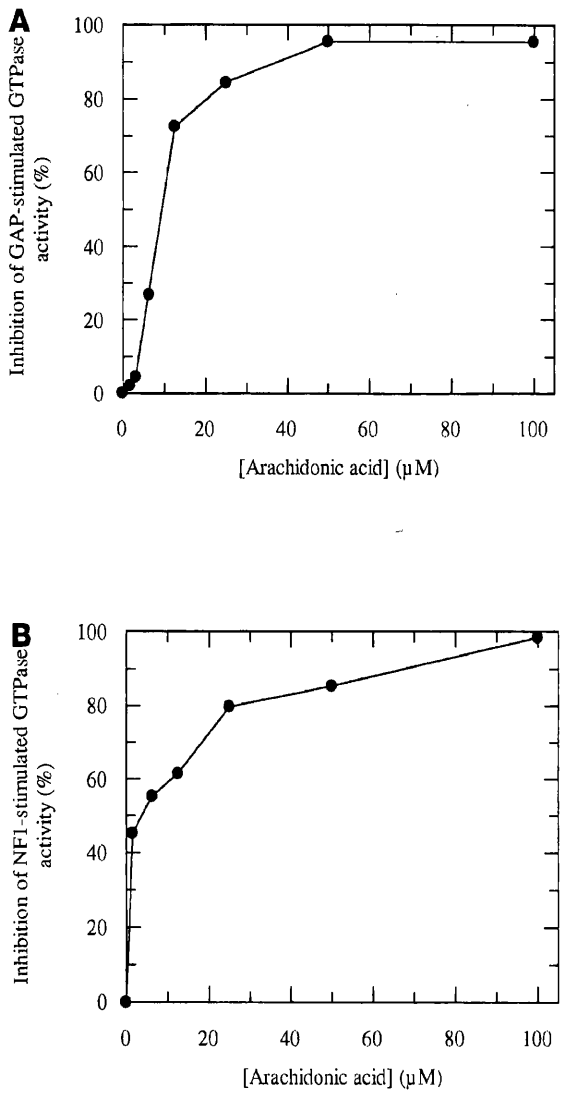

FIG. 1. **Inhibition of the GAP-344- and NF1–334-stimulated Ras GTPase by arachidonic acid.** A solution containing 7 μM Ras·[^{3}H]GTP was incubated with either 0.040 μM GAP-344 (*panel A*) or 0.014 μM NF1–334 (*panel B*) in 20 mM Tris/HCl, pH 7.5, 1 mM $MgCl_2$, 0.1 mM dithiothreitol at 25 °C. Arachidonic acid (●) was added to the mixture from a stock solution in ethanol. After 10 min, the extent of [^{3}H]GTP hydrolysis was measured by HPLC separation of [^{3}H]GTP from [^{3}H]GDP. Inhibition of GTPase activity was calculated as a percentage relative to incubations without arachidonic acid.

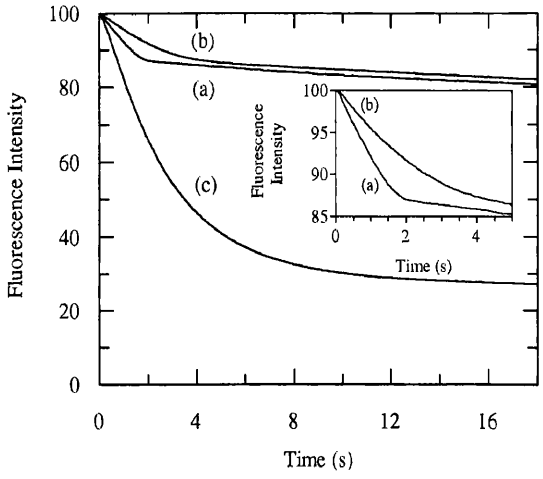

FIG. 2. **Effect of arachidonic acid on the rate of NF1–334 catalyzed Ras·mantGTP hydrolysis, under multiple turnover conditions.** Stopped-flow fluorescence experiments were performed in which 1 μM Ras·mantGTP was mixed with 0.1 μM NF1–334 at 30 °C. Both proteins were in 20 mM Tris/HCl, pH 7.5, 1 mM $MgCl_2$, 0.1 mM dithiothreitol. Fluorescence recordings are shown for experiments in the absence of arachidonic acid (*trace a*) and with 20 μM arachidonic acid added to both the NF1–334 and Ras·mantGTP solutions (*trace b*). To convert fluorescence changes into molar concentrations, in separate experiments 1 μM Ras·mantGTP was mixed with500 μM GDP dissolved in 20 mM Tris/HCl, pH 7.5, 1 mM $MgCl_2$, 0.1 mM dithiothreitol, containing additionally 40 mM EDTA and 400 mM ammonium sulfate to promote rapid nucleotide exchange (*trace c*) (see "Experimental Procedures"). The *inset* shows the initial phases of *traces a* and *b* on a larger scale.

included the detergent Nonidet P40 in all assays so that presumably mixed micelles were formed. We assayed the inhibitory potency of arachidonic acid on p120-GAP in the presence of 0.1% Nonidet P40, and found only 18% inhibition at 30 μM, whereas in the absence of Nonidet nearly complete inhibition was obtained at that concentration. This suggested that partitioning of arachidonic acid into detergent micelles reduced its inhibitory potency and so all subsequent experiments were performed with lipids in the absence of detergent.

With GAP-344, the relationship between inhibitor concentration and inhibition achieved was not strictly hyperbolic, but rather was sigmoid, but with NF1–334 the data were more variable. More pronounced sigmoid curves had been observed with GAP by Serth *et al.* (24). In those experiments the steep phase occurred at ~40–50 μM, which was the same as their experimentally determined CMC value. We also found that CMC, as determined either by light scattering of arachidonic acid itself or by the use of DPH fluorescence enhancement, was around 40 μM. However, this concentration was clearly much higher than the I_{50} values seen under our experimental conditions, showing that micelle formation is not required for inhibition.

Steady-state Kinetic Analysis of the Inhibition of NF1-activated Ras·mantGTPase by Arachidonic Acid—The mechanism of inhibition was investigated further by analyzing the kinetics under multiple turnover conditions. A continuous record of the hydrolysis process was obtained by replacing GTP by its close analogue mantGTP, as Ras·mantGTP hydrolysis is accompanied by a 10% decrease in fluorescence (31). Experiments were performed under multiple turnover (steady-state) conditions, *i.e.* with the concentration of NF1–334 well below the concentrations of Ras·mantGTP (Fig. 2).

Using 1 μM Ras·mantGTP and 0.1 μM NF1–334, the initial rate of Ras·mantGTP hydrolysis was calculated from Fig. 2*a* to be 1.1 μM·s^{-1}. This corresponds to a turnover rate of 11 s^{-1}, similar to that seen under single turnover conditions (Ref. 27 and data not shown) and consistent with the Ras·mantGTP concentration being well above K_m and the NF1–334 being fully active. Inclusion of 20 μM arachidonic acid reduced the initial rate of Ras·mantGTP hydrolysis by 45% (Fig. 2, *trace b*). The shape of the reaction progress curves in the absence of arachidonic acid (*trace a*) was typical for the substrate concentration being higher than K_m (linear phase followed by a sharp decrease in rate), whereas with arachidonic acid the progress curve (*trace b*) fitted a single exponential, consistent with arachidonic acid increasing the value of the K_m.

The inhibitory potency of arachidonic acid was influenced by ionic strength. With increasing concentrations of NaCl up to 300 mM NaCl, an increase in inhibition by arachidonic acid was seen, but further increases in NaCl concentration resulted in a decrease in the level of inhibition (data not shown). Thus, 20 μM arachidonic acid inhibited by 45% with no added NaCl, 80% with 300 mM added NaCl and 41% with 1000 mM NaCl. At 150 mM NaCl, arachidonic acid inhibited NF1-stimulated Ras·mantGTPase with I_{50} ~20 μM. The biphasic effect on inhibition with increasing ionic strength is likely to be caused by an

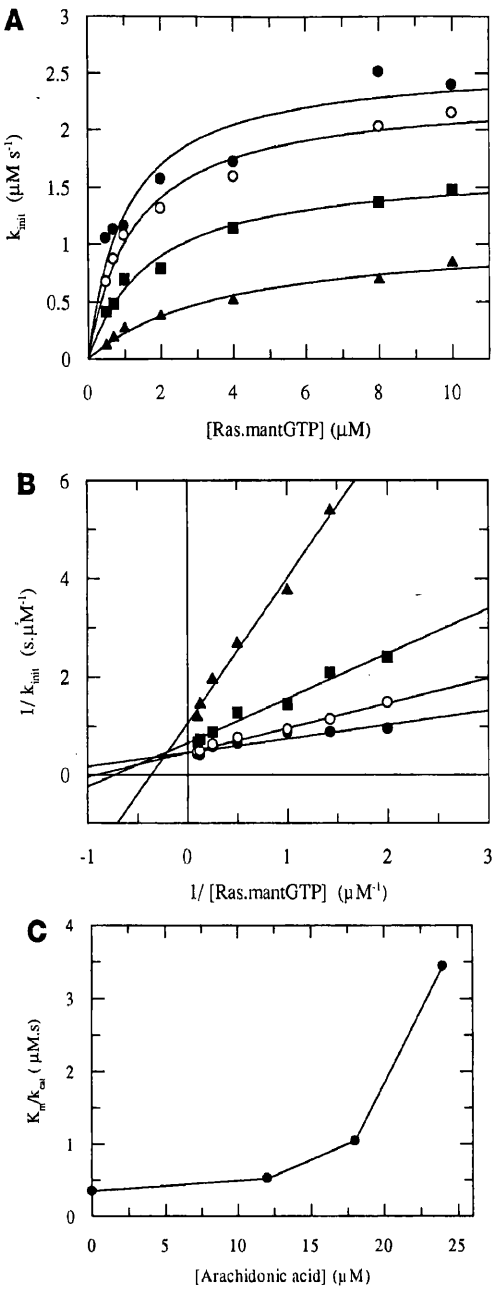

FIG. 3. **Steady-state kinetic analysis of the inhibition of NF1–334-catalyzed Ras·mantGTPase by arachidonic acid.** Initial rates (k_{init}) of NF1–334 catalyzed Ras·mantGTP hydrolysis were measured in experiments similar to those shown in Fig. 3. Experiments were performed with 0 μM (●), 12 μM (○), 18 μM (■), or 24 μM (▲) arachidonic acid. The data at each concentration of arachidonic acid were fitted by non-linear regression to the Michaelis-Menten equation to obtain values of K_m and k_{cat}. In *A* and *B*, the *solid lines* are based on these constants. K_m at 0, 12, 18, and 24 μM arachidonic acid were 1.1, 1.3, 1.8, and 3.8 μM, respectively. k_{cat} at 0, 12, 18, and 24 μM arachidonic acid were 2.6, 2.3, 1.7, and 1.1 $\mu M \cdot s^{-1}$, respectively. In *C*, the ratio of K_m to k_{cat} obtained from this curve-fitting has been plotted against the concentration of arachidonic acid used.

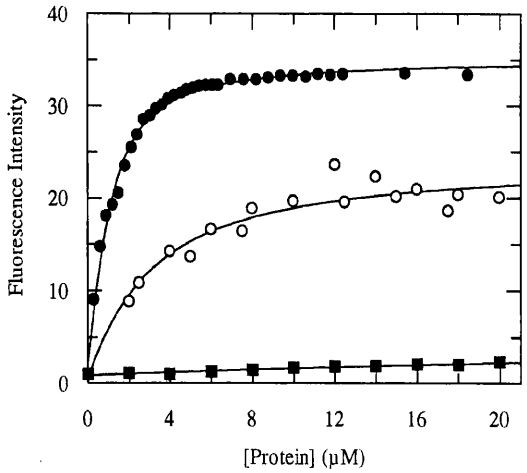

FIG. 4. **Effect of GAP-344, NF1–334 or bovine serum albumin on the fluorescence of DPH-carboxylic acid.** GAP-344 (■), NF1–334 (○), or bovine serum albumin (●) was titrated into a solution of 1 μM DPH-carboxylic acid dissolved in 20 mM Tris/HCl, pH 7.5, such that the concentration of DPH-carboxylic acid was not reduced significantly. Fluorescence was recorded with excitation at 357 nm and with emission at 435 nm. Data have been normalized on the initial level of fluorescence so that the fluorescence increases on addition of proteins are directly comparable. The *solid lines* show the best fit to binding isotherms for simple association of two molecules, with K_d = 2.6, 0.55, and 62 μM, with NF1–334, albumin, and GAP-344, respectively. Data at concentrations of GAP-344 up to 120 μM were obtained but are not shown on this scale for clarity.

increase in the K_m for Ras·mantGTP (27), resulting in more potent inhibition countered by a reduction in the affinity for arachidonic acid.

To measure values of K_m and k_{cat}, initial rates of hydrolysis were measured varying both the concentrations of Ras·mantGTP and of arachidonic acid. The experiment was performed in the presence of 50 mM NaCl such that the K_m was around 1 μM. The data obtained are shown in Fig. 3. The pattern of inhibition displayed in the Lineweaver-Burk double-reciprocal plot (Fig. 3*B*) is typical of mixed inhibition, in which the inhibitor both decreases k_{cat} and increases K_m. If the data are interpreted as fitting a mixed inhibition model (32), then it can be calculated from the intersection point of the lines that K_m (or K_S if the components are in rapid equilibrium) was around 1 μM and αK_m is ~5, where α represents the ratio of K_{iu} to K_{ic} (Scheme 1).

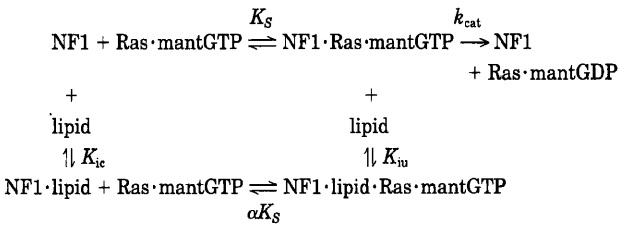

SCHEME I.

This value of α suggests that the mixed inhibition is predominantly of a competitive character, but the uncompetitive component is still significant. However, the data clearly do not fit this simple model in that the relationship between inhibition and the concentration of arachidonic acid at any fixed concentration of Ras is distinctly sigmoid and plots of either K_m/k_{cat} (Fig. 3*C*) or $1/k_{cat}$ (not shown) against arachidonic acid concentration are non-linear, parabolic upward.

Characterization of the Interaction of Arachidonic Acid with NF1 and GAP Using the Fluorescent Probe DPH-carboxylic Acid—As the kinetic mechanism of inhibition of GAP activity by arachidonic acid is complex, we examined other methods to show whether arachidonic acid binds at the Ras-binding site, or at some other site, on GAPs. We postulated that *p*-((6-phenyl)-1,3,5-hexatrienyl)benzoic acid (DPH-carboxylic acid) might be a sufficiently close analogue of arachidonic acid that it would act as a fluorescent probe of the lipid-binding site. An increase in fluorescence of DPH-carboxylic acid (1 μM) occurred when it was mixed with NF1–334, GAP-344 or bovine serum albumin (Fig. 4). At 10 μM protein, the increase was 18-, 1.6-, and 32-fold, respectively. Arachidonic acid (10 μM) abolished the enhancement of fluorescence of DPH-carboxylic acid caused by

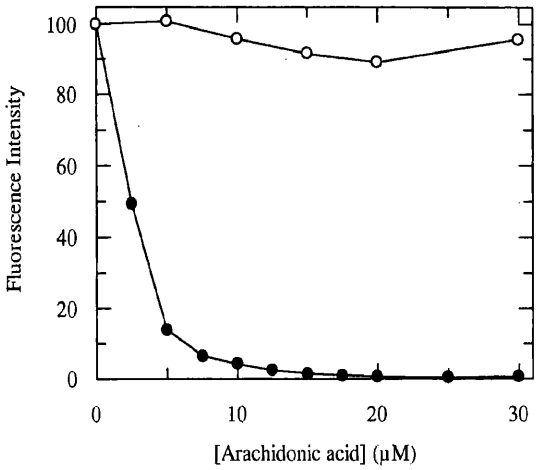

FIG. 5. **Effect of arachidonic acid on the fluorescence of a mixture of DPH-carboxylic acid with NF1–334 or serum albumin.** Arachidonic acid, from a stock solution in ethanol, was added to a solution of 1 μM DPH-carboxylic acid in 20 mM Tris/HCl, pH 7.5, containing either 0.5 μM bovine serum albumin (●) or 2 μM NF1–334 (○). The final concentration of ethanol was <1%. Fluorescence was recorded with excitation at 357 nm and emission at 435 nm. Data were corrected for light scattering caused by proteins and arachidonic acid, and for the fluorescence of 1 μM DPH-carboxylic acid in the absence of added protein. The maximum correction was 3.7% and 11.6% of the maximum fluorescence with albumin and NF1–334, respectively. The corrected fluorescence in the absence of arachidonic acid was taken to be 100. With albumin this represented 2.9-fold more fluorescence than with NF1–334.

mixture with albumin, as expected if arachidonic acid competed with DPH-carboxylic acid for binding to albumin (Fig. 5). However, at concentrations of arachidonic acid up to 40 μM, there was no significant reduction in the fluorescence of DPH-carboxylic acid mixed with either NF1 (Fig. 5) or GAP. Indeed with GAP, an increase was seen. This suggested that with the latter two proteins the probe was binding at a site distinct from the arachidonic acid-binding site. However, we were still able to use DPH-carboxylic acid as a probe for ligands interacting with GAPs since the fluorescence of the protein-bound probe was sensitive to addition of ligands.

The fluorescence of a solution containing 1 μM DPH-carboxylic acid and 2 μM NF1–334 was dramatically reduced by addition of [Leu^{61}]Harvey-Ras·GTP protein (Fig. 6). The reduction in fluorescence was nearly proportional to the concentration of added Ras, with half-maximal effect occurring at about 1 μM Ras·GTP. This is consistent with a relatively high affinity of interaction of Ras with NF1–334, as expected for the binding of NF1–334 to the [Leu^{61}]Ras mutant. Since several species were present in this experiment, it was necessary to determine whether Ras·GTP was binding to NF1–334 or to the probe. Therefore, Ras·GTP was titrated into a mixture of 2 μM DPH-carboxylic acid and 1 μM NF1–334. In this experiment, the curve was shifted to the left with half-maximal reduction occurring at 0.5 μM Ras·GTP. These data are consistent with Ras binding to NF1–334 rather than to DPH-carboxylic acid. As a further control, normal Ras·GDP was titrated into the mixture of DPH-carboxylic acid and NF1–334, but only 20% reduction of fluorescence occurred at 4 μM Ras, consistent with the known weaker affinity of NF1 for Ras·GDP as compared with Ras·GTP.

These data suggested that the probe was able to monitor the interaction between Ras and NF1. Therefore, the effect of arachidonic acid on the fluorescence changes induced by Ras was examined (Fig. 6). The decrease in fluorescence caused by addition of Ras to the mixture of DPH-carboxylic acid and NF1–334 was largely abolished by 20 μM arachidonic acid,

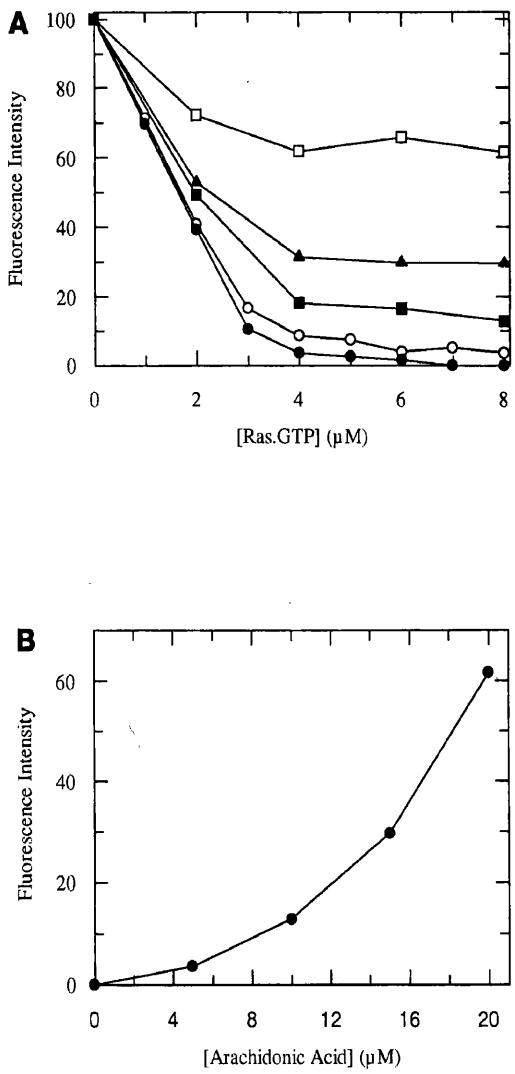

FIG. 6. **Effects of Ras·GTP and of arachidonic acid on the fluorescence of a mixture of DPH-carboxylic acid and NF1–334.** [Leu^{61}]Ras·GTP was added to a solution of 1 μM DPH-carboxylic acid in 20 mM Tris/HCl, pH 7.5, and 2 μM NF1–334 containing 0 μM (●), 5 μM (○), 10 μM (■), 15 μM (▲), or 20 μM (□) arachidonic acid. Fluorescence was recorded with excitation at 357 nm and emission at 435 nm. Data were corrected for light scattering caused by proteins and arachidonic acid, and for the fluorescence of 1 μM DPH-carboxylic acid in the absence of added protein. The maximum correction was 12.8% of the maximum fluorescence. The corrected fluorescence in the absence of Ras·GTP was taken to be 100. In *B*, the effect of arachidonic acid on the observed fluorescence in the presence of 8 μM Ras·GTP is shown.

strongly suggesting competition between Ras and the lipid for binding to NF1. However, the dependence on concentration of arachidonic acid was not hyperbolic (Fig. 6*B*).

NF1/Ras Binding Scintillation Proximity Assay—The data from the kinetic characterization and use of the fluorescent probe suggested that arachidonic acid might, at least in part, be competing with Ras for binding to NF1 or GAP. We therefore tested whether arachidonic acid might block binding of Ras to NF1 by a more direct method. The recently described scintillation proximity assay procedure (28) was used to monitor the binding of Ras·GTP to NF1–334 and to test the effects of arachidonic acid on this interaction. In this assay, GST-NF1–334 fusion protein bound via an anti-GST antibody to protein A coated fluoromicrosphere beads interacts with a Ras·[^{3}H]GTP complex. When the Ras is in close proximity to the beads, *i.e.* when bound to NF1–334, scintillation occurs, whereas Ras in free solution does not cause any light emission. A key feature of the system is that it allows direct measurements of binding at

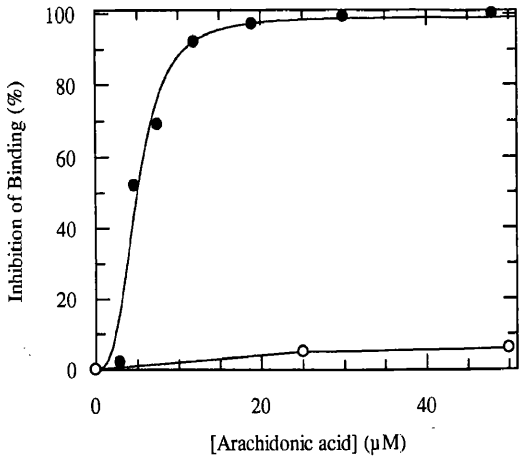

FIG. 7. **Inhibition of binding of GST-NF1–334 to Ras·GTP by arachidonic acid as monitored by scintillation proximity assay.** Arachidonic acid was added at the indicated concentrations to scintillation proximity assays containing protein A scintillation beads, anti-GST and either 0.04 μM [Leu^{61}]Ras·[^{3}H]GTP and 0.09 μM GST-NF1–334 (●) or 0.04 μM GST-[Leu^{61}]Ras·[^{3}H]GTP (○).

equilibrium.

Arachidonic acid completely abolished the signal produced in this assay, with 50% inhibition occurring at 5–10 μM arachidonic acid (Fig. 7). As a control that the reduction in signal truly represented disruption of binding between Ras and NF1, arachidonic acid was added to a mixture of scintillation proximity assay beads, anti-GST and a GST-Ras·[^{3}H]GTP complex (Fig. 7). In this case, at concentrations of arachidonic acid up to 50 μM, negligible inhibition was observed. This control demonstrated that arachidonic acid was not affecting binding of nucleotide to Ras, or binding between Protein A and antibody or between antibody and GST. In most experiments there was a non-hyperbolic dependence of inhibition on concentration of arachidonic acid, with a distinct lag at low inhibitor concentrations.

DISCUSSION

There are conflicting literature reports on the potency of arachidonic acid and phosphatidic acid, on their ability to differentially inhibit NF1 and p120-GAP activation of Ras·GTPase, and the mechanism by which this is achieved. We therefore investigated the effect of arachidonic acid on the interaction of Ras and GAPs using three different techniques in the simplest system possible.

Kinetic methods showed that in the absence of detergent, arachidonic acid inhibited the NF1- and p120-GAP activated activity of Ras·GTPase to similar extents with I_{50} values of ~5–15 μM (Fig. 1). These potencies are similar to those observed by Golubic *et al.* (23). In the presence of Nonidet detergent, the inhibitory potency of arachidonic acid on GAP activity was markedly reduced to levels reported by Bollag and McCormick (16) when they also used this detergent. We therefore performed all subsequent experiments in the absence of detergent. Under these conditions, we found phosphatidic acid to be only a weak reversible inhibitor of either GAP-334 or NF1–334 catalytic activity (data not shown), as Golubic *et al.* (23) had concluded, and in contrast to the more potent inhibition seen by other groups. These data suggested to us that some of the reported differential inhibition effects of NF1 and p120-GAP by lipids might be artifactual.

The mechanism of the inhibition of the NF1-activated Ras·GTPase was investigated in more detail by using the fluorescent analogue of GTP, mantGTP. The fluorescence decrease that occurs between Ras·mantGTP and Ras·mantGDP allowed the hydrolysis to be monitored continuously (Fig. 2). This has many advantages over the use of radiolabeled GTP, which requires analysis of many single time points. By varying the concentrations of both Ras·mantGTP and arachidonic acid, the effect of arachidonic acid on K_m and k_{cat} was established (Fig. 3). The inhibition was of a mixed character but predominantly competitive.

The second method to study the effect of arachidonic acid was to use the fluorescent probe DPH-carboxylic acid in equilibrium measurements of the interaction of Ras·GTP with NF1. Although DPH-carboxylic acid did not compete for the proposed arachidonic acid-binding site on NF1 (Fig. 5), as had been hoped, it still provided a probe on the interaction of NF1 with Ras·GTP, since the fluorescence of bound DPH-carboxylic acid was reduced on the binding of Ras·GTP (Fig. 6). Arachidonic acid largely abolished this effect (Fig. 6), strongly suggesting competition between the Ras and lipid for binding to NF1.

The third method to study the effect of arachidonic acid was to use a scintillation proximity assay (Fig. 7). Arachidonic acid completely abolished the interaction between [Leu^{61}]Ras·GTP and NF1, with 50% inhibition occurring at 5–10 μM.

All of the data above support the argument that arachidonic acid competitively inhibits the interaction of Ras·GTP with NF1. Furthermore, the inhibitory effects occur well below the CMC for arachidonic acid under the conditions used, showing that the effect is not caused by micelle formation, as had been suggested by Serth *et al.* (24).

Despite this evidence for competitive inhibition, our results suggest that arachidonic acid can exert other effects on the interaction. For example, the inhibition of the GAP-activated Ras·GTPase (Figs. 1 and 3) show a sigmoid or non-hyperbolic dose-response curve. In addition, the effect of arachidonic acid on the binding of Ras·GTP to NF1 as monitored by DPH-carboxylic acid (Fig. 6) or by the scintillation proximity assay (Fig. 7) is not hyperbolic. We do not know the explanation for this phenomenon, but similar behavior has been seen previously with arachidonic acid (23, 24).It is possible that self-association of arachidonic acid to structures smaller than full micelles is required for maximal inhibitory effects.

A further deviation from a simple competitive pattern was seen from the kinetic analysis (Fig. 3), which showed that arachidonic acid not only raised K_m but also reduced k_{cat}. The effect on k_{cat} is consistent with an irreversible inhibitory component for which we have some additional evidence (data not shown). In the scintillation proximity assay, we noted that when certain lipids (arachidic acid and phosphatidic acid, but not noticeably arachidonic acid) were added to NF1 before addition of Ras they were more potent inhibitors than when added after Ras, suggesting that the inhibitory mechanism was not always rapidly reversible on the time-scale of these experiments. Also, arachidonic acid caused slow time-dependent effects on the fluorescence of DPH-COOH bound to GAP, consistent with denaturation, which were significantly prevented by the inclusion of Ras.

Although these non-competitive effects occur, the predominantly competitive nature of the interaction makes us conclude that arachidonic acid does not act in the way that phosphatidic acid was reported to do by Bollag and McCormick (16). They reported two mains lines of evidence that phosphatidic acid does not block binding of Ras to NF1 (16). First, the inhibitor displayed non-competitive kinetics, in which the inhibitor reduced V_{max} without affecting K_m, typical of depletion of both substrate-bound and free enzyme forms by inhibitor. However, such an inhibitory pattern is also seen with an irreversible or slowly reversible type of action. Second, phosphatidic acid did not block binding of Ras·GTP to NF1 immobilized on beads (16).

No detailed quantitation (*e.g.* yield of bound proteins) or controls were given for this assay other than that SDS blocked binding. Experiments from our own laboratory (27, 28) showed that the rate of dissociation of NF1 from Ras is fast, such that no significant binding of Ras to NF1 should have been observed under the experimental conditions of Bollag and McCormick (16). Thus, the binding observed might not have been true reversible binding of NF1 to Ras. We found that dodecylmaltoside blocks binding of Ras to NF1 (28), again supporting the hypothesis that a primary mode of inhibition of amphipathic molecules such as lipids and detergents might be by preventing Ras binding to GAPs.

On the basis that certain lipids differentially inhibited p120-GAP and NF1 and on the assumption that one could extrapolate from data with phosphatidic acid that lipids in general do not block binding of Ras to GAPs, Bollag and McCormick (16) suggested a hypothesis with these key features. (*a*) p120-GAP and NF1 are differentially regulated by lipids. (*b*) Lipids activate Ras signaling by inhibiting NF1 GTPase stimulating activity. (*c*) Lipid-inhibited NF1 binds to Ras·GTP propagating a signal through NF1. (*d*) NF1 and p120-GAP are alternative effectors for Ras. (*e*) The mitogenic activity of certain lipids is through their modification of GAP activity in the cell. However, the data presented in this paper are not in accordance with this hypothesis, as (*a*) no significant differential inhibition of activity was observed, and (*b*) lipid-inhibited GAPs do not bind to Ras. We would suggest two alternative hypotheses consistent with our data. If GAPs are indeed Ras effectors for a mitogenic pathway, the mitogenic activity of arachidonic acid cannot be accounted for through inhibition of GAP catalytic activities, since arachidonic acid also blocks binding between Ras and these putative effectors. Alternatively, the mitogenic activity of arachidonic acid may be accounted for by inhibition of GAP catalytic activity, but in this case GAPs are unlikely to be effectors for a mitogenic pathway.

Acknowledgments—We acknowledge the help of Geoff Brownbridge and Martin Webb in obtaining initial data using fluorescence anisotropy suggesting that arachidonic acid blocks Ras/GAP binding. We thank James Rowedder and Al Brown for obtaining some preliminary data on inhibition of GAP activity.

REFERENCES

1. Lowy, D. R., and Willumsen, B. M. (1993) *Annu. Rev. Biochem.* **62,** 851–891
2. Bourne, H. R., Sanders, D. A., and McCormick, F. (1991) *Nature* **349,** 117–127
3. Bourne, H. R., Sanders, D. A., and McCormick, F. (1990) *Nature* **348,** 125–132
4. Satoh, T., Nakafuku, M., and Kaziro, Y. (1992) *J. Biol. Chem.* **267,** 24149–24152
5. Barbacid, M. (1987) *Annu. Rev. Biochem.* **56,** 779–827
6. Boguski, M. S., and McCormick, F. (1993) *Nature* **366,** 643–654
7. Marshall, M. S. (1994) *Trends Biochem. Sci.* **18,** 250–254
8. Lowe, P. N., and Skinner, R. H. (1994) *Cell. Signalling* **6,** 109–123
9. Moodie, S. A., Willumsen, B. M., Weber, M. J., and Wolfman, A. (1993) *Science* **260,** 1658–1661
10. Zhang, X. F., Settleman, J., Kyriakis, J. M., Takeuchi-Suzuki, E., Elledge, S. J., Marshall, M. S., Bruder, J. T., Rapp, U. R., and Uvruch, J. (1993) *Nature* **364,** 308–313
11. Warne, P. H., Rodriguez-Viciana, P., and Downward, J. (1993) *Nature* **364,** 352–355
12. Koide, H., Satoh, T., Nakafuku, M., and Kaziro, Y. (1993) *Proc. Natl. Acad. Sci. U. S. A.* **90,** 8683–8686
13. VanAelst, L., Barr, M., Marcus, S., Polverino, A., and Wigler, M. (1993) *Proc. Natl. Acad. Sci. U. S. A.* **90,** 6213–6217
14. Amrein, K. E., Panholzer, B., Molnos, J., Flint, N. A., Scheffler, J., Lahm, H. W., Bannwarth, W., and Burn, P. (1994) *Biochim. Biophys. Acta* **1222,** 441–446
15. Kikuchi, A., Demo, S. D., Ye, Z. H., Chen, Y. W., and Williams, L. T. (1994) *Mol. Cell. Biol.* **14,** 7483–7491
16. Bollag, G., and McCormick, F. (1991) *Nature* **351,** 576–579
17. Rozengurt, E. (1991) *Cancer Cells* **3,** 397–398
18. Yu, C. L., Tsai, M. H., and Stacey, D. W. (1990) *Mol. Cell. Biol.* **10,** 6683–6689
19. Tsai, M. H., Yu, C. L., Wei, F. S., and Stacey, D. W. (1989) *Science* **243,** 522–526
20. Sumida, C, Graber, R, and Nunez, E (1993) *Prostaglandins Leukotrienes Essent. Fatty Acids* **48,** 117–122
21. Ferguson, J. E and Hanley, M. R (1991) *Curr. Opin. Cell Biol.* **3,** 206–212
22. Yu, C. L., Tsai, M. H., and Stacey, D. W. (1988) *Cell* **52,** 63–71
23. Golubic, M., Tanaka, K., Dobrowolski, S., Wood, D., Tsai, M. H., Marshall, M., Tamanoi, F., and Stacey, D. W. (1991) *EMBO J.* **10,** 2897–2903
24. Serth, J., Lautwein, A., Frech, M., Wittinghofer, A., and Pingoud, A. (1991) *EMBO J.* **10,** 1325–1330
25. Tsai, M. H., Hall, A., and Stacey, D. W. (1989) *Mol. Cell. Biol.* **9,** 5260–5264
26. Bollag, G., McCormick, F., and Clark, R. (1993) *EMBO J.* **12,** 1923–1927
27. Eccleston, J. F., Moore, K. J. M., Morgan, L., Skinner, R. H., and Lowe, P. N. (1993) *J. Biol. Chem.* **268,** 27012–27019
28. Skinner, R. H., Picardo, M., Gane, N. M., Cook, N. D., Morgan, L., Rowedder, J., and Lowe, P. N. (1994) *Anal. Biochem.* **223,** 259–265
29. Skinner, R. H., Bradley, S., Brown, A. L., Johnson, N. J. E., Rhodes, S., Stammers, D. K., and Lowe, P. N. (1991) *J. Biol. Chem.* **266,** 14163–14166
30. Pingoud, A., Wehrmann, M., Pieper, U., Gast, F. U., Urbanke, C., Alves, J., Feuerstein, J., and Wittinghofer, A. (1988) *Biochemistry* **27,** 4735–4740
31. Neal, S. E., Eccleston, J. F., and Webb, M. R. (1990) *Proc. Natl. Acad. Sci. U. S. A.* **87,** 3562–3565
32. Segel, I. H. (1975) *Enzyme Kinetics*, pp. 170–204, Wiley-Interscience, New York